Functional and mechanistic properties of lapatinib in selective breast cancer cells

Author

Chintala Ramulu, Naveen Kumar

Published

2021-02-10

Thesis Type

Thesis (PhD Doctorate)

School

School of Environment and Sc

DOI

10.25904/1912/4089

Functional and mechanistic properties of lapatinib in selective breast cancer cells

Naveen Kumar Chintala Ramulu
B.Pharm., MS (Biotechnology)

School of Environment and Science
Griffith Sciences Group

Submitted in fulfilment of the requirements of the degree of
Doctor of Philosophy

September 2019

Statement of Originality

This work has not previously been submitted for a degree or diploma in any university. To the best of my knowledge and belief, the thesis contains no material previously published or written by another person except where due reference is made in the thesis itself.

Phd student: Naveen Kumar Chintala Ramulu

Signed: 

Dated: 14/09/2019

Dedication

"There are special people in our lives
who never leave us…
Even after they are gone"

This thesis is dedicated to my late father, Ramulu Chintala

Publications arising from this thesis

- Naveen Chintalaramulu[1], Raja Vadivelu[2,3], Nam-Trung Nguyen[2], Ian Edwin Cock[1,4]; *Lapatinib inhibits doxorubicin induced migration of HER2-positive breast cancer cells.* Inflammopharmacology, 2020. https://doi.org/10.1007/s10787-020-00711-9

Additional publication(s) during PhD candidature

- Jun Zhang***,** Naveen Chintalaramulu***,** Raja Vadivelu, Hongjie An, Dan Yuan, Jing Jin, Chin Hong Ooi, Ian Edwin Cock, Weihua Li, Nam-Trung Nguyen; *Inertial Microfluidic Purification of Floating Cancer Cells for Drug Screening and Three-Dimensional Tumor Models.* Analytical Chemistry, 2020. **92**(17): p. 11558-11564.

Abstract

Breast cancer is a complex heterogenous disease with distinct molecular subtypes and metabolic behaviour, disparate responses to therapies, and considerable differences in the overall survival of the patients. Insights into the biological heterogeneity of the disease has led to the development of therapeutic strategies for the effective treatment of breast cancer. The current treatment options include hormone therapy for estrogen positive (ER-positive); anti-HER2 antibody (trastuzumab) therapy for human epidermal growth factor receptor 2 (HER2)-amplified, and general chemotherapy for triple-negative (TN) breast cancers. Unfortunately, therapeutic outcomes remain poor due to inherent or acquired resistance of the cells to the treatments and the toxicity associated with therapy. Metabolic adaptation of breast cancer cells is considered to play a crucial role in enabling the cells to become resistant to therapy and acquire metastatic potential. Bioenergetic alteration (the Warburg effect) is fundamental to all forms of cancer and is regarded as one of the hallmarks. The Warburg effect is characterized by the presence of glycolytic phenotypes within the tumor tissue. Like most cancers, an increase in lactate production observed in breast cancers may be related to the upregulation of lactate dehydrogenase (LDH) enzyme that catalyses the conversion of pyruvate to lactate. Recently, human RasGAP -SH3 domain binding protein (G3BP), an RNA binding protein, was shown to interact with the mRNA of mitochondrial H^+-ATP synthase subunit β (β-F1-ATPase), an enzyme that the mediates ATP production through oxidative phosphorylation in mitochondria. That study implicated the role of G3BP in the glycolytic phenotype observed in cancers. Indeed, G3BP is overexpressed in all forms of cancers including breast cancer. The focus of this study was to investigate the potential relevance of G3BP-1 as a breast cancer biomarker and targeting G3BP-1 by lapatinib (Lap) to inhibit the morphological adaptation and cell migration of SKBR3 breast cancer cell line.

Whilst, much of the signaling mechanisms have been elucidated, the role of G3BP in the glycolytic switch remains elusive. The first part of this study investigated the potential role of G3BP in the regulation of lactate dehydrogenase A (LDH-A), a key regulator of the glycolytic shift in cancer cells.

Thus far, research has not addressed this regulation. In order to achieve this, small interfering RNA (siRNA)-mediated knockdown of G3BP-1 and G3BP-2 (isoforms of G3BP) was performed in MDA-MB-435 breast cancer cell line. Following the knockdown of G3BP, changes in the expression of LDH-A at the transcriptional and translational level were evaluated. The results showed that G3BP-1 (but not G3BP-2) was implicated in the translational regulation of LDH-A. Whilst, depletion of endogenous G3BP-1 resulted in a significant downregulation of LDH-A protein, silencing of G3BP-2 had no effect on the translational regulation of LDH-A. Furthermore, depletion of G3BP-1 and G3BP-2 had no effect on the endogenous mRNA levels of LDH-A. These findings suggest the role of G3BP-1 (but not G3BP-2) in regulating the bioenergetic phenotype of MDA-MB-435 breast cancer cells.

Furthermore, the effect of Lap on the protein levels of G3BP-1 and LDH-A was explored in a panel of breast cancer cell lines including SKBR3 (HER2-positive), MDA-MB-231 (triple-negative), and T47D (ER-positive/PR-positive). The data indicated that Lap significantly downregulated the protein levels of G3BP-1 and LDH-A, independent of HER2 status. There was a significant reduction of G3BP-1 and LDH-A protein levels in Lap-sensitive SKBR3, and Lap-insensitive MDA-MB-231 and T47D cell lines. Furthermore, the findings also indicate that irrespective of the breast cancer subtypes (based on the receptor status), G3BP-1 regulates the protein levels of LDH-A. This argument supports the data obtained from the translational regulation of LDH-A upon G3BP-1 knockdown in MDA-MB-435 breast cancer cell line. Hence these findings have updated the role of G3BP-1 in the glycolytic shift observed in cancers, in this context by regulating the expression of LDH-A protein in a panel of breast cancer cell lines. On a side note, the endogenous levels of G3BP-1 and LDH-A were found to be significantly higher in the breast cancer cell lines used in the study. This observation may justify the potential relevance of G3BP-1 and LDH-A as breast cancer biomarkers.

Since its initial identification as a RasGAP binding protein, several studies have implicated the role of G3BP in signaling pathways including Ras signaling, HER2 signaling, NF-κB signaling, and *c-myc* mRNA turnover. Indeed, these pathways are often derailed in cancer. In addition, findings in this study have reported significantly higher levels of endogenous G3BP-1 in breast cancer cell lines.

Based on these evidences, G3BP-1 may be a relevant breast cancer biomarker. Therefore, strategies to target G3BP may provide therapeutic advantages over currently available standard treatment modalities to induce sensitivity of resistant breast cancers to anti-G3BP therapy.

In the past, the mechanism of action of some anticancer drugs, including resveratrol and epigallocatechin gallate (EGCG), was elucidated by their direct interaction with the recombinant G3BP. Hence, the strategy of recombinant G3BP production was adopted in this study to identify potential anticancer agents that interact with G3BP. Since, Lap downregulated the protein levels of G3BP-1 in breast cancer cell lines (as reported in this study), protein thermal shift assays (PTS) were performed to investigate a potential interaction of recombinant G3BP-1 with Lap.

The first part of study in Chapter 4 concerns construct design, expression, and purification of the full length G3BP-1 and G3BP-2 respectively. This was achieved by inserting the respective gene sequences into the bacterial pRSETC vector with N-terminal histidine $His_{(6)}$-tag, transformation into competent BL21 (DE3) *E.coli* cells, isopropyl-β-D-thiogalactoside (IPTG) induction, and nickel-nitrilotriacetic acid (Ni-NTA) purification of His-tagged recombinant G3BPs. The results showed that purified full length G3BP-1 and G3BP-2 corresponded to molecular weights of 65-kDa and 68-kDa respectively. The identity of the proteins was also confirmed by immunoblot analysis using protein-specific antibodies for G3BP-1 and G3BP-2. Upon testing for the expression as well as the recovery of the protein in the soluble fraction, it was observed that G3BP-1 was more efficiently recovered at 25^{o}C compared to G3BP-2. The observed difference in the protein recovery may be attributed to the divergent primary structure of these related, yet distinct proteins. Differences in the composition of the catalytic domains between G3BP-1 and G3BP-2 may have an impact on the recovery of the proteins in the soluble fraction. Nevertheless, $his_{(6)}$-G3BP-1 was purified using Ni-NTA resin with high purity and a yield of 6mg/l culture.

In the next step, the effect of Lap on thermal stabilization of purified G3BP-1 protein was studied using PTS assay. The results showed that the melting temperature (t_m) of G3BP-1 in the presence of Lap was higher than for the control. Such thermal stabilization was greatest at the 4:1 stochiometric ratio of Lap to G3BP-1, with an observed thermal shift (Δt_m) of $\sim\leq 1^oC$ at 15µM of G3BP-1. To distinguish the effect of Lap on thermal stabilization of G3BP-1, Lap was compared to 5-flourouracil (5-FU), a non-ATP-interacting thymidylate synthase inhibitor. G3BP-1 thermal stability in the presence of 5-FU was measured under the same experimental conditions of 4:1 stochiometric ratio of the compound to the protein. In contrast to the earlier observation, the results showed that 5-FU did not induce thermal stabilization of G3BP-1. These findings confirmed that the observed thermal stabilization of G3BP-1 was specific to Lap. In addition, a slightly higher shift in the t_m of G3BP-1 may be indicative of a weak interaction of Lap with the protein.

Metastasis is a process that involves migration of cancer cells from the primary tumor site to the distant organs. Approximately 90% of the breast cancer related mortalities have been attributed to the metastatic spread of the disease. Like other cancers, breast cancer metastasis is associated with poor prognosis. Of all the subtypes of breast cancers, HER2-amplified and triple-negative (TN) forms are known to be highly metastatic in nature. Currently, the ability to accurately predict the risk for metastatic potential poses a substantial challenge for clinical management of the disease. Interestingly, adaptive responses are induced in cancer cells following low doses of some chemotherapeutic agents.

In chapter 5, it was observed that 0.1µM doxorubicin (Dox) treatment increased the cell viability of SKBR3 breast cancer cell line. Such an increase in cell viability following Dox treatment was not observed in MDA-MB-231, T47D and HMF cell lines. Furthermore, Dox treatment also induced migratory phenotypes in SKBR3 cells. The observations based on the immunofluorescence images of the Dox treated cells revealed that there was a significant increase in the prominent F-actin filaments and the mitochondrial spread as compared to the corresponding controls.

In line with these observations, an *in vitro* scratch wound assay revealed that Dox treated cells showed an enhanced ability to migrate into the scratch wound area as compared to the control cells. However, a combination dose of 0.1µM Dox+5µM Lap not only decreased the viability of SKBR3 cells, but also effectively suppressed the migratory phenotype compared to Dox treated cells. In addition, cells that received the combination therapy showed a significant decrease in the percentage of wound closure compared with the corresponding Dox treated controls. Furthermore, Western blot analysis indicated that SKBR3 cells treated with Lap in combination with Dox showed a significant reduction in the protein levels of G3BP-1 and LDH-A when compared to either vehicle control or Dox treatment alone. Collectively, Lap treatment inhibited Dox-induced migratory phenotypes of SKBR3 breast cancer cell line with a significant downregulation of endogenous G3BP-1 and LDH-A proteins in these cells.

Acknowledgments

This PhD has been a tough and strange journey. Although it was difficult, the journey has been an incredible experience. Now that I am submitting my thesis. I owe a great debt of gratitude to many people who have been a part of this journey. Whilst this section acknowledges the people involved, it is necessarily incomplete.

First and foremost, I would like to thank my supervisors, most especially Dr. Ian Edwin Cock for his faith of accepting me into his group at the ESC, Griffith University. Your constant support, inspiration and criticism has made this thesis possible. Ian's supervisory approach has been a valuable credential for me aspiring to a career as a researcher. I am thankful to Griffith University for my studentship, and scholarship during the time of my candidature.

I would also like to express my gratitude to Prof. Nam-Trung Nguyen, QMNC, Griffith University, for allowing me to use his spectroscopy facility to conduct fluorescence imaging. In addition, his input(s) in the form of constructive criticism during my thesis and manuscript preparation were critical. I must offer special thanks to Dr. Raja Vadivelu, a previous postdoctoral fellow in Prof. Nguyen laboratory, for his guidance and practical assistance in developing the final phase of the project. Thanks to your patience, my fluorescence imaging never felt like work, even though we have been clocking long hours. I would like to like to express my gratitude to Dr. Leisa Osborne, ESC, Griffith University for allowing me to access the teaching lab facilities to perform my experiments.

Assoc. Prof. Andreas Hofmann, GRIDD, Griffith University, and all his previous laboratory members are acknowledged for their willingness to allow me to use their structural biology facility and reagents to perform protein thermal shift assays. Special thanks goes to Dr. Lyn Mason, Dr. Ulla-Maja Bailey who taught me recombinant biology techniques that were required as a part of my research.

Finally, I thank my parents and family including my sisters for their unconditional love and support over the years, without which I would not be who I am today. I especially thank my mum Mrs. Anjani Chintala for all her prayers and sacrifices to see me complete my PhD thesis. Although my dad Mr. Ramulu Chintala is no longer with us, I am sure he would have wished me good luck for thesis examination. My daughter, Ananya endured gentle reminders that her father needs study-time to get 'his homework' done. I should thank her for being patient all through those times. Special thanks goes to my wife Mrs. Kamala Manda who has been waiting patiently to see me complete my PhD. I am sure at this stage, together with my rest of the family, she will be among the four most relieved people to see this coming to an end. Last but never the least, I would like to acknowledge my friends Dr. Sushrut Arora and Dr. Vijayalakshmi Ayyar for their moral support. Thank you for being with me in thicks and thins of life.

Contents

Abstract..... v

Acknowledgements..... x

Contents..... xii

List of figures..... xviii

List of tables..... xviii

Abbreviations..... xix

1 General introduction 1

1.1 Cancer..... 2

1.1.1 Hallmarks of cancer..... 3

1.1.1a Self-sufficiency in growth signals..... 4

1.1.1b Insensitivity to antigrowth signals..... 4

1.1.1c Evading apoptosis..... 5

1.1.1d Limitless replicative potential..... 5

1.1.1e Sustained angiogenesis..... 5

1.1.1f Tissue invasion and metastasis..... 6

1.1.2 Enabling characteristics and emerging hallmarks..... 6

1.1.2a The Warburg effect..... 7

1.1.2b Lactate dehydrogenase and the Warburg effect..... 8

1.2 Breast Cancer..... 10

1.2.1 Breast cancer subtypes..... 12

1.2.2 Breast cancer metastasis..... 15

1.2.3 Breast cancer biomarkers..... 17

1.2.3a Established breast cancer biomarkers..... 18

1.2.3b Emerging breast cancer biomarkers..... 24

1.2.3c G3BP as a novel biomarker and therapeutic target..... 26

1.2.4 Proteomic approaches for biomarker identification and drug discovery..... 29

1.3 HER2/ErbB2-targeted therapy…….. 30

1.3.1 Monoclonal antibody-based therapy for HER2-positive breast cancer……..... 30

1.3.2 Lapatinib-based therapy for HER2-positive metastatic breast cancer……33

1.4 Doxorubicin as a front-line cytotoxic chemotherapeutic agent……. 35

1.5 Combination therapies against cancer…….. 37

1.5.1 Combination therapies targeting HER2-positive breast cancer 38

1.6 Project objectives……. 40

2 General materials and methods……... 41

2.1 Materials……...… 42

2.1.1 Devices used in the study……...…... 42

2.1.2 Consumables used in the study……. 43

2.1.3 Reagents used in the study…… 44

2.1.4 Commercially available kits used in the study……..... 45

2.1.5 Bacterial strains used in the study……..... 46

2.1.6 Antibodies used in the study……. 46

2.2 Methods…… 47

2.2.1 Cell lines and culture conditions……... 47

2.2.2 Transient transfection…… 47

2.2.3 RNA Extraction and cDNA synthesis……... 47

2.2.4 Polymerase chain reaction (PCR)……. 48

2.2.5 Determination of DNA concentration and purity……. 49

2.2.6 Restriction enzyme digestion…… 49

2.2.7 Agarose gel electrophoresis…….. 49

2.2.8 Ligation of the DNA fragments…… 49

2.2.9 Transformation of chemically competent *E.coli* cells…….. 50

2.2.10 Miniprep of the plasmid DNA……... 50
2.2.11 DNA sequencing…… 50
2.2.12 Recombinant protein expression…… 51
2.2.13 Polyacrylamide gel electrophoresis…… 52
2.2.14 Western blot …….. 53
2.2.15 Recombinant protein purification…….. 53
2.2.16 Determination of protein concentration…… 54
2.2.17 Densitometric analysis……... 54
2.2.18 Statistical analysis…….. 55

3 The role of G3BP in the regulation of LDH-A in breast cancer cells…….. 56

3.1 Introduction…….. 57

3.2 Materials and methods……..... 61

3.2.1 Cell culture and reagents…… 61
3.2.2 siRNA transfection……. 61
3.2.3 Western blot……... 62
3.2.4 Quantification of mRNA by qRT-PCR……. 62

3.3 Results……... 64

3.3.1 Endogenous expression of G3BP-1 and LDH-A proteins in a panel of breast cancer cell lines …… 64
3.3.2 Endogenous expression of LDH-A protein after G3BP-1 knockdown……. 66
3.3.3 Endogenous expression of LDH-A protein after G3BP-2 knockdown……. 67
3.3.4 Endogenous levels of LDH-A mRNA after G3BP-1 knockdown……..…… 68
3.3.5 Effect of G3BP-2 knockdown on endogenous levels of LDH-A mRNA……... 69
3.3.6 Effect of Lap on the protein levels of G3BP-1 and LDH-A in a panel of breast cancer cell lines …… 70

3.4 Discussion…….. 72
3.5 Conclusion…… 75

4 Investigating the binding of purified G3BP-1 protein to lapatinib…….. 76

4.1 Introduction…….. 77
4.2 Materials and methods…… 80
4.2.1 Cell culture and reagents…… 80
4.2.2 Polymerase chain reaction…….. 81
4.2.3 Generation of fusion protein construct……... 82
4.2.4 Expression of the fusion protein constructs of G3BP……. 82
4.2.5 Western blot…… 83
4.2.6 Affinity purification of $his_{(6)}$-tag G3BP…….. 83
4.2.7 Protein thermal shift…… 84
4.3 Results…… 85
4.3.1 Generation of fusion protein constructs of G3BP-1 and G3BP-2..... 85
4.3.2 Effect of temperature on the expression of recombinant protein constructs of G3BP…… 86
4.3.3 Confirmation of the identity of G3BP……..... 88
4.3.4 Purification and concentration of G3BP-1…….. 89
4.3.5 Protein thermal shift assay of purified G3BP-1 protein with lapatinib…..... 90
4.3.6 Protein thermal shift assay of purified G3BP-1 protein with lapatinib and 5-Fluorouracil…… 92
4.4 Discussion…….. 94
4.5 Conclusion…… 100

5 The role of lapatinib in the suppression of doxorubicin induced migration of SKBR3 breast cancer cells 101

5.1 Introduction 102

5.2 Materials and methods 106

5.2.1 Cell culture and reagents 106

5.2.2 Cell viability assay 106

5.2.3 Cell proliferation assay 106

5.2.4 Immunofluorescence 107

5.2.5 Acridine orange/propidium iodide assay 107

5.2.6 Scratch wound closure assay 108

5.2.7 Microscopy 108

5.2.8 Western blot 109

5.2.9 Statistical analysis 109

5.3 Results 110

5.3.1 Effect of doxorubicin and lapatinib on cell viability 110

5.3.2 Effect of 0.1µM doxorubicin on the proliferation of SKBR3 breast cancer cell line 112

5.3.3 Impact of drug treatment on F-actin distribution in SKBR3 breast cancer cell line 114

5.3.4 Effect of drug treatment on the mitochondrial distribution in SKBR3 breast cancer cell line 117

5.3.5 Effect of drug treatment on the cell migration of SKBR3 breast cancer cell line 118

5.3.6 Morphological assessment of apoptotic SKBR3 cells by AO/PI double staining 120

5.3.7 Effect of drug treatment on the protein levels of G3BP-1 and LDH-A in SKBR3 breast cancer cell line 122

5.4 Discussion 124

5.5 Conclusion 128

6 General discussion and perspectives.....129

6.1 General discussion.....130

6.2 Perspectives.....136

7 References.....138

List of figures

1.1 Global map presenting the ranking of countries in relation to cause of cancer related deaths at ages below 70 years in 2015……..….. 2

1.2 The hallmarks of cancer…….……. 3

1.3 Schematic representation of the Warburg effect in tumor cells…….……. 8

1.4 The reaction catalyzed by lactate dehydrogenase (LDH)…….…….. 9

1.5 Pie chart distribution of the incidence and mortality for the common forms of cancer in women in 2018……..…..…. 11

1.6 Schematic representation of the various breast cancer subtypes……..…….. 14

1.7 Phases of cancer metastasis……..…….. 16

1.8 Schematic representation of the domain structure of G3BP family of proteins…. 27

1.9 Illustration of the anti-HER2 targeted therapies……..……... 39

3.1 Implications of G3BP-1 in the glycolytic shift in cancers…….. 59

3.2 Western blot analysis to detect the expression of G3BP-1 and LDH-A in a panel of breast cancer cell lines.……..…… 65

3.3 Relative expression of LDH-A protein after knockdown of G3BP-1 in MDA.MB-435 breast cancer cell line……..…….. 66

3.4 Relative expression of LDH-A protein after knockdown of G3BP-2 in MDA-MB-435 breast cancer cell line……..….. 67

3.5 Relative levels of LDH-A mRNA after knockdown of G3BP-1 in MDA-MB-435 breast cancer cell line……..……... 68

3.6 Relative levels of LDH-A mRNA after G3BP-2 knockdown in MDA-MB-435 breast cancer cell line……..…….. 69

3.7 Effect of Lap treatment on the protein levels of G3BP-1 and LDH-A in a panel of breast cancer cell lines……... 71

4.1 Map of pRSETC……..…….. 81

4.2 Schematic representation of the fusion protein constructs……..…….. 82

4.3 Generation of fusion protein constructs of G3BP-1 and G3BP-2……..……... 86

4.4 Effect of temperature on the expression of recombinant G3BP-1 and G3BP-2… 87

4.5 Confirmation of the identity of G3BP……..…….. 88

4.6 Purification and concentration of $his_{(6)}$-G3BP-1……..…..……. 90

4.7 Effect of lapatinib on thermal stabilization of purified G3BP-1 protein…… 92

4.8 Protein thermal shift assay of purified G3BP-1 protein with lapatinib and 5-fluorouracil……... 93
4.9 Alignment of amino acid sequences of G3BP-1 and G3BP-2……..... 96
4.10 Sequence homology of glycine-rich C-terminal of nucleolin and RGG-rich C-terminal stretch of G3BP-1……...……. 98
5.1 Effect of doxorubicin and lapatinib on the cell viability of breast cancer cell lines.……...……..... 111
5.2 Effect of 0.1 µM doxorubicin on the cell proliferation of SKBR3 breast cancer cell line……. 113
5.3 Changes in the actin cytoskeleton structure upon treatment of SKBR3 breast cancer cells with 0.1µM Dox, 5µM Lap and 0.1µM Dox+5µM Lap…… 115
5.4 Changes in the cell morphology of SKBR3 breast cancer cells following the drug treatment…….. 116
5.5 Changes in the mitochondrial distribution upon drug treatment of SKBR3 breast cancer cell line……. 117
5.6 Effect of drug combination on the migration of SKBR3 breast cancer cells……. 119
5.7 AO/PI double stained SKBR3 breast cancer cells following the respective drug treatment…….……... 121
5.8 Effect of drug combination on the protein levels of G3BP-1 and LDH-A in SKBR3 breast cancer cell line…… 123

List of tables

1.1 Molecular subtypes of breast cancer……..……... 13

2.1 List of devices used in the study…….…. 42

2.2 List of consumables used in the study…… 43

2.3 List of reagents used in the study…….…… 44

2.4 List of commercially available kits used in the study…….……. 45

2.5 List of bacterial strains used in the study …….……..... 46

2.6 List of antibodies used in the study……..…… 47

2.7 Recipe for preparing denaturating polyacrylamide gels……... 52

3.1 Target siRNA sequences for G3BP-1, G3BP-2 and nontargeting control…….. 61

3.2 List of qRT-PCR primers used…….…… 63

4.1 List of primers used to amplify the G3BP genes……..…… 80

4.2 t_m and Δt_m values (^oC) of purified G3BP-1 protein in the presence of lapatinib…… 91

4.3 t_m and Δt_m values (^oC) of purified G3BP-1 protein in the presence of lapatinib and 5-fluorouracil…….. 93

Abbreviations

ABC	ATP binding cassette
AC-T	Adriamycin/cyclophosphamide-docetaxel
ADC	Antibody-drug conjugate
ADCC	Antibody-dependent cellular cytotoxicity
AMPK	Adenosine monophosphate-activated protein kinase
APS	Ammonium persulfate
ATP	Adenosine triphosphate
BBB	Blood-brain barrier
BRCA	Breast cancer susceptibility gene
CA	Carcinoma antigen
CDK	Cyclin dependent kinase
CEA	Carcinoembryonic antigen
CGH	Comparative genomic hybridization
CLEOPATHRA	Clinical Evaluation of Pertuzumab and Trastuzumab
CXCR4	C-X-C chemokine receptor type 4
DFS	Differential scanning fluorimetry
DMEM	Dulbecco’s modified eagle medium
Dox	Doxorubicin
ECD	Extracellular domain
ECM	Extracellular matrix
EDTA	Ethylenediaminetetraacetic acid
EGCG	Epigallocatechin gallate
EGFR	Epidermal growth factor receptor
ELISA	Enzyme linked immunosorbent assay
EMT	Epithelial-mesenchymal transition
ER	Estrogen receptor
FASN	Fatty acid synthase
FISH	Fluorescence in situ hybridization
GAP	GTPase-activating protein
GEF	Guanine nucleotide exchange factor
GEP	Gene expression profile

GLUT	Glucose transporter
G3BP	RasGAP-SH3 domain binding protein
HBMEC	Human brain microvascular endothelial cell
HBOC	Hereditary breast and ovarian cancer
HER2	Human epidermal growth factor 2
HIF-1	Hypoxia inducible factor 1
HMFs	Human mammary fibroblasts
hPSC-CMs	human pluripotent stem cell-derived cardiomyocytes
HRG	Heregulin
ICAM	Intercellular cell adhesion molecule
IC_{50}	Half-inhibitory concentration
IGFR	Insulin-like growth factor receptor
IHC	Immunohistochemistry
Ikβα	Inhibitor kappa β
IL-1	Interleukin 1
iNOS	inducible nitric oxide synthase
IPTG	Isopropyl-β-D-thiogalactoside
Lap	Lapatinib
LB	Luria-bertani
LDH-A	Lactate dehydrogenase A
LKB1	Liver kinase B1
MAPK	Mitogen activated protein kinase
MMP	Matrix metalloproteinase
mRNP	messenger RNA protein
mTOR	mammalian target of rapamycin
MUC-1	Mucin 1
NAD	Nicotinamide adenine dinucleotide
NF-kβ	Nuclear factor kappa β
Ni-NTA	Nickel-charged nitrilotriacetic acid
NTF2	Nuclear transport factor 2
OXPHOS	Oxidative phosphorylation
PCNA	Peripheral cell nuclear antigen
PDK	Phosphoinositide-dependent kinase

PH	Pleckstrin homology
PI3K	Phosphoinositide 3-kinase
PKM2	Pyruvate kinase isozyme M2
PR	Progesterone receptor
pRB	Retinoblastoma protein
PRIMA-1	p53 reactivation and induction of massive apoptosis
PTEN	Phosphatase and tensin homolog
PTS	Protein thermal shift
PxxP	Proline rich motif
RasGAP	Ras-GTPase activating protein
RBP	RNA binding protein
RGG	Arginine/glycine rich motif
ROS	Reactive oxygen species
RRM	RNA recognition motif
RTK	Receptor tyrosine kinase
SDS-PAGE	Sodium dodecyl sulphate-polyacrylamide gel
SELDI-TOF	Surface enhanced laser desorption ionization-time of flight
SG	Stress granule
STK11	Serine/threonine kinase 11
TCH	Docetaxel/carboplatin plus trastuzumab
T-DM1	Trastuzumab emtansine
TEMED	Tetramethylethylenediamine
TGF β	Tumor growth factor beta
t_m	Melting temperature
Δt_m	Shift in melting temperature
TN	Triple negative
TNBC	Triple negative breast cancer
TNF α	Tumor necrotic factor α
Topo IIα	Topoisomerase II α
TP53	Tumor suppressor protein 53
TSP-1	Thrombospondin 1
TtGlnRS	Glutaminyl-tRNA synthetase
U.S FDA	United States Food and Drug Administration

UTR	Untranslated region
VEGF	Vascular endothelial growth factor
2-DG	2-deoxyglucose
2D-PAGE	Two-dimensional polyacrylamide gel electrophoresis
5-FU	5-Fluorouracil

Chapter 1

General introduction

1.1 Cancer

Cancer is among the leading causes of death worldwide. According to the GLOBOCAN database 2018, International Agency for Research on Cancer (IARC), approximately 18.1 million new cancer cases were diagnosed, and 9.6 million cancer-related deaths were reported in 2018 (**Fig 1.1**) [1] . According to IARC, cancer is expected to rank as the leading cause of death worldwide by the 21st century.

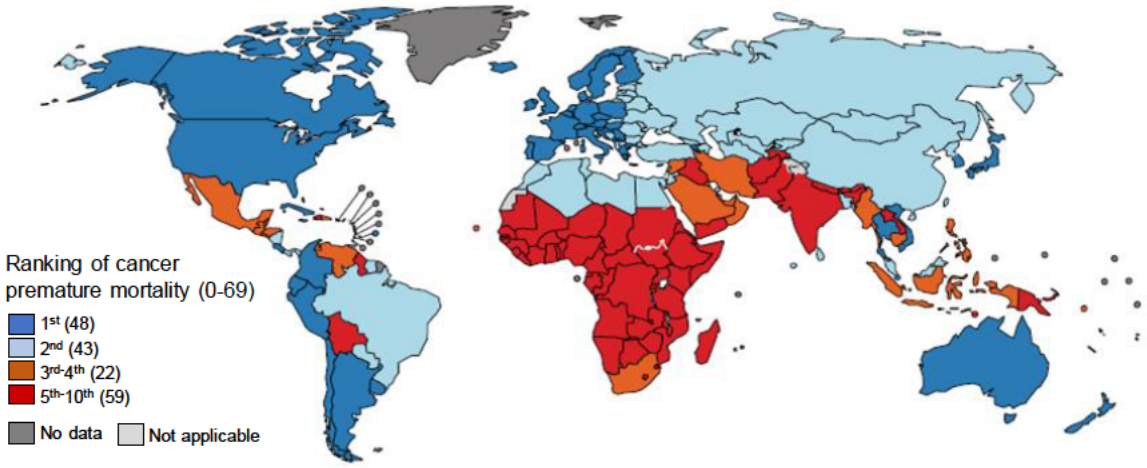

Figure 1.1: **Global map presenting the ranking of countries in relation to cause of cancer related deaths at ages below 70 years in 2015.** The number of countries represented in each ranking groups are indicated in the legends. The Figure was adapted from [1] and is presented here with permission of the corresponding author and the journal editor.

A tumor may develop in any tissue of the body. The tumor may progress into various forms of cancer following different mechanisms and may display different symptoms. However, uncontrolled cell proliferation is fundamental to all forms of cancer and compromises normal cellular homoeostasis. Target specific cancer therapy requires an understanding of the genetics of cancer to better design novel drugs to qualify for personalized treatment.

Cancer has been extensively studied as a genetic disease. As early as 1914, Boveri reported that imperfect division of chromosomal complexes cause cancer [2]

Based on the long latency time between exposure to mutagenic radiation and the appearance of a tumor, it was suggested that a cell must contain more than one mutation to develop into a solid tumor [3]. Tumor progression was considered as a stepwise process by which a cell acquires different qualities at each step; for example, mitogenic signals, antiapoptotic or metastatic capabilities [4]. Hereditary mutations may be considered as predisposing factors for carcinogenesis [5] . As cancer progresses, mutations accumulate and there is a tendency to deviate more from the normal type. Hence, metastatic tumors are often more malignant than primary tumors [6]. Interestingly, cancer is one of the few diseases where a somatic mutation is pathogenic to its carrier [7]. Additional somatic mutations and genome rearrangements enable the cancer cells to proliferate and form colonies. As a result, late-stage cancers often consist of polyclonal tumors, where each clone has unique mutations, pathologies, and drug resistances [8, 9].

1.1.1 Hallmarks of cancer

Cancer cells acquire certain functional characteristics during their multistep development into tumors (**Fig 1.2**). These characteristics are best referred to as 'Hallmarks of cancer' [10].

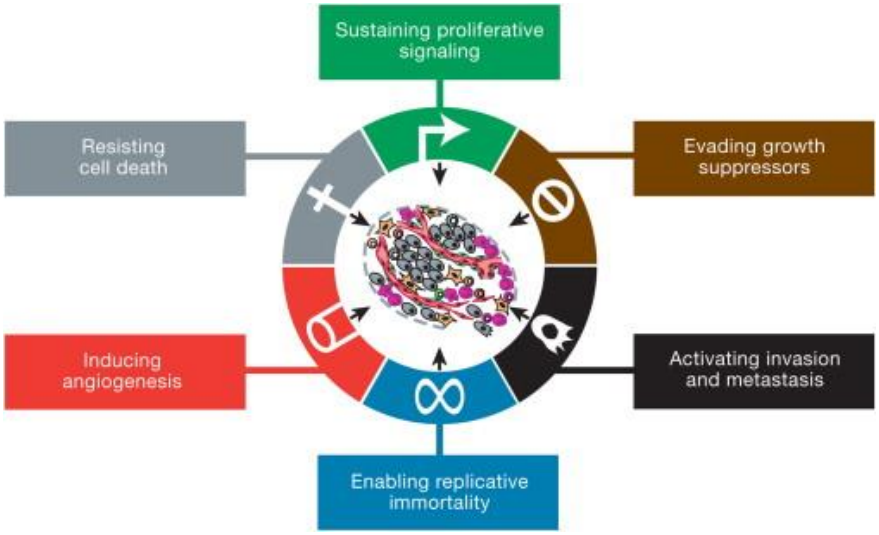

Figure 1.2: The hallmarks of cancer. Schematic representation of the functional characteristics acquired by a cancer cell during multistep development into a tumor. The Figure was reproduced from [10] with permission of the corresponding author and the journal editor.

1.1.1a Self-sufficiency in growth signals

Cancer cells have evolved to be independent in generating mitogenic signals by producing growth factor ligands themselves. Alternatively, they may signal adjacent normal cells to produce growth factors [11]. For example, a mutation resulting in structural changes in B-Raf protein leads to constitutive signaling through the mitogen activated protein kinase (MAPK) pathway [12]. Another example includes mutations in the catalytic domains of phosphoinositide 3-kinase (PI3K) isoforms that result in hyperactivity through PI3K circuitry in several types of cancers [13, 14].

1.1.1b Insensitivity to antigrowth signals

Multiple antiproliferative signals operate within cells to maintain tissue homeostasis. Most importantly, these signals are mediated through retinoblastoma protein (pRb). Retinoblastoma in its hypophosphorylated state sequesters E2F transcription factors and prevents the genes that enable the G1 to S phase transition [15-17]. Tumor growth factor β (TGF β) acts in several ways to maintain the pRb circuit within the cell. One of the mechanisms by which TGF β governs the pRb pathway is via the synthesis of $p15^{INK4B}$ and p21 proteins, which block the cyclin:cyclin dependent kinase (cyclin:CDK) complex from phosphorylating pRb [18]. In addition, TGF β suppresses the expression of *c-myc* [19]. Deregulation of the TGF β pathway has deleterious effects on the cell cycle regulation. Several mechanisms including insensitivity of the receptor to its ligand, inactivating mutations in the TGF β receptors [20, 21], deletion of the locus encoding $p15^{INK4B}$ [22] , and mutations in Smad4 (effector protein downstream of ligand activated TGF β) may result in the cessation of pRb-mediated antiproliferative signaling. On the other hand, overexpression of *c-myc* enhances the myc/max transcriptional complex, thereby enabling unrestrained proliferation [23].

1.1.1c Evading apoptosis

The role of apoptosis as a natural barrier to cancer development has been studied extensively over the last two decades [24-26]. Antiapoptotic proteins (Bcl-2, Bcl-xl, Bcl-w, Mcl-1 and A1) suppress proapoptotic responses induced by Bax and Bak. In response to substantial DNA breaks, the tumor suppressor protein p53 upregulates the expression of Noxa and Puma BH3-only proteins [27]. These interact with anti-apoptotic Bcl-2 and release Bax and Bak from antiapoptotic inhibition. When relieved of such inhibition, Bax and Bak cause the release of cytochrome c from the mitochondrial membrane [28]. Cytochrome c in turn activates a cascade of caspases to induce apoptosis [29]. Mutations in the p53 gene are reported in approximately 50% of human cancers [30], which result in the downregulation of Noxa and Puma BH3-only proteins, thus evading apoptosis.

1.1.1d Limitless replicative potential

Every cell has finite replicative potential and once it reaches its threshold it stops dividing and enters a state of senescence. Mutations in pRb and p53 enable cells to divide beyond this point until they attain a state of crisis. Occasionally a variant cell emerges out of this state (1 in 10^7) and acquires a state of immortalization [31]. Maintenance of constant telomere length is evident in such cell types and is characteristic of malignant cells [32, 33]. Cells achieve this by upregulating the expression of the telomerase enzyme that adds hexanucleotide repeats onto the ends of telomeric DNA [34]. Alternatively, chromosomal recombination maintains telomeric repeats by strand invasion of the sub-telomeric region followed by replicative copying of the sub-telomeric region onto the chromosomal ends [35].

1.1.1e Sustained angiogenesis

Angiogenesis ensures an adequate supply of oxygen and nutrients to the rapidly proliferating cells and helps in tumor progression [15]. Signals for neovascularization are conveyed by vascular endothelial growth factor (VEGF) and acidic and basic fibroblast growth factor (FGF1/2). These signals are transduced by transmembrane tyrosine kinase receptors present on endothelial cells [36, 37].

Thrombospondin 1 (TSP-1) binding to CD36 on endothelial cells recruits Src-like tyrosine phosphatase that dephosphorylates VEGF [38], enabling a balance between homeostasis and vascularization. Cancer cells undergo an 'angiogenic switch' that allows normally quiescent cells to transform into tumors [39]. Mutations in p53 reduce the levels of TSP-1, allowing endothelial cells to favor angiogenesis [40]. Many tumors have increased expression of VEGF, and FGFs compared to their normal tissue counterparts [41, 42].

1.1.1f Tissue invasion and metastasis

Distant spread of the tumor cells (metastasis) is the cause of approximately 90% of the cancer-related deaths [43]. Cell-cell adhesion molecules including E-cadherins, intercellular cell adhesion molecules (ICAMs) function in conveying the antigrowth signals across cells via cytoplasmic connections [44, 45]. Loss of E-cadherin expression is associated with epithelial-mesenchymal transition (EMT), a frequent occurrence during tumor metastasis [44, 46]. Similarly, changes in N-CAM expression from adhesive to poorly adhesive form has been reported in several cancers [45, 47].

1.1.2 Enabling characteristics and emerging hallmarks

Acquisition of the functional capacity of cancer cells is enhanced by certain intrinsic characteristics. The most predominant characteristic is the development of genomic instability. During tumor progression, the functions of various components of the DNA maintenance machinery are compromised through inactivating mutations [48-50]. Comparative genomic hybridization (CGH) studies have revealed widespread genomic aberration as conclusive evidence for the loss of genomic integrity. Recurrence of specific aberrations at sites in the genome indicates that those sites harbor genes whose manipulations cause cancer [51]. Together with defects in the maintenance and repair systems, destabilization of gene copy number and nucleotide sequence augment the genomic instability. A second enabling characteristic is the promotion of tumor inflammation. In response to neoplastic lesions, there is an influx of cells from both innate and adaptive immune arms [52]. This inflammatory response provides the cancer cells with a rich supply of bioactive molecules, growth factors, survival signals, and proangiogenic factors that are utilized by the cancer cells to thrive [53-55] .

1.1.2a The Warburg effect

Cancer cells exhibit metabolic reprogramming to generate considerable amounts of energy to ensure the demands of rapidly proliferating cells are met. This phenomenon is fundamental to all forms of cancer [56-58]. The bioenergetic reprogramming is enabled by alterations of carbohydrate metabolism. In general, energy requirements of a normal cell are met through the generation of adenosine triphosphate (ATP) molecules from glucose by oxidative phosphorylation [59]. In contrast, cancer cells have a propensity to produce lactate from glucose by aerobic glycolysis, even under normaxic conditions (**Figure 1.3**). This phenomenon is called the 'Warburg effect' [60, 61]. Although the efficiency of ATP production via glycolysis is approximately 18-fold lower when compared to mitochondrial oxidative phosphorylation, the cells maintain their energy requirement by upregulating glucose transporters (GLUT1) to increase glucose import into the cytoplasm [62, 63]. The Warburg effect is beneficial to cancer cells in several ways. Firstly, the glycolytic shift enables cancer cell to produce the building blocks, such as nucleotides, amino acids, lipids and NADPH to support its structure [62, 64, 65]. The second most evident consequence is the decrease in the mitochondrial oxidative phosphorylation [66, 67]. Accordingly, less reactive oxygen species (ROS) are generated that may enable cancer cells to avoid oxidative stress and escape apoptosis. Moreover, the Warburg effect has been directly linked to the activation of oncogenes such as *c-myc*, Ras, and Akt [63, 68-71]. Additionally, the hypoxic microenvironment in tumors promotes the upregulation of hypoxia-inducible factor (HIF-1) [72, 73]. HIF-1 is a critical transcription factor that enables the transcriptional activation of glycolytic enzyme genes, including lactate dehydrogenase-A (LDH-A) [74].

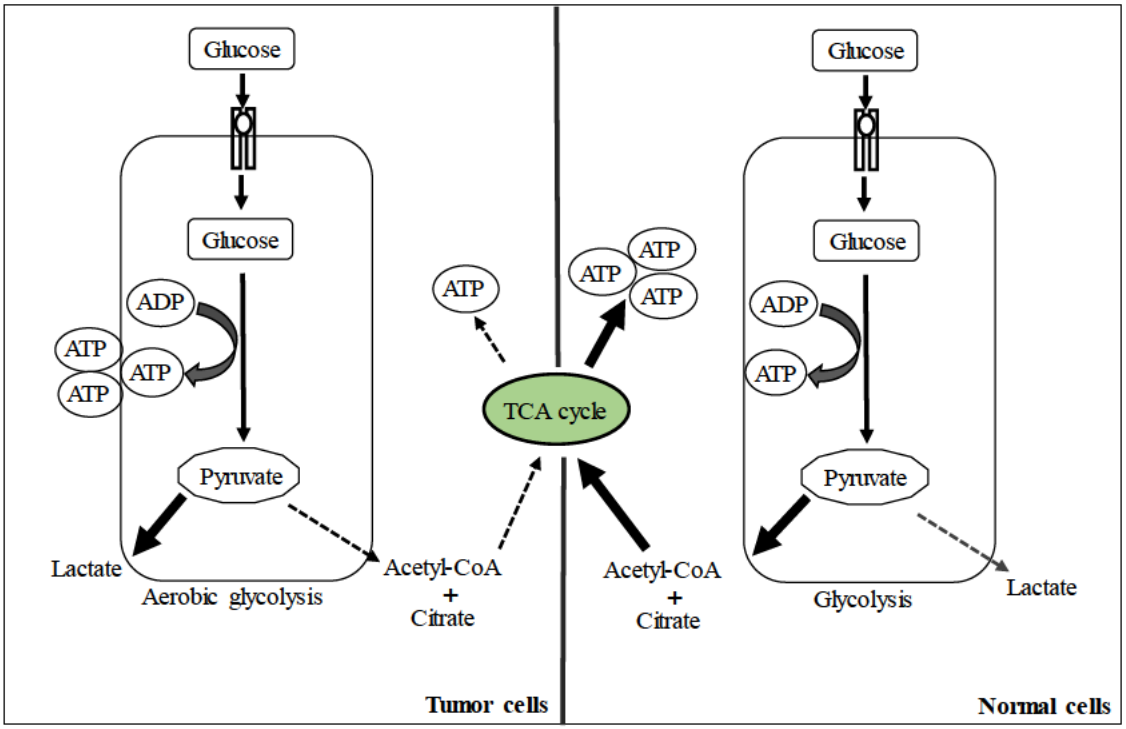

Figure 1.3: **Schematic representation of the Warburg effect in tumour cells.** In normal cells, pyruvate is converted to acetyl-CoA. Acetyl-CoA enters the TCA cycle along with citrate to generate ATP through mitochondrial oxidative phosphorylation. However, in cancer cells, aerobic glycolysis converts glucose to lactate with the generation of ATP. Mitochondrial ATP production is rather limited in cancer cells.

1.1.2b Lactate dehydrogenase and the Warburg effect

The lactate dehydrogenase gene is located on chromosome 11p15.4 [75]. The resulting protein is a polypeptide of 332 amino acids and has a molecular weight of 37-kDa. It is a tetrameric enzyme consisting of two major subunits A and/or B resulting in five isoenzymes, (A4, A3B1, A2B2, A1B3, and B4). Evidence suggests that LDH-A and LDH-B are the gene products from duplication of a single LDH-A like LDH gene [76]. Lactate dehydrogenase catalyses the reversible conversion of pyruvate to lactate coupled with the recycling of NAD^+ (**Figure 1.4**) [74, 77]. Whilst, LDH-A is predominantly present in the skeletal muscle and converts pyruvate to lactate [75], LDH-B is found in heart muscle and favours the conversion of lactate to pyruvate that is further oxidized [75].

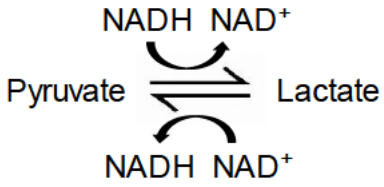

Figure 1.4: **The reaction catalysed by lactate dehydrogenase (LDH).** LDH catalysed the reversible conversion of pyruvate to lactate. Figure adapted from [75] and is presented here with permission of the corresponding author and the journal editor.

The LDH-A promoter region contains a consensus binding site for major transcription factors including HIF-1 and *c-myc* [74, 78-80]. As a result of pervasive hypoxic conditions in cancer cells, HIF-1α is stabilized and along with the constitutively expressed subunit, HIF-1β, forms the transcription factor HIF-1. Thus HIF-1 promotes the transcription of LDH-A. Human epidermal growth factor receptor (HER2/ErbB2/neu) also induces the expression of LDH-A via activation of phosphoinositide 3-kinase (PI3K)/Akt pathway, which results in the activation of HIF-1 and upregulation of LDH-A gene expression [81]. Yang *et al*., [82] demonstrated that LDH-A was induced upon activation of the extracellular signal-regulated kinase. Subsequently, ERK2 phosphorylates pyruvate kinase isozyme M2 (PKM2). This leads to the recruitment of isomerase Pin1, that allows the translocation of PKM2 to the nucleus. In the nucleus PKM2 induces *c-myc* expression via transcriptional coactivation of β-catenin, which in turn induces the expression of LDH-A gene [82]. Other transcriptional factors that are linked to LDH-A expression include FOXM1 and KLF4 [83, 84].

Lactate dehydrogenase A is upregulated in many cancers, including breast, pancreatic, gastric, renal, oesophageal and colorectal cancers [83, 85-88]. Fantin *et al.,* [56] demonstrated that cell proliferation was severely affected in LDH-A deficient clones of tumor cell lines Neu 4145, nNeu, NF980, SMF, NAF derived from mouse mammary gland. Several other reports [89-92] have indicated that LDH-A suppression leads to the inhibition of tumor cell proliferation and survival.

Increased lactate production leads to the acidification of the microenvironment. The resulting acidosis precedes the pH-dependent activation of matrix metalloproteinases (MMPs), cathepsins, which promote cell invasion [93-96]. Sheng *et al.*, [97] demonstrated that knockdown of LDH-A reduced the expression of MMP-2 and suppressed the metastatic potential of HCCLM3 human hepatocellular carcinoma cells. Studies [98-101], have shown that the acidic microenvironment within the tumor promotes the expression of VEGF that stimulates angiogenesis. Koukourakis *et al.*, [102-104] demonstrated that LDH-A activation leads to the upregulation of VEGF expression in several cancers, including endometrial, colorectal and non-small-cell lung cancer. Collectively, these evidences demonstrate that LDH-A is required for tumor survival and progression. Therefore, targeting LDH-A may prevent or suppress cancer progression.

1.2 Breast Cancer

Uncontrolled proliferation of the cells in the breast leads to breast cancer. Depending on the origin, breast cancers can be either lobular (within the lobules that produce milk), or ductal (tubes that carry milk) carcinomas [105]. Whilst invasive lobular carcinoma accounts for approximately 10% of all breast cancers [106], invasive ductal carcinomas are the most common form of breast cancers [107]. **Figure 1.5** shows that of all the ten cancer types reported for incidence and death in women worldwide, breast cancer is the most diagnosed form (24.2% of the total incidence) and the leading cause of cancer related death (15% of the total mortality) [1].

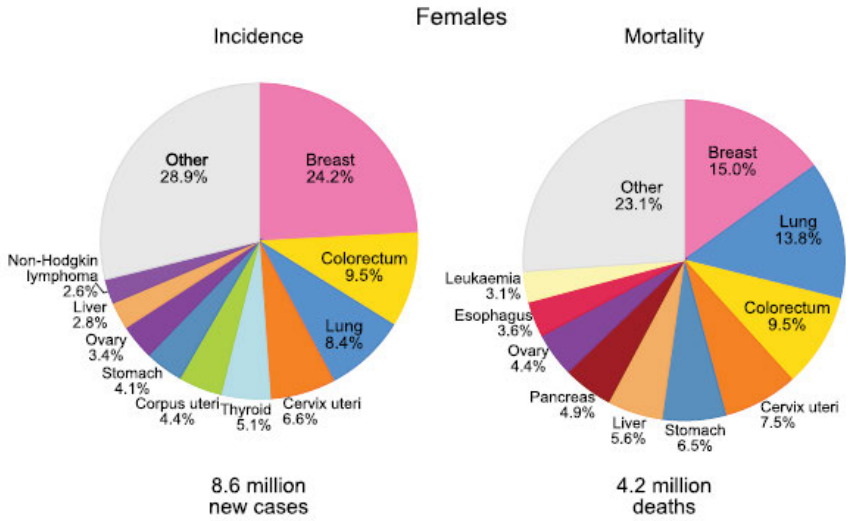

Figure 1.5: **Pie chart distribution of the incidence and mortality for the common forms of cancer in women in 2018**. The area of the pie chart represents the proportion of the total number of cases for incidence or mortality. Most common forms of cancer are indicated as the proportion of the total incidence or mortality. 'Other' category includes nonmelanoma skin cancers. Figure adapted from [1] and is presented here with permission of the corresponding author and the journal editor.

In recent years, genetic predisposition to breast cancer has been studied extensively. It was reported that 20-25% of the patients diagnosed with breast cancer had positive family history, of which 5-10% demonstrated an autosomal dominant inheritance [108, 109]. Several reports [110-113] indicated that mutations in tumor suppressor genes including BRCA1 and BRCA2 (breast cancer susceptibility gene), TP53 (tumor protein p53), PTEN (phosphatase and tensin homolog), and STK11 (serine/threonine kinase 11) confer 40-85% lifetime risk of developing breast cancer. Although, hereditary factors have been implicated in breast cancer, non-hereditary factors including, reproduction (nulliparity, late age at first birth), exogenous hormone intake (use of oral contraceptives and hormone replacement therapy), alcohol consumption, and obesity also increase the rate of breast cancer incidence [114].

1.2.1 Breast cancer subtypes

Based on the morphological characteristics, breast cancer is categorized into several subtypes. Invasive ductal carcinoma (IDC), represents approximately 80% of the invasive breast cancers that grow in the milk ducts and has invaded the tissues of the breast outside of the ducts [115]. Next most common form of the disease is the invasive lobular carcinoma (ILC) representing approximately 10% of the invasive forms of the disease. Invasive lobular carcinoma refer to cancers that have originated in the milk-producing lobules and invaded the surrounding tissues of the breast [115]. Other subtypes of breast cancer that are less common include mucinous, micropapillary, papillary, tubular, cribriform and inflammatory carcinomas.

Gene expression profiling (GEP) studies (based on ~500 intrinsic genes that are highly variable in their level of expression between different tumours but are consistent within the same tumour over a period) have broadly classified breast cancer into two groups based on the expression of estrogen receptor (ER) [116]. These two groups were further subdivided into- ER-positive (luminal A, and luminal B); ER-negative (basal-like and human epidermal growth factor receptor-HER2) [116, 117]. Recent studies have updated the breast cancer classification to include two additional but less common subtypes: claudin-low, and molecular apocrine [116].

Breast cancers of the luminal A and B subtypes are distinguished based on the relative expression of ER, ER-regulated genes, PR and other genes that include GATA-binding protein 3, X-binding proteins and hepatocyte nuclear factor 3α [118, 119]. Importantly, ER-positive cancers are also subtyped depending on their HER2 status and proliferation rate. Cheng *et al*., [120] have studied the relative expression levels of Ki67 (proliferative marker) and established a Ki67 cut-off of 14% to distinguish between the luminal A and luminal B subtypes. ER negative (ER-) breast cancers are subcategorized into HER2-positive, and basal-like breast cancers. Basal-like breast cancers are distinguished from triple-negative (ER-, PR-, HER2-) breast cancers by the expression of cytokeratin 5/6 and/or 17, and/or EGFR [115].

Whilst, claudin-low molecular subtype tumors are characterized by the low expression of claudins (3, 4 and 7), E-cadherin and CD24; molecular apocrine tumors express relatively high levels of androgen receptors and lack ER [116]. Interestingly, routine subclassification of breast cancers is achieved by immunohistochemical (IHC) staining analysis of the tumor tissues for the expression of receptors-ER, progesterone (PR) and HER1 and HER2 [115]. Whilst, such classification is used as a surrogate for GEP (**Table 1.1**), clinical decision(s) are reliably made based on the receptor status.

Table 1.1: Molecular subtypes of breast cancer. GEP, gene expression profiling; IHC, immunohistochemical; ER, estrogen receptor; PR, progesterone receptor; HER2, human epidermal growth factor receptor 2. Table adapted from [117] and is presented here with permission of the corresponding author and the journal editor.

Intrinsic subtypes (GEP)	IHC classification	Agreement IHC/GEP
Luminal A	Luminal A •ER and/or PR positive •HER2-negative •Ki67<14%	73%-100%
Luminal B	Luminal B (HER2-negative) •ER and/or PR positive •HER2-negative •Ki67≥14% Luminal B (HER2-positive) •ER and/or PR positive •HER2 overexpressed or amplified •Any Ki67	73%-100%
HER2-positive	HER2-positive (non-luminal) •HER2 overexpressed or amplified •ER and PR absent	41%-69%
Basal-like	Triple negative •ER and PR absent •HER2 absent	80%

Since breast cancer is a heterogenous disease, all breast cancer tumors may not be assigned to one of the known molecular subtypes. Sorlie *et al*., [121] have identified 35.2%, 25.8% and 6.1% of the total 115, 117, and 49 breast cancer tumors to have distinct gene expression profiles irrespective of any features of the molecular subtypes. Further studies have grouped the unclassifiable tumor samples under a new molecular subtype, termed luminal-like[116]. This new subclass of breast tumors was characterized by the elevated levels of interferon α/β, decreased metabolic processes, and integrin cell-surface interactions [116]. **Figure 1.6** is a schematic representation of the molecular subtypes of breast cancer.

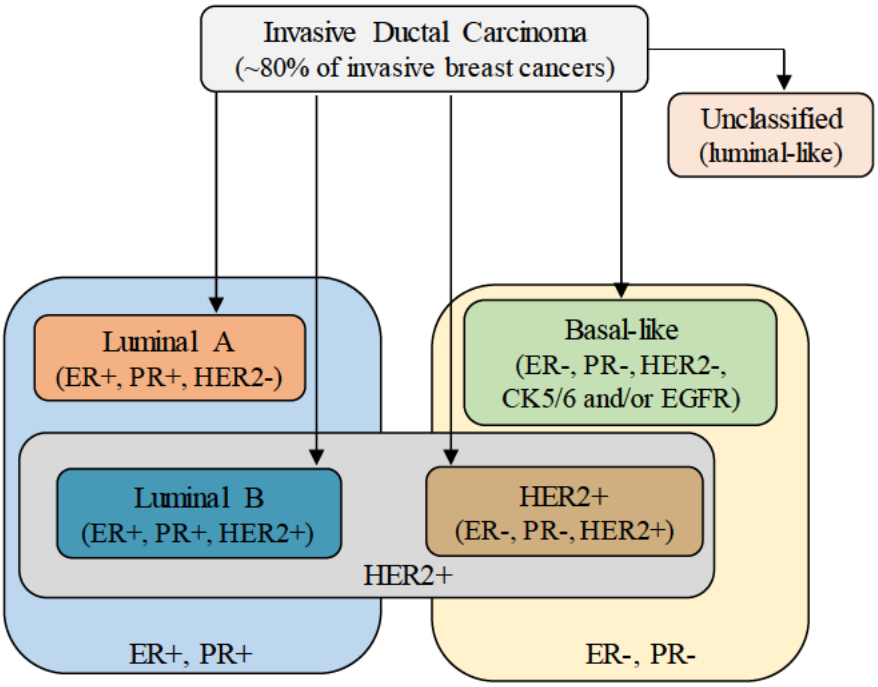

Figure 1.6: Schematic representation of the various breast cancer subtypes. The blue and yellow rectangles represent the subtypes based on the expression of ER/PR. The blue rectangle indicates ER-positive/PR-positive (luminal A and luminal B), yellow rectangle represents ER-negative/PR-negative (basal-like and HER2-positive). The central grey rectangle indicates the presence of HER2 in luminal B and HER2-positive subtypes. Some of the breast tumors are unclassified with a luminal-like molecular subtype. The figure was adapted from [115] with permission of the corresponding author and the journal editor.

1.2.2 Breast cancer metastasis

Approximately 30% of the diagnosed breast cancers acquire the ability to disseminate and colonize distant organs (metastasis), resulting in the disruption of local and systemic physiology [122, 123]. The major metastatic sites in breast cancer are bone, brain, lung and liver [124]. Metastatic tumors represent an advanced stage of the disease and is the cause of approximately 90% of cancer related deaths [125-128]. Unfortunately, the pathogenesis of metastasis is poorly understood [129].

Metastasis is one of the hallmarks of cancer [10]. It is a complex multi-stage process that consists of sequential and interrelated steps including, detachment from the primary tumor site, migration to vascular supply, entry into the blood or lymphatic systems (intravasation), survival in the blood stream, extravasation, adaptation to the foreign microenvironment, and successful proliferation and colonization [129, 130].

The metastatic cascade can be conceptually classified into two major parts (**Figure 1.7**): (a) physical translocation of the cancer cells from the primary tumor and (b) colonization [129]. Whilst, physical dissemination is widely understood, colonization is still a perplexing concept [129]. Paget *et al.,* [131] put forth a concept that certain tumor cells (seeds) have an affinity for certain organs (soil). This was deduced from the analysis of more than 900 autopsy records of breast cancer patients. According to this concept, tumors are heterogenous and consist of subpopulations of cells (clones) with different genetic profile and biological properties. Metastasis is highly selective for the specific clones that have the potential to generate metastases. Formation of successful metastases depends on the interaction between the tumor cell and the microenvironment [129, 131].

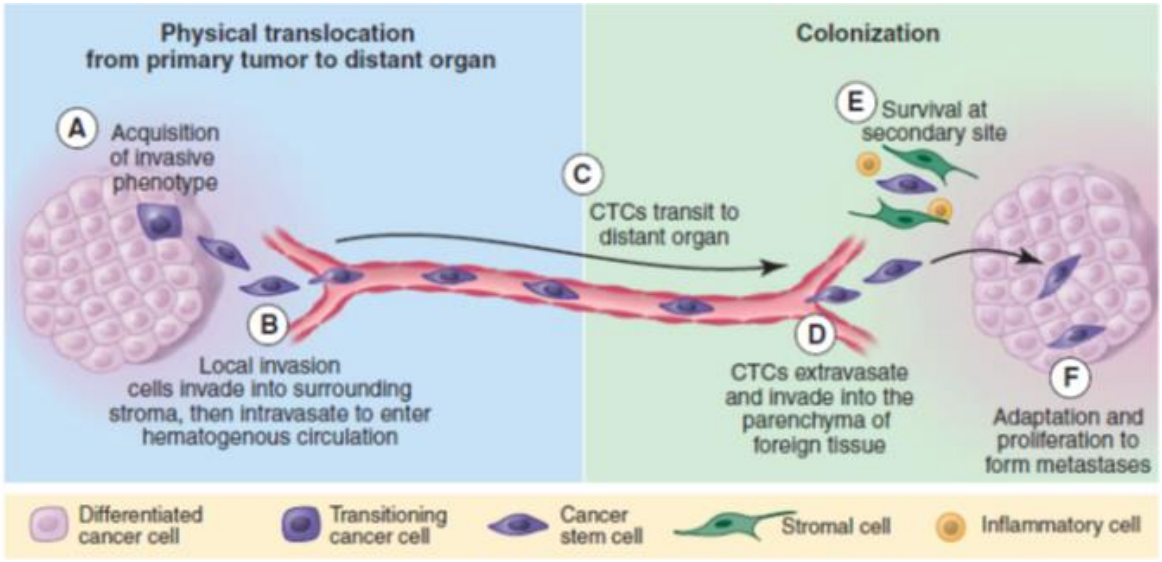

Figure 1.7: Phases of cancer metastasis. Metastatic spread of cancer involves two phases: (i) physical translocation from the primary tumor and (ii) colonization. (A) Cancer cells acquire metastatic phenotype. (B) These cells enter the local blood vessels (intravasation). (C) Cancer cells that travel through the circulatory system are termed circulating tumor cells (CTCs). (D) At the target site away from the primary tumor origin, the CTCs extravasate the blood stream and invade the foreign tissue. (E) CTCs evade the local immune response within the foreign site to enable their survival. (F) Finally, the cancer cells adapt to the new microenvironment and initiate proliferation. The Figure was reproduced from [129] and is presented here with permission of the corresponding author and the journal editor.

Since breast cancer is a heterogenous group, distinct metastatic patterns are displayed depending on the molecular subtypes [132]. ER-amplified breast cancers have the best prognosis among the three subtypes [(ER-amplified, HER2-amplfied, and triple-negative (TN)] with a low rate of incidence [133]. In contrast, HER2-amplified and TN subtypes are aggressive forms of breast cancer with poor prognosis [134, 135]. Interestingly, both HER2-amplified and TN cancers display metastatic spread to the brain in addition to the lungs [133, 136, 137]. However, the molecular mechanism for such propensity of these cells for brain metastasis is largely unknown.

Whilst, an absence of receptors may pose difficulty in therapy against TN cancers, amplification of HER2 receptor serves as a reliable indicator of aggressive nature of the disease. Perhaps, HER2-amplified breast cancers are at a particularly high risk, with approximately half of the reported cases developing brain metastasis [136, 138-143]. Indeed, HER2 is a potent oncogene that is over expressed in approximately 25-30% of the metastatic breast cancers [144-146]. Ironically, HER2-amplified metastatic breast cancer is still prevalent where therapeutic targeting of HER2 is well developed.

1.2.3 Breast cancer biomarkers

Approaches to breast cancer treatment involve the identification of tumor biomarkers that can be used for clinical management of the disease that include assisting in diagnosis, staging, evaluating the treatment response, detection of disease recurrence, and development of new therapeutic strategies. Over the past few decades, the discovery of specific predictive and prognostic biomarkers has enabled the design of more individualized therapies to target different molecular subtypes of breast cancer. Whilst, predictive biomarkers help to foretell the patient's response (associated with tumor sensitivity or resistance) to a specific treatment; prognostic markers are the indicators of the disease outcome independent of the treatment [147].

Predictive biomarkers may be the target for therapeutic intervention. For instance, ER-positive breast cancers are sensitive to hormone therapy with a significant reduction in the mortality rate in patients treated with adjuvant tamoxifen for a period of five years [148]. However, being heterogenous, the sensitivity of weakly ER-positive tumors (<10%) in comparison with strongly expressing ER-positive tumors (>10%) to adjuvant tamoxifen therapy is debatable [149]. In general, the ER-positive tumors are often associated with favourable responses [150]. Similarly, HER2 is a predictive biomarker for response to HER2-targeted therapies including the monoclonal antibody, trastuzumab (Herceptin), and small molecule tyrosine kinase inhibitors, such as lapatinib [151-153]. However, HER2-positivity indicated a poor prognosis in node-negative when compared with node-positive patients [154-156].

Likewise, Ki67 (proliferative marker) represents a strong predictive marker for response to systemic chemotherapy, although, it displays an unfavourable prognostic effect [147, 157]. In general, prognostic markers indicate if the patient requires treatment and predictive markers help to determine specific treatment.

1.2.3a Established breast cancer biomarkers

Treatment of breast cancer is guided by the measurement of specific biomarkers. Among the molecular markers, the ER, PR, HER2, BRCA1 and BRCA2, Ki67 are widely established breast cancer biomarkers. Whilst, tissue biomarkers are useful in disease prognosis and predicting the response therapy, serum biomarkers including carcinoembryonic antigen (CEA), and carcinoma antigen 15-3 are used to monitor the response following primary treatment in patients with advanced disease.

Hormone receptors

Approximately 50-70% of the invasive breast cancers are reported to be positive for hormone receptors (HR) [158, 159]. Estrogen and progesterone are the most common HRs that are identified in HR-positive breast cancers [160]. Since 1980, it has been reported that tamoxifen (antiestrogen) therapy was effective in the treatment of ER-positive tumors [161]. Evidence [162] has showed that 70-80% of invasive breast cancers that are ER-positive and PR-positive regressed with hormone therapy.

The anti-estrogenic activity of tamoxifen is due to its ability to bind to the ligand-binding domain of the ER receptor, thereby, blocking the potential for estrogen stimulation [163]. Tamoxifen therapy resulted in disease free, improved overall survival and better prognosis in patients with ER-positive tumors when compared to those with ER-negative cancers [164, 165]. The progesterone receptor is an estrogen-regulated gene, expressed in >50% of the ER-positive cancers. In the absence of ER, the expression of PR is uncommon, although such incidence is usually registered as false-negative ER, or false-positive PR status [166-171].

However, expression of PR in ER-positive cancers has prognostic significance. Whilst, lower expression of PR is associated with aggressive tumors of poor prognostic utility, cancers that are positive for both ER/PR have favorable prognosis and response to endocrine therapy [172-177].

HER2

Overexpression/amplification of HER2 is identified in approximately 25-30% of metastatic breast cancers [144-146]. Although significant therapeutic developments are made in the clinical management of HER2-positive breast cancers, most patients with the metastatic form of the disease eventually die [178, 179]. Surprisingly, brain metastasis has been reported in half of the patients with advanced HER2-positive breast cancer further limiting treatment options [139-143].

HER2 is a transmembrane receptor belonging to the family of receptor tyrosine kinases (RTK). It is structurally related to the epidermal growth factor receptor (EGFR), and is encoded by ErbB2/HER2 oncogene present on chromosome 17q21 [180, 181]. The HER family of receptors has four members: EGFR (HER1), HER2, HER3, and HER4. Whilst, HER2 does not have any known ligands, HER3 lacks the RTK activity [182]. HER2 predominantly heterodimerizes with HER3 over EGFR and/or HER4 [183-185]. Of all the heterodimers formed, HER2-HER3 is the major unit with significant oncogenic potential [138, 186, 187]. Heregulin (HRG, also known as neuregulin-1) and neuregulin-2 are two known ligands that bind to HER3. Heregulin is produced by both neurons and glial cells of the brain, where it regulates the cell proliferation, differentiation and migration [188-190]. Interestingly, breast cancers that overexpress HER3 are at a higher risk of brain metastasis [191-193].

HER2 amplification is considered as a marker of poor prognostic value and is often linked to aggressive tumors with resistance to antihormonal therapy and low overall survival [194]. HER2 status in invasive breast cancers is routinely assayed by either IHC of the HER2 protein or fluorescence in situ hybridization (FISH) analysis of the HER2 gene copy number.

In addition, enzyme linked immunosorbent assay (ELISA) is used to quantify the 'soluble'-HER2 extracellular domain (ECD), that is cleaved from the full-length receptor following proteolysis [195-198].

In cell signaling, following the ligand binding, HER2 receptors undergo homodimerization or heterodimerization. Upon dimerization of the receptor, the intracellular tyrosine residues are autophosphorylated, leading to the receptor activation. Thus, activated receptors trigger major pathways, including phosphoinositide 3-kinase/Akt (PI3K/Akt) [199, 200], mitogen activated protein kinase (MAPK) [201], phospholipase-Cγ (PLCγ) [202, 203]; protein kinase C, and the Janus kinase (Jak-STAT) [204] that result in survival and cellular proliferation. Following HER2 receptor dimerization, downstream signaling is predominantly achieved through PI3K pathway. The pathway is activated upon binding of the regulatory p85 subunit of PI3K to the phosphotyrosine site on the HER2 receptor. The binding induces allosteric activation of the p110 catalytic subunit. Subsequently, phosphorylation of phosphatidylinositol (4,5) biphosphate [$PI(4,5)P_2$] generates phosphatidylinositol (3,4,5) triphosphate [$PI(3,4,5)P_3$] [205]. Following the PI3K activation and production of $PI(3,4,5)P_3$, Akt (serine-threonine specific protein kinase) is recruited to the plasma membrane by its pleckstrin homology (PH) domain and is phosphorylated by phosphoinositide-dependent kinase (PDK-1) [206]. Phosphorylation-dependent activation of Akt results in its translocation to the nucleus, where it acts upon a huge number of downstream targets including: downstream signaling via mammalian target of rapamycin (mTOR), enhanced translation of target genes involved in angiogenesis (VEGF, HIF-1α), or cell cycle progression (cyclin D1, and *c-myc*) [207], transcription of Bcl-2, survivin, XIAP (X-linked inhibitor of apoptosis protein) [208]. In addition, ligand-induced dimerization of HER receptor also activates MAPK pathway [209]. Subsequently, docking proteins, such as Grb2 are recruited to the phosphotyrosine domain of the receptor. This results in the binding of Grb2 to SOS, a guanine nucleotide exchange factor. The docking of Grb2-SOS activates SOS to exchange GDP for GTP from Ras. Thus, activated Ras-GTP interacts with Raf and stimulates a kinase cascade eventually activating MAPK [206].

Activated MAPK phosphorylates a variety of cytoplasmic substrates and translocate to the nucleus to activate several transcription factors including *c-myc*, *c-fos*, E2F and AP1, thereby altering the transcription of genes involved in cell cycle [206]. Furthermore, RTK activation of HER2 receptor also activates PLCγ pathway. Recruitment of PLCγ to the phosphotyrosine consensus site of HER2, activates PLCγ, thereby hydrolyzing $PI(4,5)P_2$ into inositol (1,4,5) triphosphate (IP_3), and diacyl glycerol. This results in the release of calcium from the storage vesicles, thereby activating calcium/calmodulin-dependent kinases. In association with diacyl glycerol, IP3 also stimulates protein kinase C [210, 211].

Since HER2 is involved in the breast cancer pathogenesis and is overexpressed in HER2-positive breast cancer subtype, monoclonal antibody therapy to target the HER2-ectodomain has achieved significant disease regression. Trastuzumab is a monoclonal antibody that binds to the HER2-receptor [212-214] with great affinity and inhibits receptor dimerization, blocks the cleavage of ECD of the receptor, and activates antibody-dependent cellular cytotoxicity (ADCC) [213, 214]. Circulating ECD of HER2 that harbors the epitope for trastuzumab [215] has modest prognostic significance; the remainder of the HER2 (C-terminal fragment and amino-terminally truncated fragment) remains insensitive to trastuzumab. However, these fragments are responsive to tyrosine kinase inhibitors [216, 217].

Studies have revealed that HER2 receptor activation by HRG induced an upregulation of fatty acid synthase (FASN) activity, resulting in enhanced signaling and tumor progression in SKBR3 and BT474 cells [218]. An *in vivo* study has demonstrated that mice that expressed both-HER2 and TGF β under the influence of MMTV promoter (MMTV-Neu) developed tumors with enhanced metastatic potential as compared to the MMTV-Neu only mice [219, 220]. Furthermore, HER2 activation is shown to induce the overexpression of MMPs, that degrade the extra cellular matrix (ECM) resulting in migration and invasion [137, 221-224]. Collectively, these evidences show the impact of HER2 overexpression/amplification in metastatic breast cancer.

Ki67

Ki67 is a nonhistone nuclear protein that is expressed during the G_1, S, and G_2 phases of cell cycle, with a peak observed during mitosis in proliferating cells and absent in the quiescent cells [225]. Ki67 score is routinely assayed by IHC and is defined as the percentage of tumor cell nuclei positively stained. In concordance with St. Gallen Consensus of 2011 [226], the proliferative index is either positive (>14%) or negative (<14%) based on the percentage of stained carcinoma cells [226]. Ki67 has a modest prognostic significance independent of the tumor size [227-229]. In case of ER-positive tumors, Ki67 cut-off is used to distinguish between luminal A (<14%) and luminal B ($\geq$14%), representing a higher proliferative index for luminal B subtype with poor prognosis [120]. Predictive significance for the response to neoadjuvant chemotherapy was reported wherein the treatment-induced alteration(s) in Ki67 expression was found to be a strong predictor for recurrence-free and overall survival [230]. Furthermore, measuring Ki67 early in treatment was found to be a strong predictor of the clinical outcome when compared to its expression prior to treatment. For instance, the Immediate Preoperative Anastrozole, Tamoxifen or Combined with Tamoxifen (IMPACT) trial reported a decrease in Ki67 at 2 and 12 weeks of aromatase inhibitor treatment to be greater when compared to tamoxifen or the combination therapy [231-233]. Although several studies have evaluated the prognostic and predictive significance of Ki67, scoring methods need to be standardized for integration of this biomarker in breast carcinogenesis.

p53

TP53 is a tumor suppressor gene located on chromosome 17p and encodes a 53-kDa nuclear phosphoprotein [234]. Functionally, p53 acts as a transcriptional factor and regulates the expression of several genes that are involved in critical pathways including cell cycle inhibition, promotion of apoptosis, maintenance of genomic stability, and inhibition of angiogenesis [235-237].

Interestingly, TP53 is the most mutated gene in human cancers [234] and, approximately 30% of breast cancer patients display TP53 gene mutations, with frequencies ranging from >80% in basal-like to <15% in luminal A subtypes [238]. Furthermore, the TP53 gene mutation types and the consequences of such mutations also varied among different molecular subtypes of breast cancer [239]. For instance, the mutation types that were highly prevalent included missense mutations in luminal cancers, truncating mutations in basal-like, and insertion/deletion in molecular apocrine subtype [239]. As a result of gene mutation, there is an altered molecular conformation and prolonged half-life of the mutant p53 protein resulting in its nuclear accumulation [240]. This alteration is an indirect indicator of defective TP53 mutation and signifies a poor clinical outcome for breast cancer patients.

Whilst, insensitivity to therapy has been linked to dysfunctional p53 status in cancers of the small intestine, thymus, and spleen in mice models [241]; there is no direct relationship between p53 mutational status and responsiveness to therapy in human cancers [242, 243]. Despite its prognostic utility, treatment modalities that account for the p53 status are still rare.

Breast cancer susceptibility genes (BRCA1 and BRCA2)

Significant risk for developing breast cancer is the inheritance of a mutation in one of the two breast cancer susceptibility genes, BRCA1 and BRCA2 [160]. Germline mutation in these genes increases the lifetime risk of developing breast cancer by 57% and 49%; or ovarian cancer by 40% and 18% by the age of 70 years for BRCA1 and BRCA2 respectively [244]. As BRCA genes are tumor suppressors, loss of the wild-type allele by mutation results in the autosomal dominant inheritance of hereditary breast and ovarian cancer (HBOC) syndrome [244]. Individuals with HBOC syndrome have 50-80% lifetime risk of developing breast cancer, and 30-50% for ovarian cancer [244]. BRCA proteins play critical role in cellular pathways including homologous recombination (DNA repair), activation and transcriptional regulation; and cellular proliferation [244-246]. Shapira *et al.,* [247] have demonstrated that the lifetime risk of developing breast cancer was higher in individuals with an inherited paternal BRCA1 mutation. Whilst the risk associated with paternal BRCA1 mutation is modest, it was reported to be insignificant [248].

Genetic testing that involves sequencing of the patient's DNA for specific regions of BRCA genes may detect presence of BRCA mutation, thereby enabling proper diagnosis and perhaps prevention in some cases. Such screening has the potential to identify high-risk individuals, in which case, prophylactic surgery and/or chemoprevention may be favourably considered [249]. It has been reported that bilateral mastectomy in high-risk individuals reduces the risk of developing breast cancer by approximately 90% [250].

Carcinoembryonic antigen and carcinoma antigen 15-3 (CEA and CA 15-3)

Measurement of serum biomarkers is a useful tool for detection of distant metastasis. Use of CEA and CA 15-3 facilitates the early detection of metastasis in approximately 60-80% of patients with metastatic breast cancer [251]. CEA is a glycoprotein that is expressed in a variety of cancers including human colorectal, gastric, pancreatic, non-small cell lung carcinomas, as well as in breast cancers [160, 252]. Whilst serum concentrations of CEA >7.5ug/L indicate subclinical metastasis [160, 253]; CEA levels within the normal range at the time of diagnosis tend to have a favourable prognostic significance when compared to the elevated CEA levels [254]. In contrast, CA 15-3 peptides are the soluble forms of MUC-1, which are released by proteolytic activity of ADAM17 and MT-MMP1 [255, 256], and are reported to be present in approximately 90% of invasive breast cancers [257]. The prognostic significance of CA 15-3 was studied by Sandri *et al.*, [258], who demonstrated the presence of aberrant levels of CA 15-3 in luminal B and HER2-positive breast cancers to be associated with an increased risk of disease relapse and death.

1.2.3b Emerging breast cancer biomarkers

Peripheral cell nuclear antigen (PCNA) is a nonhistone nuclear protein that is involved in the recruitment of protein machinery required for DNA synthesis [259], Studies have reported that the levels of PCNA are correlated with the mitotic activity and tumor grade in several forms of cancer [260]. In addition, the presence of aberrant levels of PCNA is associated with poor overall survival in patients with metastatic breast cancer [261]. Caveolae are plasma membrane invaginations that are believed to act as membrane organizing centres to sequester and organize intracellular signaling complexes [262].

Members of caveolin family (CAV1 and CAV2) have been implicated in basal-like breast cancer subtype [263]. Furthermore, high levels of caveolin expression was associated with poor prognosis in prostate [264] and lung cancers [265].

Receptor C-X-C chemokine receptor type 4 (CXCR4) is a G-protein couple receptor, first identified as a coreceptor for T-cell tropic isolates of human immunodeficiency virus [266]. The CXCR4 has a prognostic significance in metastatic breast cancer, in which the tumor cells migrate from the primary site of origin to distant organs such as lungs, lymph nodes and bones that secrete high levels of the chemokine ligand, CXCL12 [267]. In addition, high levels of CXCR4 expression in triple negative breast cancers (TNBC) is often associated with poor prognosis and disease-free survival when compared to the TNBCs with low levels of CXCR4 expression [268]. Forkhead protein P3 (Foxp3), is involved in the immune response and plays a vital role in the differentiation, development and function of the regulatory T cells [269]. It is generally expressed in the nucleus of epithelial cells in prostate, breast and lung. In breast epithelial cells, the prognostic relevance of Foxp3 is associated with its ability to represses the expression of HER2 relevance [270]. Failure of Foxp3 recruitment to nucleus results in its limitation to cytoplasm, which has a prognostic significance in metastatic breast cancers [271]. In addition, migratory breast cancer cells show diminished levels of nuclear Foxp3 with aberrant overexpression of CXCR4, thus favouring metastasis to site-specific organs rich in CXCL12 [272, 273]. The detection of high circulatory tumor cell (CTC) count in the blood of metastatic breast cancer patients is a significant negative prognostic factor and the treatment modalities are based on the CTC measurements [274]. In the future, CTC measurements may be used to predict the efficacy of treatment and acquired resistance upon initial exposure to therapy.

Despite the progress made in developing molecular targeted therapies against breast cancer, acquired resistance has always been a limiting factor in the effective management of the disease. Hence, there is a need for novel biomarker identification with a potential to offer tailored therapeutic interventions for breast cancer patients.

1.2.3c G3BP as a novel biomarker and therapeutic target

The Ras signaling pathway is activated in approximately 30% of all cancers, leading to tumor cell proliferation, survival and motility [275, 276]. Whilst, GTPase-activating proteins (GAPs) convert the active GTP-bound form of Ras to inactive GDP-bound form, guanine nucleotide exchange-factors (GEFs) mediate the conversion back to it active form [277]. Although the molecular switch between active and inactive forms is tightly regulated, several cancers have oncogenic Ras mutations that disrupt the activity of Ras protein [275, 276]. In contrast, mutations in Ras gene are rare in breast cancers [278]. Reports have indicated that aggressive forms of breast cancer have increased mitogenic activity mediated via EGFR/HER2/RAS pathway [279-282].

Since Ras-GTPase-activating protein (RasGAP), is a critical regulator of Ras signaling pathway, studies were undertaken to identify its binding partners. Parker *et al.,* [283] reported that RasGAP -SH3 domain binding protein (G3BP), interacts with the SH3 domain of RasGAP. Following that discovery, several reports [284-288] have indicated the overexpression of G3BP in various cancers, including breast cancer.

G3BP is an evolutionary conserved RNA binding protein [288-290]. It is a member of small family of three proteins, G3BP-1, G3BP-2a and G3BP-2b, which are encoded by two different genes present on human chromosome 5 and 4 respectively [291]. Whilst G3BP-1 is a polypeptide consisting of 466 amino acids, G3BP-2 exists in two spliced isoforms (G3BP-2a and G3BP-2b) with 482 and 449 amino acids respectively [291]. G3BP is organized into four domains (**Figure 1.8**). The N-terminus contains a nuclear transport factor 2 (NTF2)-like domain that mediates its nuclear localization and protein-protein interactions [292]. G3BP is predominantly a cytoplasmic protein, although, recombinant G3BP-2a lacking the NTF2-like domain was not reported in the nucleus, suggesting the role of the NTF-2 like domain in nuclear shuttling [293]. Furthermore, the NTF2-like domain is required for G3BP auto aggregation that mediates its recruitment into the specialized RNA granules termed stress granules (SGs) [294].

Both G3BP-1 and G3BP-2 contain an RNA Recognition Motif (RRM) and Arginine/Glycine rich (RGG) regions at their C-terminus, which are recognized as RNA binding domains [291]. The RGG domain is assumed to be an auxiliary domain of the RRM [291], which usually facilitates the RRM to interact with the target RNA and with other proteins. The central region of G3BPs contains a segment that is rich in acidic residues and proline-rich (PxxP) motifs. The PxxP motif shows a minimal consensus sequence required for interacting with the SH3 domain of the RasGAP. In contrast, it was reported that the NTF2-like domain interacts with the SH3 domain [291].

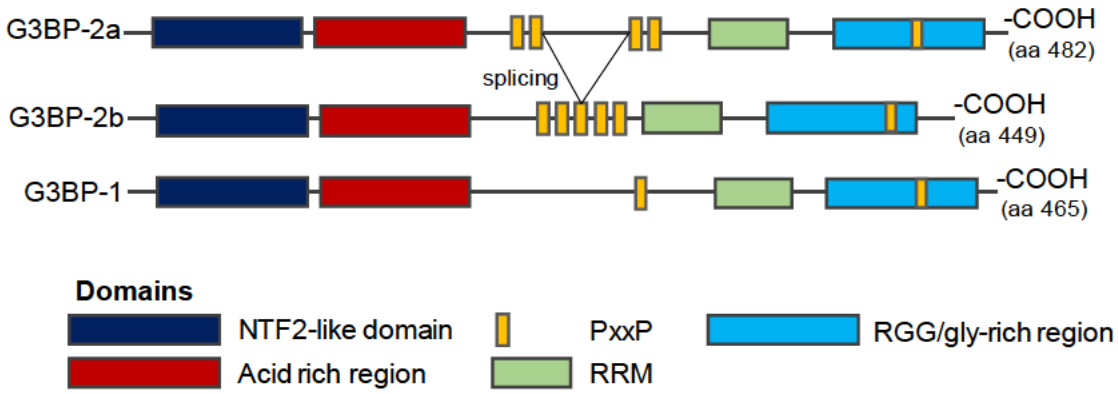

Figure 1.8: Schematic representation of the domain structure of G3BP family of proteins. G3BP consists of four domains. Nuclear transporter 2-like (NTF2-like) domain, RNA recognition motif (RRM) along with RGG/glycine-rich region, proline-rich (PxxP) region, and acid-rich region. Alternate splicing in G3BP-2a removes 33 amino acids to generate G3BP-2b. The figure was adapted from [291] and is presented here with permission of the corresponding author and the journal editor.

G3BP plays a role in the Ras signaling pathway [283, 287] through binding with RasGAP. Since RasGAP is known to function in the cytoskeletal reorganization and cell adhesion [295], G3BP may be indirectly implicated in cytoskeleton reassembly through its -SH3 domain binding function.

Zhang *et al.*, [296] have demonstrated that G3BP inhibited growth, migration and invasion of H1299 human lung carcinoma cells. In that study, siRNA mediated downregulation of G3BP had deleterious effects on the activity of ERK/MAPK mediated by reducing the phosphorylation of Src, Fak. Interestingly, downregulation of G3BP also decreased the levels of MMP-2, MMP-9 and plasminogen activator (uPA) [296]. Furthermore, G3BP downregulation also resulted in tumor regression of H1299 xenografts. Since MMP-2 and MMP-9 are important proteinases in metastasis, their regulation by G3BP emphasizes the role of G3BP in cancer metastasis.

Barnes *et al.*, [284] have reported that heregulin mediated activation of HER2 induced the expression of G3BP in SKBR3 breast cancer cells. In that study, HRG induced G3BP mRNA was significantly reduced upon pre-treatment with actinomycin D (inhibitor of transcription). However, cycloheximide induced translational inhibition showed no effect on the G3BP protein levels upon HRG stimulation in these cells. In addition, HRG treatment markedly increased the phosphorylation dependent ATPase activity of G3BP.

As an RNA binding protein, G3BP-1 plays a role in regulating the stability of mRNA transcripts [297, 298]. Gallouzi *et al.*, [297] have demonstrated that G3BP is hyperphosphoryated on serine residues, (particularly Ser149) upon serum deprivation of CCL39, Chinese hamster lung fibroblast cells. Furthermore, in this hyperphosphorylated state G3BP1 induced the cleavage of 3'-UTR (untranslated region) of *c-myc* mRNA. Dephophosporylation of G3BP-1 abolished its endoribonuclease activity. Hence, it was determined that the RNase activity of G3BP-1 was phosphorylation dependent. Furthermore, the hypophosphorylated state of G3BP-1 (lacking in the endoribonuclease activity) was assocatied with RasGAP in rapidly proliferating CCL39 cells. Consistent with these finding, Tourriere *et al.*, [298] demonstrated that G3BP-1 preferentially cleaves between cystosine and adenine bases within the 3'-UTR of the *c-myc* mRNA transcript. Such an activity was not reported in abnormal forms of G3BP-1 that lacked the ability for Ser149 phosphorylation.

The role of G3BP-1 in defining the Warburg phenotype was demonstrated by Ortego *et al.*, [288]. That study showed that G3BP-1 prevented the recruitment of β-F1-ATPase mRNA (catalytic subunit of the mitochondrial H^+-ATP synthase subunit β) to the 80S ribosomal site, thus inhibiting the translation of the ATP synthase mRNA.

In addition, G3BP-2 was reported to interact with inhibitory Iκβα [293]. Upon binding with G3BP-2, Iκβα does not exert inhibitory effect on nuclear factor kappa β (NF-κβ). As a result, NF-κβ translocates to the nucleus and induces transcription of the genes required for tumor survival and progression. G3BP is also implicated in stress granule (SG) formation [294, 299]. The SGs are dynamic cytoplasmic complexes formed in response to genotoxic stress [294] and consists of stalled translational initiation complexes. In response to genotoxic stress, G3BP-1 recruits target mRNAs to the SGs in a phosphorylation dependent manner [294]. The translation of the recruited mRNAs is temporarily aborted as an escape mechanism of the cell from the genotoxic stress. Upon cessation of the stress, the mRNAs may either be translated or degraded, depending on the cellular requirement.

Taken together, these studies implicate G3BP in several signaling pathways that provide a survival advantage to cancer cells. Importantly, its upregulation in HER2 cells may suggest a relevance of G3BP1 in HER2 subtype and qualify it as a potential biomarker for HER2 breast cancers.

1.2.4 Proteomic approaches for biomarker identification and drug discovery

The proteome of the cell consists of the entire set of proteins expressed by the genome that define the absolute functionality of the cell [300, 301]. Therefore, proteomic profiling is a promising tool for the discovery of cancer biomarkers and drug development [302, 303]. Conventional methods, including Western blot, ELISA, fluorescence-based immunoassays, and flow cytometry are employed for the detection and evaluation of protein biomarkers [304-307]. Over the last decade, more sophisticated techniques such as two-dimensional polyacrylamide gel electrophoresis (2D-PAGE) coupled with mass spectrometry, differential scanning fluorimetry (DFS), surface enhanced laser-desorption ionization-time of flight (SELDI-TOF) mass spectrometry, and X-ray crystallography are used in proteomic research [308-311]. Wulfkuhle *et al.,* [312] first reported the differential expression of fifty-seven proteins between the normal and malignant breast tissue. Several studies [309, 313-318] have reported candidate biomarkers for breast cancer. X-ray crystallography was employed to demonstrate the reactivation of mutant p53 by PRIMA-1 (p53 reactivation and induction of massive apoptosis) [319]. In a different study, Claus *et al.,* [320] employed DFS to demonstrate lapatinib (Lap)-induced thermal stabilisation of HER2 protein.

1.3 HER2/ErbB2-targeted therapy

Significant advances have been made towards targeting HER2/ErbB2-positive breast cancer. Owing to its role in breast cancer pathogenesis, and accessibility of the extracellular domain of the receptor, HER2 is a potential candidate for targeted antibody therapy.

1.3.1 Monoclonal antibody-based therapy for HER2-positive breast cancer

Trastuzumab (Herceptin), a humanized monoclonal antibody targeting HER2 receptor, entered clinical trials in the 1990s [212-214, 321]. Upon receptor binding, trastuzumab triggered internalization and degradation of HER2, by recruiting ubiquitin ligase c-Cbl [322]. Furthermore, through ADCC, trastuzumab functions to attract immune cells [323] to the tumor sites containing cells that overexpress HER2. Clynes *et al*., [324] have reported the targeting of trastuzumab coated HER2-positive tumor cells by natural killer cells via CD16-mediated cytotoxicity. In a different study, samples from patients with metastatic HER2-positive breast cancer revealed a significantly higher number of natural killer cells and cytotoxic proteins in tumor infiltrates as compared to the control group [325]. In addition, trastuzumab inhibits the PI3K/Akt and MAPK pathway by interfering with HER2 dimerization, thus blocking the receptor activation and Akt phosphorylation [326].

Whilst, several adjuvant chemotherapeutic regimens combined with trastuzumab have been studied, two of those regimens were preferred for the treatment of HER2-positive breast cancers [321, 327]. These regimens included adriamycin/cyclophosphamide-docetaxel (AC-T plus trastuzumab) and docetaxel/carboplatin plus trastuzumab (TCH) [321, 327]. The BCIRG-006 clinical study consisted of randomly assigned 3222 HER2-positive early-stage breast cancer patients receiving either AC-T, AC-T plus trastuzumab, or TCH [327]. The outcome of the study estimated disease-free survival rates at 5 years to be 75% for the AC-T group, 84% for the AC-T plus trastuzumab group, and 81% for the TCH group [327]. It was observed that the disease-free survival for the ACT-plus trastuzumab and TCH regimens were significantly higher than the AC-T. However, within the two trastuzumab regimens, significantly higher ($p < 0.001$) congestive heart failure and cardiac dysfunction were reported among the patients of the AC-T plus trastuzumab when compared with those in TCH regimen [327].

Therefore, the BCIRG-006 study favored the nonanthracycline TCH regimen over the AC-T plus trastuzumab group based on its lower risk of cardiotoxicity and leukaemia. To further investigate the therapeutic options for the treatment of higher-risk HER2 breast cancers, neoadjuvant therapeutic agents including pertuzumab and neratinib were explored with standard trastuzumab-containing regimens.

Whilst, pertuzumab is a monoclonal antibody that binds to the extracellular domain of HER2 and inhibits receptor dimerization [178, 321], neratinib, is an oral small-molecule RTK inhibitor of HER family of receptors [321, 328]. CLEOPATHRA (Clinical Evaluation of Pertuzumab and Trastuzumab) was a clinical trial that randomly assigned 808 patients with HER2-positive metastatic breast cancer to pertuzumab combined with trastuzumab/docetaxel (pertuzumab group), or trastuzumab/docetaxel alone (control group) [178]. The study revealed an overall survival of 57.1 months in the pertuzumab combined with trastuzumab/docetaxel and 40.8 months in the control group with an 8-year overall survival rates estimated to be 37% and 23% respectively [178, 329]. This study demonstrated that the combination therapy with the two antibodies significantly prolonged the overall survival with no increase in the cardiotoxicity. Although the adverse effects between the two groups during the treatment duration were generally balanced, febrile neutropenia and grade 3 diarrhea were higher in the pertuzumab group than in the corresponding control group [178]. Another clinical trial, KATHERINE, was designed to assess the therapeutic response to trastuzumab emtansine (T-DM1) in HER2-positive early breast cancer patients with residual invasive disease after neoadjuvant therapy. T-DM1 is an antibody-drug conjugate (ADC) of trastuzumab and emtansine (DM1), a microtubule inhibitor. The study involved 1486 randomly assigned patients who received either T-DM1 or trastuzumab [330]. The study revealed a significantly higher invasive disease-free survival at 3 years for the T-DM1 group over trastuzumab alone. It was estimated that 88.3% of patients in the T-DM1 group were free of invasive disease compared to a 77.0% in the trastuzumab group [330]. However, adverse effects including elevated levels of bilirubin, aspartate aminotransferase and alanine aminotransferase; thrombocytopenia, and peripheral sensory neuropathy were reported in 12.7% of the patients within the T-DM1 group as compared to an 8.1% of the control group [330].

Despite being effective, approximately 66-88% of HER2-positive breast cancer patients treated with trastuzumab alone and 20-50% of patients treated with trastuzumab in combination therapy become insensitive [331, 332]. Several mechanisms of resistance have been reported for trastuzumab insensitivity. The proteolysis of HER2 receptor generates a truncated p95HER2 isoform with constitutive kinase activity [333-335]. Scaltriti *et al.,* [335] have demonstrated that patients with metastatic breast cancer who are resistant to trastuzumab treatment acquired p95HER2 mutation, when compared to those with full-length HER2. Furthermore, overexpression of mucin-4 (O-glycosylated membrane protein) has been reported to mask the binding site of HER2 for trastuzumab [336]. Also, aberrant upregulation of RTKs, including insulin-like growth factor receptor (IGFR) [337] confers insensitivity to trastuzumab therapy. Lu *et al.,* [337] have shown that the downregulation of $p27^{Kip1}$ and $p21^{Cip1}$ with simultaneous upregulation of CDK2 activity may contribute to trastuzumab resistance in SKBR3 cells. A different study [338] observed the loss of function mutations in PTEN in ~36% of HER2-positive metastatic breast cancers that are resistant to trastuzumab therapy. Several studies [339, 340] have reported approximately 20-25% of PTEN inactivating mutations and ~25% of PI3KCA constitutive activation mutations in patients with trastuzumab resistant metastatic breast cancer. In addition, the inability of trastuzumab to penetrate through the blood-brain barrier [341] may limit its therapeutic value in treating the HER2 breast cancers that have brain metastasized.

Despite several advances in the treatment of HER2-positive breast cancers, there are notable limitations regarding the toxicities [321, 327, 342], metastasis [136, 138] and resistance [333-340] that pose additional challenges. In a quest to find novel therapeutic strategies for successful management of HER2-positive breast cancers, screening of ~3200 quinazoline and non-quinazoline compounds for potential RTK activity identified lapatinib (Lap) as a selective and potent ErbB1 and HER2/ErbB2 inhibitor [343, 344].

1.3.2 Lapatinib-based therapy against HER2-positive metastatic breast cancer

Lapatinib ditosylate (GW2016/GW572016, Tykerb) is a small-molecule RTK inhibitor of EGFR and HER2 that was approved in combination with capecitabine, for the treatment of HER2-metastatic breast cancers [151, 152]. Rusnak *et al.*, [152] have showed that Lap was effective in human tumor derived cell lines that overexpressed EGFR and HER2. In that study, the therapeutic efficiency of Lap was compared in two different breast cancer cell lines, BT474 (high levels of HER2/ErbB2 expression), and MCF7 or T47D (low expression of HER2). Findings of that study revealed a 30-40% fold difference in half maximal inhibitor concentration (IC_{50}) of Lap between the two cell lines.

Lap is a potent inhibitor of the RTK activity of both EGFR and HER2 in ErbB-driven breast cancers [152, 153]. Unlike trastuzumab, which binds to the extracellular domain of HER2, Lap elicits its antitumor activity by competing with ATP for ATP-binding pocket within the cytoplasmic domain of the RTK [345]. Binding of Lap inhibits receptor activation, thus abrogating the downstream mitogenic signaling via blocking the PI3K/Akt and Ras/MAPK pathways both *in vitro* and *in vivo* [152]. To further investigate the ErbB receptor selectivity of Lap, Zhang *et al.*, [346] have performed siRNA-mediated EGFR knockdown in HER2-overexpressing breast cancer cell lines, BT474 and SKBR3. In that study, it was demonstrated that the antitumor efficiency of Lap was independent of the EGFR status. This observation revealed that the antitumor activity of Lap relies on HER2 rather than EGFR. An independent study confirmed that Lap has higher affinity for HER2 over the EGFR monomers [347]. In contrast, the crystal structure of EGFR bound to Lap was found in an inactive-like conformation [345]. That study suggests that Lap may bind to the inactive form of EGFR, or it may induce receptor inactivation upon binding. Such an effect may have therapeutic significance in the antitumor activity of Lap as it reduces the rate of inhibitor dissociation from the receptor.

Clinical studies [335, 348-350] have reported that trastuzumab-resistant breast cancers were sensitive to Lap treatment. Importantly, potent suppression of tumor progression was observed in trastuzumab-resistant, p95HER2-expressing breast cancers [335, 348]. Furthermore, Lap significantly inhibited tumor activity in PTEN-null, trastuzumab-resistant cancers [350]. Notably, data obtained from 44 clinical studies revealed that Lap treatment of trastuzumab resistant breast cancers had lower rates of clinical cardiotoxicity, indicating its safe use [351]. A different study has reported the ability of Lap to sensitize multidrug resistance-associated protein 1 (MRP1)-overexpressing cells to conventional chemotherapy [352]. In that study, it was demonstrated that the transport function of ATP-binding cassette (ABC) was modulated by Lap thereby inhibiting the activity of MRP1, without altering the phosphorylation of Akt or ERK1/2 [352].

Being a small-molecule, Lap may have greater ability than trastuzumab (large sized monoclonal antibody) to cross the blood-brain barrier [341]. Preclinical evidence suggests that Lap treatment of BALB/c nude mice preinjected with ErbB2-overexpressing MDA-MB-231 demonstrated a significant decrease in the total number of large metastases in the brain as compared to the mice overexpressing ErbB1 alone [353, 354]. Furthermore, several clinical studies have demonstrated that Lap in combination with capecitabine was effective in reducing the tumor size in at least 20% of the patients with refractory brain metastasis [355-358].

Although Lap has significant therapeutic efficacy against trastuzumab-resistant breast cancers, acquired resistance is a serious concern. Several reports [359-363] have revealed Lap resistance in HER2 breast cancers. Comparison between the Lap-resistant (rBT474) and sensitive (BT474) breast cancer cell lines demonstrated a significant increase in the transcriptional activity and protein expression of FOXO3a and caveolin-1 of the ER signaling pathway in rBT474 cells [359]. Consistent with that report, Hedge *et al.*, [360] demonstrated an upregulation of ER and PR receptors in the Lap-resistant BT474 and T47D breast cancer cell lines. Higher incidence of HER2 mutations confer resistance to Lap treatment by inducing steric interference and reducing the conformational flexibility of the mutant HER2 to Lap [361].

Eichhorn *et al.*, [362] have reported that activating mutations in the PI3KCA gene in Lap-resistant BT474 breast cancer cells may be in part responsible for the Lap resistance. Overexpression of AXL, a membrane-bound RTK, has also been implicated in the Lap-resistance via its cross talk with hormone receptor and HER2 pathways [363]. In addition, Lap treatment is also reported to manifest common adverse effects including diarrhea, rash, nausea, arthralgia and fatigue [364, 365]. However, these adverse effects are effectively managed in routine clinical practice.

Given Lap's selectivity against ErbB1/ErbB2 receptors, and its low cardiotoxicity; Lap was tested in combination with either chemotherapy or non-chemotherapeutic agents for effective treatment of HER2-positive metastatic breast cancers. For example, Chu *et al.*, [366] demonstrated that breast cancer cell lines when treated with Lap in combination with tamoxifen had a synergetic effect in the inhibition of cell cycle progression. Such an effect was due to an upregulation of p27 expression along with a decrease in cyclin D1 and cyclin E-cdk2 activity [366]. A different study demonstrated that a combination therapy of Lap and fulvestrant had an additive effect on the growth inhibition of breast cancer cell lines by increasing the expression of p21 and p27 [342]. Furthermore, Lap in combination with paclitaxel resulted in a significant increase in the time to progression in patients with HER2-positive breast cancer, compared with paclitaxel alone [367]. Therefore, promising efficacy and safety profile of Lap has led to explore its combination with other chemotherapeutic agents such as, epirubicin, doxorubicin, docetaxel etc., for the treatment of HER2-positive breast cancer.

1.4 Doxorubicin as a front-line cytotoxic chemotherapeutic agent

Doxorubicin (Dox), also known as adriamycin, is a member of anthracycline family of antibiotics. It is used as a front-line chemotherapeutic agent in the treatment of wide range of malignancies, including breast cancer, osteosarcoma, Hodgkin's lymphoma, and leukaemia [368-371]. Upon intravenous infusion, Dox follows a triphasic plasma clearance, with a brief distribution half-life of 3-5 min, which indicates the drug's rapid uptake by cells [368-372]. Whilst, Dox is highly effective in penetrating tissues, the lipophilic nature of the molecule, together with its DNA intercalating ability, helps the drug to be retained inside the nucleated cells [368]. However, being highly effective in penetration, Dox does not readily diffuse through the blood-brain barrier [373, 374].

Doxorubicin acts by DNA intercalation [375, 376], inhibition of topoisomerase II [377, 378], and by the generation of free radicals [379-381]. Overall, Dox elicits a range of cytotoxic effects in conjunction with antiproliferation resulting in the DNA damage. Furthermore, Dox intercalates not only with nuclear DNA, but also with the mitochondrial DNA [382]. Intriguingly, the mode of action of Dox depends on the concentration of the drug, duration of the treatment, and specific form of cancer [379, 380, 383]. Several studies have demonstrated that Dox exerts its cytotoxic effects via different cellular pathways [24, 384-387].

Upon treatment of embryonic myocardial H9c2 rat cells, Dox activated ROS-dependent liver kinase B1 (LKB1), thereby upregulating AMP-activated protein kinase (AMPK) [388]. In the same study, it was demonstrated that AMPK activation induced p53-mediated apoptosis in B16 melanoma cells. Leung *et al.*, [385] have demonstrated that upon Dox treatment of MCF-7 breast cancer cells, there was a decrease in the Bcl-2 protein, whilst, the levels of Bax increased. In addition, an upregulation of p53 in these cells suggested the role of p53 pathway in modulating the levels of Bcl-2/Bax upon Dox treatment.

Interestingly, an increase in the expression of TGF β and related factors was observed upon Dox treatment of cultured mouse cardiac cells [389]. In that study, it was observed that Dox-induced cardiomyopathy was mediated through the upregulation of the TGF β pathway. Furthermore, an inhibitor of TGF β alleviated the deleterious effects caused by Dox in these cells [389]. Indeed, inactivating mutations in TGF β pathway enhance proliferation of cancer cells [390-392]. In addition, the ligands of TGF β pathway are known to be potent inducers of EMT in some cancers, thus inducing the metastatic potential in these cells. Overall, these studies may suggest an intriguing role of Dox in cancer metastasis through the modulation of TGF β pathway. Hsu *et al*., [393] reported that Dox treatment of human pluripotent stem cell-derived cardiomyocytes (hPSC-CMs), resulted in cardiotoxicity due to an upregulation of iNOS expression. Surprisingly, in a combination therapy of Lap and Dox, Lap potentiated the cardiotoxic effects of Dox in these cells. Whilst, treatment with iNOS inhibitor significantly reduced the cardiotoxicity, the anti-cancer potency of the combinational regimen was not compromised [393].

Interestingly, a combination of Lap and epirubicin (an epimer of Dox) has been tested in phase I clinical study, NCT00753207 to evaluate the safety and tolerability of fixed dose (1250 mg/day) of Lap when combined with increasing doses (75/80/90/100mg/m^2) of epirubicin to treat patients with HER2-positive/topoisomerase II-positive metastatic breast cancer [394]. The rationale for such a study was based on reports that indicated simultaneous amplification of topoisomerase II in approximately 1/3 of HER2-positive metastatic breast cancers [394, 395]. The study revealed that a combination of 1250 mg/day of Lap and 75mg/m^2 of epirubicin was relatively well tolerated and was considered for phase II trial [394].

Despite being the front-line drug of choice for breast cancer chemotherapy [396], Dox is commonly reported to induce dose-dependent cardiotoxicity [397, 398]. The deleterious effects of Dox on cardiac cells may be in part due to the upregulation of TGF β [389]. In addition, elevated levels of proinflammatory cytokines such as interleukin-1 (IL-1) and tumor necrosis factor α (TNF α) were reported in Dox treated mouse macrophages [399]. In addition, Dox-induced brain toxicity was mediated indirectly by activating the expression of inducible nitric oxide synthase (iNOS) via TNF α [400].

Although significant developments have been made in breast cancer treatment, clinical use of drugs is rather limited due to various factors including acquired resistance and/or toxicity. In this regard, novel combination therapy approaches may potentially circumvent the challenges to offer effective treatment modalities.

1.5 Combination therapies against cancer

Combination therapy is an effective treatment modality that combines therapeutic agents known to target different pathways within cancer cells [401, 402]. Such therapy offers potential advantages over single-agent therapy (monotherapy) in the treatment of cancers. Unlike monotherapy in which the tumor cells adapt themselves to overcome the therapeutic effect of a single agent (acquired resistance), simultaneous targeting of multiple pathways by combination therapy may render the cells more sensitive to treatment [401].

In addition, individual drugs in such combinations, may act in a synergistic or additive manner, thereby lowering the therapeutic dose of each drug required. Hence, the overall toxicity associated with the combination therapy is significantly reduced as compared to monotherapy. A study done by Khdair *et al.*, [403] revealed that Dox-resistant JC cells of mouse mammary adenocarcinoma overexpressed ATP-binding cassette (ABC) transporters to expel the drug out of the cells, thereby contributing towards chemoresistance. In that study, upon combination of Dox and methylene blue (in conjunction with photodynamic therapy), the cells became sensitive to Dox. Methylene blue along with photodynamic therapy in the combination, inhibited the activity of ABC transporters and enhanced the intracellular accumulation of Dox [403].

Matei *et al.*, [404] have demonstrated that the use of decitabine (hypomethylating agent) in combination with cisplatin reversed the epigenetic alterations in cisplatin-resistant ovarian cancers, thereby inducing chemosensitivity of cells to the therapeutic doses of cisplatin. In MCF-7 breast cancer cells, the use of carbonic anhydrase inhibitors in combination with sulforaphane, an anticancer drug, significantly enhanced the therapeutic potential of sulforaphane [405].

1.5.1 Combination therapies targeting HER2-positive breast cancer

Trastuzumab, pertuzumab, lapatinib, neratinib and T-DM1 are the anti-HER2 targeted agents approved by the United States Food and Drug Administration (U.S FDA) for the treatment of metastatic HER2-positive breast cancers (**Figure 1.9**) [323].

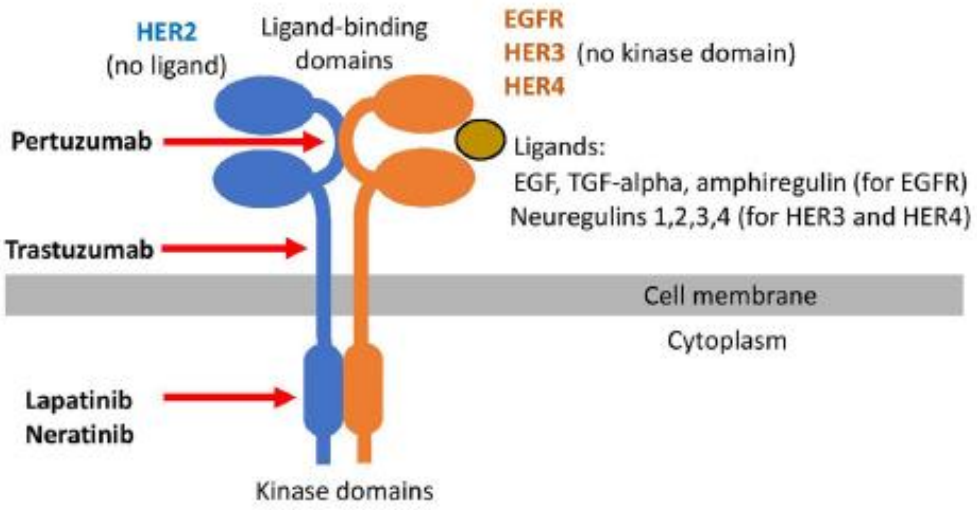

Figure 1.9: Illustration of the anti-HER2 targeted therapies. Trastuzumab binds to the extracellular domain of HER2 receptor. The binding site of the receptor for pertuzumab, within the extracellular domain of the receptor is different from trastuzumab binding site. Pertuzumab binding abrogates the HER2:HER3 dimerization. In contrast, lapatinib and neratinib are small-molecule RTK inhibitors that bind to the cytoplasmic domain of the receptor, thereby inhibiting the receptor mediated mitogenic signaling. The figure was adapted from [323] and is presented here with permission of the corresponding author and the journal editor.

Combination of trastuzumab and pertuzumab is currently the most potent combination therapy available to treat HER2-positive breast cancers [329]. Because combinations of trastuzumab and Lap have strong antitumor effect, the use of Lap as an adjunct to trastuzumab is usually considered in patients with brain metastasis [406, 407].

Whilst, trastuzumab cannot cross the blood-brain barrier [341], Lap diffuses into cells [354, 356-358, 408] and retains its antitumor activity in brain metastatic HER2-positive cancers. In high-risk HER2 breast cancers, neratinib (a small-molecule tyrosine kinase inhibitor) is used as an adjunct to trastuzumab to lower the risk of disease recurrence [328]. In addition, T-DM1 therapy offers trastuzumab mediated binding of ADC to HER2, thereby facilitating the release of maytansine from the complex to exert its antitumor activity in the cells [409, 410]. In addition, adjuvant chemotherapy regimens including AC-T plus trastuzumab and TCH demonstrated improved disease-free survival and overall survival for patients with HER2-positive BC, with disease free survival hazard ratios of 0.48 to 0.75 [327, 411, 412].

1.6 Project objectives

Despite significant advances in the diagnosis and treatment of breast cancer, the available therapies frequently fail due to the development of drug resistance. Hence, novel therapeutic targets are needed. There is substantial evidence that in breast cancers, the expression of G3BP and LDH-A are simultaneously upregulated. Interestingly, G3BP is found to regulate the expression of β-F1-ATPase. Collectively these evidences point to a critical question of whether G3BP regulates the expression of LDH-A. Although, G3BP has been studied widely as a breast cancer biomarker, efforts to target G3BP for cancer therapy are rather limited. Perhaps, anti-G3BP therapy may provide alternative treatment options for drug resistant breast cancers. Another challenge in breast cancer treatment is metastasis. Metastatic breast cancers including HER2-amplified and TN subtypes are often characterized by considerable cross-talk between the prooncogenic signaling pathways. In such cases, combination therapy that targets multiple pathways may be beneficial in tumor regression.

The project aimed to investigate the potential relevance of G3BP-1 as a breast cancer biomarker. In particular, the effect of G3BP on the regulation of LDH-A in breast cancer cell line was one of the objectives of the proposed study. In addition, the study also focussed on targeting G3BP-1 by Lap. Furthermore, use of combinational regimen of Lap and Dox to inhibit the migratory phenotypes and cell migration of Dox treated SKBR3 breast cancer cell line was also studied.

Chapter 2

General materials and methods

2.1 Materials

This section provides a list of materials used for performing various experiments described in the thesis. All the materials used are categorized into devices (**Table 2.1**), consumables (**Table 2.2**), reagents (**Table 2.3**), commercially available kits (**Table 2.4**), bacterial strains (**Table 2.5**), and antibodies (**Table 2.6**).

2.1.1 Devices used in the study

Information about the devices used to conduct experiments is mentioned in this section. **Table 2.1** provides a list of devices used and the corresponding manufacturers

Table 2.1. List of devices used in the study. The table provides a list of devices that were used to conduct experiments for the study.

Device	**Manufacturer**
Biorad VersaDoc imaging system	Bio-Rad Laboratories, Inc
Centrifuge 5810R	Eppendorf
CKX41 microscope	Olympus Life Science Solutions
Concentrator 5301	Eppendorf
Convertor oven	Sanyo Biomedical
Dry bath incubator	MS. Major Science
Dry block heater	Thermoline Scientific
Eclipse T*i*2-LAPP inverted microscope	Nikon
Freezer -20C	Westinghouse Electric
GEL Logic 200 imaging system	Kodak
Incubator shaker	Bioline Global Pty Ltd
Incu safe CO_2 incubator	Sanyo Biomedical
Inverter microwave oven	Panasonic Biomedical
Laboratory incubator	Thermoline Scientific
Laminar flow hood	Heraeus
Microcentrifuge 5424	Eppendorf
Nanodrop ND1000 spectrophotometer	Thermo Fisher Scientific
New Brunswick Innova 44 incubator shaker	Appendorf
Orbital shaker	Ratek Instruments Pty Ltd

PH meter	LabCHEM, Inc
Platform rocker	Bioline Global Pty Ltd
Precision electronic gram balance, TE1502S	Sartorius AG
Protein blotting apparatus	Bio-Rad Laboratories, Inc
Protein gel apparatus	Bio-Rad Laboratories, Inc
Powerpac 300	Bio-Rad Laboratories, Inc
Q-pod element	Millipore
Refrigerator	Fisher & Paykel, Westinghouse Electric
Revco high performance -80C freezer	Thermo Fisher Scientific
Synergy 2 multimode plate reader	Biotek Instrument, Inc
SpectraMax M3	Molecular Devices
Tomy high pressure steam sterilizer SX-500C	Alfa Medical Sterilizers
Veriti 96 well thermocycler	AB Applied Biosystems
Vortex mixer	Ratek Instruments Pty Ltd
V650 spectrophotometer	Jasco Analytical Instruments
Wisestir, magnetic stirrer with hot plate	Wisd Laboratory Instruments

2.1.2 Consumables used in the study

Information about the consumables used in the current study is provided in this section. **Table 2.2** provides information on the consumables used and their manufacturers.

Table 2.2. List of consumables used in the study. The table provides a general list of consumables that were used to conduct research.

Consumables	**Manufacturer**
Amicon-Ultra 15 centrifugal filters (MWCO 10,000)	Millipore
Conical flasks (250ml, and 1000ml)	Schott Duran® Pty. Ltd.
Falcon cell culture flasks (T25, and T75)	Corning Incorporated
96 well plates	Sarstedt Numbrecht Co.
Glass bottles (250ml, 500ml, and 1000ml)	Schott Duran® Pty. Ltd.
Immobilon-P transfer membrane	Millipore
Immobilon-Western chemiluminescent HRP substrate	Millipore
Measuring cylinders (100ml, 250ml and 1000ml)	Vitlab GmbH

Pipettes (p20, p200, p1000)	Gilson, Inc
Powder free latex gloves (medium)	Ansell Healthcare LLC
PLP100 petri plates	Techno Plas Pty. Ltd.
Reaction tubes (0.2ml, and 1.5ml)	QSP Quality Scientific Plastics, Inc.
Stripettes (5ml, 10ml and 50ml)	Corning Incorporated

2.1.3 Reagents used in the study

Information about the reagents used in this project has been provided in this section. **Table 2.3** provides information on the reagents used and their manufacturers.

Table 2.3. List of reagents used in the study. The table provides a list of general reagents that were used in the experiments.

Reagents	**Manufacturer**
Acridine Orange	Thermo Fisher Scientific
ActinGreen 488	Thermo Fisher Scientific
Ammonium persulfate	Chem-Supply Supplyline
Ampicillin	Sigma-Aldrich
Bromophenol blue	Aldrich Chemical Company, Inc
CellTiter 96 aqueous one solution reagent	Promega Co.
Complete mini EDTA-free tablets	Roche Diagnostics GmbH
DC Protein assay reagents	Bio-Rad Laboratories, Inc
D-Glucose anhydrous	Univar Pty Ltd
Dulbecco's modified eagle medium:nutrient mixture F12	Gibco Life Technologies
Dulbecco's phosphate buffer saline	Life Technologies
Dimethyl sulfoxide	Sigma-Aldrich
dNTP mix	Thermo Fisher Scientific
Ethylene diamine tetra acetic acid	Sigma-Aldrich
Fetal bovine serum	Gibco Life Technologies
HisPur Ni-NTA resin	Thermo Fisher Scientific
Imidazole ($\geq$ 99%)	Sigma-Aldrich
Isopropyl β-D-1 thiogalactopyranoside	Astral Scientific
Lapatinib	Sigma-Aldrich

Lipofectamine 2000	Invitrogen Thermo Fisher Scientific
MitoTracker Green FM	Thermo Fisher Scientific
Molecular grade agar	Oxoid Microbiology Products
Molecular grade agarose	Bio-Rad Laboratories, Inc
NucBlue Fixed CellReadyProbe	Thermo Fisher Scientific
Reduced serum medium (Opti-MEM)	Gibco Life Technologies
PageRuler plus prestained protein ladder	Thermo Fisher Scientific
Paraformaldehyde	Sigma-Aldrich
Penicillin/streptomycin	Gibco Life Technologies
Propidium Iodide	Thermo Fisher Scientific
Q5- HF DNA polymerase	New England Biolabs
Restriction enzymes and buffers	New England Biolabs
RIPA lysis and extraction buffer	Thermo Fisher Scientific
RNase-free DNase	Promega
Sodium dodecyl sulphate	Sigma-Aldrich
TEMED ($\geq$ 99%)	Sigma-Aldrich
Tris base	Amresco LLC
Tween -20	Sigma-Aldrich
Taq DNA polymerase	New England Biolabs
T4 DNA ligase	New England Biolabs
Trypsin	Gibco Life Technologies
Tryptone	Oxoid Microbiology Products
Yeast Extract	Oxoid Microbiology Products
30% Acrylamide/bis (29:1)	Bio-Rad Laboratories, Inc
1kb Plus DNA ladder	Invitrogen Thermo Fisher Scientific
10x Standard Taq. reaction buffer	New England Biolabs

2.1.4 Commercially available kits used in the study

Information about the molecular biology kits used in this project has been provided in this section. **Table 2.4** provides information on the commercially available kits used in this study.

Table 2.4. List of commercially available kits used in the study. The table provides a list of molecular biology kits used to conduct experiments.

Commercially Available Kits	Manufacturer
NucleoBond Xtra Midi Kit	Mackerey-Nagel
NucleoSpin Gel and PCR Clean-up Kit	Mackerey-Nagel
NucleoSpin Plasmid Kit	Mackerey-Nagel
QIA Quick Gel Extraction Kit	Qiagen
Quantitect RT Kit	Qiagen
RNeasy Mini Kit	Qiagen
SensiFAST Probe No-ROX One-Step kit	Bioline
DC protein assay kit	Bio-Rad Laboratories

2.1.5 Bacterial strains used in the study

Information about the chemically competent *E. coli* cells used for transformation along with the provider's details is mentioned in this section. **Table 2.5** provides a list of *E. coli* strains that were used in the experiments.

Table 2.5. List of bacterial strains used in the study. The table provides information on the chemically competent *E. coli* cells used in the transformation experiments.

***E. coli* strain**	**Genotype**	**Provider**
JM109	K strain containing recA- and endA- mutations.	Promega
BL21(DE3)	BL21(DE3) allows high-efficiency expression of protein(s) from gene(s) under the control of T7 promoter.	Promega

2.1.6 Antibodies used in the study

The antibodies used in this study have been listed in this section. **Table 2.6** provides information on various antibodies that were used for detection of the target protein(s) in this project.

Table 2.6. List of antibodies used in the study. The table provides information on the antibodies used in the current study.

Antibody	Description	Provider
Anti-6x His tag	Rabbit polyclonal anti-6x His	GeneTex
Anti-LDH-A	Rabbit polyclonal LDH-A	Abcam Plc
Anti-G3BP	Mouse monoclonal anti-G3BP	Abcam Plc
Anti-G3BP2	Rabbit polyclonal anti-G3BP2	Abcam Plc
Anti-PCNA	Rabbit monoclonal anti-PCNA	Cell Signaling Technology
Anti-β actin	Rabbit monoclonal anti--β actin	Sigma Aldrich
Anti-mouse IgG	Goat anti-mouse IgG	Invitrogen
Anti-rabbit IgG	Goat anti-rabbit IgG	Invitrogen

2.2 Methods

2.2.1 Cell lines and culture conditions

The human breast cancer cell lines including MCF-7, T47D, SKBR3, MDA-MB-435 cells, MDA-MB-231, and immortalized normal human mammary fibroblasts (HMF) were obtained from American Type Tissue Culture (ATCC, Manassas, VA, USA). The cells were cultured in T25 flasks at 37^{o}C in a humidified incubator inclusive of 5% CO_2 in DMEM/F12 with phenol red indicator supplemented with 10% fetal bovine serum (FBS) and 1% penicillin/streptomycin.

2.2.2 Transient transfection

MDA-MB-435 breast cancer cells were plated at a density of 3.5 x 10^4 cells per well in a six-well plate and incubated for 24 h. Next day, following the manufacturer's (Invitrogen) instructions the cells were transfected using lipofectamine2000. This method was followed for the transfection of the cells with target siRNA sequences along with the nontarget control sequence.

2.2.3 RNA Extraction and cDNA synthesis

After the cells were 80-85% confluent, they were trypsinized and harvested as a cell pellet by centrifugation at 3000 rpm/5 min. The cell pellet was collected, and total RNA was extracted following manufacturer's instructions (RNeasy minikit, Qiagen). Briefly, the harvested cell pellet was resuspended in RLT buffer (Qiagen) that supports the binding of RNA to the silica membrane. The lysate was briefly centrifuged at a maximum speed for 3 min at 4^{o}C.

Following the centrifugation, supernatant was removed, and equal volume of 70% ethanol was added to the lysate. The sample was then loaded on the RNeasy mini spin column placed in a collection tube and centrifuged 15 sec at ≥8000 x g. The flow-through was discarded and 700µl of wash buffer was added to the spin column and centrifuged briefly to wash the RNA bound to the silica membrane of the spin column. In the next step, the RNeasy column was placed in a collection tube and 30-50µl of RNase-free water was added to the membrane and centrifuged for 1 min at ≥8000 x g to elute the RNA. The RNA yield was estimated by NanoDrop ND 1000 spectrophotometer.

Following RNA extraction, cDNA synthesis was performed as per the manufacturer's instructions (QuantiTect reverse transcription kit, Qiagen). Briefly, genomic DNA (gDNA) elimination reaction was prepared on ice with template RNA, gDNA wipeout buffer (Qiagen), and RNase-free water. Following its incubation, the elimination reaction (template RNA with gDNA wipeout buffer) was added to the reverse-transcription master mix reaction and incubated for 15 min at 42^{o}C to allow cDNA synthesis. Further incubation at 95^{o}C for 3 min inactivated quantiscript reverse transcriptase enzyme. The synthesized cDNA was stored at 20^{o}C until use.

2.2.4 Polymerase chain reaction (PCR)

To ensure high specificity of the PCR product, optimization of the PCR protocol was done for each template/primer pair to determine appropriate annealing temperature and volume of the cDNA to be used. Optimization was done with gradient temperatures slightly above and below the expected annealing temperature of the primer pairs. The primers that bind to the template at the highest temperature are least-permissive for unspecific annealing. Thus, the first amplicons are those with highest primer specificity, which in most cases cover the region of interest. In general, 50µl PCR reaction mix consisted of 1-5µl of cDNA (not to exceed 10% of the final PCR reaction volume), 200µM dNTP mix, 0.5µM of each forward and reverse primer, 1/5th volume of 5x Q5 high fidelity reaction buffer including $MgCl_2$ as well as 0.02U/µl of Q5 high-fidelity DNA polymerase. The reaction mix was prepared on ice. The PCR was performed in a Veriti 96-well thermocycler. Presence and specificity of the amplicon(s) was confirmed by subjecting 10µl of the reaction mix to agarose gel electrophoresis (0.9% and 1.5% agarose respectively, TAE). The PCR clean-up (using NucleoSpin Gel and PCR clean-up kit) was done for the remaining DNA.

2.2.5 Determination of DNA concentration and purity

To determine the concentration of the purified DNA after clean-up, the optical density (OD) was measured at 260nm and 280nm using the NanoDrop ND 1000 spectrophotometer. The concentration was calculated as 1 unit of OD_{260} equaling 50µg/ml double-stranded DNA or 40µg/ml RNA, respectively. The purity of the product was determined by a ratio of (OD_{260}/OD_{280}). For a pure DNA sample OD_{260}/OD_{280} corresponds to 1.8.

2.2.6 Restriction enzyme digestion

Restriction enzymes used in this study included NdeI, HindIII, and NcoI. Appropriate volumes of the insert (G3BP-1, and/or G3BP-2), and the vector (pRSETC), corresponding to 1.0-2.0µg were used to set up the digestion(s). Typical reaction mixtures consisted of 1.0-2.0µg of the DNA, $1/10^{th}$ volume for each of the recommended 10x reaction buffer, 1mg/ml bovine serum albumin (BSA), 10U of the appropriate restriction enzyme and DNase-free water in a total volume of 50µl. The restriction reaction mixture was incubated for 2 h at 37^oC.

2.2.7 Agarose gel electrophoresis

Agarose gel electrophoresis was performed to analyse either PCR amplicons or the products of restriction digestion. A small volume of the reaction mixture (10µl) was run on a 0.9-1.5% (weight/volume) of non-denaturating agarose gel in 1% TAE (40mM Tris-HCl, 20mM acetic acid, and 1mM EDTA, pH 8.0) buffer at 100V for 1 h. DNA was visualized by addition of 1µg/ml of ethidium bromide to the gel(s) and analysed by GEL Logic 200 imaging system.

2.2.8 Ligation of the DNA fragments

To ligate the digested vector and insert, 50ng of the vector DNA was mixed with a 3:1 molar ratio of (each) insert DNA, 400U of T4 DNA ligase and $1/10^{th}$ volume of the 10x T4 ligase reaction buffer in a total volume of 20µl. The reaction was incubated at 4^oC for 16 h. A small volume (4.0µl) of the ligation mixture was used to transform the chemically competent *E.coli* cells.

2.2.9 Transformation of chemically competent *E. coli* cells

Competent JM109 *E. coli* cells were thawed on ice. After the cells were thawed, 50ng of DNA (in a volume not greater than 10µl) was added per 100µl of the competent cells and mixed. The tubes were left on ice for 10 min. The cells were subjected to heat shock at 42^{o}C for 45-50 sec in a water bath. Following heat shock the cells were put on ice for 2 min. A volume of 200µl of luria-bertani (LB) (10g tryptone, 5g NaCl, and 5g yeast extract per litre; pH 7.5) broth was added to the heat shock cells and incubated at 37^{o}C with shaking at 225 rpm for 2 h. The cells were plated onto LB agar plate(s) (15g/l) containing ampicillin (100mg/ml) and incubated at 37^{o}C overnight. The next day, only the transformed *E.coli* cells that were ampicillin-resistant, formed colonies on the antibiotic-selective LB agar plates.

2.2.10 Miniprep of the plasmid DNA

Single, transformed JM109 *E. coli* colonies were picked from the agar plate and inoculated into 5ml of LB broth with ampicillin and grown overnight at 37^{o}C and 225 rpm. Following growth, the bacterial cultures were centrifuged 4000 rpm at 4^{o}C to obtain the pellet. Miniprep(s) of the plasmid DNA were done according to the manufacturer's instructions (NucleoSpin Plasmid kit, Mackerey-Nagel). Briefly, 5ml of the overnight *E.coli* LB culture was harvested as a cell pellet by centrifuging 30 sec at ≥11,000 x g. The cell pellet was resuspended in an appropriate volume of lysis buffer and incubated for 5min. The lysate was centrifuged 5 min at ≥11,000 x g to separate the supernatant from the cell debris. The supernatant was decanted onto a nucleospin plasmid column consisting of a silica membrane that allows high DNA binding capacity. Following this, the column was washed with ethanolic buffer and air-dried. DNase-free water was added to a volume of 30µl to the column and DNA was eluted by centrifuging 1 min at ≥11,000 x g. Quantification of the DNA was achieved as previously described in section 2.2.5.

2.2.11 DNA sequencing

The accuracy of the generated constructs was confirmed by Griffith University DNA sequencing facility, Nathan campus, QLD. BDT v3.1 (Big Dye Terminator) was used to set-up the sequencing reaction. DNA sequencing reaction was set up with 300ng of the plasmid DNA in a total reaction volume of 20µl containing 3.2 picomoles of the primer, 1/5th volume of the recommended 5x sequencing buffer, 4µl of the BDT v3.1 dye.

DNA sequencing PCR reaction conditions included initial denaturation at 96ºC for 1 min, denaturation at 96ºC for 10 sec, annealing at 50ºC for 5 sec, and extension at 60ºC for 4 min. Denaturation and annealing steps were repeated for 25-30 times and at the end of the PCR reaction the sample was stored at 4ºC. Following the sequencing PCR reaction, clean-up of the DNA was achieved by the conventional ethanol/sodium acetate precipitation and the DNA pellet was dried. The sample was then sent for DNA sequencing facility for sequence analysis. The DNA sequencing results were analysed using chromas software (https://technelysium.com.au/wp) and clustalW (www.genome.jp/tools-bin/clustalw).

2.2.12 Recombinant protein expression

For heterologous protein expression, BL21(DE3) *E. coli* cells were used. Transformation was done as previously described in section 2.2.9. Following transformation, single isolated colonies were inoculated into 5ml of the LB-broth culture with ampicillin at 37ºC/225 rpm. Next day, 1ml of the overnight culture was inoculated into 100ml of LB-broth containing ampicillin (100mg/ml). The culture was grown at 37ºC/225 rpm and OD_{600} was monitored until it reached 0.66. Once the OD_{600} was 0.66, the culture was induced with isopropyl-β-D-thiogalactoside (IPTG) at a final concentration of 1mM and expression was achieved at room temperature unless otherwise indicated. Following IPTG induction, samples were collected at 4 h, 8 h and overnight to monitor the protein yield over the time-course.

After protein expression, the cultures were centrifuged 20 min ≥ 4,000 rpm and the pellet was stored at -20ºC. The cell pellet was suspended in the lysis buffer [(50mM Tris-HCl, 250mM NaCl, 10% glycerol, 1% Triton X-100, 1mM PMSF, mini EDTA-free protease inhibitor tablets, one table for every 10ml of buffer), RNase-free DNase (1U/µl)]. The resuspended pellet was incubated at 4ºC for 2 h to ensure the pellet was completely resuspended in the lysis buffer. Following resuspension, the lysate was sonicated to shear DNA until the turbidity resembled that of a clear protein solution. The sonicated lysate was centrifuged 45 min ≥15,000 x g at 4ºC to separate the soluble and insoluble fractions. Since the recombinant protein(s) carry N-terminal $his_{(6)}$-tag, protein expression was verified by Western blot analysis using anti-6x His tag antibody (Genetex).

2.2.13 Polyacrylamide gel electrophoresis

Protein(s) samples were prepared for sodium dodecyl sulphate-polyacrylamide gel (SDS-PAGE) analysis. SDA-PAGE electrophoresis allows the protein(s) to be separated by size under denaturating conditions. Equal volumes for each protein sample were loaded on a 10-12.5% gels, depending on the size of the protein. **Table 2.7** provides recipe for preparing 10 and 12.5% polyacrylamide gels.

Table 2.7: Recipe for preparing denaturating polyacrylamide gels. Protocol was making 10 and 12.5% SDS-polyacrylamide gels.

Component	**Resolving gel**		**Stacking gel**
Gel Percentage	10%	12.5%	6%
Water	3.20ml	2.50ml	2.60ml
30% Acrylamide/bis (29:1)	2.67ml	3.33ml	1.00ml
1.5M Tris pH 8.8 (resolving gel)/ 0.5M Tris pH 6.8 (stacking gel)	2.00ml	2.00ml	1.25ml
10% SDS	80µl	80µl	50µl
10% Ammonium persulfate (APS)	80µl	80µl	50µl
Tetramethylethylenediamine (TEMED)	8µl	8µl	5µl

Polyacrylamide gels were prepared as per the recipe outlined in **Table 2.7** and poured into a Mini-PROTEAN 3-gel system (Bio-Rad Laboratories). The gel was set to polymerize for about 45 min. Prior to loading, the protein samples were denatured by heating at 95^{o}C for 5 min. SDS-PAGE electrophoresis was performed in 1x SDS-running buffer (25mM Tris, 1% SDS, 200mM glycine) at 100V until adequate separation was achieved. Prestained protein ladder (a mixture of purified prestained proteins with a wide range of molecular weights from 10 to 250-kDa) of 3µl volume was loaded alongside the samples to estimate the molecular weight(s) of the proteins in consideration. Following SDS-PAGE, the gel was either stained with Commassie dye, or the protein(s) were detected by Western blot as described in section 2.2.14.

2.2.14 Western blot

Following separation by SDS-PAGE, proteins were transferred from the gel onto Immobilin-P transfer membrane (Millipore). Electroblotting was performed at 100V for 180 min at 4^{o}C in a mini trans-blot electrophoretic transfer cell (Bio-Rad Laboratories), using 1x transfer buffer (25mM Tris, 200mM glycine, 20% methanol).

Prior to the transfer, membrane was activated by briefly soaking in 100% methanol, followed by its equilibration in transfer buffer for 5 min. Following the transfer of proteins, the membrane was blocked in 5% skim milk/TBS-T [(150mM NaCl, 10mM Tris-HCl (pH 8.0), 0.05% Tween-20)] for 1 h at 25^{o}C to saturate unspecific protein binding sites. Detection of the target protein(s) was achieved by incubating the membrane with specific antibodies (1/500-1/4,000 dilution) in 5% skim-milk/TBS-T at 4^{o}C overnight. Next day, the membrane was washed three times with TBS-T to remove unbound antibody. Following the washes, membrane was incubated with HRP-conjugated secondary antibody (1/2,000 dilution) in 5% skim-milk/TBS-T for 1 h at 25^{o}C. After three washes with TBS-T, the target protein(s) were visualized using Immobilon-western chemiluminescent horseradish peroxidase (HRP) substrate detection kit (Millipore), with a ChemiDoc MP Imaging System (Bio-Rad Laboratories).

2.2.15 Recombinant protein purification

Since the recombinant protein(s) carry N-terminal $his_{(6)}$-affinity tag HisPur Ni-NTA resin (Thermo Fisher Scientific) was used for protein purification. The resin was composed of nickel-charged nitrilotriacetic acid (NTA) chelate immobilized onto 6% crosslinked agarose. Approximately 4ml of the resin (Ni-NTA resin has a binding capacity of $\leq$60mg of a 28-kDa $his_{(6)}$-tag protein/ml of the resin) was used to purify the recombinant protein from a litre culture. After the column was settled, the storage buffer (50% slurry in 20% ethanol) was drained from the resin and the protein sample was prepared by mixing the protein extract with an equal volume of the equilibration buffer (50mM Tris-HCl, 250mM NaCl, and 10mM imidazole, pH 7.4). Equilibration of the column was performed with two resin-bed volumes of the equilibration buffer. Following equilibration, the protein lysate was loaded onto the column. The flow-through that contained proteins (other than the protein of interest) was collected.

The column was then washed with three resin-bed volumes of wash buffer (50mM Tris-HCl, 250mM NaCl, and 25mM imidazole, pH 7.4) to ensure that all the lysate was washed form the column leaving only the recombinant protein bound to the column. The final step involved the elution of the recombinant protein with elution buffer (50mM Tris-HCl, 250mM NaCl, and 50-500mM imidazole, pH 7.4). Gradient elution with increasing concentration(s) of imidazole was analysed to determine the optimum concentration of imidazole for protein elution. Three fractions were collected for each imidazole concentration during gradient elution. Once the elution was completed, equal volumes of flow-through, wash, and elution fractions were run on SDS-PAGE and stained with Commassie to determine the imidazole concentration for elution and the quality of the purified protein.

2.2.16 Determination of protein concentration

Protein concentration was determined using a DC protein assay kit (Bio-Rad Laboratories). Manufacturer's instructions were followed to determine the concentration of the protein using a 96-well multimode plate reader (Biotek Instruments). The concentration of the protein (analyte) was determined in mg/ml by comparison to a BSA standard curve established using serial dilutions of the BSA and measuring the absorbance at 750nm.

2.2.17 Densitometric analysis

The immunoblot data was analysed using Quantity One software (Bio-Rad Laboratories) to study the relative intensity of the normalized target protein band(s) by comparison to their control(s). Prior to analysis, normalization of the target band(s) was performed against actin that was used as an internal loading control. A volume rectangle toolbox was created around the target band and its corresponding actin control. The volume analysis report was generated to show the values for the protein expression densities for the target protein and its corresponding actin control. The density values of the protein(s) were normalized to that of the related actin controls. The normalized values that were obtained for each of the target(s) were compared to the respective experimental controls.

2.2.18 Statistical analysis

Each assay was performed in triplicate and independently repeated at least three times. Data are represented as mean values ± SD (standard deviation). Statistical analysis was performed using Graphpad Prism 6 software (San Diego, CA, USA). Student t-tests or one-way analysis of variance (ANOVA), followed by a Bonferroni test (unless otherwise stated) were performed. All statistical analysis was performed at $p < 0.05$ level of significance.

Chapter 3

The role of G3BP in the regulation of LDH-A in breast cancer cells

3.1 Introduction

Breast cancer, a complex heterogenous disease, is the second most prevalent cancer worldwide after lung cancer and is the major cause of cancer-related deaths among women [1, 413]. The complexity of breast cancer is due to the mutations in the genes that regulate several mitogenic pathways including PI3k/Akt, Ras/MAPK, pRb/E2F and TP53 signaling [199-201, 414, 415]. Furthermore, the heterogeneity of the disease is characterized by the distinct receptor status including ER/PR, HER2, or TN breast tumors [115, 321] as noted by IHC analysis. These differences have served as the basis for making clinical decisions pertaining to the specific treatment modalities for management of the disease. Although significant advances have been made in the development of targeted therapies, breast cancer remains a huge challenge with poor prognosis and high mortality.

Breast cancer, like all other cancers, is characterized by dysregulated bioenergetic metabolism [58, 416]. The propensity of cancer cells to convert glucose to lactate through aerobic glycolysis (the Warburg effect) is critical for cancer cell survival and tumor progression [60-64]. As a result of this metabolic switch, there is reduced usage of the mitochondrial respiratory chain. Such an adaptation leads to a lower production of ROS by mitochondria, which enables the cancer cells to evade apoptosis [66, 67]. The observed alteration in the metabolic pathway is mediated by an upregulation of glycolytic enzymes, including LDH-A that catalyses the conversion of pyruvate to lactate coupled with the regeneration of NAD^+ [74, 75]. Different studies [417, 418] have demonstrated an upregulation of LDH-A in breast cancers. Hou *et al.*, [417] have demonstrated that low doses of taxol resulted in the upregulation of LDH-A in breast cancer cell lines including BT474, MCF-7, SKBR3 and MDA-MB-231. In addition, the study also showed an increase in the glycolytic flux upon taxol treatment. In the same study, it was demonstrated that taxol resistant MCF-7 cells were characterised by a significant upregulation of LDH-A. Hence, it was suggested that altered glycolytic switch via upregulation of LDH-A enabled the survival and progression of the taxol resistant MCF-7 cells. A different study by Van Poznak *et al.*, [419] has demonstrated that oral treatment with gossypol, an inhibitor of LDH-A, resulted in the tumor regression in patients with refractory metastatic breast cancers.

In another study, an overexpression of HER2 in the breast cancer cell lines including MCF-7/HER2 and MDA-MB-435/HER2 upregulated the levels of LDH-A [81]. In that study, inhibition of glycolysis by 2-deoxyglucose (2-DG) and oxamate demonstrated a stronger inhibitory effect in MCF-7/HER2 and MDA-MB-435/HER2 cells compared to the corresponding MCF-7 and MDA-MB-435 neo cells that expressed lower levels of HER2. Several lines of evidence suggest that upregulation of LDH-A is correlated with the metastatic ability of cancers [102-104, 420, 421].

There is substantial evidence that G3BP family of proteins, consisting of G3BP-1 and G3BP-2, are overexpressed in human cancers, especially in breast, head and neck, colon and lung cancers [283-288]. G3BP is implicated in a variety of mitogenic signaling pathways in carcinogenesis and metastasis, including NF-κβ [293], Ras-signaling [283, 287], and the ubiquitin proteasome system [422-424]. Zhang *et al.,* [296] have demonstrated that the downregulation of G3BP-1 in H1299 human lung carcinoma cells significantly decrease the levels of MMP-2 and MMP-9. It has been reported that G3BP-2 interacts with inhibitory Iκβα, to enable the induction of NF-κβ mediated transcription of genes that regulate tumor survival and progression [293]. Interestingly, Barnes *et al*., [284] have demonstrated that HRG stimulation of HER2-amplified SKBR3 breast cancer cells induced the expression of G3BP-1. Taken together with other studies, it may be deduced that there is a simultaneous overexpression of G3BP-1 and LDH-A in breast cancers. However, the mechanistic link between the overexpression of G3BP-1 and the glycolytic shift is poorly understood.

Ortega *et al*., [288] have demonstrated a potential role of G3BP-1 in defining the Warburg phenotype in breast cancer cells. In that study, it was shown that G3BP-1 inhibits the translation of β-F1-ATPase mRNA by interacting with it. The β-F1-ATPase is a mitochondrial complex V subunit that is involved in the synthesis of ATP molecules via oxidative phosphorylation [288]. Downregulation of β-F1-ATPase may result in the reduced oxidative phosphorylation activity to favour enhanced glycolysis in cancers [425]. Hence, the role of G3BP-1 may be implicated in the energy generation pathway. **Figure 3.1** illustrates the altered bioenergetic metabolism in cancers with an implication of G3BP-1 in the glycolytic flux.

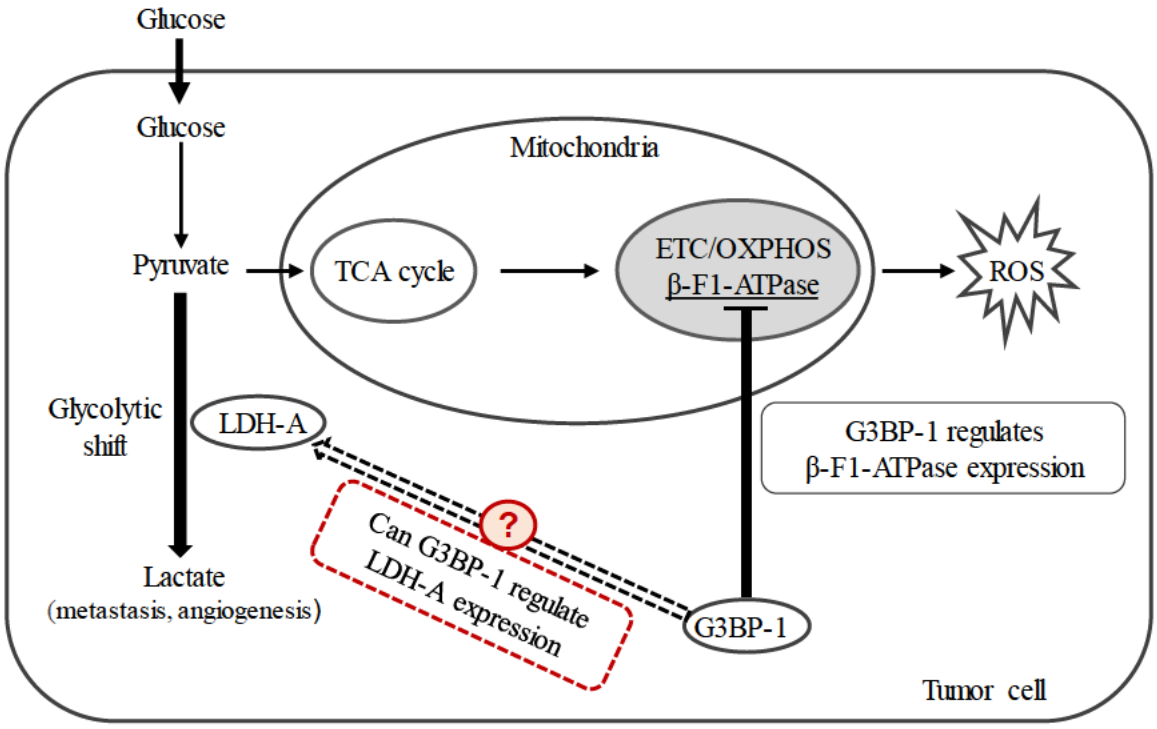

Figure 3.1: Implications of G3BP-1 in the glycolytic shift in cancers. Alteration to glucose metabolism involve the conversion of pyruvate to lactate catalysed by LDH-A. A glycolytic shift leads to reduced mitochondrial oxidative phosphorylation activity, thereby enabling cancer cells to reduce the levels of reactive oxygen species. G3BP-1 inhibits the translation of β-F1-ATPase mRNA. The potential role of G3BP-1 in the regulation of LDH-A expression was investigated. ETC=electron transport chain, LDH-A=lactate dehydrogenase-A, OXPHOS=oxidative phosphorylation, ROS=reactive oxygen species, TCA=tricarboxylic acid.

Lapatinib, a small molecule tyrosine kinase inhibitor, is widely used in the treatment of breast cancers that overexpress EGFR and HER2 [151-153]. Whilst Lap is effective in blocking the RTK activity of HER2, it also impacts the metabolic status of cancer cells [426, 427]. Although Lap treatment may result in HER2 inhibition, its role in regulating the activation of LDH-A may be indirect. Jin *et al.,* [426] have demonstrated that targeting HER2 or Src attenuated LDH-A activity, anoikis resistance and metastatic potential in breast cancer, and head and neck cancer cells.

In that study, it was demonstrated that phosphorylation of LDH-A at tyrosine 10 (Y10) by upstream kinases, such as, HER2 and Src enhanced cancer cell invasion, and tumor metastasis. In the same study, it was shown that Lap-mediated inhibition of HER2 caused a significant decrease in the levels of Y10-phosphorylated LDH-A in HER2-positive SKBR3 and BT474 breast cancer cells. Similarly, saracatinib (Src inhibitor) treatment of MDA-MB-231 (HER2-negative), and UM-SCC1 (head and neck squamous carcinoma) cells decreased LDH-A Y10 phosphorylation [426]. It was also observed that the drug treatment sensitized cells to anoikis induction and inhibited their migratory potential. In a different study, it was observed that the cell proliferation of MDA-MB-231 and SKBR3 breast cancer cells was inhibited by Lap via its regulation of pyruvate kinase type M2 (PKM2) expression [427]. In the glycolytic pathway, PKM2 catalyzes the irreversible conversion of phosphoenol pyruvate (PEP) to pyruvate along with the production of an ATP molecule [428]. It has been reported that the serum levels of PKM2 are elevated in several forms of cancer, including breast [429], colon [430], lung, and cervical cancers [431]. Interestingly, upregulation of PKM2 is associated with hypoxic adaptation in cancer cells [432]. The induced hypoxic condition results in the stabilization of HIF-1, which results in the transcription of genes including LDH-A, GLUT1, GLUT3 and hexokinase [428]. Guan *et al.*, [427] have demonstrated that Lap treatment of MDA-MB-231 and SKBR3 breast cancer cells induced downregulation of PKM2 through its inhibition of EGFR and HER2 respectively. Collectively, these evidences suggest the role of Lap in the metabolic status of cancer cells. Interestingly, both G3BP-1 [283-288] and LDH-A [417, 418] are overexpressed in breast cancer and have been implicated in the glycolytic shift [74, 75, 288] observed in breast tumor cells. Therefore, a potential effect of Lap treatment on the expression of G3BP-1 was investigated.

The experiments in this chapter were designed to (a) assess the protein levels of G3BP-1 and LDH-A in different breast cancer cell lines (representative of distinct molecular subtypes based on the receptor status) with a view to interrogate these markers as clear targets in breast cancer (b) determine the effect of G3BP knockdown on the regulation of LDH-A expression at both transcription and translation levels in MDA-MB-435 breast cancer cell line and (c) extend the study to investigate the effect of Lap on the protein levels of G3BP-1 and LDH-A in a panel of breast cancer cell lines used in this study.

3.2 Materials and Methods

3.2.1 Cell culture and reagents

Human breast cancer cell line, MDA. MB435 cells were cultured in DMEM/F-12 (Gibco, Life Technologies) supplemented with 10% FBS (Gibco, Life Technologies) and penicillin/streptomycin (Gibco, Life Technologies).

The small interfering RNA (siRNA) sequences for targeting G3BP-1, and G3BP-2 were synthesized by Dharmacon Inc., (Colorado, USA). **Table 3.1** provides the details of siRNA sequences used in this study.

Table 3.1: Target siRNA sequences for G3BP-1, G3BP-2 and nontargeting control. Table provides information on the siRNA sequences used in this study to knockdown G3BP-1 and G3BP-2.

Target Gene	siRNA	Target sequence
G3BP-1	SiGENOME SMART pool siRNA D-012099-18	GUGCGAGAACAACGAAUAA
G3BP-2	SiGENOME SMART pool siRNA D-015329-02	GGAAGUACGUUUAAAUGUG
Nontargeting control	siGENOME non-targeting siRNA D-001206-14	UAAGGCUAUGAAGAGAUAC

3.2.2 siRNA transfection

MDA-MB-435 breast cancer cells were plated at a density of 3.5 x 10^4 cells per well in a six-well plate and incubated for 24 h. Next day, the cells were transfected with siRNA(s) for the target gene(s) including G3BP-1, G3BP-2 and nontargeting siRNA using lipofectamine 2000 (Invitrogen).

Following the manufacturer's instructions, lipofectamine was diluted to 1/4th volume in Opti-MEM (reduced serum medium; a modification of Eagle's minimum essential medium; Gibco, Life Technologies). Similarly, siRNA was diluted to a concentration of 50nM in Opti-MEM. Equal volumes of the diluted siRNA and lipofectamine reagent were mixed and the siRNA:lipofectamine complex was incubated at 25^{o}C for 5 min. Following the incubation, the complex was added to the cells. The siRNA transfected cells were further incubated for 96 h before extracting the protein or mRNA for analysing the efficiency of knockdown.

3.2.3 Western blot

Whole-cell lysates were used for immunoblotting. Briefly, the cells were washed with cold phosphate-buffered saline (PBS) and then lysed with RIPA lysis buffer (Thermo Fisher Scientific). The protein concentrations were determined using the DC protein assay kit (Bio-Rad Laboratories) as previously described in section 2.2.16. Equal amounts of the protein samples were run on SDS-PAGE. Following the separation, proteins were transferred to Immobilin-P transfer membranes (Millipore). Western blot was performed as described in section 2.2.14. The primary antibodies used in this study included anti-G3BP, anti-G3BP-2, anti-LDH-A (Abcam Plc), and anti-β-actin (Sigma-Aldrich). HRP-conjugated secondary antibodies were purchased from Invitrogen.

3.2.4 Quantification of mRNA by qRT-PCR

Following 96 h transfection with siRNA targeting G3BP-1, G3BP-2, and nontargeting siRNA, the total RNA was isolated from MDA-MB-435 cells as described previously in section 2.2.3 using RNeasy Mini Kit (Qiagen). Quantitative real time PCR (qRT-PCR) was performed using SensiFAST Probe No-ROX One-Step kit (Bioline). **Table 3.2** provides information on the primers used for qRT-PCR. All samples were processed in rotor gene 6000 real-time PCR machine (Corbett Research). The cycling program was 45^{o}C for 10 min, followed by 40 cycles of 95^{o}C for 15 sec and 60^{o}C for 20 sec. The relative amounts of mRNA were calculated using the comparative $\Delta\Delta C_T$ method [433] with β-actin as an internal control and all the values are reported relative to the nontargeting siRNA transfected cells.

Table 3.2 List of qRT-PCR primers used. Table provides information on the gene specific primers used to detect the corresponding mRNA levels by qRT-PCR

Gene	**Primer direction**	**Primer sequence (5'-3')**
G3BP-1	Forward	GCCTGTTGCTGAACCAGAGCCT
G3BP-1	Reverse	TGGACGGGGCTGTGAAGCTG
G3BP-2	Forward	CAAGAGAGCGAGAAACCAGAG
G3BP-2	Reverse	GTTCCTCTTCCAGAGCCAAGT
LDH-A	Forward	AGCCCGATTCCGTTACCT
LDH-A	Reverse	CACCAGCAACATTCATTCCA
Actin	Forward	CACCATTGGCAATGAGCGGTTC
Actin	Reverse	AGGTCTTTGCGGATGTCCACGTT

3.3 Results

3.3.1 Endogenous expression of G3BP-1 and LDH-A proteins in a panel of breast cancer cell lines

Endogenous protein levels of G3BP-1 and LDH-A were assayed in a panel of breast cancer cell lines including SKBR3 (HER2-positive), MDA-MB-231 (triple-negative), T47D (ER-positive/PR-positive), and HMF (human mammary fibroblast) respectively. To study the expression of these markers, equal amount of the extracted protein from the above-mentioned cell lines was run on SDS-PAGE followed by Western blot. **Fig. 3.2A** represents the immunoblot using anti-G3BP-1 and anti-LDH-A antibody to detect the bands corresponding to the proteins. Analysis of the blot showed that the expression of G3BP-1 and LDH-A proteins was significantly higher in breast cancer cell lines when compared to HMF as a control **(Fig. 3.2B)**.

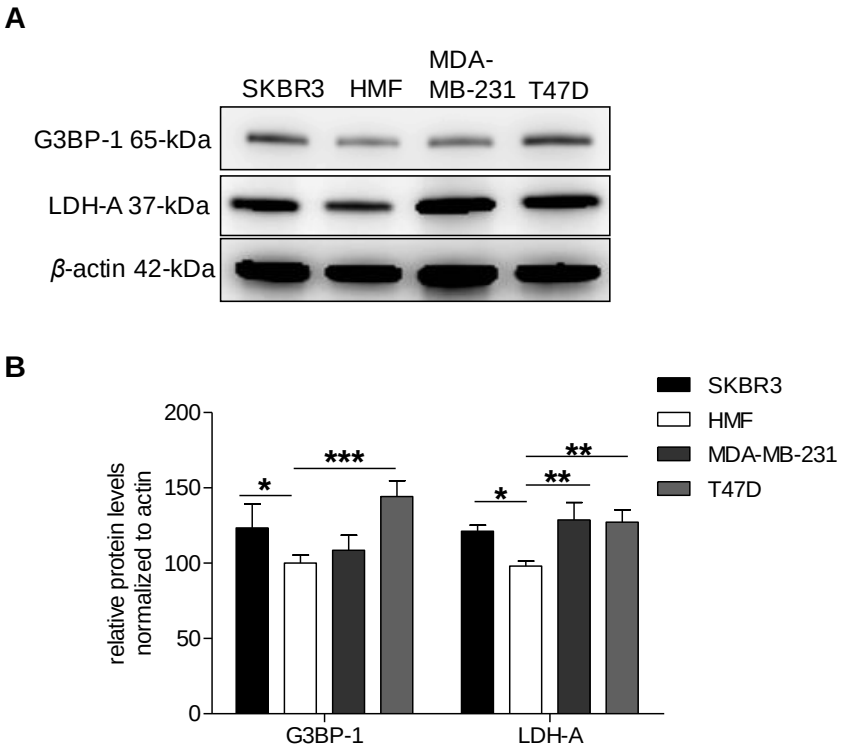

Figure 3.2: Western blot analysis to detect the expression of G3BP-1 and LDH-A in a panel of breast cancer cell lines. **Fig. 3.2A**. Shows the immunoblot result of the expression of G3BP-1 and LDH-A in SKBR3, HMF, MDA-MB-231 and T47D cells when anti-G3BP-1 and -LDH-A antibodies were used at a dilution of 1:1000. *β*-actin was used as a loading control. **Fig. 3.2B.** Shows the histogram obtained from the immunoblot data that represents the relative expression of G3BP-1 and LDH-A proteins in the breast cancer cells when compared to HMF as control. Statistical significance is represented as *** $p<0.001$, ** $p<0.01$, and * $p<0.05$ between the respective breast cancer cells versus HMF as control. Bars represent mean $\pm$ SD of three independent experiments. The data obtained was analyzed using one-way analysis of variance (ANOVA) followed by Bonferroni's multiple comparison test.

3.3.2 Endogenous expression of LDH-A protein after G3BP-1 knockdown

To investigate the potential relation between G3BP-1 and LDH-A, siRNA targeting G3BP-1 was used to knockdown G3BP-1 protein in the breast cancer cell line, MDA-MB-435. **Fig. 3.3A** shows the immunoblot using anti-G3BP-1 antibody to confirm the knockdown of G3BP-1 following siRNA transfection. It was observed that G3BP-1 protein was significantly reduced in the siRNA treated cells when compared to the nontargeting siRNA control. After the knockdown was confirmed, the samples were probed with anti-LDH-A antibody to study the effect of G3BP-1 knockdown on LDH-A regulation. Analysis of the blot showed that LDH-A protein was significantly reduced in the G3BP-1 knockdown cells as compared to the controls (**Fig. 3.3B**)

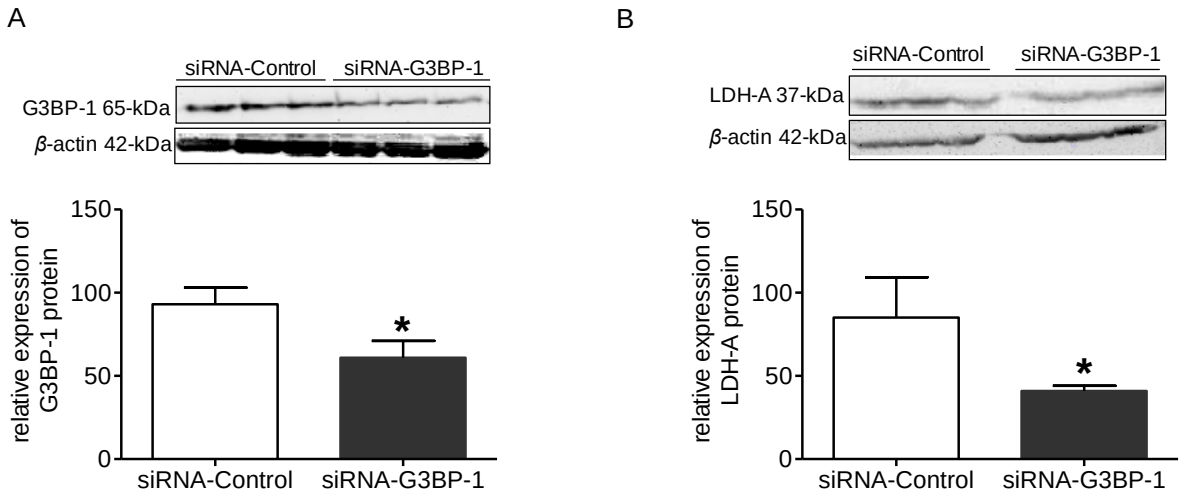

Figure 3.3: Relative expression of LDH-A protein after knockdown of G3BP-1 in MDA-MB-435 breast cancer cell line. Fig. 3.3A. Confirmation of G3BP-1 knockdown at the protein level. The top panel shows the immunoblot result of the expression of G3BP-1 following transfection of MDA-MB-435 cells with siRNA-G3BP-1. *β*-actin was used as a loading control. The bottom panel shows the relative expression of G3BP-1 compared to the control sample obtained by the densitometric analysis of the immunoblot data. Downregulation of G3BP-1 was statistically significant. *, $p<0.05$, student's t test was performed. The data was expressed as mean $\pm$ SD of three independent experiments. **Fig. 3.3B.** Regulation of LDH-A protein after knockdown of G3BP-1. Top panel shows the immunoblot of LDH-A in the G3BP-1 knockdown versus the control samples. *β*-actin was used as the loading control. The bottom panel represents the histogram obtained from the immunoblot data. A statistically significant difference was observed in the relative expression of LDH-A between G3BP-1 knockdown versus control cells. *, $p<0.05$, n=3; student's t test was performed.

3.3.3 Endogenous expression of LDH-A protein after G3BP-2 knockdown

To further assess the potential role of G3BP-2 in regulating LDH-A, the protein expression levels of G3BP-2 after treatment with siRNA-G3BP-2 were determined. **Fig. 3.4A** shows that the knockdown of G3BP-2 protein was statistically significant when siRNA targeting G3BP-2 was used. After confirming the G3BP-2 knockdown, the samples were probed with anti-LDH-A antibody to study the relative expression of LDH-A protein in G3BP-2 knockdown cells, and their respective controls. Surprisingly, there was no difference in the relative expression levels of LDH-A protein between G3BP-2 knockdown and control cells (**Fig. 3.4B**).

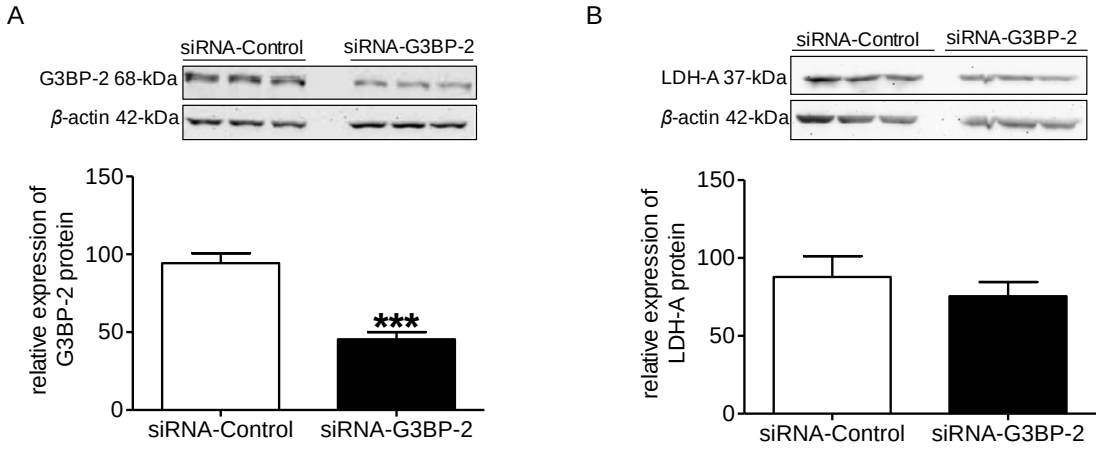

Figure 3.4: Relative expression of LDH-A protein after knockdown of G3BP-2 in MDA-MB-435 breast cancer cell line. Fig. 3.4A. Confirmation of G3BP-2 knockdown at the protein level. The top panel shows the immunoblot result after transfection of the MDA-MB-435 cells with siRNA-G3BP-2. *β*-actin was used as a loading control. The bottom panel shows the relative expression of G3BP-2 compared to the control sample. Downregulation of G3BP-2 was statistically significant. ***, $p<0.001$, student's t test was performed. The data was expressed as mean $\pm$ SD of three independent experiments. **Fig. 3.4B.** Regulation of LDH-A protein after knockdown of G3BP-2. The top panel shows the immunoblot of LDH-A in the G3BP-2 knockdown versus the control samples. *β*-actin was used as the loading control. The bottom panel represents the relative expression of LDH-A in G3BP-2 knockdown cells as compared to the corresponding controls. It was observed that knockdown of G3BP-2 had no statistical significance on the expression of LDH-A protein as compared to the control.

3.3.4 Endogenous levels of LDH-A mRNA after G3BP-1 knockdown

Following the study on the translational regulation of LDH-A by G3BPs, the effect of G3BP knockdown on the endogenous levels of LDH-A mRNA was also investigated. Briefly, MDA-MB-435 cells were transfected with siRNA targeting G3BP-1. The total RNA was isolated, and the mRNA levels of G3BP-1 were studied by performing qRT-PCR. *β*-actin was used as the house keeping gene for normalisation. **Fig. 3.5A** shows significant reduction in the mRNA levels of G3BP-1 after siRNA knockdown. Upon confirmation of G3BP-1 knockdown, the relative levels of LDH-A mRNA between G3BP-1 knockdown and control samples were analysed. Results showed that the mRNA of LDH-A was not regulated upon knockdown of G3BP-1 (**Fig. 3.5B**).

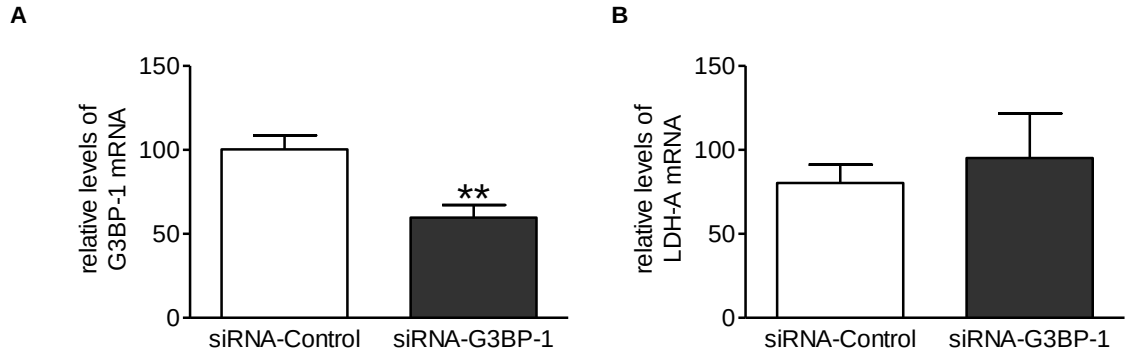

Figure 3.5: Relative levels of LDH-A mRNA after knockdown of G3BP-1 in MDA-MB-435 breast cancer cell line. qRT-PCR was performed to study the endogenous levels of LDH-A mRNA in G3BP-1 knockdown cells. **Fig. 3.5A.** Significant downregulation in the mRNA levels of G3BP-1 was observed in the siRNA-G3BP-1 treated MDA-MB-435 breast cancer cells when compared to the corresponding controls. *β*-actin was used as a house keeping gene. **, $p<0.01$, student's t test was performed. The data was expressed as mean $\pm$ SD of three independent experiments. **Fig. 3.5B.** There was no statistically significant difference in the endogenous levels of LDH-A mRNA between G3BP-1 knockdown cells versus controls. *β*-actin was used as a house keeping gene.

3.3.5 Effect of G3BP-2 knockdown on endogenous levels of LDH-A mRNA

Next, the association between the levels of LDH-A mRNA in G3BP-2 knockdown versus the control cells was also studied. The siRNA-G3BP-2 treatment led to statistically significant downregulation of G3BP-2 mRNA (**Fig. 3.6A**). However, no significant difference in the levels of LDH-A mRNA was observed between G3BP-2 knockdown cells and the related controls (**Fig. 3.6B**).

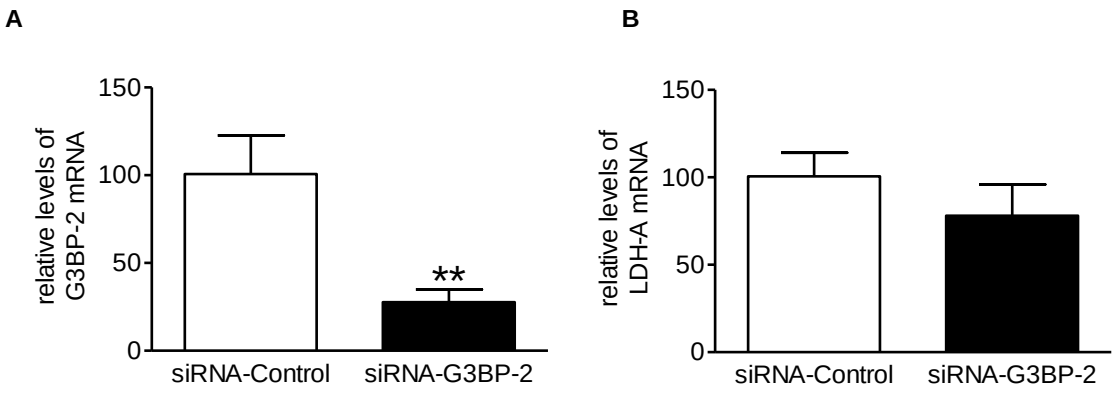

Figure 3.6: Relative levels of LDH-A mRNA after G3BP-2 knockdown in MDA-MB-435 breast cancer cell line. Fig. 3.6A. Statistically significant downregulation in the mRNA levels of G3BP-2 was observed in the siRNA-G3BP-2 treated cells when compared to the corresponding controls. β-actin was used as a house keeping gene. **, $p<0.01$, student's t test was performed. The data was expressed as mean $\pm$ SD of three independent experiments. **Fig. 3.6B.** Significant difference was not observed in the endogenous levels of LDH-A mRNA between G3BP-2 knockdown cells versus controls. β-actin was used as a house keeping gene.

3.3.6 Effect of Lap on the protein levels of G3BP-1 and LDH-A in a panel of breast cancer cell lines

Observed translational downregulation of LDH-A upon G3BP-1 knockdown in MDA-MB-435 breast cancer cell line has indicated an association between G3BP-1 and LDH-A in these cells. Such an association was further explored in a panel of breast cancer cell lines including SKBR3 (HER2-positive), MDA-MB-231 (triple-negative) and T47D (ER-positive/PR-positive) representing distinct molecular subtypes based on the receptor status. Since Lap is known to regulate the expression of LDH-A in the glycolytic pathway [426, 427], the inhibitor concentration (IC_{50}) of Lap was determined in the respective cell lines that were included in the study. Following IC_{50} determination, SKBR3, MDA-MB-231 and T47D cell lines were treated with Lap at the concentration of 5µM, 121µM and 110µM respectively. The cell viability data for Lap treatment of breast cancer cell lines has been provided in the relevant section-5.3.1 (Figure 5.1) of the thesis. Following the drug treatment, protein was extracted from the cells. **Fig. 3.7A, 3.7B,** and **3.7C** represents the protein levels of G3BP-1 and LDH-A in SKBR3, MDA-MB-231 and T47D breast cancer cell lines respectively. The top panel in each indicates the immunoblot using anti-G3BP-1 and anti-LDH-A antibody to study the protein levels of G3BP-1 and LDH-A upon Lap treatment. It was observed that the intensity of bands corresponding to G3BP-1 and LDH-A in drug treated cells when compared to the corresponding controls was reduced in all the breast cancer cell lines included in the study. The bottom panel in each represents the histogram obtained upon analysis of the blot. The data revealed that the protein levels of G3BP-1 and LDH-A were significantly reduced in Lap treated cells versus controls for the respective cell lines.

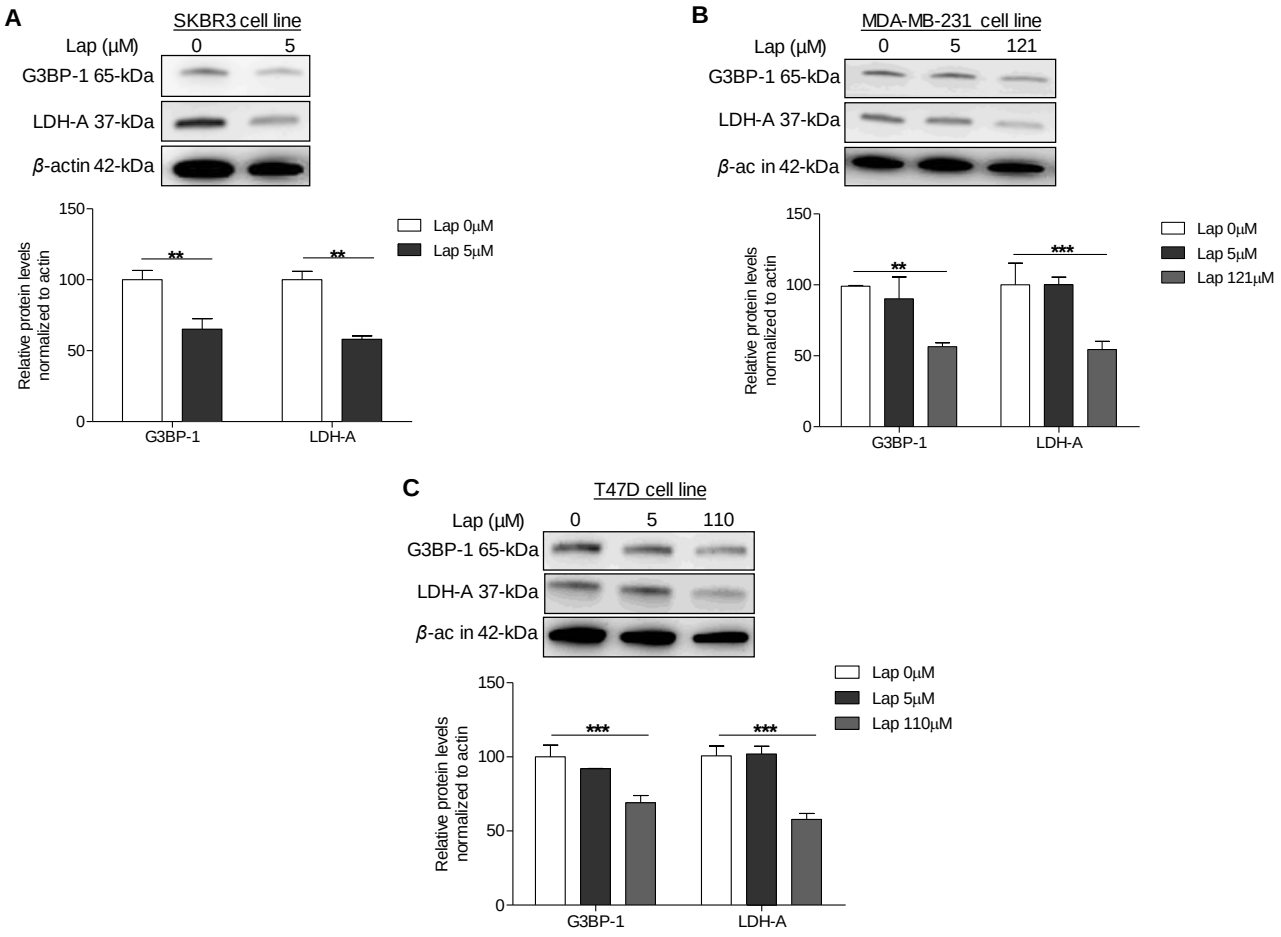

Figure 3.7: Effect of Lap treatment on the protein levels of G3BP-1 and LDH-A in a panel of breast cancer cell lines. Fig. 3.7A, 3.7B, and **3.7C** represent the effect of treating SKBR3, MDA-MB-231 and T47D breast cancer cells with IC_{50} of 5, 121, and 110μM Lap, respectively. The top panel in each represents the immunoblot result of the expression of G3BP-1 and LDH-A following Lap treatment of the indicated cell line. *β*-actin was used as a loading control. The bottom panel shows the relative expression of G3BP-1 and LDH-A compared to the untreated sample obtained by the densitometric analysis of the immunoblot data. Upon Lap treatment, the protein levels of G3BP-1 and LDH-A were significantly reduced. **, $p<0.01$, ***, $p<0.001$; student's t test was performed. The data was expressed as mean ± SD of three independent experiments.

3.4 Discussion

Although studies have implicated the role for G3BP in the mitogenic signaling pathways including NF-κβ [293], Ras signaling [283, 287] and the ubiquitin proteasome system [422-424], its role in regulating the glycolytic pathway in cancer is still unclear. However, Ortega *et al.,* [288] have demonstrated that G3BP-1 regulates the translation of mitochondrial β-F1-ATPase mRNA. Data reported in this chapter have updated the role of G3BP-1 in the glycolytic switch through its translational regulation of LDH-A in MDA-MB-435 breast cancer cell line. Furthermore, Lap treatment of different breast cancer cell lines, which are distinct in their receptor status, has revealed a significant reduction in the protein levels of G3BP-1 and LDH-A respectively. Collectively, findings in this chapter support a role for G3BP-1 in the glycolytic shift observed in breast cancer cell lines.

Interestingly, several studies have shown that G3BP is overexpressed in breast cancers [283-288]. Likewise, upregulation of LDH-A was reported to promote tumor growth and metastasis [434], anoikis resistance and tumor cell invasion [426] of breast cancer cells. Based on the limited evidence to support the role of G3BP-1 in the glycolytic shift, a potential link between G3BP-1 and LDH-A was investigated in this chapter. Initial experiments were designed to examine the endogenous levels of G3BP-1 and LDH-A in a panel of breast cancer cell lines including SKBR3 (HER2-positive), MDA-MB-231 (triple-negative), T47D (ER-positive/PR-positive) and HMF cells. Data obtained from Western blot analysis (**Figure 3.2**) revealed that the endogenous protein levels of G3BP-1 and LDH-A in the breast cancer cell lines were significantly higher when compared to HMF as control. This clearly indicated the potential relevance of G3BP-1 and LDH-A as targets for breast cancer therapy.

Cancer cells in general, display Warburg phenotype to meet the demands of proliferating cells for macromolecular synthesis and energy production [63, 435]. As a result, there is a reprogramming in the bioenergetic pathway to enable enhanced reuptake of glucose and produce higher amounts of lactate [60, 436]. In this process, cancer cells enable the upregulation of critical enzymes in the glycolytic pathway. Lactate dehydrogenase-A is one such enzyme that is often upregulated in breast cancer [417, 418].

The current study investigated the potential link between G3BP and LDH-A in MDA-MB-435 breast cancer cell line by siRNA-mediated knockdown of G3BP in these cells. Upon depletion of G3BP-1, an inhibition in the translation of LDH-A was observed in the cells (**Figure 3.3**). In contrast, such regulation at the level of translation was not observed when G3BP-2 was depleted. The precise mechanism of action of G3BP-1 in the translational regulation of LDH-A, and the specificity of G3BP-1 but not G3BP-2 for such regulation remains elusive. However, it may be speculated that being an RNA binding protein, G3BP-1 may function as a linker RBP in the mRNA-protein complex (mRNP) complex. In its role as a linker RBP, G3BP may regulate the transport of LDH-A mRNA to the appropriate subcellular localization (target site) for translation. Perhaps, upon depletion of G3BP-1, LDH-A mRNA may not be transported to its target site for translation resulting in the reduced levels of LDH-A protein, although this is yet to be tested.

Interestingly, the translational downregulation of LDH-A upon G3BP-2 depletion was not observed (**Figure 3.4**). This may indicate that G3BP-1 and G3BP-2 may have different functions in breast cancer cells. Although, G3BP-1 and G3BP-2 belong to G3BP family of RBPs and share approximately 70% sequence homology [289, 290], subtle differences exist in the subcellular localization of these proteins [285]. French *et al.,* [285] have reported the nuclear localization of G3BP-2 upon serum starvation, in contrast to G3BP-1 that remained cytosolic. Furthermore, G3BP-1 but not G3BP-2 is implicated in the transcript stability of mRNAs. Whilst, G3BP-1 degrades the mRNA of c-*myc* [297], BART [437], PMP22 [438], it stabilizes tau mRNA transcript [439]. Such reports on the role of G3BP-2 in regulating gene expression are limited. The data obtained from translational regulation of LDH-A (**Figures 3.3** and **3.4**) upon depletion of G3BP-1 and G3BP-2 is in accordance with the published reports that indicate functional differences between the two proteins.

At the mRNA level, depletion of either G3BP-1 or G3BP-2 had no effect on the transcript stability of LDH-A mRNA (**Figures 3.5** and **3.6**). This may be due to an indirect role of G3BP in regulating the transcript stability of LDH-A mRNA. Such an argument may be in line with reports that implicate the role of G3BP-1 in the regulation of the transcript stability of tau mRNA [439]. In that study, it was identified that G3BP-1 did not directly associate with tau mRNA. Instead, it associated with insulin like growth factor-1 (IMP-1), a translational regulator within the tau mRNA-protein complex, thereby regulating the translation of tau mRNA.

It is thus conceivable that, although G3BP-1 does not affect the transcript stability, it may act as a linker RBP to transport the LDH-A mRNA to the appropriate site to induce its translation. G3BP-1 depletion may induce a variability in the LDH-A mRNP code that does not facilitate the transport of LDH-A mRNA to the target site for translation. Such an outcome may not necessarily require G3BP-1 to directly associate with LDH-A mRNA. Collectively, these findings have implicated the role of G3BP-1 in the glycolytic shift via its effect on the translational downregulation of LDH-A in MDA-MB-435 breast cancer cell line.

Lapatinib is a potent inhibitor of EGFR and HER2 that is used in the treatment of HER2-positive breast cancers [151-153]. Lap-mediated HER2 inhibition was reported to block the phosphorylation of LDH-A at tyrosine 10 residue, thereby regulating the glycolytic switch in SKBR3 and BT474 breast cancer cells [426]. In a different study, Lap was found to inhibit cell proliferation of MDA-MB-231 and SKBR3 cells by regulating the expression of PKM2 (a glycolytic enzyme) [427]. On a side note, HER2-positive cells upregulate the expression of (a) LDH-A via activation of PI3k/Akt [81] and Erk/PKM2 pathways [82] and (b) G3BP-1 upon HRG stimulation [284]. Based on these reports, it was hypothesized that Lap may have a potential role in the glycolytic shift in breast cancers through its regulation of G3BP-1 and LDH-A.

Treatment of SKBR3 (HER2-positive), MD-MB-231 (triple-negative) and T47D (ER-positive/PR-positive) cell lines with IC_{50} dose of 5, 121, and 110µM Lap resulted in a significant decrease in the protein levels of G3BP-1 and LDH-A (**Figure 3.7**) in all the cell lines included in the study. Although the breast cancer cell lines used in this study represent distinct molecular subtypes based on the receptor status, significant reduction in the protein levels upon Lap treatment was evident in all the indicated cell lines. The findings also revealed that the effect of Lap in downregulating G3BP-1 and LDH-A was independent of HER2. This speculation is based on the data (**Figure 3.7**) that showed a significant decrease in the levels of G3BP-1 and LDH-A upon drug treatment of Lap-sensitive SKBR3, and Lap-insensitive MDA-MB-231 and T47D cell lines.

Furthermore, this observation seems to corroborate the argument that endogenous protein levels of LDH-A may be influenced by G3BP-1 independent of the receptor status. Collectively, the data (**Figures 3.3** and **3.7**) may speculate a role for G3BP-1 in regulating the endogenous protein levels of LDH-A in the breast cancer cell lines used in the study.

3.5 Conclusion

Overall, the findings in this chapter have updated the role of G3BP-1 in regulating the altered glycolytic pathway in breast cancer, and in this context, through its regulation of the endogenous protein levels of LDH-A in a panel of breast cancer cell lines. Since, the data (**Figures 3.5** and **3.6**) does not indicate G3BP-1 to regulate the transcript stability of LDH-A mRNA, experiments to determine the binding of G3BP-1 to LDH-A mRNA may not add value to the findings. The objective of this chapter was to investigate G3BP-1 as a potential biomarker for targeted breast cancer therapy, and hence the experiments to validate its RNA binding ability are out of the scope of the current investigation.

Chapter 4

Investigating the binding of purified G3BP-1 protein with lapatinib

4.1 Introduction

The G3BP family of proteins, including G3BP-1 and G3BP-2, are a class of RNA binding proteins that are highly conserved throughout the eukaryotic evolution [289, 297]. G3BP was discovered as a SH3-domain interacting protein of RasGAP [283]. Although these proteins are ubiquitously expressed, the precise function of G3BP is unclear. This may be because the efforts to understand their role have taken diverse and non-processive paths.

Both G3BP-1 and G3BP-2 are overexpressed in various human cancers, particularly in breast cancer [283-288]. Guitarda *et al.,* [286] have demonstrated an upregulation of G3BP-1 in several tumors including breast, lung, colon, neck, and bladder cancers. A different study by French *et al*., [285] has shown that G3BP-2 was overexpressed in 88% of 56 breast tumors as compared to the surrounding normal tissue. Furthermore, Barnes *et al.,* [284] have reported an upregulated of G3BP-1 in human breast carcinoma biopsy samples when compared to normal tissue. In the same study, it was observed that the mRNA and protein levels of G3BP-1 were upregulated upon stimulation of HER2 with heregulin. In agreement with this observation, MCF-7/HER2 breast cancer cells, when stimulated with heregulin, overexpressed G3BP-1 [284]. Collectively, these evidences indicate the potential relevance of G3BP-1 in the pathology of breast cancer.

G3BP is implicated in several mitogenic signaling pathways that are frequently derailed in cancer [283, 287, 288, 293, 294, 299, 422-424]. Through its binding to SH3-domain of RasGAP [283], G3BP mediates global gene transcription and translation downstream of Ras [440-442]. As an RNA binding protein, G3BP-1 is known to regulate the mRNA stability of several transcripts, including c-myc [297], BART [437], PMP22 [438], and tau mRNA [439]. Surprisingly, such regulation of mRNA stability has not been reported for G3BP-2. This suggests that although G3BP-1 and G3BP-2 belong to G3BP family of RNA binding proteins, they are distinctly separated with respect to their function. Findings from chapter 3 of the current study have corroborated this statement as it was observed that G3BP-1, but not G3BP-2, regulate the translational expression of LDH-A protein in the MDA-MB-435 breast cancer cell line. All experimental evidence gathered to-date supports a pro-tumorigenic role for G3BP-1 in breast cancer. Therefore, targeting G3BP-1 may offer a potentially new paradigm in breast cancer therapy.

Over the past decade, several studies [305-307] have demonstrated direct targeting of G3BP to be a promising strategy for cancer treatment. Oi *et al*., [305] have reported that induction of apoptosis in resveratrol treated SK-MEL-5 melanoma cell line was due to targeting of G3BP-1. In that study, purified recombinant NTF-2 like domain of G3BP-1 was found to interact with resveratrol. Another study demonstrated that epigallocatechin gallate (EGCG) suppressed the growth of H1299 non-small cell lung carcinoma cell line by targeting G3BP-1 [306]. In that study, it was observed that direct interaction of EGCG with SH3-domain binding region of G3BP-1 inhibited Ras signaling in the treated cells. Zhang *et al.*, [307] have reported a synthetic peptide GAP161 to target G3BP-1, thereby inducing apoptosis in HCT116 colon cancer cell line. In that study, it was observed that the interaction of GAP161 with NTF-2 like domain of G3BP-1 blocked Ras signaling in the treated HCT116 cells, thus inhibiting cell growth. The above-mentioned studies indicated a direct interaction of recombinant G3BP-1 with the drug candidate(s).

Lapatinib, is a potent RTK inhibitor of EGFR and HER2 that is effective in the treatment of HER2-amplified breast cancers [151-153]. Lap-induced HER2 inhibition is mediated by competitive blocking of the receptor access to ATP molecules [151, 345]. Lapatinib functions as an ATP-competitive inhibitor to interact with ATP-interacting residues within the ATP-binding pocket of RTK, thus preventing the receptor access to ATP. Wood *et al*., [345] have reported the crystal structure of Lap bound to EGFR. In that study it was demonstrated that Lap preferentially binds to the purified cytoplasmic domain of EGFR and HER2 over other EGFR inhibitors. In addition, the slow off-rate of Lap from the receptor indicated a prolonged inactivation of the receptor [345].

An interesting clue to the function of G3BP-1 came from the identification of a non-canonical human DNA helicase VIII (HDH VIII) from the nuclear extract of HeLa cells [443]. DNA helicases are enzymes with ATPase activity that and are implicated in DNA replication, repair and recombination [443]. HDH VIII was found to be analogous to G3BP-1 and contained sequences rich in RGG boxes [443]. Two independent studies [283, 297] have reported the RNase activity of G3BP-1 (cleavage of c-*myc* mRNA transcript) to be ATP-dependent. Barnes *et al.,* [284] have demonstrated that heregulin stimulation of SKBR3 breast cancer cells resulted in a two-fold increase in the ATPase activity of G3BP-1 in the reaction that contained breast mRNA as compared to the control group without mRNA.

Surprisingly, the amino acid residues at the C-terminal RGG rich region in G3BP-1 were found to be 75% identical to the glycine-rich C-terminal of nucleolin, a canonical DNA and RNA helicase (HDH IV) [443]. It is through this glycine-rich C-terminal domain that HDH IV binds to ATP molecule [444].

Since RGG rich domain of G3BP-1 shares ~75% sequence homology with glycine-rich C-terminal of HDV IV [443], it may be speculated that RGG of G3BP-1 harbours ATP-interacting residues. Hence, Lap (an ATP-competitive inhibitor) may be a good candidate for exploring potential drug-interactions with G3BP-1.

Protein thermal shift (PTS) assays were adopted to study the potential interaction of G3BP-1 with Lap. PTS is an increasingly popular technique that is used to identify small-molecule based compounds that stabilize purified proteins [445]. The assay measures temperature at which the target protein unfolds [i.e., the melting temperature (t_m)] as a readout for its thermal stability. Upon addition of ligand to the purified protein, changes in the melting temperature (Δt_m) are assayed to identify compound(s) that stabilize the protein of interest [445].

Several studies [320, 446] have reported novel intermolecular interactions using the PTS technique. Claus *et al.*, [320] have demonstrated that in comparison with bosutinib (an ATP-competitive Src/Abl inhibitor), Lap significantly induced thermal stabilization of purified HER2 receptor. Nachiappan *et al.*, [446] have reported an increase in thermal stability of glutaminyl-tRNA synthetase (TtGlnRS) as a result of rigid binding of substate to the enzyme. Initial experiments in this chapter were focussed on cloning, expression and purification of recombinant G3BP-1 and G3BP-2. In the later stages of this study, purified G3BP was tested for potential drug-interactions with Lap by PTS assay.

4.2 Materials and Methods

4.2.1 Cell culture and reagents

SKBR3, human breast cancer cell line was cultured as previously described in section 2.2.1. Total RNA isolation from the cells and synthesis of cDNA was performed as previously described in section 2.2.3. Oligonucleotides used in this study were synthesized by Geneworks Pty, Ltd. The purity of the synthesized nucleotides was of the transfection grade. **Table 4.1** provides information on the oligonucleotides that were designed to amplify full length G3BP-1 (Genebank NM_ 005754.2) and G3BP-2 (Genebank NM_ 203505.2) respectively.

Table 4.1: List of primers used to amplify the G3BP genes. PCR amplification of G3BP-1 and G3BP-2 was done using the primer sequences listed in the table.

Gene	**Accession number**	**Forward primer (5'-3') †**	**Reverse primer (5'-3') †**
G3BP-1	NM_005754.2	tcagatctcatatgcggggttct**catcatc atcatcatcat**ggtATGGTGATG GAGAAGCCTAGTC	gggaagcttTCACTGCCGT GGCGCAAGCC
G3BP-2	NM_203505.2	tcagatctcatatgcggggttct**catcatc atcatcatcat**ggtATGGTTATG GAGAAGCCCAGTC	catgccatggTCAGCGACGC TGTCCTGTGAAG

† Lower-case underlined text represents the restriction sites that were added to the primer sequences (catatg-NdeI, aagctt-HindIII, and ccatgg-NcoI*).* The lowercase letters represent the additional nucleotides that were added for the ease of restriction digestion. The lowercase bold letters indicate the nucleotide sequence for $His_{(6)}$-affinity tag. The uppercase letters indicate the gene sequence(s) for G3BP-1 and G3BP-2 respectively.

pRSETC bacterial expression vector (Thermo Fisher Scientific) was used for generating fusion protein constructs of G3BP-1 and G3BP-2. Under the influence of an inducible T7 promoter the cloned DNA sequences are expressed with high efficiency in bacterial *E.coli* cells. The presence of the N-terminal his tag allows purification of the expressed proteins. **Figure 4.1** shows the features of pRSETC vector.

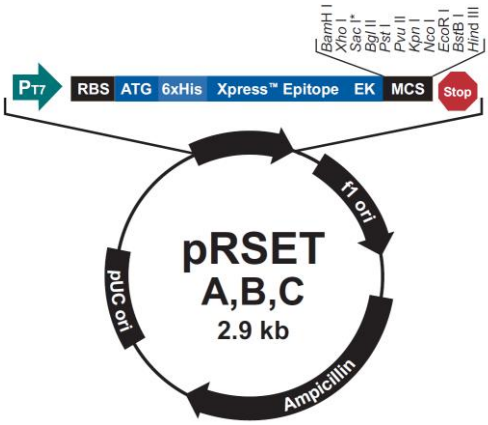

Figure 4.1. Map of pRSETC. Bacterial expression vector pRSETC with T7 promoter, ribosome binding site, $his_{(6)}$-affinity tag, and multiple cloning site. The figure was reproduced from [Invitrogen Cat: V351-20, manual part: 25-0213] with all relevant permissions.

Lap was purchased from Sigma-Aldrich Co., and was stored at a stock concentration of 10mM in dimethyl sulfoxide (DMSO) at -20 °C

4.2.2 Polymerase chain reaction

PCR reactions to amplify full-length G3BP-1 and G3BP-2 were carried out using 0.02U/µl of Q5 high-fidelity DNA polymerase and standard 10x buffer supplied by the manufacturer (New England Biolabs). The reaction(s) contained 2µl of DNA template or 100pg of the control plasmid (pGEX4T3+hsaG3BP-1 and/or pGEX4T3+hsaG3BP-2), and 0.5µM of each forward and reverse primer. Cycling conditions included initial denaturation of DNA at 98ºC for 30 secs, annealing at 66ºC for 30 secs, and final extension at 72ºC for 2 min for 25 cycles.

4.2.3 Generation of fusion protein constructs

cDNAs representing the target sequences were cloned into pRSETC vector (Invitrogen). **Figure 4.2** shows the recombinant plasmids generated in this study. The plasmids were generated by inserting the DNA sequence(s) of full-length G3BP-1 into the NdeI/HindIII linearized pRSETC vector. Similarly, the recombinant pRSETC plasmids for full-length G3BP-2 were generated by cloning the sequence between the NdeI/NcoI digested vector.

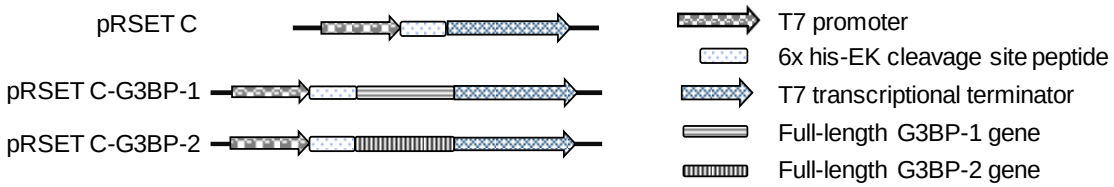

Figure 4.2: Schematic representation of the fusion protein constructs. pRSETC expression vector was used to generate the fusion protein constructs of full-length G3BP-1, and/or G3BP-2. The expression of G3BP(s) is under the influence of an inducible T7 promoter. The protein(s) are expressed with an N-terminal $his_{(6)}$-tag to allow affinity purification of the recombinant G3BPs. In addition, the enterokinase (EK) cleavage site present in the vector allows for cleavage of the fusion tag.

4.2.4 Expression of the fusion protein constructs of G3BP

BL21(DE3) *E. coli* cells were transformed with G3BP fusion construct(s) and protein expression was induced with 1mM IPTG. Expression of the proteins was performed at 37^{o}C, 25^{o}C and 20^{o}C to optimize the expression temperature. Following IPTG induction aliquots of bacterial cultures were collected at 4 h, 8 h, and 16 h to monitor protein intensity over the expression time-course. Following protein expression, bacterial lysates were processed as previously described in section 2.2.12. Briefly, the lysates were sonicated with 10 sec ≥30 (amplitude) and 40 sec off cycle at 4^{o}C. Following sonication, the samples were centrifuged 45 min ≥15,000 x g at 4^{o}C to separate the soluble and insoluble fractions.

4.2.5 Western blot

Following preparation of the proteins in the soluble and insoluble fractions, 5µl of the protein fractions were added to an equal volume of 50 mM Tris, pH 7.4; 250 mM NaCl and mixed with SDS-PAGE loading dye to a final concentration of 1x dye in the total volume. Samples were heated for 5 min at 95^{o}C and run on a 10% polyacrylamide gel until adequate separation was achieved. Following the electrophoresis, Western blot was performed as previously described in section 2.2.14. The blot(s) were probed with rabbit polyclonal anti-6x His antibody (Genetex) overnight at 4^{o}C. Next day, the blot was washed and incubated at 25^{o}C for 1 h with anti-rabbit IgG (Invitrogen). ECL detection was performed using the Western chemiluminescent HRP substrate detection kit (Millipore). The identity of the protein(s) was confirmed using protein-specific antibodies for G3BP-1 and G3BP-2 (Abcam Plc).

4.2.6 Affinity purification of his$_{(6)}$-tag G3BP

Following the expression of his$_{(6)}$-tag G3BP in a litre culture volume, the protein was purified using HisPur Ni-NTA resin (Thermo Fisher Scientific) by gravity flow chromatography. The soluble fraction was mixed with an equal volume of the equilibration buffer containing 50mM Tris, pH 7.4, 250mM NaCl and 10mM imidazole. The prepared protein extract was clarified using a 0.2µm syringe filter. The clarified protein extract was incubated in a tube with preequilibrated HisPur Ni-NTA resin (binding capacity: $\leq$ 60mg/ml resin) and mixed on an end-over-end rotator for 30 min at 4^{o}C. Following incubation, the flow-through was collected and the resin was washed with ten resin-bed volumes of wash buffer containing 50mM Tris, pH 7.4; 250mM NaCl and 25mM imidazole. Elution was achieved with gradient imidazole concentration in the elution buffer containing 50mM Tris, pH 7.4; 250mM NaCl and 50–500mM imidazole. Three-column volumes of elution buffer for each gradient imidazole concentration was used for elution and the eluate fractions were collected at each step.

4.2.7 Protein thermal shift assay (PTS)

PTS assays were carried out as described by Niesen *et al*., [445]. This assay measures the T_m of the purified protein in the presence or absence of a stabilizing ligand. As the temperature increases the protein unfolds and the hydrophobic parts are exposed. SYPRO Orange (Thermo Fisher Scientific), a fluorescent dye used in the assay has affinity for the hydrophobic patches and binds to the exposed parts of the protein to induce fluorescence upon binding. In a 96-well RT-PCR plate (Life Technologies), the ratio of G3BP-1 and SYPRO Orange dye (fluorescent dye) was optimized by testing a 4x5 matrix of conditions. The optimization conditions included the protein concentration from 10 to 25µM and SYPRO Orange concentration from 5x to 20x in a sample volume of 20µl containing 100mM NaCl and 20mM HEPES (pH 7.5). The optimal conditions for the assay were determined at 15µM of G3BP-1 and 6.5x SYPRO Orange dye. Three technical replicates were then tested for each ligand (Lap and 5-FU) using the optimized protein:dye ratio. Experiments were conducted on a Roche LightCycler 480, (Roche, Switzerland) and analysed using DMAN software.

4.3 Results

4.3.1 Generation of fusion protein constructs of G3BP-1 and G3BP-2

Generation of the fusion constructs involved PCR amplification of G3BP-1 and G3BP-2 (**Fig. 4.3A**), cloning the amplified DNA sequences into pRSETC vector, transformation of JM109 *E. coli* cells with the fusion construct(s), and screening the transformed bacterial cells for G3BP-1 and G3BP-2 inserts (**Fig. 4.3B and 4.3C**).

Based on the optimization of conditions for PCR amplification of G3BP-1 and G3BP-2, the annealing temperature of 66^{o}C was selected for PCR amplification of the genes. cDNA extracted from MCF-7 breast cancer cell line was used as the template and control plasmids included pGEX4T3+hsaG3BP-1, pGEX4T3+hsaG3BP-2 and pGEX4T3 +NDUFV1. The results indicated an amplification of G3BP-1 and G3BP-2 at the expected band sizes of 1.4-kb, and 1.5-kb (**Fig. 4.3A**) respectively. Following the transformation of JM109 *E. coli* cells with the fusion constructs, the bacteria was grown overnight on LB agar plates containing ampicillin at 37^{o}C. Next day, the transformed colonies were screened to confirm the identity of the G3BP insert(s). Whilst, NdeI/HindIII were used to screen for G3BP-1, inserts for G3BP-2 were screened by NdeI/NcoI. Upon restriction digestion, the fusion plasmids showed bands corresponding to G3BP-1 (**Fig. 4.3B**), and G3BP-2 (**Fig. 4.3C**). The fusion constructs thus generated were sequenced by DNA sequencing to confirm the identity of the nucleotide sequences for G3BP-1 and G3BP-2.

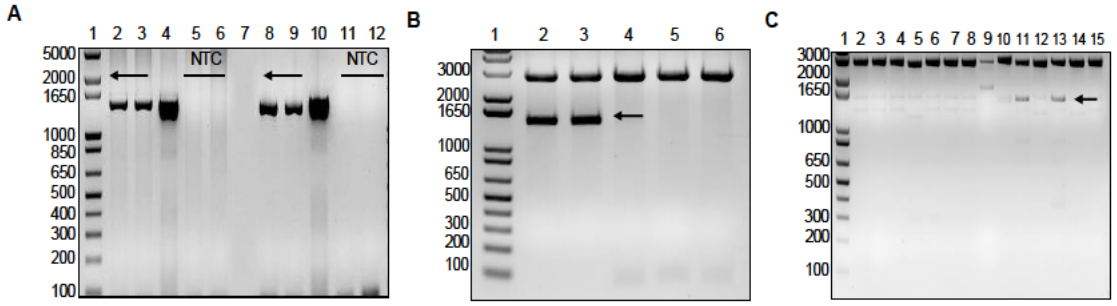

Figure 4.3: Generation of fusion protein constructs of G3BP-1 and G3BP-2. Fig.4.3A. 0.9% agarose gel image of PCR amplification products for the cDNA extracted from MCF-7 cells (lanes 2-3) amplified with G3BP-1 primers; (lanes 8-9) amplified with G3BP-2 primers. Lanes 4 and 10 include control plasmids- pGEX4T3+hsaG3BP-1, pGEX4T3+hsaG3BP-2 respectively. NTC indicates no template control. Lane 1 shows a 1-kb plus DNA ladder. **Fig. 4.3B:** 0.9% agarose gel image of restriction enzyme digested recombinant pRSETC+G3BP-1 plasmids (lanes 2-6), using NdeI/HindIII enzymes. Lanes 2-3 show band at ~1.4-kb indicative of G3BP-1. Lane 1 represents a 1-kb plus DNA ladder. **Fig. 4.3C.** Restriction enzyme digestion of the recombinant pRSETC+G3BP-2 plasmids (lanes 2-15), using NdeI/NcoI enzymes when run on 0.9% agarose gel. Lanes 11-13 show band at ~1.5-kb corresponding to G3BP-2. Lane 1 shows a 1-kb plus DNA ladder. Arrows indicate either G3BP-1 or G3BP-2

4.3.2 Effect of temperature on the expression of recombinant protein constructs of G3BP

It has been reported that a decrease in expression temperature reduces protein aggregation and improves the solubility of a recombinant protein [447]. Hence, the effect of temperature on the expression of G3BP-1 and G3BP-2 was studied. It was observed that when G3BP-1 was expressed at 37°C, the protein was recovered in both the soluble and the insoluble fraction. Lowering the temperature to 25°C resulted in the efficient recovery of the protein in the soluble fraction. However, induction at 20°C was not favourable for G3BP-1 expression. In addition, the intensity of the protein band in the soluble fraction at both expression temperatures (37°C and 25°C) was reduced over the expression time-course (**Fig. 4.4A**). Therefore, the optimum temperature for the expression of G3BP-1 was 25°C with the protein recovery within 8 h following IPTG induction.

In contrast, lowering the expression temperature to 20ºC favoured the recovery of major proportion of G3BP-2 in the soluble fraction, although there was still some protein in the insoluble fraction. Whilst, the expression at 25ºC resulted in protein degradation, such degradation was not observed when induced at 20ºC (**Fig. 4.4B**). The expressed G3BP-1 and G3BP-2 had apparent molecular weights of 65-kDa and 68-kDa respectively as determined by immunoblot analysis using anti-6x-His antibody (Genetex).

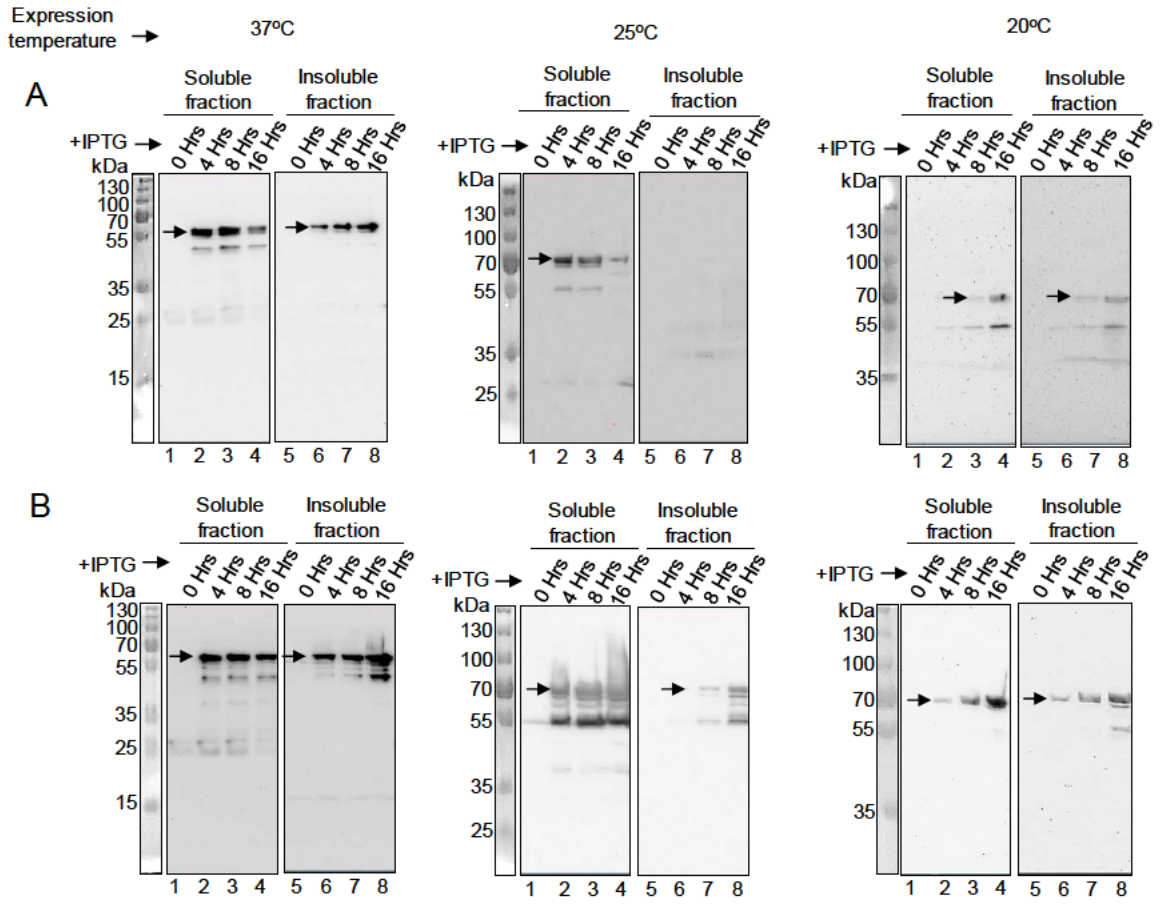

Figure 4.4: Effect of temperature on the expression of recombinant G3BP-1 and G3BP-2. Fig. 4.4A and 4.4B represent the immunoblot using anti-6x His antibody showing the expression of G3BP-1 and G3BP-2 at 37ºC, 25ºC and 20ºC respectively. Following 1mM IPTG induction of BL21(DE3) cells, samples were collected at 4 h, 8 h and 16 h. Lanes (2-4) indicate the protein in the soluble fraction at 4, 8 and 16 h respectively after IPTG induction. Similarly, lanes (6-8) indicate the protein present in the insoluble fraction at the respective time points. Lane 1 and 5 represent the soluble and insoluble fractions prior to IPTG induction. kDa represents the molecular weight standard. Arrows indicate either G3BP-1 or G3BP-2 accordingly.

4.3.3 Confirmation of the identity of G3BP

To further confirm the identity of the expressed G3BP proteins, immunoblotting was performed using protein-specific antibodies for G3BP-1 and G3BP-2. Anti-G3BP (epitope recognition: 214-303 amino acids) and anti-G3BP-2 (epitope recognition: 275-325 amino acids) antibodies were purchased from Abcam Plc. Protein samples prepared by expression at 37°C were used for immunoblotting. Western blot analysis using anti-G3BP-1 (**Fig. 4.5A**), or anti-G3BP-2 antibody (**Fig. 4.5B**), revealed protein band(s) whose molecular weights were identical to those when probed with anti-6x His antibody. Hence, the observed bands of molecular weights 65-kDa and 68-kDa were confirmed to be of G3BP-1 and G3BP-2 respectively.

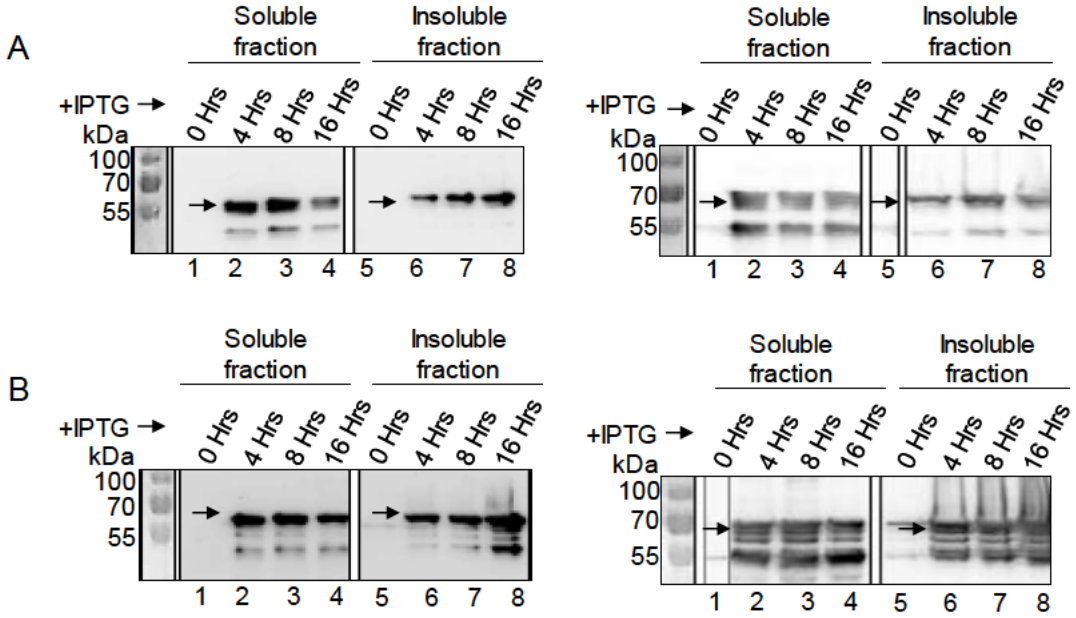

Figure 4.5: Confirmation of the identity of G3BP. Immunoblot using protein-specific antibodies for detection of G3BP. **Fig. 4.5A**: Western blot analysis using anti-G3BP antibody indicated a band of molecular weight 65-kDa. Similarly, **Fig. 4.5B** showed a band of 68-kDa when the immunoblot was probed with anti-G3BP-2 antibody. Immunoblot images on the left panel were adapted from [**Figure 4.4**], which showed the expression of G3BP-1 and G3BP-2 at 37°C upon detection with anti-6x His antibody. Arrows indicate either G3BP-1 or G3BP-2 accordingly.

4.3.4 Purification and concentration of G3BP-1

Based on the results obtained from the recovery of the recombinant protein in the soluble fraction, purification of $his_{(6)}$-G3BP-1 was conceived. Following 1mM IPTG induction of BL21(DE3) *E. coli* cells containing the pRSETC-G3BP-1 plasmid, the expressed $His_{(6)}$-G3BP-1 was collected in the soluble fraction and purified using Ni-NTA resin as previously described in section 4.2.7. A volume of 5µl of flow-through, wash and the gradient eluate fractions were mixed with equal volume of 50mM Tris, pH 7.4, 250mM NaCl buffer and run on a 10% polyacrylamide gel. **Fig. 4.6A** shows the image of the protein gel after staining with Coomassie stain. It indicates that $His_{(6)}$-G3BP-1 was bound to the Ni-NTA resin and eluted in the fractions containing 125mM and 250mM imidazole in the elution buffer, the highest amount of the protein was eluted at 125mM imidazole. Purified $his_{(6)}$-G3BP-1 was passed through an amicon ultra-15 filter (Millipore), with a 10K molecular weight cut off (MWCO) and the protein was exchanged into a buffer containing 50mM Tris, pH 7.4; 250mM NaCl. Following buffer exchange, $his_{(6)}$-G3BP-1 was concentrated to a final volume of ~4ml. A small aliquot of the concentrated G3BP-1 was run on a 10% SDS-gel to check the quality of the protein (**Fig. 4.6B**). Concentration of the protein was estimated to be 1.5mg/ml by UV_{500} scan and the yield of purified G3BP-1 was estimated to be 6mg/l of the culture.

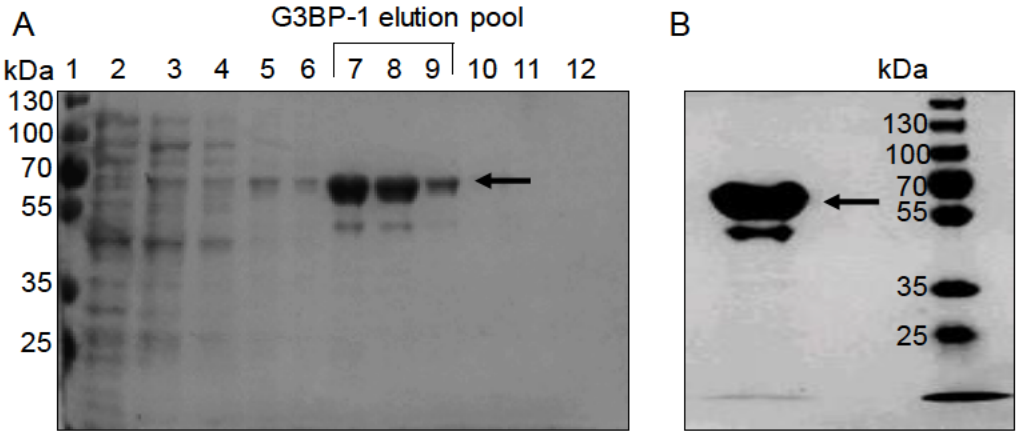

Figure 4.6: Purification and concentration of his$_{(6)}$-G3BP-1. Fig. 4.6A. shows the Commassie stained polyacrylamide gel image of his$_{(6)}$-G3BP-1 purification using Ni-NTA resin. Lanes 2, (3–4) indicate flow-through and wash fractions respectively. Lanes (5–12) indicate eluate fractions with increasing concentration of imidazole in the elution buffer. Lanes (7–8) corresponding to 125mM imidazole concentration showed G3BP-1 band at the expected molecular weight of 68-kDa. Some proportion of the protein was eluted at 250mM imidazole concentration as shown in lane 9. Lane 1 is the protein marker. **Fig. 4.6B**. Coomassie stained gel image of the concentrated G3BP-1. The purified his$_{(6)}$-G3BP-1 was buffer exchanged and concentrated using amicon-ultra 15 centrifugal filters, with a MWCO 10K. Arrow indicates His$_{(6)}$-G3BP-1 band that appears to be relatively pure.

4.3.5 Protein thermal shift assay of purified G3BP-1 protein with lapatinib

Purified G3BP-1 was tested in PTS assay across a range of concentrations of Lap (**Figure 4.7**). Briefly, 15µM of the purified G3BP-1 was mixed with 6.5x SYPRO Orange dye. Lap was added at a concentration ranging between 30–120µM (2x to 8x stoichiometric ratio of the compound to the protein) to investigate the effect of Lap on the thermal unfolding of G3BP-1. The inflection point of the Boltzmann sigmoidal curve was taken as the t_m of G3BP-1. Thermal shift (Δt_m) values were obtained by subtracting the t_m value of G3BP-1 in DMSO control. The data indicated that the t_m (°C) of G3BP-1 in the absence of Lap, at 15µM was 49.0 $\pm$ 0.10°C. Lap stabilized G3BP-1 by ~ ≤1°C for the concentrations ranging from 30-120µM of Lap.

The greatest thermal stabilization of G3BP-1 (up to 50.1 ± 0.10°C) was observed at 60µM of Lap (**Figure 4.7**). However, beyond the 4:1 stoichiometric ratio of Lap to G3BP-1, the t_m value decreased as observed at 120µM of Lap. **Table 4.2** summarizes the t_m and Δt_m values of G3BP-1 in the presence of Lap at different stoichiometric ratios of the compound to the protein.

Table 4.2: t_m and Δt_m values (^{o}C) of purified G3BP-1 protein in the presence of lapatinib

Table showing the t_m and Δt_m values (^{o}C) of G3BP-1 in the presence or absence of Lap at different stoichiometric ratios of the compound to the protein.

Stoichiometric ratio	**t_m value (^{o}C)**	**Δt_m (^{o}C)**
DMSO control (0:1)	49.0 ± 0.10	0.00
Lapatinib: G3BP-1 (2:1)	49.8 ± 0.29	0.80
Lapatinib: G3BP-1 (4:1)	50.1 ± 0.10	1.11
Lapatinib: G3BP-1 (8:1)	48.5 ± 0.19	-0.46

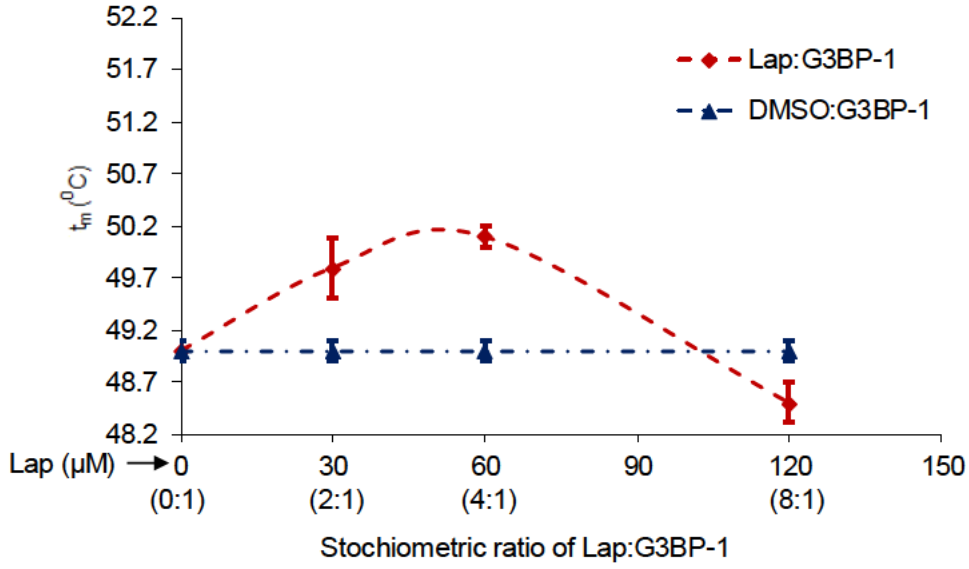

Figure 4.7. Effect of lapatinib on thermal stabilization of purified G3BP-1 protein. Lap was tested at different concentrations ranging from 30-120μM (red, square) at a stochiometric ratio of 2x to 8x of the compound to the protein, at 15μM of purified G3BP-1. Thermal shift was greatest at 60μM of Lap. At 120μM of Lap the t_m of G3BP-1 decreased below the control. G3BP-1 in DMSO (blue, triangle) was the control for the experiment. Data was represented as mean ± SD of three independent experiments. t_m = thermal shift.

4.3.6 Protein thermal shift assay of purified G3BP-1 protein with lapatinib and 5-fluorouracil

To investigate the specificity of Lap-induced thermal stabilization of recombinant G3BP-1, 5-fluorouracil (a thymidylate synthase inhibitor) [448] was tested for its effect on thermal stability of the protein. Thus far, 5-FU has not been reported to interact with ATP binding proteins. Since, the 4:1 stochiometric ratio of Lap:G3BP-1 resulted in the greatest thermal stabilization (~ ≤1°C) of G3BP-1 (as previously observed in section 4.3.5), this ratio was selected to test the effect of 5-FU on thermal stability of the protein (**Figure 4.8**). **Table 4.3** reports the t_m values for G3BP-1 in DMSO, Lap and 5-FU to be 49.9 ± 0.08, 51.0 ± 0.14, and 49.0 ± 0.07°C respectively.

The data revealed that Lap induced thermal stabilization ($\Delta t_m \geq 1^oC$) of G3BP-1, which was not observed when 5-FU was tested (**Figure 4.8**), suggesting that the interaction of G3BP-1 may be specific to Lap via the ATP-interacting residues present within the C-terminal of the protein.

Table 4.3: t_m and Δt_m values (^oC) of purified G3BP-1 protein in the presence of lapatinib and 5-fluorouracil. Table showing the t_m and Δt_m (^oC) values of G3BP-1 in the presence of Lap and 5-FU at 4:1 stoichiometric ratio of the compound(s) to the protein.

Stoichiometric ratio	t_m value (^oC)	Δt_m (^oC)
DMSO control (0:1)	49.9 ± 0.08	0.00
Lapatinib: G3BP-1 (4:1)	51.0 ± 0.14	1.05
5-FU: G3BP-1 (4:1)	49.0 ± 0.07	-0.89

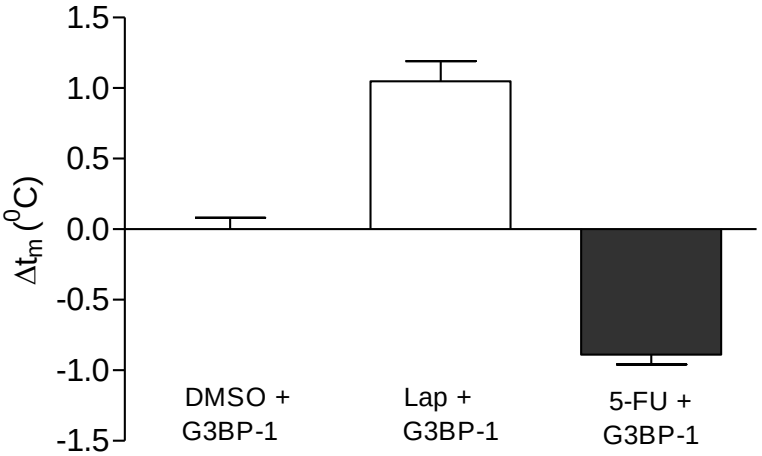

Figure 4.8. Protein thermal shift assay of purified G3BP-1 protein with lapatinib and 5-fluorouracil. The effect of Lap versus 5-FU on thermal stabilisation of G3BP-1 was studied at 4:1 stoichiometric ratio of compound(s) to the protein respectively. At 60µM of Lap, Δt_m of G3BP-1 was $\geq 1^oC$. 5-FU induced a negative shift in the t_m of G3BP-1 by $\leq 1^oC$. G3BP-1 in DMSO was used as the control. Data was represented as the mean ± SD of three independent experiments. Δt_m = thermal shift.

4.4 Discussion

Over the last decade, protein-ligand interaction studies have identified novel interactions between ligands and protein targets [305, 319, 320, 345, 449]. For example, Claus *et al*., [320] have demonstrated thermal stabilization of purified HER2 receptor by Lap. In a different study, Oi *et al*., [305] have reported the direct interaction of G3BP-1 to resveratrol-conjugated sepharose beads. Similarly, studies [319, 449] have demonstrated that PRIMA-1 (p53 re-activation and induction of massive apoptosis) stabilized mutant p53 through its covalent interaction with the DNA binding domain of the mutant protein. An independent study by Wassman *et al*., [450] has reported stabilization of mutant p53 by p53-reactivating compounds. Findings in this chapter report Lap-induced thermal stabilization of recombinant G3BP-1 by protein thermal shift assay. Furthermore, such stabilization was specific to Lap, as treatment of G3BP-1 with 5-fluorouracil (a negative control) did not induce thermal stability of the protein.

The first part of this chapter involved the production of recombinant G3BP. Fusion protein constructs of G3BP were generated by cloning the respective gene sequences into the pRSETC expression vector with inducible T7 promoter. **Figure 4.2** illustrated the cloning strategy to generate fusion protein constructs in pRSETC bacterial expression vector. The accuracy of the protein constructs was confirmed by restriction digestion (**Figure 4.3**) and DNA sequencing. The fusion protein constructs were expressed in BL21(DE3) *E. coli* cells (**Figure 4.4**). This strain of bacteria is well-known for its versatility, rapid cultivation and inexpensive cost. Following IPTG induction, the fusion proteins with the N-terminal $his_{(6)}$-tag were expressed as detected by the immunoblot analysis using anti-$his_{(6)}$ antibody. Consistent with the observations made by Kennedy *et al*., [289], in this study, the immunoblot data estimated the molecular weight of G3BP-1 and G3BP-2 to be approximately 65-kDa and 68-kDa respectively (**Figure 4.4**). In contrast, the predicted molecular sizes for G3BP-1 and G3BP-2 were 54.9 and 58.2-kDa [283]. Such an increase in the observed molecular weight may be due to the posttranslational modification commonly observed in these proteins [298].

In addition, it was observed that the efficiency of protein recovery in the soluble fraction was improved when the expression temperatures were lowered (**Figure 4.4**). This observation supports the general argument that lower temperature enables slow rate of protein production to ensure proper folding of the proteins [447]. However, the expression of G3BP-1 was not favoured when the temperature was lowered from 25^{o}C to 20^{o}C. This may be due to the repression of the T7 promoter activity as the temperature was lowered below the optimum of 25^{o}C. However, promoter repression was less likely to occur, as the recovery of G3BP-2, whose expression is controlled by the same promoter was more efficient as the temperature was lowered from 25^{o}C to 20^{o}C.

A more plausible explanation for the differences in the recovery of G3BP-1 and G3BP-2 may be due to the distinctive nature of these proteins. Although, G3BP-1 and G3BP-2 belong to the G3BP family, they have distinct catalytic domain compositions [289]. Kennedy *et al*, [289] have shown the presence of two and five proline rich (PxxP) motifs in G3BP-1 and G3BP-2 respectively. In that study, it was demonstrated that the two proteins differed considerably in the arginine-glycine rich RGG boxes. Therefore, the differences in the composition of these catalytic domains between G3BP-1 and G3BP-2 may affect the overall stability of the proteins, and hence their recovery in the soluble fraction. **Figure 4.9** shows the aligned amino acid sequences of G3BP-1 and G3BP-2 to indicate the distinct nature of these proteins.

Figure 4.9: Alignment of amino acid sequences of G3BP-1 and G3BP-2. Clustal alignment of G3BP-1 and G3BP-2 amino acid sequences reveal distinct catalytic domains. Amino acids are shown in single letter format. Numbering at the end of the line indicates the amino acid position within the indicated protein. Spaces within the aligned proteins indicate gaps inserted into the sequences to maintain collinearity. Sequences in italics indicate the acid-rich domain. Whilst, black underlined sequences represent RNP-2, blue underlined indicate RNP-1. Sequences in red indicate the RGG rich domain within the proteins. Boxes represent the proline-rich sequences (PxxP). The amino acid residues in the blue box represent the ATP-interacting residues within the RGG rich domain of G3BP-1. The figure was adapted from [289, 443] and is presented here with permission of the corresponding author and the journal editor.

Immunoblot analysis using protein-specific antibodies, anti-G3BP and anti-G3BP-2 revealed bands that were identical to those when probed with anti-6x His antibody (**Figure 4.5**). This observation confirmed the identity of the expressed fusion proteins. Interestingly, an additional band of relatively lower molecular size than that of a full length G3BP protein was observed. This band may be due to an incomplete translation of the full-length cDNA encoding the protein or due to the degradation of the expressed protein. Generating the protein construct with a C-terminal affinity tag may circumvent the problem by ensuring only those cDNAs that are completely translated to be detected by the tag-specific antibody. Once the expression conditions for the protein were optimized, G3BP-1 was purified using Ni.NTA resin and eluted with 125mM imidazole. Upon purification and SDS-PAGE electrophoresis, the eluate sample showed an intense band at molecular size of 68-kDa corresponding to the purified G3BP-1 (**Fig. 4.6A**). The purified protein was concentrated to a final volume of 4ml at 1.5mg/ml (**Fig. 4.6B**).

The second part of this chapter investigated the effect of Lap on thermal stabilization of purified G3BP-1 using PTS assay. PTS identifies molecular interactions between ligands and target proteins depending on the changes in melting temperature (t_m) of the target protein in the presence or absence of the ligand [451]. The binding efficiency correlates with a shift in the melting temperature ($\Delta t_{m)}$ upon interaction of the target protein with the ligand. Such an interaction may provide potential insights into thermal stability of the target protein.

G3BP-1 was tested in the PTS assay with a range of concentrations of Lap. The results demonstrated that Lap treatment induced thermal shifts (increase in the t_m value) that were slightly higher than the vehicle control. Although minor, thermal stabilization was greatest at a concentration of 60µM of Lap (**Figure 4.7**). Such an observation may be a result of weak association between the ATP-interacting residues of G3BP-1 and Lap.

Wood *et al.*, [345] have demonstrated that Lap strongly interacts with the ATP-residues within the ATP-binding cleft of EGFR and HER2 receptors. The presence of a well-defined ATP binding pocket in the receptor enables a strong interaction between HER2 and Lap [345]. Based on that report, it may be speculated that the weakly induced thermal stabilization of G3BP-1 in the presence of Lap may be due to weak interactions of the ATP-interacting residues of the protein with Lap. Costa *et al.*, [443] have shown that the RGG rich region of G3BP-1 is homologous to the glycine-rich C-terminal of nucleolin, (a known DNA and RNA helicase with ATPase activity). Srivastava *et al.*, [444] have reported that glycine-rich terminal domain of nuclelin binds strongly to ATP. In fact, mapping a 23 residue stretch of RGG rich domain of G3BP-1 with homologous glycine-rich C-terminal domain of nucleolin revealed 75% sequence homology as indicated in **Figure 4.10** [443].

Nucleolin 658 G**RGG**FGG**RGG**G**RGG** . **RGG**FG**GRG**R 682
G3BP 428 L**RGP**GGP**RGG** L**GGG**M**RGP** . P**RGG**M 450

Figure 4.10: Sequence homology of glycine-rich C-terminal of nucleolin and RGG-rich C-terminal stretch of G3BP-1. Mapping of glycine-rich C-terminal of nucleolin with a 23-residue stretch of RGG rich C-terminal region of G3BP-1 revealed around 75% sequence identity. The glycine-rich carboxy terminal domain of nucleolin binds strongly to ATP. Letters in bold indicate homology. Numbering at the start and the end of each line indicates the amino acid position within the respective proteins. Dots indicate gaps inserted into the sequences to maintain collinearity. The figure was adapted from [443] and is presented here with permission of the corresponding author and the journal editor.

Despite the presence of ATP-interacting residues within the RGG rich stretch of G3BP-1, a well-defined ATP-binding pocket has not been reported for this protein. Hence, strong binding of G3BP-1 to Lap was not achieved. However, the observed thermal shift may be due to weak interactions between the ATP-binding residues of G3BP-1 and Lap, although this is yet to be determined.

Interestingly, as the stochiometric ratio of Lap:G3BP-1 was increased to 8:1 at 120µM of Lap, it was observed that there was a negative shift in the t_m of G3BP-1. Such an observation is not uncommon for multidomain proteins. Guillermo *et al*., [452] have demonstrated that increasing concentrations of Ca^{+2} stabilized the calcium-binding domain (β-domain) of equine lysozyme, whilst the t_m of α-domain did not change. The effect of Ca^{+2} on the overall stability of equine lysozyme resulted in transition intermediates of which some retained the native-like structure whilst others were devoid of the native conformation. In line with that argument, in this chapter, it may be speculated that an observed negative shift in the t_m of G3BP-1 at 120µM of Lap may be due to reduced interdomain cooperativity during G3BP-1 denaturation. On a side note, Wassman *et al*., [450] have argued that a slightly higher shift in the t_m of mutant p53 in the presence of PRIMA-1 may be due to the inherently unstable nature of the protein. Whilst, such an argument may have general limitations, the slightly induced thermal stabilization of G3BP-1 by Lap may be a result of weak protein-ligand interactions. In contrast, the presence of a well-defined binding pocket enabled complex formation between HER2 and Lap, where Lap induced thermal stabilization of HER2 at a concentration of 1µM [320]. Based on the evidence presented (**Figure 4.7** and **4.8**) and reports elsewhere [320], it may be speculated that Lap binds to G3BP-1 with weak affinity, whilst its binding affinity to HER2 is relatively high. Indeed, Korcsmaros *et al.*,[453] have proposed that it is unlikely that a multi-target drug binds to different targets with equally high affinity.

For most applications, data from thermal shift is a measure of correlation and given the complexity of the cellular environment with a high level of molecular crowding in cells, it may be difficult to predict the clinical relevance of the observation. Nevertheless, these findings provide mechanistic details on the interaction of Lap with G3BP-1.

To validate the specificity of Lap induced stabilization of G3BP-1, 5-fluorouracil (5-FU) [448] was tested at 4:1 stochiometric concentration of the compound to the protein. In contrast to Lap, 5-FU had no stabilizing effect on G3BP-1 suggesting that the interactions were specific to Lap. The negative shift in the t_m of G3BP-1 in the presence of 5-FU may be due to the stabilization of the non-native forms of the protein by the compound. Cimmperman *et al*., [454] have argued that ligand binding to the native state (folded conformation) tends to increase the t_m of the protein, whilst, its interaction with the non-native state (unfolded conformation) decreases the t_m.

Based on this argument, it may be speculated that 5-FU preferentially binds to the unfolded conformations of G3BP-1. In line with this hypothesis, Lap-induced thermal shift may stabilize the folded conformation of G3BP-1. On a different note, Lap induced thermal stabilization of purified HER2 protein reported elsewhere [320] could not be included as a positive control in this study due to unavailability of purified HER2 protein. This limitation reduces the conclusions of this study. Although, inclusion of positive control in this study was not feasible, significance of the interaction between purified G3BP-1 protein and Lap may be further evaluated using HER2 or EGFR in future studies.

4.5 Conclusion

In conclusion, this chapter demonstrated the effect of Lap on thermal stabilization of G3BP-1. In the presence of Lap the t_m of G3BP-1 was slightly increased with a greatest thermal stabilization at 60µM of Lap when 4:1 stochiometric concentration of the compound to the protein was tested. The specificity of Lap interaction was confirmed by assessing the interaction of G3BP-1 with 5-FU (negative control), which showed no effect on thermal stability of G3BP-1 when compared to Lap.

Chapter 5

The role of lapatinib in the suppression of doxorubicin induced migration of SKBR3 breast cancer cells

5.1 Introduction

Breast cancer is the second most prevalent cancer worldwide after lung cancer and it is the major cause of cancer-related deaths among women [1]. Metastatic breast cancer is the invasive form of the disease that has spread from the breast to other parts of the body. Reports indicate that approximately 30% of the cases diagnosed with breast cancer are metastatic in nature [123], and often lead to death [125, 126]. Interestingly, distant metastatic disease is frequently observed in inflammatory breast cancer (IBC), a rare, yet highly aggressive form of the disease [455]. Although, IBC accounts for less than 5% of all breast cancers [456], 85% of those patients had regional lymph node invasion, and over 30% were reported to have distant metastasis at the time of diagnosis [455]. The unfavourable prognosis in invasive breast cancer is mainly attributed to its inherent ability to metastasize [455]. Unfortunately, the pathogenesis of metastasis remains poorly understood [129]. Currently, the ability to accurately predict the risk for metastatic potential poses a substantial challenge for clinical management of the disease.

Metastasis is one of the hallmarks of cancer [10]. It begins with the removal of cancer cells from the primary tumor site, followed by intravasation of blood vessels [10, 457]. Upon their journey through the vascular system, the metastatic cells extravasate into a new microenvironment where they attach and proliferate to produce secondary tumors [457]. Metastasis is an enormously complex process that involves a wide array of cellular changes, including alterations in cell morphology and expression of cell adhesion molecules [10, 126, 458]. One of the crucial steps in acquiring metastatic potential is the formation of lamellipodia [459-461]. Lamellipodia formation is dependent on the dynamic reorganization of the actin cytoskeleton [461, 462]. Such a modulation of actin network during lamellipodia assembly may relate to a surge in the levels of ATP [463, 464]. In agreement with this speculation, Campello *et al.*, [465] have reported the redistribution of mitochondria to the polarized cytoskeletal organization to regulate the motor activity of the migrating lymphocytes. Hence, it was argued that changes in mitochondrial dynamics were essential to lymphocyte function in the inflamed tissue [465]. Reorganization of the actin cytoskeleton during metastasis is also characterized by the loss of cell adhesion molecule, E-cadherin [10, 466].

Several studies have reported the link between loss of E-cadherin expression and the induction of EMT in cancer cells [467-469]. For example, induction of *c-Fos* oncogene in normal mouse mammary epithelial cell line induced EMT and was associated with a downregulation of E-cadherin expression [467]. Interestingly, several studies [470-472] have reported the formation of binucleated cells upon treatment with anticancer drugs. For example, treatment of MDA-MB-231 breast cancer cells with Dox induced the formation of micronucleated binucleated cells due to intrinsic chromosomal instability of the cell line [471]. Generation of binucleated cells was considered as a compensatory mechanism to maintain the genetic balance to enable cancer progression [471]. Overall, cancer cells undergo cellular adaptations to enable survival of the tumor cells during metastasis.

Doxorubicin (Dox, Adriamycin) is a widely used anthracycline chemotherapeutic agent for the treatment of several cancers including breast, leukaemia, lung, stomach and ovarian cancers [368-371]. Dox is reported to elicit its therapeutic effect by DNA intercalation [375, 376], generation of free radicals [379-381], and inhibition of topoisomerase II [377, 378]. Campiglio *et al.,* [378] have demonstrated that expression of HER2 may play a role in regulating the levels of topoisomerase II, thus predicting the response to Dox therapy in breast cancers. In that study it was revealed that HER2-positive breast tumors were frequently responsive to Dox therapy as compared to HER2-negative cancers, upon administration of 3 cycles of Dox as neoadjuvant chemotherapy. BCIRG-006, a clinical study, reported an overall disease-free survival rate of 75% for adriamycin/cyclophosphamide-docetaxel (ACT), 84% for ACT plus trastuzumab, and 81% for docetaxel/carboplatin plus trastuzumab (TCH) groups in a study population of 3222 patients with HER2-positive metastatic breast cancer [327]. Despite being effective, the ACT plus trastuzumab group had a significantly higher incidence of cardiac dysfunction and heart failure [327]. Although Dox is effective, long-term administration of the drug results in elevated risk of congestive cardiomyopathy [473-475] and chemoresistance [371, 476], thereby limiting its use.

Interestingly, adaptive responses are induced in cancer cells following sublethal doses of some chemotherapeutic agents [477]. For example, exposure of mouse EMT-6 and human MDA-MB-231 breast cancer cell lines to cisplatin for five days induced transient but substantial resistance to the drug [478]. In that study, it was observed that exposure to cisplatin was accompanied by the formation of compact multicellular spheroids in the breast cancer cell lines.

In a different study, Yoshida *et al.,* [479] have reported acquired resistance to tumor necrosis factor-related apoptosis-inducing ligand (TRAIL) induced cytotoxicity in MDA-MB-231 breast cancer cell lines upon exposure to subtoxic doses of TRAIL. Similarly, depending on the dosage regimen and cell type, Dox may elicit multiple mechanisms of action [370, 480]. For example, Amalina *et al.,* [480] have reported that low doses of Dox induced lamellipodia formation and promoted migration in 4T1 and MDA-MB-231 breast cancer cell lines at 24 h after drug treatment. However, prolonged exposure of the cell lines to Dox treatment beyond 48 h resulted in cell death in both the cell lines. In a different study, Liu *et al.,* [370] have demonstrated that treatment with Dox augmented cell migration and invasion of MCF-7 and BT474 breast cancer cell lines via activation of Rho/MLC pathway. Prior treatment with RhoA inhibitor suppressed the migration and invasion promoting effects of Dox in these cell lines [370]. Hence, an investigation of some possible effects of Dox treatment in the metastatic potential of breast cancer cell lines may provide insights into cancer chemotherapy.

Over the past decade, combination therapies have become a promising method in the treatment of cancers that are resistant to monotherapy [401]. Lapatinib (Lap) is a dual-EGFR/HER2 inhibitor [151-153] that is effectively used in combination with capecitabine to treat trastuzumab-resistant advanced HER2-amplified breast cancers [481-484]. Boccardo *et al.,* [485] have reported that Lap in combination with capecitabine increased the response rate, time to disease progression, and progression-free survival in patients with refractory HER2-positive breast cancer when compared to those who received capecitabine treatment alone. A phase III randomized study (EGF100151) that included 399 patients with locally advanced metastatic breast cancer, compared the use of Lap along with capecitabine versus capecitabine alone [486]. In that study, it was reported that very few patients on Lap and capecitabine therapy developed brain metastasis, with a 20% lower risk of death when compared to those who were treated with capecitabine alone.

Lapatinib was also studied in combination with other anticancer chemotherapies including taxanes [487], anthracyclines [369, 488], and carboplatin [489]. Since, one-third of the advanced HER2-amplified breast cancers have potential for brain relapse [137, 488, 490, 491], combination therapy of Lap with anthracyclines may offer therapeutic advantage in the clinical management of the disease.

In such a combination regimen, Lap may have greater ability to cross the blood-brain barrier [341], whilst Dox is retained in the cells due to its DNA intercalating ability [368]. Interestingly, combination of Lap with epirubicin (epimer of Dox) was tested in a phase I clinical study, NCT00753207 [394]. The study reported that the combination therapy was well tolerated in patients with HER-positive/topoisomerase II-positive metastatic breast cancer and suitable for further investigation in a phase II study.

The present study aimed to investigate the phenotypic alterations in breast cancer cell lines induced by low doses of chemotherapeutic agent(s). In this study, the cell viability of different breast cancer cell lines including SKBR3 (HER2-positive), MDA-MB-231 (triple-negative), T47D (ER-positive/PR-positive) and HMF (human mammary fibroblast) in response to varying doses of Dox and Lap was assayed. Furthermore, phenotypic alterations including reorganization of actin filaments, mitochondrial localization and migration of SKBR3 cells in response to 0.1µM Dox treatment were studied. In addition, the IC_{50} of 5µM Lap was used to study its inhibitory effects on Dox-induced morphological changes in these cells. Following respective drug treatments, morphological parameters were examined and their effects on migration of SKBR3 breast cancer cell line were studied by MTS assays, scratch wound healing assays and fluorescence microscopy respectively. Also, the effect of drug treatment on the protein levels of G3BP-1 and LDH-A was assessed using Western blot analysis to investigate if such treatment regulated the expression of these biomarkers.

5.2 Materials and Methods

5.2.1 Cell lines and reagents

The SKBR3, MDA-MB-231, and T47D breast cancer cell lines, along with human mammary fibroblasts used in this study were obtained from American Type Tissue Culture (ATCC, USA) and cultured as previously described in section 2.2.1. Lapatinib was purchased from Sigma-Aldrich Co., and Dox was a generous gift from Assoc. Prof. Kathryn Tonissen, School of Environment and Science, Griffith University, Australia. The drugs were stored at a stock concentration of 10mM in DMSO at -20 °C. Paraformaldehyde (PFA) was purchased from Sigma-Aldrich Co. ActinGreen 488, NucBlue Fixed Cell ReadyProbes, and MitoTracker Green FM were obtained from Thermo Fisher Scientific.

5.2.2 Cell viability assay

Cells were seeded in a 96-well plate (Sarstedt Co., Numbrecht, Germany) at a density of 5 x 10^3 cells per well in 100 µL of complete medium and incubated at 37 °C for 48 h. Post-seeding, the medium was removed and 100 µL of fresh medium containing different concentrations of either Dox (0.01-10µM) or Lap (0.01-100µM) were added and incubated for 24 h. Following the drug treatment, 20µl of MTS was added and further incubated for 1 h at 37 °C. The optical density (O.D) was read at 490 nm with SpectraMax M3-Molecular devices (San Jose, CA, USA). The percentage of DMSO in the medium was 0.1% (v/v).

5.2.3 Cell proliferation assay

SKBR3 cells were seeded at a density of 2 x 10^5 cells/well in a 6-well plate and incubated at 37ºC in a humidified incubator inclusive of 5% CO_2. Two days after seeding, the cells were treated with 0.1µM Dox for 24, 48 and 72 h respectively. Following the duration of Dox treatment, the cells were washed with PBS to discard the dead cells. The adherent cells were trypsinized and the pellet was resuspended in PBS. A single wash of the cells with PBS was followed with incubation with 4% PFA at room temperature. PFA fixed cells were washed with PBS. Following manufacturer's instructions, the cells were incubated with two drops of NucBlue ReadyProbes reagent per ml for 30 min to stain the nuclei.

A volume of 20µl was pipetted on the hemocytometer and fluorescent images of the cells were captured using Nikon Eclipse Ti2-LAPP inverted microscope. The cells in four peripheral squares of the hemocytometer were counted for 0.1µM Dox treated and control SKBR3 cells for the respective time points.

5.2.4 Immunofluorescence

SKBR3 cells treated with either 0.1µM Dox, 5µM Lap, 0.1µM Dox+5µM Lap, or DMSO alone (vehicle control) for 24 h were rinsed three times using analytical grade PBS. Cells were fixed for 30 min at room temperature using 4% PFA, followed by washing once in PBS. Following manufacturer's instructions, the PFA fixed cells were incubated with 2 drops each of ActinGreen488 and NucBlue ReadyProbes reagent per ml of the medium for 30 min. Staining with MitoTracker Green FM was achieved by resuspending the live cells in 100µl of PBS containing 15ng/ml of the dye and incubation for 45 min. Cells were then washed twice in PBS prior to imaging.

5.2.5 Acridine orange/propidium iodide assay

SKBR3 at a density of 2 x 10^5 cells/well were seeded in a 6-well plate and 48 h post seeding the cells were treated with 0.1µM Dox, 5µM Lap, 0.1µM Dox+5µM Lap, or DMSO alone for 24 h respectively. Following the drug treatment, culture supernatant containing the dead cells was collected. The adherent cells were trypsinized and the cell pellet was resuspended in the culture supernatant that was previously collected. After resuspending the cells, 5µl of acridine orange (10µg/ml)+5µl propidium iodide (10µg/ml) was added to the cell suspension and incubated briefly at room temperature. A small aliquot of cell suspension for each treatment condition was pipetted onto a glass slide and representative fluorescent images of the cells stained with acridine orange (green) and/or propidium iodide (orange to red) were captured using Nikon Eclipse inverted microscope.

5.2.6 Scratch wound closure assay

SKBR3 cells were seeded at a density of 2 x 10^4 cells per well in 100µl of complete medium in a 96-well plate and incubated at 37 °C for 72 h. Thereafter, a scratch (wound) was made in the bottom center of the well within the confluent cell layer by using a 100µl yellow pipette tip. The medium was subsequently aspirated, and the cells were gently washed twice in PBS to remove detached cells. The cells were treated with either 0.1µM Dox, 5µM Lap, 0.1µM Dox+5µM Lap, or DMSO alone respectively in 100µl of fresh medium per well and incubated for 24 h at 37 °C. Following drug treatment, a brief rinse in PBS was performed and the cells were fixed with 4% PFA for 30 min at room temperature, washed once in PBS and stained with ActinGreen 488 and NucBlue ReadyProbes reagent for 30 min. Cells were then washed twice in PBS prior to imaging. The cell migration was visualized using a Nikon Eclipse T*i*2-LAPP fluorescent microscope. Representative magnification images were acquired at 10x lens magnification at 0 and 24 h after drug treatment. The area of the wound in the microscopic images was measured using ImageJ. Migration was reported as the percentage of gap closure at 24 h relative to the total wound area at 0 h of the same wound spot.

5.2.7 Microscopy

Fluorescent images were acquired using the Nikon Eclipse T*i*2-LAPP Inverted Microscope System. Image analysis was performed with NIS-Elements AR Software (Nikon Instruments Inc.). Representative high magnification images were acquired at either 10x or 20x lens magnification for actin (490nm), nucleus (360nm) and mitochondria (490nm) respectively. Images were acquired from each assay well with a minimum of 100 cells in each experiment. All tests consisted of three biological repeats. Quantification of the images was performed using ImageJ 1.51*v* software (National Institutes of Health, USA).

5.2.8 Western blot

Whole-cell lysates were used for immunoblotting. Following the respective drug treatment(s), the cells were washed with cold phosphate-buffered saline (PBS) and then lysed with RIPA lysis buffer (Thermo Fisher Scientific). The protein concentrations were determined using the DC protein assay kit (Bio-Rad Laboratories) as previously described in section 2.2.16. Equal amounts of the protein samples were run on SDS-PAGE. Following the separation, proteins were transferred to Immobilin-P transfer membranes (Millipore). Western blot analysis was performed as described in section 2.2.14. The primary antibodies used in this study included anti-G3BP, anti-LDH-A (Abcam Plc), anti-PCNA (Cell Signaling Technology), and anti-β-actin (Sigma-Aldrich). HRP-conjugated secondary antibodies were purchased from Invitrogen.

5.2.9 Statistical analysis

Each assay was performed in triplicate and independently repeated at least three times. Data are presented as mean $\pm$ SD (standard deviation). Statistical analysis was achieved using Graphpad Prism 6 software (San Diego, CA, USA). Student t-tests or one-way analysis of variance (ANOVA), followed by a Bonferroni test (unless otherwise stated) were performed. All statistical analysis was performed at $p < 0.05$ level of significance.

5.3 Results

5.3.1 Effect of doxorubicin and lapatinib on cell viability

A study was undertaken to evaluate the *in vitro* cytotoxic effects of Dox and Lap in breast cancer cells at increasing concentrations of the drugs for 24 h. HMF, SKBR3 and MDA-MB-231 breast cancer cells were treated with varying doses (0.01-10µM) of Dox (**Fig. 5.1A**). Dox significantly inhibited the viability of HMF cells at 1.0µM and 10µM ($p < 0.001$). However, a similar inhibition of cell viability was observed only at 10µM in SKBR3 cells. Interestingly, at 0.1µM Dox, there was a significant increase in the viability of SKBR3 cells ($p < 0.01$) as compared to the vehicle control. In case of MDA-MB-231 cells, the cell viability was inhibited ($p < 0.01$) at 10µM of Dox treatment. The potency (half maximal inhibitor concentration; IC_{50}) was estimated to be 0.70µM, 8.33µM, and 14.91µM for HMF, SKBR3, and MDA-MB-231 breast cancer cell lines respectively. **Fig. 5.1B** shows the effect of varying concentrations (0.01-100µM) of Lap on HMF, SKBR3, MDA-MB-231, and T47D breast cancer cells. The results indicate that Lap significantly inhibited HMF cell viability ($p < 0.01$) at 10µM and 100µM respectively. In contrast, Lap was more effective in SKBR3 cells, which showed significant decrease in the cell viability ($p < 0.01$) between 0.1µM to 100µM of the drug concentration. In the case of MDA-MB-231 cells, Lap significantly inhibited the cell viability ($p < 0.01$) at 10µM and 100µM respectively. The effect of Lap on T47D cells was significant between 1.0µM and 100µM respectively. Furthermore, there was no increase in the cell viability of SKBR3 cells at lower doses of Lap. The IC_{50} values were calculated to be 117.00µM, 5.00µM, 121.80µM, and 110.00µM for HMF, SKBR3, MDA-MB-231, and T47D breast cancer cell lines respectively. To further investigate the effect of 0.1µM of Dox on the viability of SKBR3 cells over time; a time-dependent incubation (24, 48 and 72 h) of cells with 0.1µM Dox was performed (**Fig. 5.1C**). The results obtained from the study showed that the viability of control cells increased exponentially between 0 to 72 h. In the 0.1µM Dox treated cells, there was a significant increase in the viability ($p < 0.01$) at 24 h after drug treatment as compared to the control cells. However, such increase in viability was not observed at 48 and 72 h in the Dox treated cells. Since 0.1µM Dox significantly increased the viability of SKBR3 cells (**Fig. 5.1A**), the IC_{50} dose of 5µM Lap in combination with 0.1µM Dox was used to investigate its effect on the cell viability of SKBR3 cells. The results indicated a significant decrease in the viability ($p < 0.001$) of 0.1µM Dox+5µM Lap treated cells when compared to the 0.1µM Dox alone treated cells (**Fig. 5.1D**).

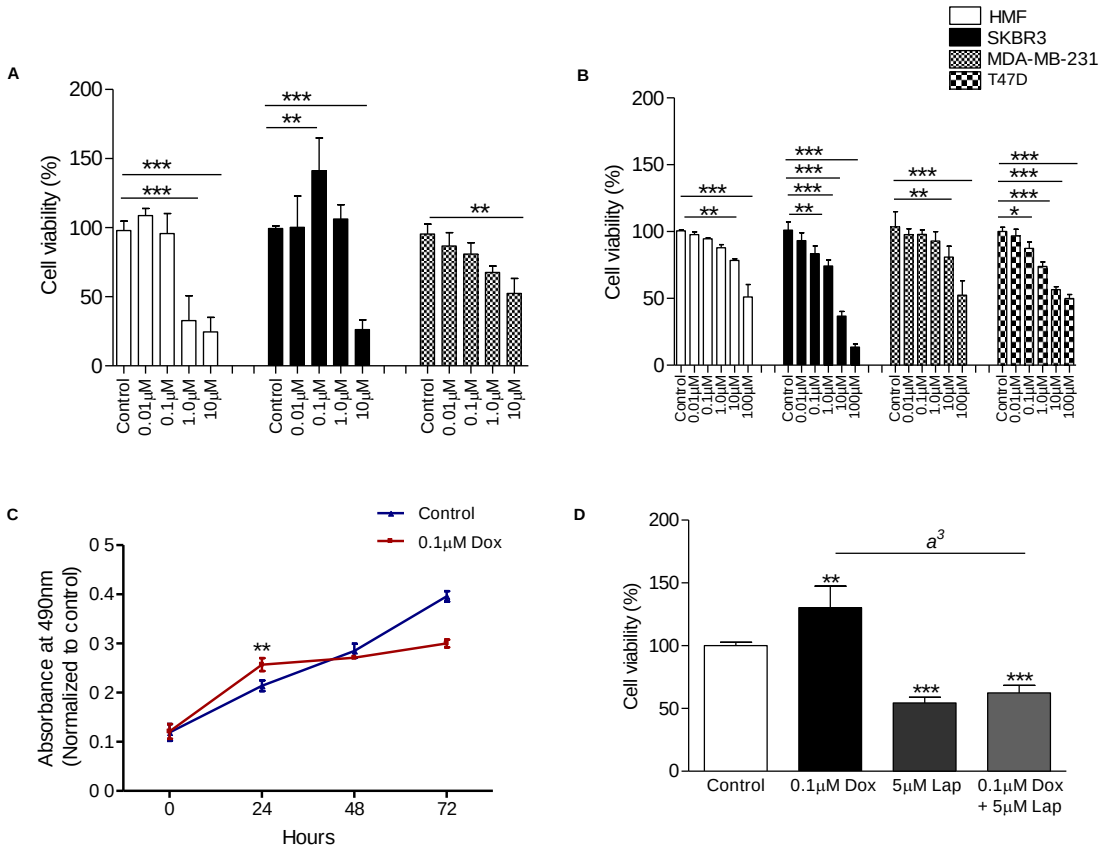

Figure 5.1: Effect of doxorubicin and lapatinib on the cell viability of breast cancer cell lines. Effect of doxorubicin (0-10µM) and lapatinib (0-100µM) on the cell viability of HMF, SKBR3, MDA-MB-231, and T47D breast cancer cells has been represented in **Fig. 5.1A** and **Fig. 5.1B** respectively. Cell lines were treated with varying doses of either Dox (0-10µM) or Lap (0-100µM) and incubated for 24 h respectively. Following the drug treatment, cell viability was determined by using MTS assay at OD_{490nm}. Data are expressed as the percentage of control (untreated) cell viability upon treatment with either Dox or Lap respectively. **Fig. 5.1C**: Effect of 0.1µM Dox on the cell viability of SKBR3 cells at different time points. SKBR3 cells were treated with 0.1µM Dox for 24, 48 and 72 h respectively. Following the drug treatment cell viability was determined. Absorbance values of the treated samples at each time point were normalized to the respective controls. Statistical analysis was done using Student's t-test and ** $p<0.01$, indicated a significant increase in the cell viability at 24 h as compared to the control. **Fig. 5.1D**: Effect of drug combination on the cell viability of SKBR3 cells. Cells were treated with either 0.1µM Dox, 5µM Lap or a combinational dose of 0.1µM Dox+5µM Lap for 24 h respectively. Cell viability was expressed as the percentage of control cell viability following drug treatment. Statistical significance is represented as ** $p<0.01$, *** $p<0.001$ when compared to the control. Also, a^3 $p<0.001$ indicates 0.1µM Dox versus 0.1µM Dox+5µM Lap. Bars represent mean ± SD of three independent experiments. The data obtained was analyzed using one-way analysis of variance (ANOVA) followed by Bonferroni's multiple comparison test; unless otherwise stated. Dox=Doxorubicin, Lap=Lapatinib.

5.3.2 Effect of 0.1µM doxorubicin on the proliferation of SKBR3 breast cancer cell line

Further study was undertaken to evaluate the effect of 0.1µM Dox on the proliferation of SKBR3 cells. The cells were treated with the indicated dose of Dox for 24, 48, and 72 h respectively. Following a protocol published elsewhere [492, 493] with minor amendments, the cell proliferation was studied based on the increase in the cell count by staining the nuclei with NucBlue™ Ready Probes™ reagent. **Fig. 5.2A**. Left panel represents merged bright field and fluorescent images of the cells on hemocytometer following the respective drug treatment. The right panel revealed that 0.1µM Dox treatment for 24 h did not induce proliferation of SKBR3 cells as the cell count of the drug treated versus control was not significantly different. In contrast, Dox treatment for 48 and 72 h resulted in a statistically significant decrease in the cell count when compared to the respective controls. To further assess the effect of 24 h treatment of SKBR3 cell line with 0.1µM Dox, protein expression levels of peripheral cell nuclear antigen (PCNA), a cell proliferative marker used in cancers including breast cancer [229, 494, 495] were determined in drug treated and the corresponding control cells (**Fig. 5.2B**). The top panel represents the immunoblot using anti-PCNA to study the protein levels of PCNA following 24 h treatment of SKBR3 cell line with 0.1µM Dox and the respective control. The bottom panel that represents the histogram obtained by the analysis of the blot revealed no significant difference in the relative expression of PCNA between 0.1µM Dox treated and the corresponding control. These findings verified that the previously observed increase in cell viability of SKBR3 cells upon treatment with 0.1µM Dox (**Fig. 5.1A**) was not due to enhanced proliferation.

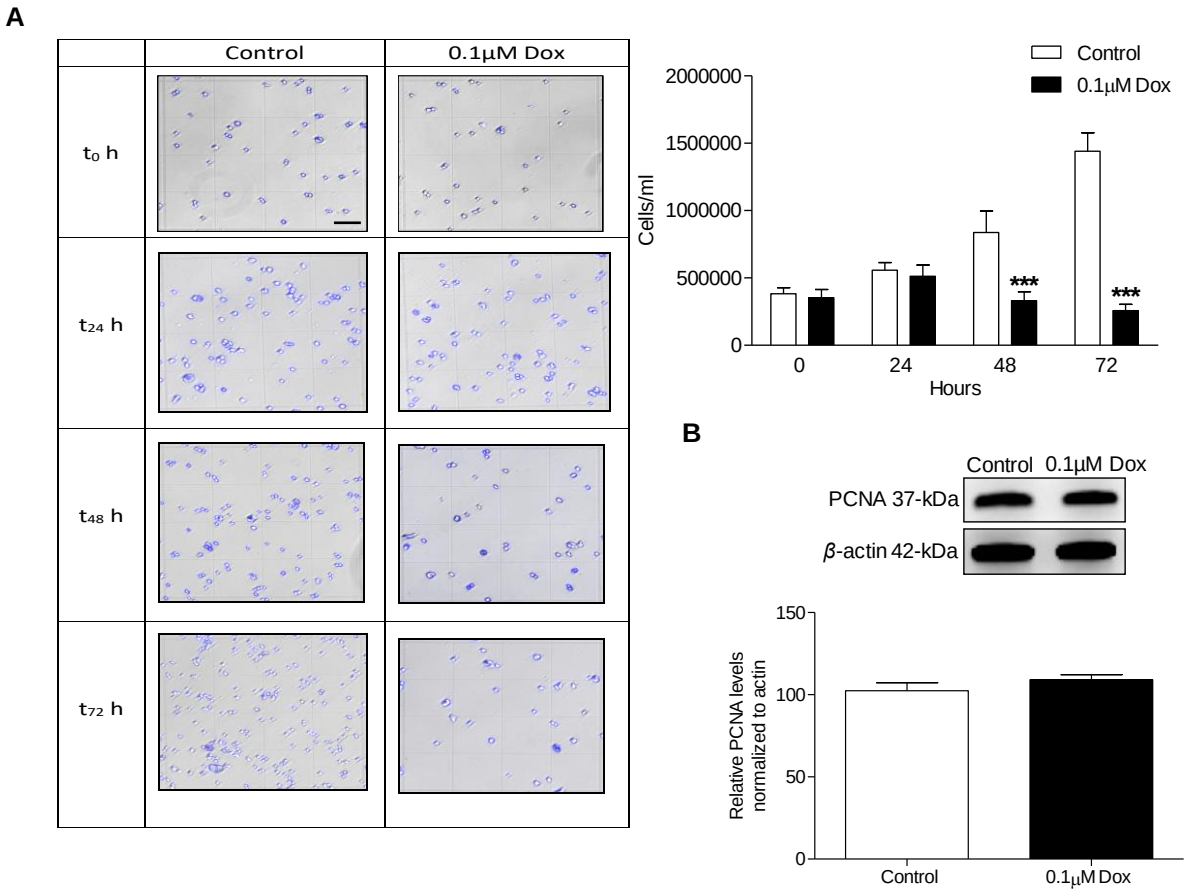

Figure 5.2: Effect of 0.1µM doxorubicin on the cell proliferation of SKBR3 breast cell line. Cells were treated with 0.1µM Dox for 24, 48 and 72 h respectively. Following the drug treatment, cells were fixed with PFA and incubated with NucBlue Fixed Cell ReadyProbes reagent to stain the nuclei (blue fluorescence). **Fig. 5.2A.** Left panel represents the merged-bright field and fluorescent images of the cells loaded on the hemocytometer for cell counting. Image of one of the sets of 16 squares on hemocytometer that was used for cell counting has been represented in the images. Images were taken at original magnification of 4x using Nikon Eclipse Ti2-LAPP inverted microscope. Scale bar: 250µm. Right panel represents the histogram obtained from the cell count using hemocytometer for each treatment condition. Statistical significance is represented as *** p<0.001 between 0.1µM Dox treated versus the respective control for the indicated duration of Dox treatment. Bars represent mean $\pm$ SD of three independent experiments. The data obtained was analyzed using one-way analysis of variance (ANOVA) followed by Bonferroni's multiple comparison test. **Fig. 5.2B**. Top panel represents the immunoblot result of the expression of PCNA following 0.1µM Dox treatment of SKBR3 cell line for 24 h. β-actin was used as a loading control. The bottom panel shows the relative expression of PCNA compared to the untreated sample obtained by densitometric analysis of the immunoblot data. Upon Dox treatment, there was no statistical significance in the protein levels of PCNA between 0.1µM Dox treatment and the respective control. Student's t test was performed. The data was expressed as mean $\pm$ SD of three independent experiments. Dox=Doxorubicin, PCNA=peripheral cell nuclear antigen.

5.3.3 Impact of drug treatment on F-actin distribution in SKBR3 breast cancer cell line

To further investigate the impact of drug treatment on the cell morphology, a study on changes in the organization of actin cytoskeleton upon 0.1µM Dox treatment of SKBR3 cells was undertaken. Following 0.1µM Dox, 5µM Lap, and 0.1µM Dox+5µM Lap treatment for 24 h, the cells were fixed and stained with ActinGreen™ 488 and NucBlue™ ReadyProbes reagent. Fluorescent images of the treated cells were acquired and the cells were divided into three categories (**Fig. 5.3A**)- normal F-actin (normal filamentous actin), F-actin aggregates (absence of detectable actin fibres), and prominent F-actin (barbed end formation) depending on the structure of their actin cytoskeleton as described elsewhere [496, 497]. These results (**Fig. 5.3B**) demonstrated a significant decrease ($p < 0.001$) in the normal F-actin fibres when the cells were treated with either-0.1µM Dox, 5µM Lap or 0.1µM Dox+5µM Lap when compared with the respective control. Regarding F-actin aggregates, 5µM Lap and 0.1µM Dox+5µM Lap formed high ($p < 0.001$) F-actin aggregates in contrast with the control. Importantly, 0.1µM Dox treatment significantly ($p < 0.001$) enhanced the formation of prominent F-actin fibres when compared to the control. In addition, there was a decrease ($p < 0.001$) in the prominent F-actin upon 0.1µM Dox+5µM Lap treatment versus 0.1µM Dox treatment alone.

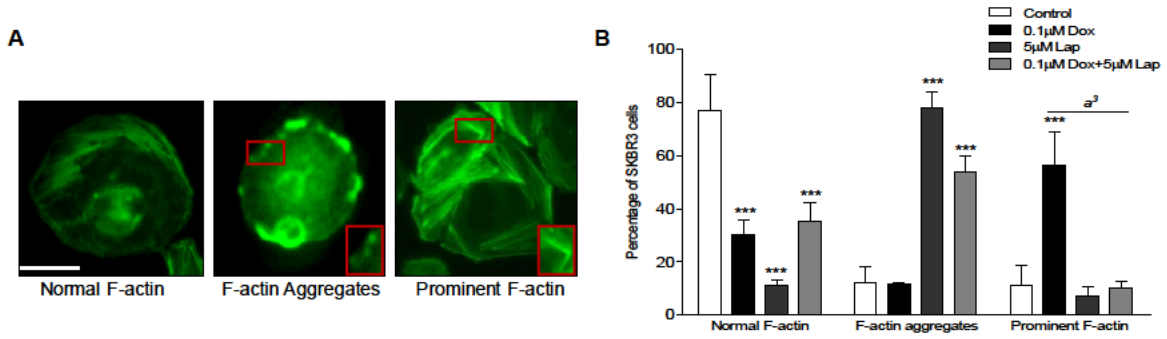

Figure 5.3: Changes in the actin cytoskeleton structure upon treatment of SKBR3 breast cancer cells with 0.1μM Dox, 5μM Lap and 0.1μM Dox+5μM Lap. Cells were treated with either- 0.1μM Dox, 5μM Lap or a combinational dose of 0.1μM Dox+5μM Lap for 24 h respectively. **Fig. 5.3A**: Cells were categorized into three categories based on their F-actin organization-normal F-actin, F-actin aggregates (magnified inset), prominent F-actin (magnified inset); as stained with ActinGreen 488 ReadyProbes reagent to detect actin. Images were taken at original magnification of 20x using Nikon Eclipse Ti2-LAPP inverted microscope. Scale bar: 100μm. **Fig. 5.3B**: Cells were scored according to their F-actin organization as in (**A**) and presented as percentage of total cells. Statistical significance is represented as ***$p<0.001$ when compared to the respective controls. Also, within the prominent F-actin, a^3 $p<0.001$ indicated 0.1μM Dox versus 0.1μM Dox+5μM Lap. Bars represent mean ± SD of three independent experiments, n ≥100 cells in each experiment. The data obtained was analyzed using one-way analysis of variance (ANOVA) followed by Bonferroni's multiple comparison test. Dox=Doxorubicin, Lap=Lapatinib.

Interestingly, fluorescent microscopic images of 0.1µM Dox and 5µM Lap revealed distinct morphological features. Following 0.1µM Dox treatment, the SKBR3 cells showed migratory phenotypes, characterized by membrane protrusions such as lamellipodia or filopodia at the leading edge of the cells (**Fig. 5.4A**). In contrast, the cells treated with 5µM Lap showed a higher proportion of actin aggregates when visualized (**Fig. 5.4B**).

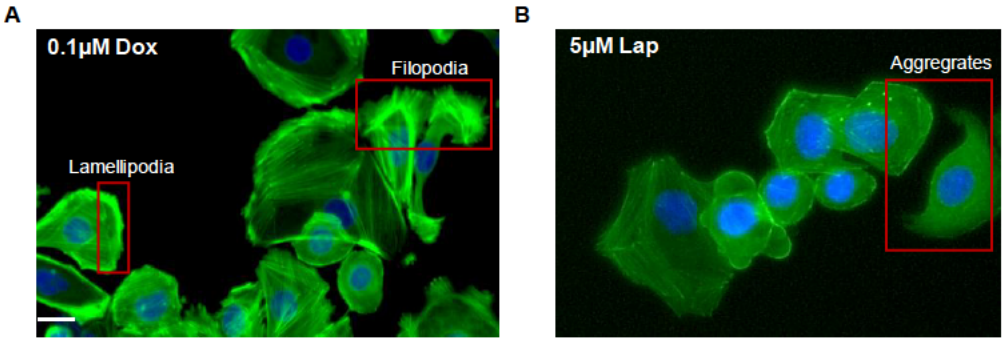

Figure 5.4: Changes in the cell morphology of SKBR3 breast cancer cells following the drug treatment. Representative fluorescent images of SKBR3 cells upon treatment with 0.1µM Dox (**Fig. 5.4A**) and 5µM Lap (**Fig. 5.4B**) for 24 h respectively. Images were taken at original magnification of 40x using Nikon Eclipse Ti2-LAPP inverted microscope. Scale bar: 100µm. **Fig. 5.4A**. SKBR3 cells treated with 0.1µM Dox showed characteristic migratory phenotypes with lamellipodia or filopodia at the leading edge of the cells. **Fig. 5.4B**. Cells treated with 5µM Lap showed actin aggregation and an absence of migratory phenotype.

5.3.4 Effect of drug treatment on the mitochondrial distribution in SKBR3 breast cancer cell line

Observed changes in the F-actin cytoskeleton of drug treated SKBR3 cells suggested the need for abundant ATP supply to enable cell reorganization. Therefore, the extent of mitochondrial spread in the drug treated SKBR3 breast cancer cell line was investigated. Following the dosage regimen of 0.1µM Dox, 5µM Lap and 0.1µM Dox+5µM Lap respectively for 24 h, SKBR3 cells were stained with MitoTracker Green FM and fluorescent images of the treated cells were acquired (**Fig. 5.5A**). Using ImageJ, the images of the cells were manually traced for mitochondrial localization. The extent of mitochondrial spread in the drug treated cells was obtained upon normalization with the control cells. Data shown in **Fig. 5.5B** indicated that 0.1µM Dox induced a significant 2-fold increase ($p < 0.01$) in the mitochondrial spread, as compared to the control. In contrast, 5µM Lap, and 0.1µM Dox+5µM Lap treatments effectively decreased ($p < 0.05$) the mitochondrial spread when compared to 0.1µM Dox treatment

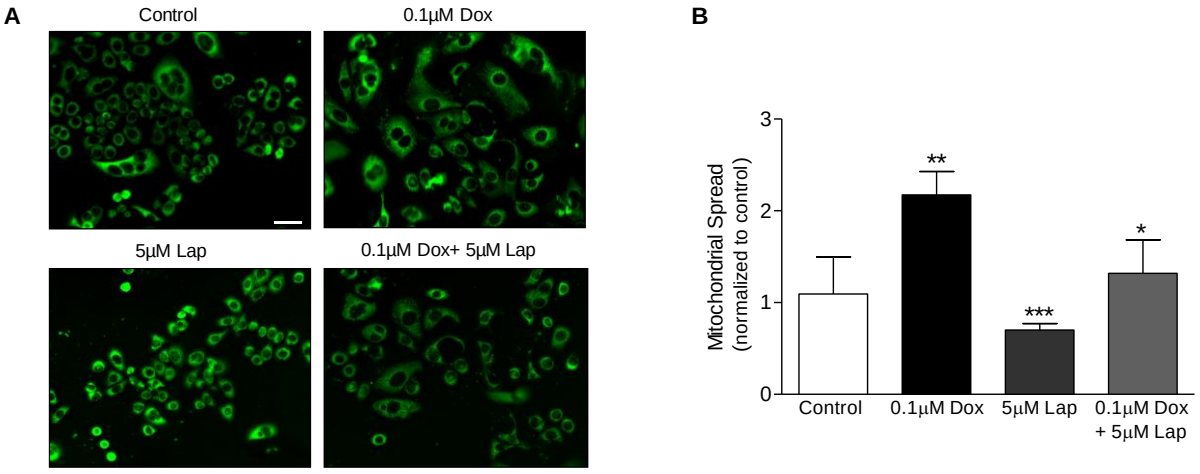

Figure 5.5: Changes in the mitochondrial distribution upon drug treatment of SKBR3 breast cancer cell line. Cells were treated with either 0.1µM Dox, 5µM Lap or a combination dose of 0.1µM Dox+5µM Lap for 24 h respectively. **Fig. 5.5A**. Representative images of the SKBR3 cells stained to detect mitochondria (green fluorescence from MitoTracker Green FM), show the mitochondrial spread. Images were taken at original magnification of 20x using Nikon Eclipse Ti2-LAPP inverted microscope. Scale bar: 50µm. **Fig. 5.5B**. Data were analyzed by measuring the mitochondrial spread for each of the drug treatments normalized to the control. Statistical significance is represented as ** p<0.01 when compared to control; *** p<0.001, * p<0.05 0.1µM Dox versus 5µM Lap and 0.1µM Dox+5µM Lap respectively. Bars represent mean $\pm$ SD of three independent experiments. The data obtained were analyzed using one-way analysis of variance (ANOVA) followed by Bonferroni's multiple comparison test. Dox=Doxorubicin, Lap=Lapatinib.

5.3.5 Effect of drug treatment on the cell migration of SKBR3 breast cancer cell line

Investigation into the reorganization of actin cytoskeleton and changes in the mitochondrial spread upon drug treatment of SKBR3 cells suggested a potential impact on the cell migration. Hence, an *in vitro* scratch wound healing assay was performed to assess the effect of drug treatment on the migration of these cells. Cell migration was measured as the percentage of gap closure over a period of 24 h upon treatment of the cells with either 0.1µM Dox, 5µM Lap and 0.1µM Dox+5µM Lap respectively. At the end of 24 h treatment, the cells were fixed and stained with ActinGreen™ 488 and NucBlue ReadyProbes™ reagent and fluorescent images of the cells were acquired (**Fig. 5.6A**). Quantitative analysis of the bright field images (**Fig. 5.6B**) revealed that compared to the control, 0.1µM Dox treated cells significantly enhanced the migration of SKBR3 cells ($p < 0.001$), whilst cell migration was inhibited significantly by 5µM Lap ($p < 0.001$) and 0.1µM Dox+5µM Lap treatment ($p < 0.05$) respectively. Furthermore, there was a significant inhibition of cell migration ($p < 0.001$) between 0.1µM Dox versus 0.1µM Dox+5µM Lap treatment (**Fig. 5.6C**).

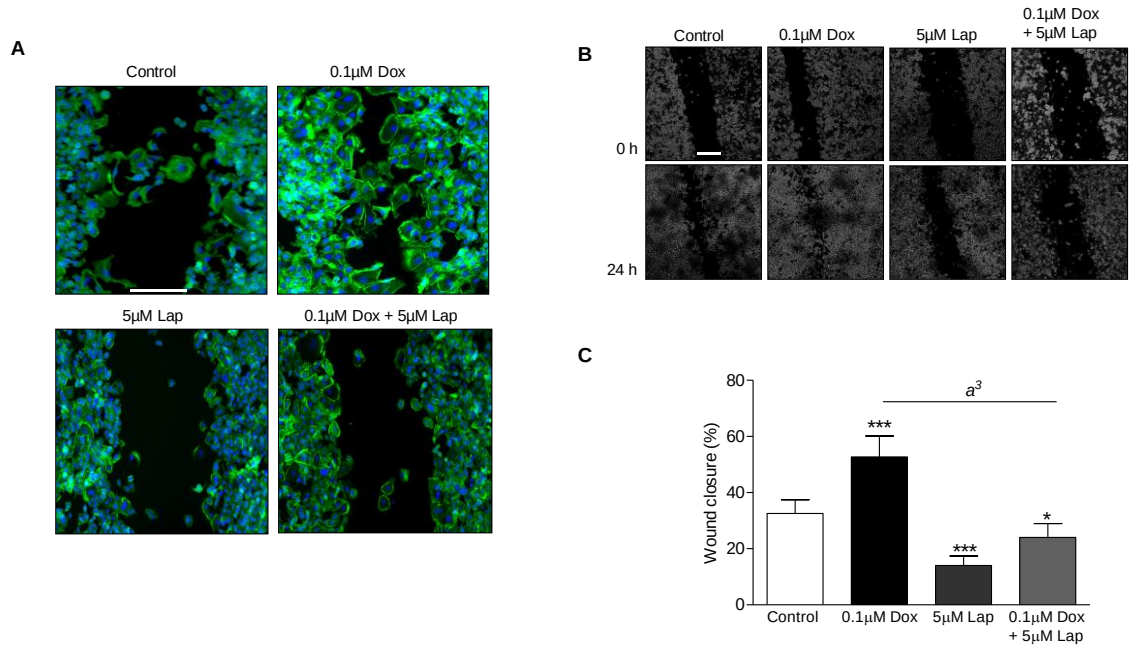

Figure 5.6: Effect of drug combination on the migration of SKBR3 breast cancer cells. **Fig. 5.6A**. Representative fluorescent images of the scratch wound healing after 24 h of control, 0.1µM Dox, 5µM Lap or a combination dose of 0.1µM Dox+5µM Lap treated SKBR3 cells. Cells were stained to detect- actin (green fluorescence from ActinGreen 488 ReadyProbes reagent) and nuclei (blue fluorescence from NucBlue Fixed Cell ReadyProbes reagent). Images were taken at original magnification of 10x using Nikon Eclipse Ti2-LAPP inverted microscope. **Fig. 5.6B**. Representative brightfield images of the drug treated SKBR3 cells at 0 and 24 h post-scratch. **Fig. 5.6C**. Data is expressed as the percentage of gap closure after 24 h of the respective drug treatments. Scale bar: 200µm. Statistical significance is represented as *** $p<0.001$,* $p<0.05$, when compared to the control. Also, a^3 $p<0.001$ indicates 0.1µM Dox versus 0.1µM Dox+5µM Lap. Bars represent mean ± SD of three independent experiments. The data obtained was analyzed using one-way analysis of variance (ANOVA) followed by Bonferroni's multiple comparison test. Dox=Doxorubicin, Lap=Lapatinib.

5.3.6 Morphological assessment of apoptotic SKBR3 cells by AO/PI double staining

Since the cell viability studies revealed a significant reduction in the viability of SKBR3 cells upon 5μM Lap and 0.1μM Dox+5μM Lap treatment (**Fig. 5.1D**), acridine orange/propidium iodide double staining was used to further investigate the induction of apoptosis. Following the dosage regimen of 0.1μM Dox, 5μM Lap and 0.1μM Dox+5μM Lap for 24 h, SKBR3 cells were stained with AO/PI and fluorescent images of the cells were acquired (**Fig. 5.7A**). The control and 0.1μM Dox showed diffuse green fluorescence that was indicative of viable cells. In contrast, 5μM Lap and 0.1μM Dox+5μM Lap treatment groups showed an increase in the number of cells with orange/red fluorescence that suggested an apoptotic induction. Apoptotic features including membrane blebbing, chromatin condensation, nuclear fragmentation, and apoptotic bodies were observed in the cells treated with 5μM Lap and 0.1μM Dox+5μM. Necrotic cells stained red with PI, which penetrated the nuclear matter where the cell membrane was compromised. Data shown in **Fig. 5.7B** indicated a significant increase in the apoptotic cells between 5μM Lap versus either-control or 0.1μM Dox treatment. Whilst, the apoptotic cell population increased from 4.3% to 41.8% ($p < 0.001$) compared between 0.1μM Dox and 5μM Lap or 0.1μM Dox+5μM Lap, the necrotic cell subpopulation was 2.0% and 6.1% for 0.1μM Dox, and Lap treatment respectively. Interestingly, the difference in apoptotic induction between 5μM Lap and 0.1μM Dox+5μM Lap treatment was not significant. Consistent with the reports presented elsewhere [498], in this study, treatment of SKBR3 breast cancer cell line with 5μM Lap and 0.1μM Dox+5μM Lap significantly induced apoptosis when compared to the corresponding control or 0.1μM Dox treatment alone.

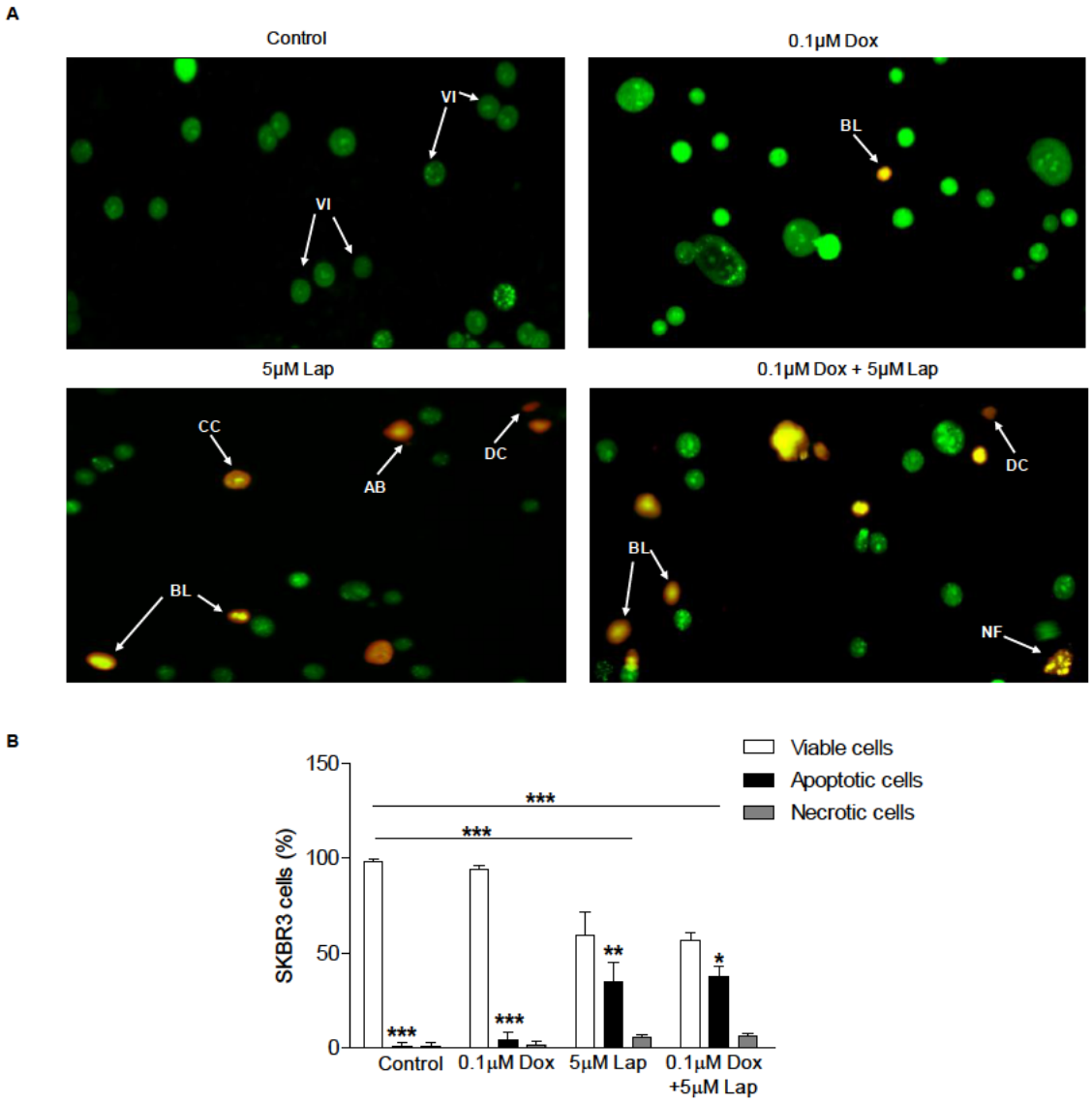

Figure 5.7: AO/PI double stained SKBR3 breast cancer cells following the respective drug treatment. Cells were treated with either- 0.1μM Dox, 5μM Lap or a combinational dose of 0.1μM Dox+5μM Lap for 24 h. **Fig. 5.7A**. Representative fluorescent images of the AO/PI stained SKBR3 cells revealed normal cell structure for control, and a subpopulation of cells with enlarged cell structure when treated with 0.1μM Dox. Treatment with 5μM Lap and 0.1μM Dox+5μM Lap predominantly showed characteristics of apoptosis including membrane blebbing, chromatin condensation, nuclear fragmentation and apoptotic bodies. Images were taken at original magnification of 20x using Nikon Eclipse Ti2-LAPP inverted microscope. Scale bar is 100μm. **Fig. 5.7B**. Cells were scored based on the AO/PI staining and presented as percentage of total cells. Statistical significance is represented as * $p<0.05$, ** $p<0.01$, and *** $p<0.001$ when compared to the corresponding viable cells within each treatment condition. Also, a significant increase in apoptosis was observed in 5μM Lap and 0.1μM Dox+5μM Lap groups when compared to the viable cell population of the control group. Bars represent mean ± SD of three independent experiments, n ≥100 cells in each experiment. The data obtained was analyzed using one-way analysis of variance (ANOVA) followed by Bonferroni's multiple comparison test. VI=Viable, CC=Chromatin condensation, BL=Membrane blebbing, AB=Apoptotic bodies, NF=Nuclear fragmentation, DC=Dead cell. Dox=Doxorubicin, Lap=Lapatinib.

5.3.7 Effect of drug treatment on the protein levels of G3BP-1 and LDH-A in SKBR3 breast cancer cell line

Since Lap treatment was shown to regulate the protein expression levels of G3BP-1 and LDH-A in a panel of breast cancer cell lines including SKBR3 (**Figure 3.7**), the effect of 0.1µM Dox, 5µM Lap and 0.1µM Dox+5µM Lap on the expression of G3BP-1 and LDH-A in SKBR3 cell line was also studied. **Figure 5.8** shows the immunoblot using anti-G3BP-1 and anti-LDH-A antibodies to study the protein levels of G3BP-1 and LDH-A upon respective drug treatment(s). The intensity of bands corresponding to G3BP-1 and LDH-A in 5µM Lap and 0.1µM Dox+5µM Lap was reduced when compared to the control (**Fig. 5.8A**). *β*-actin was used as a loading control. Analysis of the blot showed that the protein levels of G3BP-1 and LDH-A were significantly downregulated ($p < 0.01$) in 5µM Lap and 0.1µM Dox+5µM Lap in comparison to the control. However, 0.1µM Dox treatment did not regulate the levels of these biomarkers (**Fig. 5.8B**).

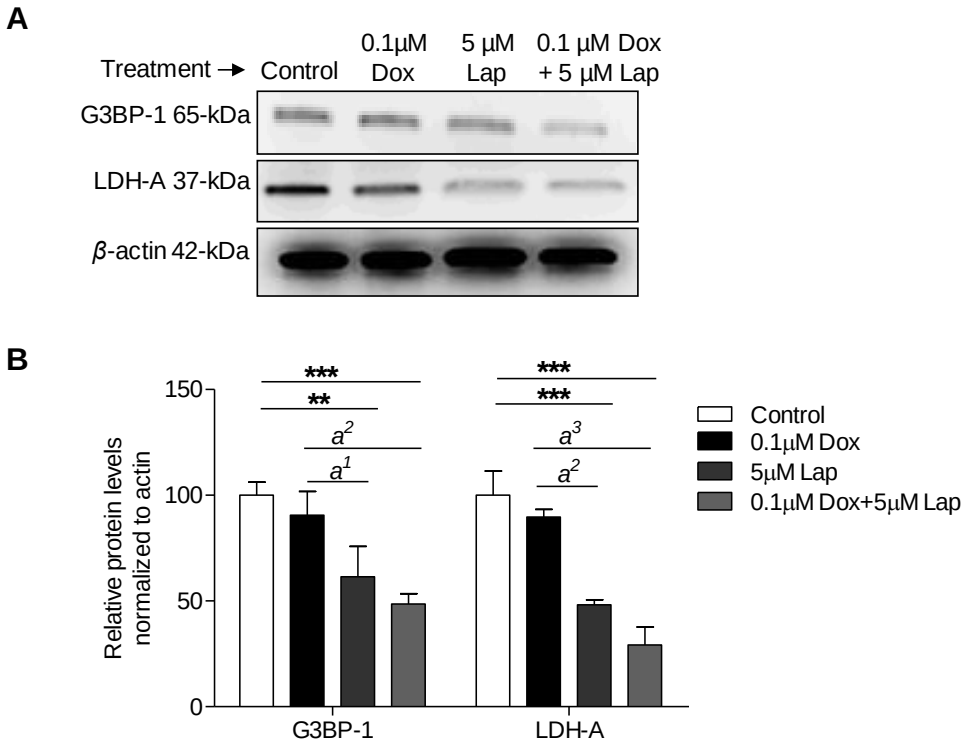

Figure 5.8: Effect of drug combination on the protein levels of G3BP-1 and LDH-A in SKBR3 breast cancer cell line. Fig. 5.8A. Immunoblot analysis of the expression of G3BP-1 and LDH-A following 0.1µM Dox, 5µM Lap, and 0.1µM Dox+5µM Lap treatment of SKBR3 cells when anti-G3BP-1 and –LDH-A antibodies were used at a dilution of 1:1000. *β*-actin was used as a loading control. **Fig. 5.8B**. The histogram obtained from the immunoblot data showing the relative expression of G3BP-1 and LDH-A when compared to the control. Statistical significance is represented as $^{**}p<0.01$, and $^{***}p<0.001$ between the indicated drug treatment versus the corresponding control for G3BP-1 and LDH-A respectively. Also, a^1 $p<0.05$, a^2 $p<0.01$, a^3 $p<0.001$ indicated 0.1µM Dox versus and 5µM Lap and 0.1µM Dox+5µM Lap for G3BP-1 and LDH-A respectively. Bars represent mean $\pm$ SD of three independent experiments. The data obtained was analysed using one-way analysis of variance (ANOVA) followed by Bonferroni's multiple comparison test. Dox=Doxorubicin, Lap=Lapatinib.

5.4 Discussion

Metastasis represents the final and the most devastating stage of cancer and remains the cause of 90% deaths from solid tumors [125, 127]. For decades, the use of anthracyclines has been a mainstay of therapy for patients with high-risk breast cancer [499]. Furthermore, several clinical trials including Anthracyclines in Early Breast Cancer (ABC), Western German Study (WSG) Plan B, and Microarray In Node-Negative and 1 to 3 Positive Lymph Node Disease May Avoid Chemotherapy (MINDACT) have compared nonanthracycline taxane-based and adjuvant anthracycline chemotherapy regimens in HER2-negative breast cancer patients and suggested the later to be superior to a taxane regimen in high risk patients with extensive lymph node involvement [499]. However, the use of an adjuvant anthracycline regimen has been put into question due to the risk of congestive cardiomyopathy [473-475] and chemoresistance [371, 476] associated with anthracyclines.

Interestingly, some studies [370, 480, 500] have implicated the role of Dox in inducing migration and invasion of MCF-7, BT474, MDA-MB-231 breast cancer cells. To investigate such effects of Dox in *in vitro* studies, a panel of breast cancer cell lines were tested herein. Data acquired in this chapter has demonstrated that 0.1µM of Dox significantly increased the cell viability of SKBR3 breast cancer cell line in comparison to other breast cancer cell lines included in the study. Further investigation of the effect of 0.1µM Dox treatment on SKBR3 cell line revealed the induction of migratory phenotypes in these cells. However, a combinational dose of 0.1µM Dox+5µM Lap was effective in inhibiting the migratory phenotypes induced by 0.1µM Dox alone treatment. Since Lap treatment downregulated the expression of G3BP-1 and LDH-A in a variety of breast cancer cell lines (**Figure 3.7**), it was interesting to examine the effect of combinational dose of Dox and Lap on the protein levels of these biomarkers in SKBR3 cell line. Indeed, the combinational dose of 0.1µM Dox+5µM Lap significantly downregulated the expression of both- G3BP-1 and LDH-A in the drug treated SKBR3 cells when compared to control and 0.1µM Dox alone treatment.

Cell viability experiments aimed to investigate the chemosensitivity to Dox and Lap of SKBR3, MDA-MB-231, T47D breast cancer cell lines, along with HMF, revealed a significant increase in the viability of 0.1µM Dox treated SKBR3 cells (**Figure 5.1**). The findings in this study have also demonstrated that the enhanced viability of SKBR3 breast cancer cells upon 0.1µM Dox treatment was not due to an increase in the cell proliferation as the data showed that the cell count of 0.1µM Dox treated cells at 24 h did not increase when compared to the corresponding control (**Fig. 5.2A**). Also, there was no difference in the expression levels of PCNA between 0.1µM Dox treated versus control cells at 24 h (**Fig. 5.2B**). Hence, the observed increase in cell viability may be due to the increased levels of NADH produced by cellular dehydrogenase enzymes within the metabolically active SKBR3 cells. Consistent with this speculation, Alam *et al.,* [501] have demonstrated that Dox treatment of E006AA and LNCaP prostate cancer cell lines increased the mitochondrial activity and the production of NADH. Results obtained from the proliferation assay upon 0.1µM Dox treatment over different time points indicated that there was no difference in the proliferation of 0.1µM Dox treated SKBR3 cells beyond 24 h time point (**Fig. 5.2A**). Similar results were obtained when cell viability of SKBR3 cells was assayed in response to 0.1µM Dox treatment over time (**Fig. 5.1C**). Such an observation may be justified by the fact that Dox, being a lipophilic molecule, rapidly diffuses into the cells and binds to DNA, thereby accumulating intracellularly [375, 502]. With time, there may be a decrease in drug uptake by the cells or an increased efflux, resulting in no observable difference in the viability over longer periods of treatment. Since the increase in cell viability upon 0.1µM Dox treatment was observed only in SKBR3 breast cancer cell line, this dose was used in further studies.

Consistent with previous literature [346], SKBR3 cells were more sensitive to increasing doses of Lap (**Fig. 5.1B**). Therefore, an IC_{50} dose of 5µM Lap in combination with 0.1µM Dox was chosen to be tested in SKBR3 cells in further experiments. Since 0.1µM Dox+5µM Lap significantly suppressed the cell viability of SKBR3 cells when compared with 0.1µM Dox alone (**Fig. 5.1D**), the metabolic alteration observed in these cells may be regulated by Lap.

Reports indicate that chemoresistant tumors comprise intrinsically resistant cells that adapt themselves to display increased propensity for cancer progression and metastasis [503]. Such cellular adaptations are required during metastatic dissemination. The current study investigated the morphological changes in drug treated SKBR3 cells. The data (**Figure 5.3**) indicated that 0.1µM Dox had an impact on the reorganization of actin cytoskeleton. Interestingly, the majority of 0.1µM Dox treated cells had prominent F-actin filaments. This data is consistent with the observations made by Avtanski *et al.,* [504] that reported cytoskeletal reorganization of F-actin into finger like protrusions in MCF-7 and MDA-MB-231 cells. In agreement with those findings, in this study it was observed that 0.1µM Dox induced membrane protrusions including lamellipodia and filopodia at the leading edge of the cells (**Fig. 5.4A**). Studies have reported that actin polymerization at these sites generates protrusive force required for migration [505, 506]. Findings reported in this study have shown that the migratory phenotype of 0.1µM Dox induced SKBR3 cells was effectively suppressed when treated with a combinatory dose of 0.1µM Dox+5µM Lap. Indeed, morphological changes upon 5µM Lap treatment have revealed actin aggregation within the cells (**Fig. 5.4B**). Collectively, it may be proposed that the inhibitory effect of 5µM Lap may be due to the disruption of the cytoskeletal organization to reduce or eliminate the prominent F-actin filaments. Thus, the use of Lap in combination with Dox inhibited the migratory phenotype of 0.1µM Dox induced SKBR3 cells.

Of note, altered mitochondrial dynamics may enhance the acquisition of metastatic potential in cancer cells [507]. Thus, we next studied the mitochondrial spread in drug treated SKBR3 cells. Notably, the mitochondrial spread was significantly higher in the 0.1µM Dox treated cells when compared to the cells that received 0.1µM Dox+5µM Lap (**Figure 5.5**). These findings correlated with actin cytoskeleton reorganization that was observed in this study. Since metastasis requires higher levels of energy, an increase in the mitochondrial spread in 0.1µM Dox treated cells may be a cellular adaptation to provide survival advantage to these cells. This data is consistent with findings presented elsewhere [508, 509] that indicated a heightened mitochondrial dynamics during metastasis.

Since 0.1µM Dox treatment induced migratory phenotypes in SKBR3 cells, it was relevant to evaluate the effect of combinatory treatment with Dox and Lap in terms of Dox-induced cell migration. The data presented in this study has shown that 0.1µM Dox induced the migratory phenotypes of SKBR3 cells through cellular adaptations including F-actin reassembly, membrane protrusions (lamellipodia and filopodia), and increased mitochondrial localization. The wound closure (**Figure 5.6**) in 0.1µM Dox treated cells may be due to the migration of the cells upon drug treatment. It was also demonstrated that the inhibition of migration was at least partially dependent on the reduction or elimination of prominent F-actin filaments upon combinatory treatment of Lap and Dox. Consistent with these observations, a different study demonstrated that the migratory potential in the PC3 prostate cancer cell line was reduced due to the elimination of filopodia [510]. The present study has also revealed that 5µM Lap treatment significantly increased the proportion of actin aggregates (77%) in contrast to the Dox and control groups in which the aggregates were around 12%. Interestingly, the viable cells within 0.1µM Dox treatment had a significantly higher (56%) proportion of prominent F-actin when compared to 7% in 5µM Lap group, which may have enhanced migration. Lee *et al.,* [511] have reported that upon drug treatment, the cells with an increased proportion of actin aggregates tend to migrate at a slower rate than the corresponding controls cells. Hence, in the present study, the combinatory treatment with Dox and Lap may have inhibited the migration of cells predominantly due to accumulation of actin aggregates.

A crucial factor that determines the metastatic potential of cancer cells is their motility [512]. In this study, it has been demonstrated that a combinatory dose of Lap with Dox suppressed the migratory phenotypes of 0.1µM Dox induced SKBR3 cells. These findings suggests a potential role of Lap in inhibiting the invasive capacity induced by Dox in SKBR3 breast cancer cell line.

Reports indicate that G3BP-1 participates in several signaling pathways that are implicated in cell proliferation and migration [283, 287, 288, 293, 296]. For example, silencing of G3BP in human H1299 non-small cell lung carcinoma cell line downregulated the expression of matrix metalloproteinase-2 (MMP-2), MMP-9 and plasminogen activator (uPA), thereby inhibiting cell migration [296].

In this study, Western blot analysis revealed that upon treatment of SKBR3 cells with 5µM Lap and 0.1µM Lap+5µM Dox, the endogenous protein levels of G3BP-1 and LDH-A were significantly reduced when compared to control and 0.1µM Dox alone (**Figure 5.8**). However, 0.1µM Dox alone (when compared to control) did not alter the endogenous levels of these biomarkers. Based on the findings reported in this study (**Figures 5.6** and **5.8**), and evidences presented elsewhere [291, 293, 296], it may be speculated that inhibition of cell migration upon Lap treatment in SKBR3 breast cancer cell line may be mediated by downregulation of G3BP-1. In addition, downregulation of LDH-A in Lap treated cells may suggest an association in the regulation between G3BP-1 and LDH-A in SKBR3 breast cancer cell line. Consistently, earlier findings (**Figure 3.7**) that reported downregulation of G3BP-1 and LDH-A upon Lap treatment in a panel of breast cancer cell lines including SKBR3 cells corroborate the argument that the endogenous expression of these two biomarkers is associated in SKBR3 breast cancer cell line that was used in this study (**Figure 5.8**). Although, studying the impact of Lap-mediated downregulation of G3BP-1 on cell migration in a broader panel of breast cancer cell lines may add value, it does not necessarily alter the significance of the findings reported herein.

5.5 Conclusion

Taken together, these results suggest that 0.1µM Dox induced migration in SKBR3 breast cancer cell line occurs via actin reorganization and alteration of the mitochondrial localization. Such effects were effectively suppressed through a combinatory treatment of 0.1µM Dox+5µM Lap. Furthermore, the combinational dose also downregulated the expression levels of G3BP-1 and LDH-A proteins in drug treated cells. This *in vitro* study provided evidence to support the justification for investigating Lap combination therapy for treatment of HER2-positive metastatic breast cancers.

Chapter 6

General discussion and perspectives

6.1 General discussion

Since the discovery of G3BP as a GAP SH3-binding protein [283], several reports have indicated its frequent upregulation in various human cancers, including breast cancers [283-288]. Furthermore, it is also implicated in pathways that control cell proliferation and survival [283, 287, 288, 293, 296]. Collectively, these studies provide evidence that G3BP plays an important role in breast cancer and therefore may be a promising target for treatment of breast cancer. The findings reported herein, investigate the potential relevance of G3BP as a biomarker for breast cancer. In this study, it was demonstrated that G3BP-1 (but not G3BP-2) regulates the translational expression of LDH-A in MDA-MB-435 breast cancer cell line. Interestingly, the study also revealed that Lap interacts with G3BP-1 and stabilizes the protein. In addition, it was also reported that Lap-mediated inhibition of migratory phenotypes induced by Dox treatment of SKBR3 breast cancer cell line was through downregulation of endogenous G3BP-1. Collectively, these evidences support the role of G3BP-1 in breast cancer progression and that targeting G3BP-1 with Lap may significantly inhibit cell migration of HER2-positive breast cancer cell lines.

Although studies have reported that G3BP-1 plays a role in several mitogenic pathways, its impact on the metabolic alteration in cancers is less well studied. Interestingly, Ortega *et al.*, [288] have reported that G3BP-1 inhibits the translation of β-F1-ATPase mRNA. The current study investigated the role of G3BP-1 in the glycolytic shift observed in breast cancers, by examining the effect of silencing G3BP-1 on endogenous levels of LDH-A in MDA-MB-435 breast cancer cell line. Indeed, LDH-A, which catalyses the conversion of pyruvate to lactate, is upregulated in breast cancers [417, 418]. Initial experiments revealed that the endogenous protein levels of G3BP-1 and LDH-A were significantly higher in breast cancer cell lines when compared to HMF cells used as a control (**Figure 3.2**). This finding clarified the potential relevance of G3BP-1 and LDH-A as breast cancer biomarkers. Further experiments revealed that depletion of G3BP-1 (**Figure 3.3**), but not G3BP-2 (**Figure 3.4**) downregulated the endogenous levels of LDH-A protein. However, there was no effect on the mRNA transcript stability of LDH-A upon knockdown of G3BP-1 (**Figure 3.5**) or G3BP-2 (**Figure 3.6**).

Indeed, translational regulation of target mRNAs is not uncommon for RBPs. The interaction of RNPs with mRNA creates an mRNP code, which regulates the post-transcriptional processing, subcellular localization, stability, and translation of the transcript [513]. Therefore, depletion of G3BP-1 may induce variability in the mRNP code for LDH-A transcript, although this is yet to be verified. Such a variation may not facilitate the transport of LDH-A mRNA to its destination. Another plausible explanation for regulation of the target mRNAs by RNP is the recruitment of translational initiation factors upon the RNP binding to the target mRNA transcript, thereby inducing translation. In addition, the RBPs may temporarily repress several mRNAs and enhance the translation of specific mRNAs to meet the bioenergetic and biosynthetic requirements of rapidly proliferating cancer cells.

An important feature that determines the regulation of mRNA transcripts is the interaction of the RBPs with the cis-acting elements in the UTRs of the target mRNAs [288, 298, 514]. In the current study, it was shown that G3BP-1 depletion did not affect the transcript stability of LDH-A mRNA. The significance of this result is unclear, although it would be tempting to speculate that the transcriptional regulation of LDH-A mRNA within the mRNP complex may be indirect via other transcriptional regulators. Indeed, another study revealed that G3BP-1 associates with translational regulators such as IMP-1 to regulate the translation of tau mRNA by G3BP-1, without directly binding to the mRNA transcript [439]. Collectively, the findings reported in Chapter 3 (**Figures 3.3-3.6**) implicated the role of G3BP-1 in defining the Warburg phenotype of MDA-MB-435 breast cancer cell line.

Several reports have implicated the role of Lap in the metabolic shift in breast cancer cell lines through its regulation of glycolytic enzymes involving LDH-A [426] and PKM2 [427]. In this study, the potential link between Lap and G3BP-1 in regulating the glycolytic switch in breast cancer cell lines was investigated. The findings revealed that Lap downregulated the endogenous protein levels of G3BP-1 and LDH-A and such effects were independent of receptor status in the breast cancer cell lines included in the study (**Figure 3.7**). Similarly, as rescue experiments to examine whether the observed alterations in endogenous LDH-A are due to siRNA mediated knockdown of G3BP-1 could not be performed, the conclusions of this study may be limited.

Whilst evidence suggests that G3BP is overexpressed in several cancers, including breast cancer, and is implicated in various mitogenic signaling pathways in cells, studies to target G3BP for cancer therapy are rather limited. Based on the evidence reported in Chapter 3 on the impact of Lap on downregulating the endogenous protein levels of G3BP-1 in breast cancer cell lines (**Figure 3.7**), it was speculated that Lap may interact with G3BP-1 to manifest the observed effect. Hence, in chapter 4, potential interaction between Lap and purified G3BP-1 protein was examined using protein thermal shift assays.

In this regard, fusion protein constructs of G3BP-1 (**Fig. 4.3B**) and G3BP-2 (**Fig. 4.3C**) were generated using pRSETC expression vector with N-terminal $His_{(6)}$ tag. To determine the optimum induction temperature for the expression of the protein constructs, different expression temperatures were considered, and the protein expression was analysed. As depicted by the **Fig. 4.4A**, G3BP-1 was efficiently recovered when the temperature was lowered from 37^{o}C to 25^{o}C. Surprisingly, further lowering of the temperature to 20^{o}C did not favour the expression of G3BP-1. In contrast (as shown in **Fig. 4.4B**), the recovery of G3BP-2 in the soluble fraction was more efficient as the temperature was lowered from 37^{o}C to 20^{o}C. However, the recovery was not complete compared to that of G3BP-1 at 25^{o}C. This observation is in line with reports that suggest the divergent nature of G3BP-1 and G3BP-2 [289]. Whilst, these proteins are involved in similar biochemical processes, the differences in their structure may be attributed to their distinct stabilities. Also, the identity of G3BP-1 and G3BP-2 was confirmed using protein-specific antibodies (**Figure 4.5**). Affinity purification of $His_{(6)}$-G3BP-1 was performed using Ni-NTA resin and the protein yield was estimated to be 6mg/l of culture (**Figure 4.6**).

In the next step, the effect of Lap (an ATP-competitive inhibitor of RTK of HER2) [151, 345] on thermal stability of purified G3BP-1 protein was investigated by protein thermal shift assays (**Figure 4.7**). In the presence of Lap, the t_m of G3BP-1 was increased compared to the control. The shift in t_m was greatest at 60µM of Lap at 4:1 stochiometric concentration of the compound to the protein. The observed thermal stabilization was speculated to be a result of weak interaction between the ATP interacting residues within the RGG-rich carboxy terminal of G3BP-1 and Lap.

Indeed, Costa *et al.,* [443] reported that residues within RGG domain of G3BP-1 were approximately 75% homologous to those present in nucleolin (human DNA/RNA helicase with ATPase activity), that binds to ATP. Under these assay conditions, stabilization of G3BP-1 in the presence of 5-FU (inhibitor of thymidylate synthase) [448] was studied to examine if the observed thermal stabilization of G3BP-1 was specific to Lap. Since 5-FU so far has not been reported to interact with ATP binding proteins, its inclusion as a negative control in the assay may be justified. Thermal stabilization of purified G3BP-1 protein was specific to Lap as such stability of G3BP-1 was not induced in the presence of 5-FU (**Figure 4.8**).

Since the crystal structure of the C-terminal domain of G3BP-1 was not available, ligand docking studies with Lap were not feasible. On a side note, Oi *et al*., [305] predicted the binding of resveratrol to G3BP-1 by performing ligand docking studies using the crystal structure of NTF2-like domain of G3BP-1 [305]. The choice of PTS technique warrants careful consideration of the solvents in which the test compounds are dissolved. For example, Sorrell *et al.,* [515] reported that higher concentrations of DMSO destabilized the protein, thereby inducing a negative shift in the t_m of anthrax protein protective antigen (PA). In that study, it was recommended that the DMSO concentration be kept to a maximum limit of 2% and ligand induced Δt_m of the protein be compared with the solvent control. Following the recommendation, in this study, the DMSO concentration was kept below 1% to ensure that the shift in t_m was primarily due to the interaction of Lap with G3BP-1, whilst the DMSO effect was negligible. Wassman *et al*., [450] showed that mutant p53-reactivating compounds including [PRIMA-1, methylene quinuclidinone (MQ), and stictic acid] induced thermal stabilization of both wild-type and mutant p53. Indeed, these mutations were single amino acid substitutions in the DNA binding domain of the protein. Nevertheless, in this study, the observed effect of Lap on G3BP-1 may not be generalized across the G3BP family including G3BP-2 as these two proteins differ in the composition of their catalytic domains [289].

It is intriguing to find that cancer cells develop adaptive responses to low doses of chemotherapeutic agents. For example, treatment of MCF-7, BT474 and MDA-MB-231 breast cancer cell lines by Dox induced cell migration and invasion [370, 480]. Such responses may enable cancer cells to adapt to a new environment and colonize distant organs. Perhaps, these adaptations attribute to tumor metastasis, which accounts for 90% deaths from solid tumors [125, 127]. Hence, it would be interesting to examine drug induced cellular adaptations, as these studies can contribute to the design of novel strategies for therapeutic intervention.

Herein, a panel of breast cancer cell lines were evaluated for cell viability in response to treatment with Dox and Lap (**Figure 5.1**). Interestingly, the MTS assay revealed an enhanced cell viability of SKBR3 cell line upon treatment with 0.1µM Dox when compared to the corresponding untreated controls (**Fig. 5.1A**). Also, it was revealed that 0.1µM Dox did not alter the cell proliferation between drug treated and control cells (**Figure 5.2**) providing conclusive evidence that the observed effect of 0.1µM Dox was due to enhanced cell viability. Further investigation into the effect of 0.1µM Dox treatment on cellular adaptations of SKBR3 cells revealed morphological changes consistent with a significant increase in the formation of prominent F-actin filaments (**Figure 5.3**), formation of lamellipodia and filopodia that are indicative of migratory phenotypes (**Figure 5.4**) and increased mitochondrial spread (**Figure 5.5**) compared with the control cells. Consistently, treatment of SKBR3 cell line with 0.1µM Dox enhanced migration when compared to control cells (**Figure 5.6**). In contrast, a combinational dose of 0.1µM Dox+5µM Lap significantly inhibited the cell viability of SKBR3 breast cancer cell line induced by 0.1µM Dox alone treatment (**Fig. 5.1D**). Furthermore, the combinational dose was effective in suppressing the observed phenotypic alterations induced by 0.1µM Dox alone. The findings revealed a significant difference in the prominent F-actin filaments (**Figure 5.3**), migratory phenotypes (**Figure 5.4**) and mitochondrial spread (**Figure 5.5**) between 0.1µM Dox alone treatment versus 0.1µM Dox+5µM Lap. In addition, the combinational dose also showed a significant decrease in the percentage of wound closure when compared to the control (**Figure 5.6**).

Consistent with the reports presented elsewhere [346], in this study, 5µM Lap and 0.1µM Dox+5µM Lap significantly induced apoptosis of SKBR3 breast cancer cells when compared to the corresponding control or 0.1µM Dox alone treatment (**Figure 5.7**). Further studies on the effect of drug treatment on G3BP-1 and LDH-A revealed a significant downregulation in the expression levels of these biomarkers between 5µM Lap and 0.1µM Dox+5µM Lap versus control and 0.1µM Dox alone treatment (**Figure 5.8**). However, the expression levels of these biomarkers did not significantly alter between 5µM Lap and 0.1µM Dox+5µM Lap treatments. Collectively, findings in Chapter 5 demonstrated that a combinational dose of 0.1µM Dox+5µM Lap treatment was effective in inhibiting the migratory phenotypes induced by 0.1µM Dox treatment and such inhibition may be mediated through the ability of Lap to downregulate the endogenous expression of G3BP-1in SKBR3 breast cancer cell line. Similarly, investigating the impact of Lap-mediated downregulation of G3BP-1 on the migration of cells in a broader panel of breast cancer cell lines may add value to the current study, although, it does not necessarily undermine the significance of findings reported in Chapter 5.

In summary, the current study has demonstrated the potential relevance of G3BP-1 as a biomarker in breast cancer. Findings concerning (a) the higher expression levels of endogenous G3BP-1 in several breast cancer cell lines (distinct in the molecular subtypes), and (b) its implication in the Warburg effect has clearly demonstrated the significance of G3BP-1 in breast cancers. Interestingly, both the effects (an increased cell viability and induction of migratory phenotypes of SKBR3 breast cancer cell line upon Dox treatment) were inhibited by the combinational therapy of Lap and Dox. Furthermore, such inhibition may be mediated by the downregulation of G3BP-1 by Lap independent of HER2 status. This study has also demonstrated a clear and robust link between G3BP-1 and breast cancer (especially HER2-positive breast cancer), and also a link between G3BP-1 and Lap. This evidence gives a glimpse into the potential relevance of G3BP-1 in HER2-positive breast cancers that are often associated with a high rate of metastasis to the bone and brain. It would be interesting to study the potential impact of G3BP-1 expression levels on the innate resistance to Dox treatment. Such studies may offer higher levels of G3BP-1 to be a selection biomarker to predict which patients would benefit the most from the combinational therapy of Dox and Lap.

6.2 Perspectives

In order to validate the effect of G3BP-1 on the translational regulation of LDH-A mRNA, rescue experiments as reported elsewhere [516] should be performed in future studies. This may be done by re-expressing G3BP-1 from a transiently transfected vector that carries the mRNA for G3BP-1. Following the expression of exogenous G3BP-1, it is speculated that translational inhibition of LDH-A mRNA may be rescued. This experiment would provide evidence that the observed changes in the expression of LDH-A mRNA after depletion of G3BP-1 are due to siRNA mediated G3BP-1 knockdown and not an off-target effect. Since G3BP-1 is implicated in the Ras signaling pathway [283, 287], assessing the impact of G3BP-1 silencing on Ras/MAPK signaling may further validate the findings of this study. A previous study demonstrated that knockdown of G3BP-1 inhibited cell migration of human lung carcinoma H1299 cells by downregulating the expression of MMP-2, MMP-9 and uPA respectively [296]. Similarly, measuring lactate levels as reported elsewhere [517, 518], may demonstrate decreased production of metabolic lactate as a result of downregulation of LDH-A upon silencing of G3BP-1 in MDA-MB-435 breast cancer cell line. Such an effect may provide a functional validation of the effect of G3BP-1 knockdown on LDH-A regulation in MDA-MB-435 breast cancer cells. Study by Oi *et al.,* [305] analysed *in vitro* binding of G3BP-1 with resveratrol-conjugated sepharose beads to confirm G3BP-1 as a potential target of resveratrol. Similarly, Lap-conjugated sepharose beads may be used in *in vitro* binding assays to confirm the interaction of Lap with G3BP-1.

Findings reported in Chapter 5 of this study have implicated increased cell viability and mitochondrial spread of SKBR3 breast cancer cell line upon Dox treatment. Another study has reported increased mitochondrial activity and NADH production upon Dox treatment of prostate cancer cell lines including E006AA and LNCaP [501]. Similarly, measuring the impact of Dox treatment on the production of NADH in SKBR3 breast cancer cell line may confirm the effect of Dox in these cells. Treatment of Dox was reported to induce EMT via upregulation of TGF β activity in 4T1 and MCF7/HER2 breast cancer cell line [480].

Although assessing the impact of drug treatment on changes in TGF β activity was outside the scope of this study, insights from such studies may inform the future development of effective drug combinational trials. A further enhancement of the hypothesized multidrug therapy of Lap plus Dox could be the addition of resveratrol and/or EGCG that would make an interesting and relevant future study.

In summary, the work presented in this thesis demonstrated that (a) siRNA mediated knockdown of G3BP-1 in MDA-MB-435 breast cancer cell line downregulated the endogenous protein levels of LDH-A. However, (b) such regulation was not observed at the level of mRNA. In addition, (c) Lap treatment of different breast cancer cell lines (that differ in their receptor status) indicated downregulation of G3BP-1 and LDH-A independent of the receptor status, (d) Lap induced thermal stabilization of purified G3BP-1 protein as assessed by protein thermal shift assays, and (e) the effect of Lap on inhibiting the migratory phenotypes of Dox-induced SKBR3 breast cancer cells was mediated by the downregulation of G3BP-1 and LDH-A. Overall, findings reported in this thesis provide substantial evidence that G3BP-1 is a potential relevant biomarker of breast cancer and targeting G3BP-1 may have therapeutic significance in breast cancer treatment. In general, such studies provide mechanistic insights for the development of molecular-based targeted therapies to treat breast cancers.

Chapter 7

References

1. Bray, F., et al., *Global cancer statistics 2018: GLOBOCAN estimates of incidence and mortality worldwide for 36 cancers in 185 countries.* CA Cancer J Clin, 2018. **68**(6): p. 394-424.
2. Manchester, K.L., *Theodor Boveri and the origin of malignant tumours.* Trends in Cell Biology, 1995. **5**(10): p. 384-387.
3. Muller, H.J., *Radiation damage to the genetic material.* Am Sci, 1950. **38**(1): p. 33-59.
4. Foulds, L., *Tumor progression.* Cancer Res, 1957. **17**(5): p. 355-6.
5. Hemminki, K., J. Lorenzo Bermejo, and A. Forsti, *The balance between heritable and environmental aetiology of human disease.* Nat Rev Genet, 2006. **7**(12): p. 958-65.
6. Whitman, R., *Somatic Mutations as a Factor in the Production of Cancer: A Critical Review of v. Hansemann's Theory of Anaplasia in the Light of Modern Knowledge of Genetics.* The Journal of Cancer Research, 1919. **4**(2): p. 181-202.
7. Vogelstein, B. and K.W. Kinzler, *Cancer genes and the pathways they control.* Nat Med, 2004. **10**(8): p. 789-99.
8. Gerlinger, M., et al., *Intratumor heterogeneity and branched evolution revealed by multiregion sequencing.* New England journal of medicine, 2012. **366**(10): p. 883-892.
9. Landau, D.A., et al., *Evolution and impact of subclonal mutations in chronic lymphocytic leukemia.* Cell, 2013. **152**(4): p. 714-726.
10. Hanahan, D. and R.A. Weinberg, *Hallmarks of cancer: the next generation.* Cell, 2011. **144**(5): p. 646-74.
11. Cheng, N., et al., *Transforming growth factor-β signaling–deficient fibroblasts enhance hepatocyte growth factor signaling in mammary carcinoma cells to promote scattering and invasion.* Molecular Cancer Research, 2008. **6**(10): p. 1521-1533.
12. Davies, M. and Y. Samuels, *Analysis of the genome to personalize therapy for melanoma.* Oncogene, 2010. **29**(41): p. 5545.
13. Jiang, B.H. and L.Z. Liu, *PI3K/PTEN signaling in angiogenesis and tumorigenesis.* Advances in cancer research, 2009. **102**: p. 19-65.
14. Yuan, T. and L. Cantley, *PI3K pathway alterations in cancer: variations on a theme.* Oncogene, 2008. **27**(41): p. 5497.
15. *<Hallmarks of cancer_1.pdf>*.
16. Massagué, J., *G1 cell-cycle control and cancer.* Nature, 2004. **432**(7015): p. 298.

17. Classon, M. and E. Harlow, *The retinoblastoma tumour suppressor in development and cancer.* Nature Reviews Cancer, 2002. **2**(12): p. 910.
18. Datto, M.B., et al., *The viral oncoprotein E1A blocks transforming growth factor beta-mediated induction of p21/WAF1/Cip1 and p15/INK4B.* Molecular and cellular biology, 1997. **17**(4): p. 2030-2037.
19. Moses, H.L., E.Y. Yang, and J.A. Pietenpol, *TGF-β stimulation and inhibition of cell proliferation: new mechanistic insights.* Cell, 1990. **63**(2): p. 245-247.
20. Fynan, T. and M. Reiss, *Resistance to inhibition of cell growth by transforming growth factor-beta and its role in oncogenesis.* Critical reviews in oncogenesis, 1993. **4**(5): p. 493-540.
21. Markowitz, S., et al., *Inactivation of the type II TGF-beta receptor in colon cancer cells with microsatellite instability.* Science, 1995. **268**(5215): p. 1336-1338.
22. Chin, L., J. Pomerantz, and R.A. DePinho, *The INK4a/ARF tumor suppressor: one gene—two products—two pathways.* Trends in biochemical sciences, 1998. **23**(8): p. 291-296.
23. Foley, K.P. and R.N. Eisenman, *Two MAD tails: what the recent knockouts of Mad1 and Mxi1 tell us about the MYC/MAX/MAD network.* Biochimica et Biophysica Acta (BBA)-Reviews on Cancer, 1999. **1423**(3): p. M37-M47.
24. Adams, J.M. and S. Cory, *The Bcl-2 apoptotic switch in cancer development and therapy.* Oncogene, 2007. **26**(9): p. 1324.
25. Lowe, S.W., E. Cepero, and G. Evan, *Intrinsic tumour suppression.* Nature, 2004. **432**(7015): p. 307.
26. Evan, G. and T. Littlewood, *A matter of life and cell death.* Science, 1998. **281**(5381): p. 1317-1322.
27. Junttila, M.R. and G.I. Evan, *p53—a Jack of all trades but master of none.* Nature reviews cancer, 2009. **9**(11): p. 821.
28. Green, D.R. and J.C. Reed, *Mitochondria and apoptosis.* science, 1998. **281**(5381): p. 1309-1312.
29. Thornberry, N.A. and Y. Lazebnik, *Caspases: enemies within.* Science, 1998. **281**(5381): p. 1312-1316.
30. Harris, C.C., *p53 tumor suppressor gene: from the basic research laboratory to the clinic-an abridged historical perspective.* Carcinogenesis, 1996. **17**(6): p. 1187-1198.

31. Wright, W.E., O.M. Pereira-Smith, and J.W. Shay, *Reversible cellular senescence: implications for immortalization of normal human diploid fibroblasts.* Molecular and cellular biology, 1989. **9**(7): p. 3088-3092.
32. Blasco, M.A., *Telomeres and human disease: ageing, cancer and beyond.* Nature Reviews Genetics, 2005. **6**(8): p. 611.
33. Shay, J.W. and W.E. Wright, *Hayflick, his limit, and cellular ageing.* Nature reviews Molecular cell biology, 2000. **1**(1): p. 72.
34. Bryan, T.M. and T.R. Cech, *Telomerase and the maintenance of chromosome ends.* Current opinion in cell biology, 1999. **11**(3): p. 318-324.
35. Bryan, T.M., et al., *Telomere elongation in immortal human cells without detectable telomerase activity.* The EMBO journal, 1995. **14**(17): p. 4240-4248.
36. Fedi, P., S. Tronick, and S. Aaronson, *Growth factors.* Cancer medicine, 1997: p. 41-64.
37. Veikkola, T. and K. Alitalo. *VEGFs, receptors and angiogenesis*. in *Seminars in cancer biology*. 1999. Elsevier.
38. Bull, H.A., P.M. Brickell, and P.M. Dowd, *Src-related protein tyrosine kinases are physically associated with the surface antigen CD36 in human dermal microvascular endothelial cells.* FEBS letters, 1994. **351**(1): p. 41-44.
39. Hanahan, D. and J. Folkman, *Patterns and emerging mechanisms of the angiogenic switch during tumorigenesis.* cell, 1996. **86**(3): p. 353-364.
40. Dameron, K.M., et al., *Control of angiogenesis in fibroblasts by p53 regulation of thrombospondin-1*. Science, 1994. **265**(5178): p. 1582-1584.
41. Rak, J., et al., *Oncogenes as inducers of tumor angiogenesis.* Cancer and Metastasis Reviews, 1995. **14**(4): p. 263-277.
42. Maxwell, P.H., et al., *The tumour suppressor protein VHL targets hypoxia-inducible factors for oxygen-dependent proteolysis.* Nature, 1999. **399**(6733): p. 271.
43. Sporn, M.B., *The war on cancer.* Lancet (London, England), 1996. **347**(9012): p. 1377-1381.
44. Christofori, G. and H. Semb, *The role of the cell-adhesion molecule E-cadherin as a tumour-suppressor gene.* Trends in biochemical sciences, 1999. **24**(2): p. 73-76.
45. Johnson, J.P., *Cell adhesion molecules of the immunoglobulin supergene family and their role in malignant transformation and progression to metastatic disease.* Cancer and Metastasis Reviews, 1991. **10**(1): p. 11-22.

46. Petrova, Y.I., L. Schecterson, and B.M. Gumbiner, *Roles for E-cadherin cell surface regulation in cancer.* Molecular biology of the cell, 2016. **27**(21): p. 3233-3244.
47. Kaiser, U., B. Auerbach, and M. Oldenburg, *The neural cell adhesion molecule NCAM in multiple myeloma.* Leukemia & lymphoma, 1996. **20**(5-6): p. 389-395.
48. Negrini, S., V.G. Gorgoulis, and T.D. Halazonetis, *Genomic instability--an evolving hallmark of cancer.* Nat Rev Mol Cell Biol, 2010. **11**(3): p. 220-8.
49. Jackson, S.P. and J. Bartek, *The DNA-damage response in human biology and disease.* Nature, 2009. **461**(7267): p. 1071.
50. Kastan, M.B., *DNA damage responses: mechanisms and roles in human disease: 2007 GHA Clowes Memorial Award Lecture.* Molecular Cancer Research, 2008. **6**(4): p. 517-524.
51. Korkola, J. and J.W. Gray, *Breast cancer genomes—form and function.* Current opinion in genetics & development, 2010. **20**(1): p. 4-14.
52. Pages, F., et al., *Immune infiltration in human tumors: a prognostic factor that should not be ignored.* Oncogene, 2010. **29**(8): p. 1093.
53. DeNardo, D.G., P. Andreu, and L.M. Coussens, *Interactions between lymphocytes and myeloid cells regulate pro-versus anti-tumor immunity.* Cancer and Metastasis Reviews, 2010. **29**(2): p. 309-316.
54. Grivennikov, S.I., F.R. Greten, and M. Karin, *Immunity, inflammation, and cancer.* Cell, 2010. **140**(6): p. 883-899.
55. Qian, B.-Z. and J.W. Pollard, *Macrophage diversity enhances tumor progression and metastasis.* Cell, 2010. **141**(1): p. 39-51.
56. Fantin, V.R., J. St-Pierre, and P. Leder, *Attenuation of LDH-A expression uncovers a link between glycolysis, mitochondrial physiology, and tumor maintenance.* Cancer Cell, 2006. **9**(6): p. 425-34.
57. Ward, P.S. and C.B. Thompson, *Metabolic reprogramming: a cancer hallmark even warburg did not anticipate.* Cancer cell, 2012. **21**(3): p. 297-308.
58. Cairns *et al*., *Regulation of cancer cell metabolism.* Nat Rev Cancer, 2011. **11**(2): p. 85-95.
59. Rolfe, D. and G.C. Brown, *Cellular energy utilization and molecular origin of standard metabolic rate in mammals.* Physiological reviews, 1997. **77**(3): p. 731-758.
60. Warburg *et al*., *On the Origin of Cancer Cells.* Science, 1996.
61. Gatenby, R.A. and R.J. Gillies, *Why do cancers have high aerobic glycolysis?* Nat Rev Cancer, 2004. **4**(11): p. 891-9.

62. DeBerardinis, R.J., et al., *The biology of cancer: metabolic reprogramming fuels cell growth and proliferation.* Cell metabolism, 2008. **7**(1): p. 11-20.
63. Hsu, P.P. and D.M. Sabatini, *Cancer cell metabolism: Warburg and beyond.* Cell, 2008. **134**(5): p. 703-707.
64. Cantor, J.R. and D.M. Sabatini, *Cancer cell metabolism: one hallmark, many faces.* Cancer discovery, 2012. **2**(10): p. 881-898.
65. Jadvar, H., A. Alavi, and S.S. Gambhir, *18F-FDG uptake in lung, breast, and colon cancers: molecular biology correlates and disease characterization.* Journal of Nuclear Medicine, 2009. **50**(11): p. 1820-1827.
66. Brand, K.A. and U. Hermfisse, *Aerobic glycolysis by proliferating cells: a protective strategy against reactive oxygen species.* The FASEB journal, 1997. **11**(5): p. 388-395.
67. Ruckenstuhl, C., et al., *The Warburg effect suppresses oxidative stress induced apoptosis in a yeast model for cancer.* PloS one, 2009. **4**(2): p. e4592.
68. DeBerardinis, R.J., et al., *Brick by brick: metabolism and tumor cell growth.* Current opinion in genetics & development, 2008. **18**(1): p. 54-61.
69. Kroemer, G. and J. Pouyssegur, *Tumor cell metabolism: cancer's Achilles' heel.* Cancer cell, 2008. **13**(6): p. 472-482.
70. Frezza, C. and E. Gottlieb. *Mitochondria in cancer: not just innocent bystanders*. in *Seminars in cancer biology*. 2009. Elsevier.
71. Dang, C.V. and G.L. Semenza, *Oncogenic alterations of metabolism.* Trends in biochemical sciences, 1999. **24**(2): p. 68-72.
72. Zhong, H., et al., *Overexpression of hypoxia-inducible factor 1α in common human cancers and their metastases.* Cancer research, 1999. **59**(22): p. 5830-5835.
73. Talks, K.L., et al., *The expression and distribution of the hypoxia-inducible factors HIF-1α and HIF-2α in normal human tissues, cancers, and tumor-associated macrophages.* The American journal of pathology, 2000. **157**(2): p. 411-421.
74. Semenza, G.L., et al., *Hypoxia response elements in the aldolase A, enolase 1, and lactate dehydrogenase A gene promoters contain essential binding sites for hypoxia-inducible factor 1.* Journal of Biological Chemistry, 1996. **271**(51): p. 32529-32537.
75. Valvona, C.J., et al., *The Regulation and Function of Lactate Dehydrogenase A: Therapeutic Potential in Brain Tumor.* Brain Pathol, 2016. **26**(1): p. 3-17.
76. Markert, C.L., J.B. Shaklee, and G.S. Whitt, *Evolution of a gene.* Science, 1975. **189**(4197): p. 102-114.

77. Burgner, J.W. and W.J. Ray Jr, *On the origin of the lactate dehydrogenase induced rate effect.* Biochemistry, 1984. **23**(16): p. 3636-3648.
78. Firth, J.D., B.L. Ebert, and P.J. Ratcliffe, *Hypoxic regulation of lactate dehydrogenase A Interaction between hypoxia-inducible factor 1 and cAMP response elements.* Journal of Biological Chemistry, 1995. **270**(36): p. 21021-21027.
79. Lewis, B.C., et al., *Identification of putative c-Myc-responsive genes: characterization of rcl, a novel growth-related gene.* Molecular and cellular biology, 1997. **17**(9): p. 4967-4978.
80. Shim, H., et al., *c-Myc transactivation of LDH-A: implications for tumor metabolism and growth.* Proceedings of the National Academy of Sciences, 1997. **94**(13): p. 6658-6663.
81. Zhao *et al*., *Upregulation of lactate dehydrogenase A by ErbB2 through heat shock factor 1 promotes breast cancer cell glycolysis and growth.* Oncogene, 2009. **28**(42): p. 3689-701.
82. Yang, W., et al., *ERK1/2-dependent phosphorylation and nuclear translocation of PKM2 promotes the Warburg effect.* Nature cell biology, 2012. **14**(12): p. 1295.
83. Cui *et al.*, *FOXM1 promotes the warburg effect and pancreatic cancer progression via transactivation of LDHA expression.* Clin Cancer Res, 2014. **20**(10): p. 2595-606.
84. Shi, M., et al., *A novel KLF4/LDHA signaling pathway regulates aerobic glycolysis in and progression of pancreatic cancer.* Clinical Cancer Research, 2014. **20**(16): p. 4370-4380.
85. Cai *et al*., *A Combined Proteomics and Metabolomics Profiling of Gastric Cardia Cancer Reveals Characteristic Dysregulations in Glucose Metabolism.* Molecular and Cellular Proteomics, 2010.
86. Girgis *et al*., *Lactate Dehydrogenase A is a potential prognostic marker in clear cell renal cell carcinoma.* Molecular Cancer, 2014.
87. Yao *et al*., *LDHA is necessary for the tumorigenicity of esophageal squamous cell carcinoma.* Tumour Biol, 2013. **34**(1): p. 25-31.
88. Wang *et al*., *Lactate dehydrogenase A negatively regulated by miRNAs promotes aerobic glycolysis and is increased in colorectal cancer.* Oncotarget, 2015.
89. Langhammer, S., et al., *LDH-A influences hypoxia-inducible factor 1α (HIF1 α) and is critical for growth of HT29 colon carcinoma cells in vivo.* Targeted oncology, 2011. **6**(3): p. 155-162.

90. Le, A., et al., *Inhibition of lactate dehydrogenase A induces oxidative stress and inhibits tumor progression.* Proc Natl Acad Sci U S A, 2010. **107**(5): p. 2037-42.
91. Xie, H., et al., *LDH-A inhibition, a therapeutic strategy for treatment of hereditary leiomyomatosis and renal cell cancer.* Molecular cancer therapeutics, 2009. **8**(3): p. 626-635.
92. Zhang, Y., et al., *Inhibition of LDH-A by lentivirus-mediated small interfering RNA suppresses intestinal-type gastric cancer tumorigenicity through the downregulation of Oct4.* Cancer letters, 2012. **321**(1): p. 45-54.
93. Baumann, F., et al., *Lactate promotes glioma migration by TGF-β2–dependent regulation of matrix metalloproteinase-2.* Neuro-oncology, 2009. **11**(4): p. 368-380.
94. Kato, Y., et al., *Acidic extracellular pH induces matrix metalloproteinase-9 expression in mouse metastatic melanoma cells through the phospholipase D-mitogen-activated protein kinase signaling.* Journal of Biological Chemistry, 2005. **280**(12): p. 10938-10944.
95. Rofstad, E.K., et al., *Acidic extracellular pH promotes experimental metastasis of human melanoma cells in athymic nude mice.* Cancer research, 2006. **66**(13): p. 6699-6707.
96. Swietach, P., R.D. Vaughan-Jones, and A.L. Harris, *Regulation of tumor pH and the role of carbonic anhydrase 9.* Cancer and Metastasis Reviews, 2007. **26**(2): p. 299-310.
97. Sheng, S.L., et al., *Knockdown of lactate dehydrogenase A suppresses tumor growth and metastasis of human hepatocellular carcinoma.* The FEBS journal, 2012. **279**(20): p. 3898-3910.
98. Beckert, S., et al., *Lactate stimulates endothelial cell migration.* Wound repair and regeneration, 2006. **14**(3): p. 321-324.
99. Fukumura, D., et al., *Hypoxia and acidosis independently up-regulate vascular endothelial growth factor transcription in brain tumors in vivo.* Cancer research, 2001. **61**(16): p. 6020-6024.
100. Hirschhaeuser, F., U.G. Sattler, and W. Mueller-Klieser, *Lactate: a metabolic key player in cancer.* Cancer research, 2011. **71**(22): p. 6921-6925.
101. Shi, Q., et al., *Regulation of vascular endothelial growth factor expression by acidosis in human cancer cells.* Oncogene, 2001. **20**(28): p. 3751.

102. Koukourakis *et al*., *Lactate dehydrogenase 5 (LDH5) relates to up-regulated hypoxia inducible factor pathway and metastasis in colorectal cancer.* Clin Exp Metastasis, 2005. **22**(1): p. 25-30.
103. Koukourakis, M., et al., *Lactate dehydrogenase-5 (LDH-5) overexpression in non-small-cell lung cancer tissues is linked to tumour hypoxia, angiogenic factor production and poor prognosis.* British journal of cancer, 2003. **89**(5): p. 877.
104. Koukourakis, M.I., et al., *Lactate dehydrogenase 5 expression in operable colorectal cancer: strong association with survival and activated vascular endothelial growth factor pathway—a report of the Tumour Angiogenesis Research Group.* Journal of clinical oncology, 2006. **24**(26): p. 4301-4308.
105. Friedman, L.M., et al., *Synergistic down-regulation of receptor tyrosine kinases by combinations of mAbs: implications for cancer immunotherapy.* Proceedings of the National Academy of Sciences, 2005. **102**(6): p. 1915-1920.
106. Li, C.I., et al., *Trends in incidence rates of invasive lobular and ductal breast carcinoma.* Jama, 2003. **289**(11): p. 1421-1424.
107. Rakha, E.A. and I.O. Ellis. *Lobular breast carcinoma and its variants*. in *Seminars in diagnostic pathology*. 2010. Elsevier.
108. Lynch, H.T. and J.F. Lynch, *Breast cancer genetics in an oncology clinic: 328 consecutive patients.* Cancer genetics and cytogenetics, 1986. **22**(4): p. 369-371.
109. Margolin, S., et al., *Family history, and impact on clinical presentation and prognosis, in a population-based breast cancer cohort from the Stockholm County.* Familial cancer, 2006. **5**(4): p. 309-321.
110. Lalloo, F. and D. Evans, *Familial breast cancer.* Clinical genetics, 2012. **82**(2): p. 105-114.
111. Ford, D., et al., *Genetic heterogeneity and penetrance analysis of the BRCA1 and BRCA2 genes in breast cancer families.* The American Journal of Human Genetics, 1998. **62**(3): p. 676-689.
112. Antoniou, A., et al., *Average risks of breast and ovarian cancer associated with BRCA1 or BRCA2 mutations detected in case series unselected for family history: a combined analysis of 22 studies.* The American Journal of Human Genetics, 2003. **72**(5): p. 1117-1130.
113. King, M.-C., J.H. Marks, and J.B. Mandell, *Breast and ovarian cancer risks due to inherited mutations in BRCA1 and BRCA2.* Science, 2003. **302**(5645): p. 643-646.

114. Ziegler, R.G., et al., *Migration patterns and breast cancer risk in Asian-American women.* JNCI: Journal of the National Cancer Institute, 1993. **85**(22): p. 1819-1827.
115. Sandhu, R., et al., *Microarray-based gene expression profiling for molecular classification of breast cancer and identification of new targets for therapy.* Laboratory Medicine, 2010. **41**(6): p. 364-372.
116. Dvorkin-Gheva, A. and J.A. Hassell, *Identification of a novel luminal molecular subtype of breast cancer.* PLoS One, 2014. **9**(7): p. e103514.
117. Guiu, S., et al., *Molecular subclasses of breast cancer: how do we define them? The IMPAKT 2012 Working Group Statement.* Ann Oncol, 2012. **23**(12): p. 2997-3006.
118. Perou, C.M., et al., *Molecular portraits of human breast tumours.* Nature, 2000. **406**(6797): p. 747-52.
119. Sørlie, T., et al., *Gene expression patterns of breast carcinomas distinguish tumor subclasses with clinical implications.* Proceedings of the National Academy of Sciences, 2001. **98**(19): p. 10869-10874.
120. Cheang, M.C., et al., *Ki67 index, HER2 status, and prognosis of patients with luminal B breast cancer.* J Natl Cancer Inst, 2009. **101**(10): p. 736-50.
121. Sorlie, T., et al., *Repeated observation of breast tumor subtypes in independent gene expression data sets.* Proc Natl Acad Sci U S A, 2003. **100**(14): p. 8418-23.
122. Jones, S.E., *Metastatic breast cancer: the treatment challenge.* Clinical breast cancer, 2008. **8**(3): p. 224-233.
123. Esparza-Lopez, J., et al., *Metformin reverses mesenchymal phenotype of primary breast cancer cells through STAT3/NF-kappaB pathways.* BMC Cancer, 2019. **19**(1): p. 728.
124. Smid, M., et al., *Subtypes of breast cancer show preferential site of relapse.* Cancer research, 2008. **68**(9): p. 3108-3114.
125. Pani, G., T. Galeotti, and P. Chiarugi, *Metastasis: cancer cell's escape from oxidative stress.* Cancer Metastasis Rev, 2010. **29**(2): p. 351-78.
126. Mu, X.M., et al., *Pristimerin inhibits breast cancer cell migration by up- regulating regulator of G protein signaling 4 expression.* Asian Pac J Cancer Prev, 2012. **13**(4): p. 1097-104.
127. Gupta, G.P. and J. Massagué, *Cancer metastasis: building a framework.* Cell, 2006. **127**(4): p. 679-695.
128. Siegel, R., et al., *Cancer statistics, 2014.* CA: a cancer journal for clinicians, 2014. **64**(1): p. 9-29.

129. Chaffer, C.L. and R.A. Weinberg, *A perspective on cancer cell metastasis.* science, 2011. **331**(6024): p. 1559-1564.
130. Chambers, A.F., A.C. Groom, and I.C. MacDonald, *Metastasis: dissemination and growth of cancer cells in metastatic sites.* Nature Reviews Cancer, 2002. **2**(8): p. 563.
131. Paget, S., *The distribution of secondary growths in cancer of the breast.* Cancer Metastasis Rev, 1989. **8**: p. 98-101.
132. Chiang, A.C. and J. Massagué, *Molecular basis of metastasis.* New England Journal of Medicine, 2008. **359**(26): p. 2814-2823.
133. Jin, X. and P. Mu, *Targeting breast cancer metastasis.* Breast cancer: basic and clinical research, 2015. **9**: p. BCBCR. S25460.
134. Kennecke, H., et al., *Metastatic behavior of breast cancer subtypes.* Journal of clinical oncology, 2010. **28**(20): p. 3271-3277.
135. Dent, R., et al., *Pattern of metastatic spread in triple-negative breast cancer.* Breast cancer research and treatment, 2009. **115**(2): p. 423-428.
136. Harrell, J.C., et al., *Genomic analysis identifies unique signatures predictive of brain, lung, and liver relapse.* Breast cancer research and treatment, 2012. **132**(2): p. 523-535.
137. Majid Momeny, J.M.S., Flavia Marturana, Amy E. McCart Reed, Debra Black, Gianluca Sala, Stefano Iacobelli,, D.Y. Jane D. Holland, Leonard Da Silva, Peter T. Simpson, Kum Kum Khanna, Georgia Chenevix-Trench, , and S.R. Lakhani, *Heregulin-HER3-HER2 signaling promotes matrix metalloproteinase-dependent blood-brain-barrier transendothelial migration of human breast cancer cell lines.* Oncotarget, 2015.
138. Pestalozzi, B.C., et al., *Identifying breast cancer patients at risk for Central Nervous System (CNS) metastases in trials of the International Breast Cancer Study Group (IBCSG).* Annals of Oncology, 2006. **17**(6): p. 935-944.
139. Bendell, J.C., et al., *Central nervous system metastases in women who receive trastuzumab-based therapy for metastatic breast carcinoma.* Cancer, 2003. **97**(12): p. 2972-7.
140. Brufsky, A.M., et al., *Central nervous system metastases in patients with HER2-positive metastatic breast cancer: incidence, treatment, and survival in patients from registHER.* Clin Cancer Res, 2011. **17**(14): p. 4834-43.
141. Leyland-Jones, B., *Human epidermal growth factor receptor 2-positive breast cancer and central nervous system metastases.* J Clin Oncol, 2009. **27**(31): p. 5278-86.

142. Olson, E.M., et al., *Clinical outcomes and treatment practice patterns of patients with HER2-positive metastatic breast cancer in the post-trastuzumab era.* Breast, 2013. **22**(4): p. 525-31.
143. Pestalozzi, B.C., et al., *CNS relapses in patients with HER2-positive early breast cancer who have and have not received adjuvant trastuzumab: a retrospective substudy of the HERA trial (BIG 1-01).* Lancet Oncol, 2013. **14**(3): p. 244-8.
144. Lipton, A., *Hormonal influences on oncogenesis and growth of breast cancer*, in *Breast Cancer*. 2005, Elsevier Inc. p. 42-48.
145. Owens, M.A., B.C. Horten, and M.M. Da Silva, *HER2 amplification ratios by fluorescence in situ hybridization and correlation with immunohistochemistry in a cohort of 6556 breast cancer tissues.* Clin Breast Cancer, 2004. **5**(1): p. 63-9.
146. Cronin, K.A., et al., *Population-based estimate of the prevalence of HER-2 positive breast cancer tumors for early stage patients in the US.* Cancer Invest, 2010. **28**(9): p. 963-8.
147. Weigel, M.T. and M. Dowsett, *Current and emerging biomarkers in breast cancer: prognosis and prediction.* Endocr Relat Cancer, 2010. **17**(4): p. R245-62.
148. Patani, N., L.A. Martin, and M. Dowsett, *Biomarkers for the clinical management of breast cancer: international perspective.* Int J Cancer, 2013. **133**(1): p. 1-13.
149. Iwamoto, T., et al., *Estrogen receptor (ER) mRNA and ER-related gene expression in breast cancers that are 1% to 10% ER-positive by immunohistochemistry.* J Clin Oncol, 2012. **30**(7): p. 729-34.
150. Byar, D.P., M.E. Sears, and W.L. McGuire, *Relationship between estrogen receptor values and clinical data in predicting the response to endocrine therapy for patients with advanced breast cancer.* European Journal of Cancer (1965), 1979. **15**(3): p. 299-310.
151. Rusnak, D. and T.M. Gilmer, *The discovery of lapatinib (GW572016).* Molecular cancer therapeutics, 2011. **10**(11): p. 2019-2019.
152. Rusnak, D.W., et al., *The effects of the novel, reversible epidermal growth factor receptor/ErbB-2 tyrosine kinase inhibitor, GW2016, on the growth of human normal and tumor-derived cell lines in vitro and in vivo.* Molecular cancer therapeutics, 2001. **1**(2): p. 85-94.
153. Xia, W., et al., *Anti-tumor activity of GW572016: a dual tyrosine kinase inhibitor blocks EGF activation of EGFR/erbB2 and downstream Erk1/2 and AKT pathways.* Oncogene, 2002. **21**(41): p. 6255.

154. Mass, R.D., et al., *Evaluation of Clinical Outcomes According to HER2 Detection by Fluorescence In Situ Hybridization in Women with Metastatic Breast Cancer Treated with Trastuzumab.* Clinical Breast Cancer, 2005. **6**(3): p. 240-246.
155. Piccart-Gebhart, M.J., et al., *Trastuzumab after adjuvant chemotherapy in HER2-positive breast cancer.* N Engl J Med, 2005. **353**(16): p. 1659-72.
156. Ménard, S., et al., *HER2 as a Prognostic Factor in Breast Cancer.* Oncology, 2001. **61(suppl 2)**(Suppl. 2): p. 67-72.
157. Luporsi, E., et al., *Ki-67: level of evidence and methodological considerations for its role in the clinical management of breast cancer: analytical and critical review.* Breast Cancer Res Treat, 2012. **132**(3): p. 895-915.
158. Piccart-Gebhart, M.J., *New Developments in Hormone Receptor--Positive Disease.* Oncologist, 2011. **16**.
159. Duffy, M.J., *Predictive markers in breast and other cancers: a review.* Clinical chemistry, 2005. **51**(3): p. 494-503.
160. Banin Hirata, B.K., et al., *Molecular markers for breast cancer: prediction on tumor behavior.* Disease markers, 2014. **2014**.
161. Jensen, E.V. and V.C. Jordan, *The estrogen receptor: a model for molecular medicine.* Clin Cancer Res, 2003. **9**(6): p. 1980-9.
162. Leo McGuire, W., *Current status of estrogen receptors in human breast cancer.* Cancer, 1975. **36**(S2): p. 638-644.
163. Fisher, B., et al., *Tamoxifen for Prevention of Breast Cancer: Report of the National Surgical Adjuvant Breast and Bowel Project P-1 Study.* JNCI: Journal of the National Cancer Institute, 1998. **90**(18): p. 1371-1388.
164. Harvey, J.M., et al., *Estrogen receptor status by immunohistochemistry is superior to the ligand-binding assay for predicting response to adjuvant endocrine therapy in breast cancer.* Journal of clinical oncology : official journal of the American Society of Clinical Oncology, 1999. **17**(5): p. 1474-1481.
165. Wittliff, J.L., *Steroid-hormone receptors in breast cancer.* Cancer, 1984. **53**(3 Suppl): p. 630-43.
166. Fuqua, S.A., et al., *Variant human breast tumor estrogen receptor with constitutive transcriptional activity.* Cancer Res, 1991. **51**(1): p. 105-9.
167. Daffada, A.A.I., et al., *Exon 5 Deletion Variant Estrogen Receptor Messenger RNA Expression in Relation to Tamoxifen Resistance and Progesterone Receptor/pS2 Status in Human Breast Cancer.* Cancer Research, 1995. **55**(2): p. 288.

168. McGuire, W.L., G.C. Chamness, and S.A. Fuqua, *Estrogen receptor variants in clinical breast cancer.* Mol Endocrinol, 1991. **5**(11): p. 1571-7.
169. Fisher, E.R., et al., *Solving the dilemma of the immunohistochemical and other methods used for scoring estrogen receptor and progesterone receptor in patients with invasive breast carcinoma.* Cancer, 2005. **103**(1): p. 164-73.
170. Maeyer, L.D., et al., *Does Estrogen Receptor–Negative/Progesterone Receptor–Positive Breast Carcinoma Exist?* Journal of Clinical Oncology, 2008. **26**(2): p. 335-336.
171. Rhodes, A. and B. Jasani, *The oestrogen receptor-negative/progesterone receptor-positive breast tumour: a biological entity or a technical artefact?* Journal of clinical pathology, 2009. **62**(1): p. 95-96.
172. Rakha, E.A., et al., *Biologic and clinical characteristics of breast cancer with single hormone receptor positive phenotype.* J Clin Oncol, 2007. **25**(30): p. 4772-8.
173. Dowsett, M., et al., *Relationship between quantitative estrogen and progesterone receptor expression and human epidermal growth factor receptor 2 (HER-2) status with recurrence in the Arimidex, Tamoxifen, Alone or in Combination trial.* J Clin Oncol, 2008. **26**(7): p. 1059-65.
174. Viale, G., et al., *Prognostic and predictive value of centrally reviewed expression of estrogen and progesterone receptors in a randomized trial comparing letrozole and tamoxifen adjuvant therapy for postmenopausal early breast cancer: BIG 1-98.* J Clin Oncol, 2007. **25**(25): p. 3846-52.
175. Anderson, H., et al., *Predictors of response to aromatase inhibitors.* J Steroid Biochem Mol Biol, 2007. **106**(1-5): p. 49-54.
176. Arpino, G., et al., *Estrogen receptor-positive, progesterone receptor-negative breast cancer: association with growth factor receptor expression and tamoxifen resistance.* J Natl Cancer Inst, 2005. **97**(17): p. 1254-61.
177. Stendahl, M., et al., *High progesterone receptor expression correlates to the effect of adjuvant tamoxifen in premenopausal breast cancer patients.* Clin Cancer Res, 2006. **12**(15): p. 4614-8.
178. Baselga, J., et al., *Pertuzumab plus trastuzumab plus docetaxel for metastatic breast cancer.* N Engl J Med, 2012. **366**(2): p. 109-19.

179. Swain, S.M., et al., *Pertuzumab, trastuzumab, and docetaxel for HER2-positive metastatic breast cancer (CLEOPATRA study): overall survival results from a randomised, double-blind, placebo-controlled, phase 3 study.* Lancet Oncol, 2013. **14**(6): p. 461-71.
180. Slamon, D.J., et al., *Human breast cancer: correlation of relapse and survival with amplification of the HER-2/neu oncogene.* science, 1987. **235**(4785): p. 177-182.
181. Yamamoto, T., et al., *Similarity of protein encoded by the human c-erb-B-2 gene to epidermal growth factor receptor.* Nature, 1986. **319**(6050): p. 230-4.
182. Baselga, J. and S.M. Swain, *Novel anticancer targets: revisiting ERBB2 and discovering ERBB3.* Nature Reviews Cancer, 2009. **9**(7): p. 463.
183. Lee-Hoeflich, S.T., et al., *A central role for HER3 in HER2-amplified breast cancer: implications for targeted therapy.* Cancer research, 2008. **68**(14): p. 5878-5887.
184. Zhang, Y., et al., *HER/ErbB receptor interactions and signaling patterns in human mammary epithelial cells.* BMC cell biology, 2009. **10**(1): p. 78.
185. Ueno, Y., et al., *Heregulin-induced activation of ErbB3 by EGFR tyrosine kinase activity promotes tumor growth and metastasis in melanoma cells.* International journal of cancer, 2008. **123**(2): p. 340-347.
186. Garrett, J.T., et al., *Transcriptional and posttranslational up-regulation of HER3 (ErbB3) compensates for inhibition of the HER2 tyrosine kinase.* Proceedings of the National Academy of Sciences, 2011. **108**(12): p. 5021-5026.
187. Vaught, D.B., et al., *HER3 is required for HER2-induced preneoplastic changes to the breast epithelium and tumor formation.* Cancer research, 2012. **72**(10): p. 2672-2682.
188. Bernstein, H.-G., et al., *Localization of neuregulin-1α (heregulin-α) and one of its receptors, ErbB-4 tyrosine kinase, in developing and adult human brain.* Brain research bulletin, 2006. **69**(5): p. 546-559.
189. Pinkas-Kramarski, R., et al., *Brain neurons and glial cells express Neu differentiation factor/heregulin: a survival factor for astrocytes.* Proceedings of the National Academy of Sciences, 1994. **91**(20): p. 9387-9391.
190. Lok, J., et al., *Neuregulin-1 signaling in brain endothelial cells.* Journal of Cerebral Blood Flow & Metabolism, 2009. **29**(1): p. 39-43.
191. Berghoff, A.S., et al., *Co-overexpression of HER2/HER3 is a predictor of impaired survival in breast cancer patients.* The Breast, 2014. **23**(5): p. 637-643.

192. Da Silva, L., et al., *HER3 and downstream pathways are involved in colonization of brain metastases from breast cancer.* Breast Cancer Research, 2010. **12**(4): p. R46.
193. Sun, M., et al., *HER family receptor abnormalities in lung cancer brain metastases and corresponding primary tumors.* Clinical cancer research, 2009. **15**(15): p. 4829-4837.
194. Barnes, D.M., *c-erbB-2 amplification in mammary carcinoma.* J Cell Biochem Suppl, 1993. **17g**: p. 132-8.
195. Zabrecky, J.R., et al., *The extracellular domain of p185/neu is released from the surface of human breast carcinoma cells, SK-BR-3.* J Biol Chem, 1991. **266**(3): p. 1716-20.
196. Liu, P.C., et al., *Identification of ADAM10 as a major source of HER2 ectodomain sheddase activity in HER2 overexpressing breast cancer cells.* Cancer Biol Ther, 2006. **5**(6): p. 657-64.
197. Leitzel, K., et al., *Elevated soluble c-erbB-2 antigen levels in the serum and effusions of a proportion of breast cancer patients.* Journal of clinical oncology, 1992. **10**(9): p. 1436-1443.
198. Bramwell, V.H.C., et al., *Changes over time of extracellular domain of HER2 (ECD/HER2) serum levels have prognostic value in metastatic breast cancer.* Breast Cancer Research and Treatment, 2008. **114**(3): p. 503.
199. Prigent, S.A. and W.J. Gullick, *Identification of c-erbB-3 binding sites for phosphatidylinositol 3'-kinase and SHC using an EGF receptor/c-erbB-3 chimera.* The EMBO journal, 1994. **13**(12): p. 2831-2841.
200. Peles, E., et al., *Regulated coupling of the Neu receptor to phosphatidylinositol 3'-kinase and its release by oncogenic activation.* J Biol Chem, 1992. **267**(17): p. 12266-74.
201. Ben-Levy, R., et al., *A single autophosphorylation site confers oncogenicity to the Neu/ErbB-2 receptor and enables coupling to the MAP kinase pathway.* The EMBO journal, 1994. **13**(14): p. 3302-3311.
202. Fazioli, F., et al., *The erbB-2 mitogenic signaling pathway: tyrosine phosphorylation of phospholipase C-gamma and GTPase-activating protein does not correlate with erbB-2 mitogenic potency.* Molecular and cellular biology, 1991. **11**(4): p. 2040-2048.
203. Peles, E., et al., *Oncogenic forms of the neu/HER2 tyrosine kinase are permanently coupled to phospholipase C gamma.* The EMBO journal, 1991. **10**(8): p. 2077-2086.

204. Liu, J. and J.A. Kern, *Neuregulin-1 activates the JAK-STAT pathway and regulates lung epithelial cell proliferation.* Am J Respir Cell Mol Biol, 2002. **27**(3): p. 306-13.
205. Conche, C. and K. Sauer, *Uncovering the PI3Ksome: phosphoinositide 3-kinases and counteracting PTEN form a signaling complex with intrinsic regulatory properties.* Molecular and cellular biology, 2014. **34**(18): p. 3356-3358.
206. Citri, A., K.B. Skaria, and Y. Yarden, *The deaf and the dumb: the biology of ErbB-2 and ErbB-3.* Exp Cell Res, 2003. **284**(1): p. 54-65.
207. Wullschleger, S., R. Loewith, and M.N. Hall, *TOR signaling in growth and metabolism.* Cell, 2006. **124**(3): p. 471-84.
208. Romashkova, J.A. and S.S. Makarov, *NF-kappaB is a target of AKT in anti-apoptotic PDGF signalling.* Nature, 1999. **401**(6748): p. 86-90.
209. Marshall, C.J., *MAP kinase kinase kinase, MAP kinase kinase and MAP kinase.* Curr Opin Genet Dev, 1994. **4**(1): p. 82-9.
210. Karin, M. and T. Hunter, *Transcriptional control by protein phosphorylation: signal transmission from the cell surface to the nucleus.* Curr Biol, 1995. **5**(7): p. 747-57.
211. Hunter, T., *Signaling--2000 and beyond.* Cell, 2000. **100**(1): p. 113-27.
212. Carter, P., et al., *Humanization of an anti-p185HER2 antibody for human cancer therapy*. Proceedings of the National Academy of Sciences of the United States of America, 1992. **89**(10): p. 4285-4289.
213. Molina, M.A., et al., *Trastuzumab (herceptin), a humanized anti-Her2 receptor monoclonal antibody, inhibits basal and activated Her2 ectodomain cleavage in breast cancer cells.* Cancer research, 2001. **61**(12): p. 4744-4749.
214. Hudis, C.A., *Trastuzumab—mechanism of action and use in clinical practice.* New England journal of medicine, 2007. **357**(1): p. 39-51.
215. Brodowicz, T., et al., *Soluble HER-2/neu neutralizes biologic effects of anti-HER-2/neu antibody on breast cancer cells in vitro.* Int J Cancer, 1997. **73**(6): p. 875-9.
216. Scaltriti, M., et al., *Expression of p95HER2, a truncated form of the HER2 receptor, and response to anti-HER2 therapies in breast cancer.* J Natl Cancer Inst, 2007. **99**(8): p. 628-38.
217. Xia, W., et al., *Truncated ErbB2 receptor (p95ErbB2) is regulated by heregulin through heterodimer formation with ErbB3 yet remains sensitive to the dual EGFR/ErbB2 kinase inhibitor GW572016.* Oncogene, 2004. **23**(3): p. 646-53.

218. Jin, Q., et al., *Fatty acid synthase phosphorylation: a novel therapeutic target in HER2-overexpressing breast cancer cells.* Breast Cancer Research, 2010. **12**(6): p. R96.

219. Muraoka, R.S., et al., *Increased malignancy of Neu-induced mammary tumors overexpressing active transforming growth factor β1.* Molecular and cellular biology, 2003. **23**(23): p. 8691-8703.

220. Siegel, P.M., et al., *Transforming growth factor β signaling impairs Neu-induced mammary tumorigenesis while promoting pulmonary metastasis.* Proceedings of the National Academy of Sciences, 2003. **100**(14): p. 8430-8435.

221. Asrani, K., et al., *The HER2-and Heregulin β1 (HRG)–Inducible TNFR Superfamily Member Fn14 Promotes HRG-Driven Breast Cancer Cell Migration, Invasion, and MMP9 Expression.* Molecular Cancer Research, 2013. **11**(4): p. 393-404.

222. Yao, J., et al., *Multiple signaling pathways involved in activation of matrix metalloproteinase-9 (MMP-9) by heregulin-β1 in human breast cancer cells.* Oncogene, 2001. **20**(56): p. 8066.

223. Xu, F.-J., et al., *Heregulin and agonistic anti-p185 (c-erbB2) antibodies inhibit proliferation but increase invasiveness of breast cancer cells that overexpress p185 (c-erbB2): increased invasiveness may contribute to poor prognosis.* Clinical cancer research, 1997. **3**(9): p. 1629-1634.

224. Yong, H.-Y., et al., *ErbB2-enhanced invasiveness of H-Ras MCF10A breast cells requires MMP-13 and uPA upregulation via p38 MAPK signaling.* International journal of oncology, 2010. **36**(2): p. 501-507.

225. Lopez, F., et al., *Modalities of synthesis of Ki67 antigen during the stimulation of lymphocytes.* Cytometry, 1991. **12**(1): p. 42-9.

226. Sørlie, T., et al., *Distinct molecular mechanisms underlying clinically relevant subtypes of breast cancer: gene expression analyses across three different platforms.* BMC genomics, 2006. **7**(1): p. 127.

227. Urruticoechea, A., I.E. Smith, and M. Dowsett, *Proliferation marker Ki-67 in early breast cancer.* J Clin Oncol, 2005. **23**(28): p. 7212-20.

228. De Azambuja, E., et al., *Ki-67 as prognostic marker in early breast cancer: a meta-analysis of published studies involving 12 155 patients.* British journal of cancer, 2007. **96**(10): p. 1504-1513.

229. Stuart-Harris, R., et al., *Proliferation markers and survival in early breast cancer: a systematic review and meta-analysis of 85 studies in 32,825 patients.* Breast, 2008. **17**(4): p. 323-34.
230. Jones, R.L., et al., *The prognostic significance of Ki67 before and after neoadjuvant chemotherapy in breast cancer.* Breast cancer research and treatment, 2009. **116**(1): p. 53-68.
231. Dowsett, M., et al., *Biomarker changes during neoadjuvant anastrozole, tamoxifen, or the combination: influence of hormonal status and HER-2 in breast cancer--a study from the IMPACT trialists.* J Clin Oncol, 2005. **23**(11): p. 2477-92.
232. Dowsett, M., et al., *Short-term changes in Ki-67 during neoadjuvant treatment of primary breast cancer with anastrozole or tamoxifen alone or combined correlate with recurrence-free survival.* Clin Cancer Res, 2005. **11**(2 Pt 2): p. 951s-8s.
233. Dowsett, M., et al., *Proliferation and apoptosis as markers of benefit in neoadjuvant endocrine therapy of breast cancer.* Clin Cancer Res, 2006. **12**(3 Pt 2): p. 1024s-1030s.
234. Velculescu, V.E. and W.S. El-Deiry, *Biological and clinical importance of the p53 tumor suppressor gene.* Clinical chemistry, 1996. **42**(6): p. 858-868.
235. Vogelstein, B., D. Lane, and A.J. Levine, *Surfing the p53 network.* Nature, 2000. **408**(6810): p. 307-10.
236. Freed-Pastor, W.A. and C. Prives, *Mutant p53: one name, many proteins.* Genes Dev, 2012. **26**(12): p. 1268-86.
237. Levine, A.J. and M. Oren, *The first 30 years of p53: growing ever more complex.* Nat Rev Cancer, 2009. **9**(10): p. 749-58.
238. Sørlie, T., et al., *Gene expression patterns of breast carcinomas distinguish tumor subclasses with clinical implications.* Proc Natl Acad Sci U S A, 2001. **98**(19): p. 10869-74.
239. Dumay, A., et al., *Distinct tumor protein p53 mutants in breast cancer subgroups.* International journal of cancer, 2013. **132**(5): p. 1227-1231.
240. Elledge, R.M., et al., *p53 protein accumulation detected by five different antibodies: relationship to prognosis and heat shock protein 70 in breast cancer.* Cancer Res, 1994. **54**(14): p. 3752-7.
241. El-Deiry, W.S., *The role of p53 in chemosensitivity and radiosensitivity.* Oncogene, 2003. **22**(47): p. 7486-95.

242. Elledge, R.M. and D.C. Allred, *Prognostic and predictive value of p53 and p21 in breast cancer.* Breast Cancer Res Treat, 1998. **52**(1-3): p. 79-98.
243. Soussi, T. and C. Béroud, *Assessing TP53 status in human tumours to evaluate clinical outcome.* Nat Rev Cancer, 2001. **1**(3): p. 233-40.
244. Roy, R., J. Chun, and S.N. Powell, *BRCA1 and BRCA2: different roles in a common pathway of genome protection.* Nat Rev Cancer, 2011. **12**(1): p. 68-78.
245. Welcsh, P.L., K.N. Owens, and M.C. King, *Insights into the functions of BRCA1 and BRCA2.* Trends Genet, 2000. **16**(2): p. 69-74.
246. Venkitaraman, A.R., *Cancer susceptibility and the functions of BRCA1 and BRCA2.* Cell, 2002. **108**(2): p. 171-82.
247. Shapira, I., et al., *Does maternal or paternal inheritance of BRCA mutation affect the age of cancer diagnosis?* Journal of Clinical Oncology, 2011. **29**(15_suppl): p. 1510-1510.
248. Senst, N., et al., *Parental origin of mutation and the risk of breast cancer in a prospective study of women with a BRCA1 or BRCA2 mutation.* Clin Genet, 2013. **84**(1): p. 43-6.
249. Vanstone, M., et al., *Recognizing BRCA gene mutation risk subsequent to breast cancer diagnosis in southwestern Ontario.* Canadian family physician Medecin de famille canadien, 2012. **58**(5): p. e258-e266.
250. Rebbeck, T.R., et al., *Bilateral prophylactic mastectomy reduces breast cancer risk in BRCA1 and BRCA2 mutation carriers: the PROSE Study Group.* J Clin Oncol, 2004. **22**(6): p. 1055-62.
251. Jäger, W., et al., *Serial CEA and CA 15-3 measurements during follow-up of breast cancer patients.* Anticancer Res, 2000. **20**(6d): p. 5179-82.
252. Thompson, J.A., F. Grunert, and W. Zimmermann, *Carcinoembryonic antigen gene family: molecular biology and clinical perspectives.* Journal of clinical laboratory analysis, 1991. **5**(5): p. 344-366.
253. Molina, R., et al., *Prospective evaluation of carcinoembryonic antigen (CEA) and carbohydrate antigen 15.3 (CA 15.3) in patients with primary locoregional breast cancer.* Clin Chem, 2010. **56**(7): p. 1148-57.
254. Uehara, M., et al., *Long-term prognostic study of carcinoembryonic antigen (CEA) and carbohydrate antigen 15-3 (CA 15-3) in breast cancer.* Int J Clin Oncol, 2008. **13**(5): p. 447-51.

255. Thathiah, A. and D.D. Carson, *MT1-MMP mediates MUC1 shedding independent of TACE/ADAM17.* The Biochemical journal, 2004. **382**(Pt 1): p. 363-373.
256. Hattrup, C.L. and S.J. Gendler, *Structure and function of the cell surface (tethered) mucins.* Annu Rev Physiol, 2008. **70**: p. 431-57.
257. Duffy, M.J., et al., *CA 15-3: a prognostic marker in breast cancer.* Int J Biol Markers, 2000. **15**(4): p. 330-3.
258. Sandri, M.T., et al., *Prognostic role of CA15.3 in 7942 patients with operable breast cancer.* Breast Cancer Res Treat, 2012. **132**(1): p. 317-26.
259. Moldovan, G.L., B. Pfander, and S. Jentsch, *PCNA, the maestro of the replication fork.* Cell, 2007. **129**(4): p. 665-79.
260. Elston, C.W. and I.O. Ellis, *Pathological prognostic factors in breast cancer. I. The value of histological grade in breast cancer: experience from a large study with long-term follow-up.* Histopathology, 1991. **19**(5): p. 403-10.
261. Zhao, H., et al., *Interaction of proliferation cell nuclear antigen (PCNA) with c-Abl in cell proliferation and response to DNA damages in breast cancer.* PloS one, 2012. **7**(1): p. e29416-e29416.
262. Hnasko, R. and M.P. Lisanti, *The biology of caveolae: lessons from caveolin knockout mice and implications for human disease.* Mol Interv, 2003. **3**(8): p. 445-64.
263. Elsheikh, S., et al., *Caveolin 1 and Caveolin 2 are associated with breast cancer basal-like and triple-negative immunophenotype.* British Journal of Cancer, 2008. **99**: p. 327 - 334.
264. Karam, J.A., et al., *Caveolin-1 overexpression is associated with aggressive prostate cancer recurrence.* The Prostate, 2007. **67**(6): p. 614-622.
265. Ho, C.-C., et al., *Caveolin-1 expression is significantly associated with drug resistance and poor prognosis in advanced non-small cell lung cancer patients treated with gemcitabine-based chemotherapy.* Lung cancer, 2008. **59**(1): p. 105-110.
266. Kucia, M., et al., *Trafficking of normal stem cells and metastasis of cancer stem cells involve similar mechanisms: pivotal role of the SDF-1-CXCR4 axis.* Stem Cells, 2005. **23**(7): p. 879-94.
267. Mukherjee, D. and J. Zhao, *The Role of chemokine receptor CXCR4 in breast cancer metastasis.* American journal of cancer research, 2013. **3**(1): p. 46.
268. Chen, H.-W., et al., *Cytoplasmic CXCR4 high-expression exhibits distinct poor clinicopathological characteristics and predicts poor prognosis in triple-negative breast cancer.* Current molecular medicine, 2013. **13**(3): p. 410-416.

269. Sahin, M., E. Sahin, and S. Koksoy, *Regulatory T cells in cancer: an overview and perspectives on cyclooxygenase-2 and Foxp3 DNA methylation.* Human immunology, 2013. **74**(9): p. 1061-1068.
270. Zuo, T., et al., *FOXP3 is an X-linked breast cancer suppressor gene and an important repressor of the HER-2/ErbB2 oncogene.* Cell, 2007. **129**(7): p. 1275-1286.
271. Merlo, A., et al., *FOXP3 expression and overall survival in breast cancer.* J Clin Oncol, 2009. **27**(11): p. 1746-52.
272. Harvey, J.R., et al., *Inhibition of CXCR4-mediated breast cancer metastasis: a potential role for heparinoids?* Clinical Cancer Research, 2007. **13**(5): p. 1562-1570.
273. Mellor, P., et al., *Modulatory effects of heparin and short-length oligosaccharides of heparin on the metastasis and growth of LMD MDA-MB 231 breast cancer cells in vivo.* Br J Cancer, 2007. **97**(6): p. 761-8.
274. Cristofanilli, M., et al., *Circulating tumor cells, disease progression, and survival in metastatic breast cancer.* N Engl J Med, 2004. **351**(8): p. 781-91.
275. Downward *et al*., *Targeting RAS signalling pathways in cancer therapy.* Nat Rev Cancer, 2003. **3**(1): p. 11-22.
276. Pylayeva-Gupta, Y., E. Grabocka, and D. Bar-Sagi, *RAS oncogenes: weaving a tumorigenic web.* Nature Reviews Cancer, 2011. **11**(11): p. 761.
277. Cherfils, J. and M. Zeghouf, *Regulation of small gtpases by gefs, gaps, and gdis.* Physiological reviews, 2013. **93**(1): p. 269-309.
278. van Reesema, L.L.S., et al., *RAS pathway biomarkers for breast cancer prognosis.* Clinical laboratory international, 2016. **40**: p. 18.
279. Arteaga, C.L., et al., *Treatment of HER2-positive breast cancer: current status and future perspectives.* Nature reviews Clinical oncology, 2012. **9**(1): p. 16.
280. Foulkes, W.D., I.E. Smith, and J.S. Reis-Filho, *Triple-negative breast cancer.* New England journal of medicine, 2010. **363**(20): p. 1938-1948.
281. Tebbutt, N., M.W. Pedersen, and T.G. Johns, *Targeting the ERBB family in cancer: couples therapy.* Nature reviews Cancer, 2013. **13**(9): p. 663.
282. Wright, K.L., et al., *Ras signaling is a key determinant for metastatic dissemination and poor survival of luminal breast cancer patients.* Cancer research, 2015. **75**(22): p. 4960-4972.
283. Parker *et al*., *A Ras-GTPase-Activating Protein SH3-Domain-Binding Protein.* MOLECULAR AND CELLULAR BIOLOGY, 1996.

284. Barnes *et al*., *Heregulin Induces Expression, ATPase Activity, and Nuclear Localization of G3BP, a Ras Signaling Component, in Human Breast Tumors.* CANCER RESEARCH, 2002.

285. French *et al*., *The expression of Ras–GTPase activating protein SH3*

domain-binding proteins, G3BPs, in human breast cancers. The Histochemical Journal, 2002.

286. Guitarda *et al*., *G3BP is overexpressed in human tumors and promotes S phase entry.* Cancer Letters, 2001.

287. Pazman *et al*., *Rasputin, the Drosophilahomologue of the RasGAP SH3 binding protein, functions in Ras- and Rho-mediated signaling.* Development, 2000.

288. Ortega *et al*., *Human G3BP1 interacts with beta-F1-ATPase mRNA and inhibits its translation.* J Cell Sci, 2010. **123**(Pt 16): p. 2685-96.

289. Kennedy *et al*., *Characterization of G3BPs: tissue specific expression, chromosomal localisation and rasGAP(120) binding studies.* J Cell Biochem, 2001. **84**(1): p. 173-87.

290. FABIENNE PARKER, F.M., ISABELLE DELUMEAU, MARC DUCHESNE,, L.D. DIDIER FAUCHER, ANITA DUGUE,, and F.S.A.B. TOCQUE, *A Ras-GTPase-Activating Protein SH3-Domain-Binding Protein.* MOLECULAR AND CELLULAR BIOLOGY, 1996.

291. Irvine *et al*., *Rasputin, more promiscuous than ever: a review of G3BP*. Int J Dev Biol, 2004. **48**(10): p. 1065-77.

292. Vognsen, T., I.R. Moller, and O. Kristensen, *Crystal structures of the human G3BP1 NTF2-like domain visualize FxFG Nup repeat specificity.* PLoS One, 2013. **8**(12): p. e80947.

293. Prigent *et al*., *IkappaBalpha and IkappaBalpha /NF-kappa B complexes are retained in the cytoplasm through interaction with a novel partner, RasGAP SH3-binding protein 2.* J Biol Chem, 2000. **275**(46): p. 36441-9.

294. Tourriere, H., et al., *The RasGAP-associated endoribonuclease G3BP assembles stress granules.* J Cell Biol, 2003. **160**(6): p. 823-31.

295. Leblanc, V., B. Tocque, and I. Delumeau, *Ras-GAP controls Rho-mediated cytoskeletal reorganization through its SH3 domain.* Mol Cell Biol, 1998. **18**(9): p. 5567-78.

296. Zhang, H., et al., *Downregulation of G3BPs inhibits the growth, migration and invasion of human lung carcinoma H1299 cells by suppressing the Src/FAK-associated signaling pathway.* Cancer Gene Ther, 2013. **20**(11): p. 622-9.
297. Gallouzi *et al*., *A Novel Phosphorylation-Dependent RNase Activity of GAP-SH3 Binding Protein: a Potential Link between Signal Transduction and RNA Stability.* MOLECULAR AND CELLULAR BIOLOGY, 1998.
298. Tourriere *et al*., *RasGAP-associated endoribonuclease G3Bp: selective RNA degradation and phosphorylation-dependent localization.* Mol Cell Biol, 2001. **21**(22): p. 7747-60.
299. Kedersha, N., et al., *G3BP-Caprin1-USP10 complexes mediate stress granule condensation and associate with 40S subunits.* J Cell Biol, 2016. **212**(7): p. 845-60.
300. Gam, L.-H., *Breast cancer and protein biomarkers.* World journal of experimental medicine, 2012. **2**(5): p. 86.
301. Xiao, C., et al., *Lymphoproliferative disease and autoimmunity in mice with increased miR-17-92 expression in lymphocytes.* Nature immunology, 2008. **9**(4): p. 405.
302. Montreuil, J., J.F.G. Vliegenthart, and H. Schachter, *Glycoproteins II*. Vol. 29. 1997: Elsevier.
303. Dias, M.H., et al., *Proteomics and drug discovery in cancer.* Drug discovery today, 2016. **21**(2): p. 264-277.
304. Hudler, P., N. Kocevar, and R. Komel, *Proteomic approaches in biomarker discovery: new perspectives in cancer diagnostics.* The scientific world journal, 2014. **2014**.
305. Oi *et al*., *Resveratrol induces apoptosis by directly targeting Ras-GTPase-activating protein SH3 domain-binding protein 1.* Oncogene, 2015. **34**(20): p. 2660-71.
306. Shim *et al*., *Epigallocatechin gallate suppresses lung cancer cell growth through Ras-GTPase-activating protein SH3 domain-binding protein 1.* Cancer Prev Res (Phila), 2010. **3**(5): p. 670-9.
307. Zhang *et al*., *GAP161 targets and downregulates G3BP to suppress cell growth and potentiate cisplaitin-mediated cytotoxicity to colon carcinoma HCT116 cells.* Cancer Sci, 2012. **103**(10): p. 1848-56.
308. Dwek, M.V. and S.L. Rawlings, *Current perspectives in cancer proteomics.* Molecular biotechnology, 2002. **22**(2): p. 139-152.
309. Somiari, R.I., et al., *Proteomics of breast carcinoma.* Journal of Chromatography B, 2005. **815**(1-2): p. 215-225.

310. Andreotti, G., M. Monticelli, and M.V. Cubellis, *Looking for protein stabilizing drugs with thermal shift assay.* Drug Test Anal, 2015. **7**(9): p. 831-4.
311. Jain, K., *Proteomics-based anticancer drug discovery and development.* Technology in cancer research & treatment, 2002. **1**(4): p. 231-236.
312. Wulfkuhle, J.D., et al., *Proteomics of human breast ductal carcinoma in situ.* Cancer research, 2002. **62**(22): p. 6740-6749.
313. Luo, Y., et al., *Comparative proteome analysis of breast cancer and normal breast.* Molecular biotechnology, 2005. **29**(3): p. 233-244.
314. Deng, S.-S., et al., *Comparative proteome analysis of breast cancer and adjacent normal breast tissues in human.* Genomics, proteomics & bioinformatics, 2006. **4**(3): p. 165-172.
315. Yiu, C.C., et al., *Changes in protein expression after neoadjuvant use of aromatase inhibitors in primary breast cancer: a proteomic approach to search for potential biomarkers to predict response or resistance.* Expert opinion on investigational drugs, 2010. **19**(sup1): p. S79-S89.
316. Hodgkinson, V.C., et al., *Pilot and feasibility study: comparative proteomic analysis by 2-DE MALDI TOF/TOF MS reveals 14-3-3 proteins as putative biomarkers of response to neoadjuvant chemotherapy in ER-positive breast cancer.* Journal of proteomics, 2012. **75**(9): p. 2745-2752.
317. Caldas-Lopes, E., et al., *Hsp90 inhibitor PU-H71, a multimodal inhibitor of malignancy, induces complete responses in triple-negative breast cancer models.* Proceedings of the National Academy of Sciences, 2009. **106**(20): p. 8368-8373.
318. Yang, W.S., et al., *Proteomic approach reveals FKBP4 and S100A9 as potential prediction markers of therapeutic response to neoadjuvant chemotherapy in patients with breast cancer.* Journal of proteome research, 2011. **11**(2): p. 1078-1088.
319. Lambert, J.M., et al., *PRIMA-1 reactivates mutant p53 by covalent binding to the core domain.* Cancer Cell, 2009. **15**(5): p. 376-88.
320. Claus *et al.*, *Inhibitor-induced HER2-HER3 heterodimerisation promotes proliferation through a novel dimer interface.* Elife, 2018. **7**.
321. Waks, A.G. and E.P. Winer, *Breast cancer treatment: a review.* Jama, 2019. **321**(3): p. 288-300.
322. Klapper, L.N., et al., *Tumor-inhibitory antibodies to HER-2/ErbB-2 may act by recruiting c-Cbl and enhancing ubiquitination of HER-2.* Cancer research, 2000. **60**(13): p. 3384-3388.

323. Larionov, A.A., *Current therapies for human epidermal growth factor receptor 2-positive metastatic breast cancer patients.* Frontiers in Oncology, 2018. **8**: p. 89.
324. Clynes, R.A., et al., *Inhibitory Fc receptors modulate in vivo cytotoxicity against tumor targets.* Nat Med, 2000. **6**(4): p. 443-6.
325. Arnould, L., et al., *Trastuzumab-based treatment of HER2-positive breast cancer: an antibody-dependent cellular cytotoxicity mechanism?* Br J Cancer, 2006. **94**(2): p. 259-67.
326. Junttila, T.T., et al., *Ligand-independent HER2/HER3/PI3K complex is disrupted by trastuzumab and is effectively inhibited by the PI3K inhibitor GDC-0941.* Cancer Cell, 2009. **15**(5): p. 429-40.
327. Slamon, D., et al., *Adjuvant trastuzumab in HER2-positive breast cancer.* New England Journal of Medicine, 2011. **365**(14): p. 1273-1283.
328. Martin, M., et al., *Neratinib after trastuzumab-based adjuvant therapy in HER2-positive breast cancer (ExteNET): 5-year analysis of a randomised, double-blind, placebo-controlled, phase 3 trial.* The Lancet Oncology, 2017. **18**(12): p. 1688-1700.
329. Swain, S.M., et al., *Pertuzumab, trastuzumab, and docetaxel in HER2-positive metastatic breast cancer.* N Engl J Med, 2015. **372**(8): p. 724-34.
330. von Minckwitz, G., et al., *Trastuzumab Emtansine for Residual Invasive HER2-Positive Breast Cancer.* N Engl J Med, 2019. **380**(7): p. 617-628.
331. Nahta, R. and F.J. Esteva, *HER2 therapy: molecular mechanisms of trastuzumab resistance.* Breast Cancer Res, 2006. **8**(6): p. 215.
332. Valabrega, G., F. Montemurro, and M. Aglietta, *Trastuzumab: mechanism of action, resistance and future perspectives in HER2-overexpressing breast cancer.* Ann Oncol, 2007. **18**(6): p. 977-84.
333. Scott, G.K., et al., *A truncated intracellular HER2/neu receptor produced by alternative RNA processing affects growth of human carcinoma cells.* Mol Cell Biol, 1993. **13**(4): p. 2247-57.
334. Christianson, T.A., et al., *NH2-terminally truncated HER-2/neu protein: relationship with shedding of the extracellular domain and with prognostic factors in breast cancer.* Cancer Res, 1998. **58**(22): p. 5123-9.
335. Scaltriti, M., et al., *Expression of p95HER2, a truncated form of the HER2 receptor, and response to anti-HER2 therapies in breast cancer.* Journal of the National Cancer Institute, 2007. **99**(8): p. 628-638.

336. Nagy, P., et al., *Decreased accessibility and lack of activation of ErbB2 in JIMT-1, a herceptin-resistant, MUC4-expressing breast cancer cell line.* Cancer Res, 2005. **65**(2): p. 473-82.
337. Lu, Y., et al., *Insulin-like growth factor-I receptor signaling and resistance to trastuzumab (Herceptin).* Journal of the National Cancer Institute, 2001. **93**(24): p. 1852-1857.
338. Nagata, Y., et al., *PTEN activation contributes to tumor inhibition by trastuzumab, and loss of PTEN predicts trastuzumab resistance in patients.* Cancer Cell, 2004. **6**(2): p. 117-27.
339. Berns, K., et al., *A functional genetic approach identifies the PI3K pathway as a major determinant of trastuzumab resistance in breast cancer.* Cancer cell, 2007. **12**(4): p. 395-402.
340. Kataoka, Y., et al., *Association between gain-of-function mutations in PIK3CA and resistance to HER2-targeted agents in HER2-amplified breast cancer cell lines.* Ann Oncol, 2010. **21**(2): p. 255-262.
341. Oktay, E., et al., *Nearly complete response of brain metastases from HER2 overexpressing breast cancer with lapatinib and capecitabine after whole brain irradiation.* Case reports in oncological medicine, 2013. **2013**.
342. Vogel, C., et al., *Management of ErbB2-positive breast cancer: insights from preclinical and clinical studies with lapatinib.* Japanese journal of clinical oncology, 2010. **40**(11): p. 999-1013.
343. Lackey, K., *Lessons from the drug discovery of lapatinib, a dual ErbB1/2 tyrosine kinase inhibitor.* Current topics in medicinal chemistry, 2006. **6 5**: p. 435-60.
344. FDA, D.s. *Lapatinib (Tykerb) [full prescribing information].* . 2009.
345. Wood *et al*., *A Unique Structure for Epidermal Growth Factor Receptor Bound to GW572016 (Lapatinib): Relationships among Protein Conformation, Inhibitor Off-Rate, and Receptor Activity in Tumor Cells.* CANCER RESEARCH, 2004.
346. Zhang, D., et al., *Activity of lapatinib is independent of EGFR expression level in HER2-overexpressing breast cancer cells.* Mol Cancer Ther, 2008. **7**(7): p. 1846-50.
347. Scaltriti, M., et al., *Lapatinib, a HER2 tyrosine kinase inhibitor, induces stabilization and accumulation of HER2 and potentiates trastuzumab-dependent cell cytotoxicity.* Oncogene, 2009. **28**(6): p. 803.

348. Scaltriti, M., et al., *Clinical benefit of lapatinib-based therapy in patients with human epidermal growth factor receptor 2–positive breast tumors coexpressing the truncated p95HER2 receptor.* Clinical cancer research, 2010. **16**(9): p. 2688-2695.
349. Hutchinson, L., *Lapatinib is effective in patients with p95HER2-positive tumors.* Nature Reviews Clinical Oncology, 2010. **7**(7): p. 358A-358A.
350. Xia, W., et al., *Lapatinib antitumor activity is not dependent upon phosphatase and tensin homologue deleted on chromosome 10 in ErbB2-overexpressing breast cancers.* Cancer research, 2007. **67**(3): p. 1170-1175.
351. Perez, E.A., et al., *Cardiac safety of lapatinib: pooled analysis of 3689 patients enrolled in clinical trials.* Mayo Clin Proc, 2008. **83**(6): p. 679-86.
352. Ma, S.-l., et al., *Lapatinib antagonizes multidrug resistance-associated protein 1-mediated multidrug resistance by inhibiting its transport function.* Molecular medicine (Cambridge, Mass.), 2014. **20**(1): p. 390-399.
353. Palmieri, D., et al., *Her-2 overexpression increases the metastatic outgrowth of breast cancer cells in the brain.* Cancer Res, 2007. **67**(9): p. 4190-8.
354. Gril, B., et al., *Effect of lapatinib on the outgrowth of metastatic breast cancer cells to the brain.* J Natl Cancer Inst, 2008. **100**(15): p. 1092-103.
355. Cameron, D., et al., *A phase III randomized comparison of lapatinib plus capecitabine versus capecitabine alone in women with advanced breast cancer that has progressed on trastuzumab: updated efficacy and biomarker analyses.* Breast cancer research and treatment, 2008. **112**(3): p. 533-543.
356. Geyer, C.E., et al., *Lapatinib plus capecitabine for HER2-positive advanced breast cancer.* New England Journal of Medicine, 2006. **355**(26): p. 2733-2743.
357. Lin, N.U., et al., *Phase II trial of lapatinib for brain metastases in patients with human epidermal growth factor receptor 2–positive breast cancer.* Journal of clinical oncology: official journal of the American Society of Clinical Oncology, 2008. **26**(12): p. 1993.
358. Lin, N.U., et al., *Multicenter phase II study of lapatinib in patients with brain metastases from HER2-positive breast cancer.* Clinical cancer research, 2009. **15**(4): p. 1452-1459.
359. Xia, W., et al., *A model of acquired autoresistance to a potent ErbB2 tyrosine kinase inhibitor and a therapeutic strategy to prevent its onset in breast cancer.* Proceedings of the National Academy of Sciences, 2006. **103**(20): p. 7795-7800.

360. Hegde, P.S., et al., *Delineation of molecular mechanisms of sensitivity to lapatinib in breast cancer cell lines using global gene expression profiles.* Molecular cancer therapeutics, 2007. **6**(5): p. 1629-1640.
361. Trowe, T., et al., *EXEL-7647 inhibits mutant forms of ErbB2 associated with lapatinib resistance and neoplastic transformation.* Clinical cancer research, 2008. **14**(8): p. 2465-2475.
362. Eichhorn, P.J., et al., *Phosphatidylinositol 3-kinase hyperactivation results in lapatinib resistance that is reversed by the mTOR/phosphatidylinositol 3-kinase inhibitor NVP-BEZ235.* Cancer research, 2008. **68**(22): p. 9221-9230.
363. Liu, L., et al., *Novel mechanism of lapatinib resistance in HER2-positive breast tumor cells: activation of AXL.* Cancer research, 2009. **69**(17): p. 6871-6878.
364. Benson, A.B., 3rd, et al., *Recommended guidelines for the treatment of cancer treatment-induced diarrhea.* J Clin Oncol, 2004. **22**(14): p. 2918-26.
365. Crown, J.P., et al., *Pooled analysis of diarrhea events in patients with cancer treated with lapatinib.* Breast cancer research and treatment, 2008. **112**(2): p. 317-325.
366. Chu, I., et al., *The dual ErbB1/ErbB2 inhibitor, lapatinib (GW572016), cooperates with tamoxifen to inhibit both cell proliferation- and estrogen-dependent gene expression in antiestrogen-resistant breast cancer.* Cancer Res, 2005. **65**(1): p. 18-25.
367. Di Leo, A., et al., *Phase III, double-blind, randomized study comparing lapatinib plus paclitaxel with placebo plus paclitaxel as first-line treatment for metastatic breast cancer.* J Clin Oncol, 2008. **26**(34): p. 5544-52.
368. Carvalho, C., et al., *Doxorubicin: the good, the bad and the ugly effect.* Current medicinal chemistry, 2009. **16**(25): p. 3267-3285.
369. Gordon, A.N., et al., *Recurrent epithelial ovarian carcinoma: a randomized phase III study of pegylated liposomal doxorubicin versus topotecan.* J Clin Oncol, 2001. **19**(14): p. 3312-22.
370. Liu, C.L., et al., *Doxorubicin Promotes Migration and Invasion of Breast Cancer Cells through the Upregulation of the RhoA/MLC Pathway.* J Breast Cancer, 2019. **22**(2): p. 185-195.
371. Lovitt, C.J., T.B. Shelper, and V.M. Avery, *Doxorubicin resistance in breast cancer cells is mediated by extracellular matrix proteins.* BMC Cancer, 2018. **18**(1): p. 41.
372. Zheng, Z., et al., *An ancestral haplotype defines susceptibility to doxorubicin nephropathy in the laboratory mouse.* Journal of the American Society of Nephrology, 2006. **17**(7): p. 1796-1800.

373. Bigotte, L. and Y. Olsson, *Cytofluorescence localization of adriamycin in the nervous system.* Acta neuropathologica, 1982. **58**(3): p. 193-202.
374. Tangpong, J., et al., *Adriamycin-induced, TNF-α-mediated central nervous system toxicity.* Neurobiology of disease, 2006. **23**(1): p. 127-139.
375. Tacar, O., P. Sriamornsak, and C.R. Dass, *Doxorubicin: an update on anticancer molecular action, toxicity and novel drug delivery systems.* Journal of pharmacy and pharmacology, 2013. **65**(2): p. 157-170.
376. Hilmer, S.N., et al., *The hepatic pharmacokinetics of doxorubicin and liposomal doxorubicin.* Drug metabolism and disposition, 2004. **32**(8): p. 794-799.
377. Tewey, K., et al., *Adriamycin-induced DNA damage mediated by mammalian DNA topoisomerase II.* Science, 1984. **226**(4673): p. 466-468.
378. Campiglio, M., et al., *Role of proliferation in HER2 status predicted response to doxorubicin.* Int J Cancer, 2003. **105**(4): p. 568-73.
379. Gewirtz, D.A., *A critical evaluation of the mechanisms of action proposed for the antitumor effects of the anthracycline antibiotics adriamycin and daunorubicin.* Biochem Pharmacol, 1999. **57**(7): p. 727-41.
380. Minotti, G., et al., *Anthracyclines: molecular advances and pharmacologic developments in antitumor activity and cardiotoxicity.* Pharmacol Rev, 2004. **56**(2): p. 185-229.
381. Tokarska-Schlattner, M., et al., *New insights into doxorubicin-induced cardiotoxicity: the critical role of cellular energetics.* Journal of molecular and cellular cardiology, 2006. **41**(3): p. 389-405.
382. Ashley, N. and J. Poulton, *Mitochondrial DNA is a direct target of anti-cancer anthracycline drugs.* Biochemical and biophysical research communications, 2009. **378**(3): p. 450-455.
383. Muller, I., et al., *Effect of concentration on the cytotoxic mechanism of doxorubicin--apoptosis and oxidative DNA damage.* Biochem Biophys Res Commun, 1997. **230**(2): p. 254-7.
384. Chen, M.B., et al., *Activation of AMP-activated protein kinase is involved in vincristine-induced cell apoptosis in B16 melanoma cell.* Journal of cellular physiology, 2011. **226**(7): p. 1915-1925.
385. Leung, L.K. and T.T. Wang, *Differential effects of chemotherapeutic agents on the Bcl-2/Bax apoptosis pathway in human breast cancer cell line MCF-7.* Breast cancer research and treatment, 1999. **55**(1): p. 73-83.

386. Mcgahon, A.J., et al., *Chemotherapeutic drug-induced apoptosis in human leukaemic cells is independent of the Fas (APO-1/CD95) receptor/ligand system.* British journal of haematology, 1998. **101**(3): p. 539-547.
387. Ni, C., et al., *Doxorubicin-induced cardiotoxicity involves IFNγ-mediated metabolic reprogramming in cardiomyocytes.* The Journal of pathology, 2019. **247**(3): p. 320-332.
388. Chen, M.-B., et al., *Activation of AMP-activated protein kinase contributes to doxorubicin-induced cell death and apoptosis in cultured myocardial H9c2 cells.* Cell biochemistry and biophysics, 2011. **60**(3): p. 311-322.
389. Sun, Z., et al., *The TGF-β pathway mediates doxorubicin effects on cardiac endothelial cells.* Journal of molecular and cellular cardiology, 2016. **90**: p. 129-138.
390. Strutz, F., et al., *TGF-β1 induces proliferation in human renal fibroblasts via induction of basic fibroblast growth factor (FGF-2).* Kidney international, 2001. **59**(2): p. 579-592.
391. Clark, R.A., et al., *TGF-β1 stimulates cultured human fibroblasts to proliferate and produce tissue-like fibroplasia: A fibronectin matrix-dependent event.* Journal of cellular physiology, 1997. **170**(1): p. 69-80.
392. Furuta, K., et al., *Gene mutation of transforming growth factor β1 type II receptor in hepatocellular carcinoma.* International journal of cancer, 1999. **81**(6): p. 851-853.
393. Hsu, W.-T., et al., *The HER2 inhibitor lapatinib potentiates doxorubicin-induced cardiotoxicity through iNOS signaling.* Theranostics, 2018. **8**(12): p. 3176-3188.
394. O'Connor, R., et al., *Phase I evaluation of lapatinib (L) and epirubicin (E) in patients (pts) with anthracycline (anth)-naive metastatic breast cancer (MBC).* Journal of Clinical Oncology, 2009. **27**(15_suppl): p. 1107-1107.
395. Jacobson, K.K., et al., *Gene copy mapping of the ERBB2/TOP2A region in breast cancer.* Genes Chromosomes Cancer, 2004. **40**(1): p. 19-31.
396. Giordano, S.H., et al., *Decline in the use of anthracyclines for breast cancer.* Journal of Clinical Oncology, 2012. **30**(18): p. 2232.
397. Swain, S.M., F.S. Whaley, and M.S. Ewer, *Congestive heart failure in patients treated with doxorubicin: a retrospective analysis of three trials.* Cancer: Interdisciplinary International Journal of the American Cancer Society, 2003. **97**(11): p. 2869-2879.
398. Lipshultz, S.E., et al., *Cardiovascular disease in adult survivors of childhood cancer.* Annual review of medicine, 2015. **66**: p. 161-176.

399. Wang, L., et al., *Doxorubicin-induced systemic inflammation is driven by upregulation of toll-like receptor TLR4 and endotoxin leakage.* Cancer research, 2016. **76**(22): p. 6631-6642.
400. Jansen, C.E., et al., *Preliminary results of a longitudinal study of changes in cognitive function in breast cancer patients undergoing chemotherapy with doxorubicin and cyclophosphamide.* Psycho-Oncology, 2008. **17**(12): p. 1189-1195.
401. Cock, I.E., *Is the pharmaceutical industry's preoccupation with the monotherapy drug model stifling the development of effective new drug therapies?* Inflammopharmacology, 2018. **26**(3): p. 861-879.
402. Pritchard, J.R., et al., *Defining principles of combination drug mechanisms of action.* Proceedings of the National Academy of Sciences, 2013. **110**(2): p. E170-E179.
403. Khdair, A., et al., *Nanoparticle-mediated combination chemotherapy and photodynamic therapy overcomes tumor drug resistance.* Journal of Controlled Release, 2010. **141**(2): p. 137-144.
404. Matei, D., et al., *Epigenetic resensitization to platinum in ovarian cancer.* Cancer research, 2012. **72**(9): p. 2197-2205.
405. Mokhtari, R.B., et al., *Combination therapy in combating cancer.* Oncotarget, 2017. **8**(23): p. 38022.
406. Blackwell, K.L., et al., *Overall survival benefit with lapatinib in combination with trastuzumab for patients with human epidermal growth factor receptor 2–positive metastatic breast cancer: final results from the EGF104900 study.* Journal of Clinical Oncology, 2012. **30**(21): p. 2585-2592.
407. Pivot, X., et al., *CEREBEL (EGF111438): a phase III, randomized, open-label study of lapatinib plus capecitabine versus trastuzumab plus capecitabine in patients with human epidermal growth factor receptor 2–positive metastatic breast cancer.* Journal of Clinical Oncology, 2015. **33**(14): p. 1564-1573.
408. Metro, G., et al., *Clinical outcome of patients with brain metastases from HER2-positive breast cancer treated with lapatinib and capecitabine.* Annals of oncology, 2010. **22**(3): p. 625-630.
409. Lambert, J.M. and R.V. Chari, *Ado-trastuzumab Emtansine (T-DM1): an antibody–drug conjugate (ADC) for HER2-positive breast cancer*. 2014, ACS Publications.
410. Blum, R.H., et al., *A therapeutic trial of maytansine.* Cancer clinical trials, 1978. **1**(2): p. 113-117.

411. Piccart-Gebhart, M.J., et al., *Trastuzumab after adjuvant chemotherapy in HER2-positive breast cancer.* New England Journal of Medicine, 2005. **353**(16): p. 1659-1672.
412. Romond, E.H., et al., *Trastuzumab plus adjuvant chemotherapy for operable HER2-positive breast cancer.* New England Journal of Medicine, 2005. **353**(16): p. 1673-1684.
413. Polyak *et al*., *Heterogeneity in breast cancer.* J Clin Invest, 2011. **121**(10): p. 3786-8.
414. Sledge Jr, G. and K. Miller, *Exploiting the hallmarks of cancer: the future conquest of breast cancer.* European Journal of Cancer, 2003. **39**(12): p. 1668-1675.
415. Schulz, W., *Molecular biology of human cancers: an advanced student's textbook*. 2005: Springer Science & Business Media.
416. Ruprecht *et al*., *Lapatinib Resistance in Breast Cancer Cells Is Accompanied by Phosphorylation-Mediated Reprogramming of Glycolysis.* Cancer Res, 2017. **77**(8): p. 1842-1853.
417. Hou, L., et al., *Interfering cellular lactate homeostasis overcomes Taxol resistance of breast cancer cells through the microRNA-124-mediated lactate transporter (MCT1) inhibition.* Cancer cell international, 2019. **19**(1): p. 193.
418. Feng, Y., et al., *Lactate dehydrogenase A: A key player in carcinogenesis and potential target in cancer therapy.* Cancer medicine, 2018. **7**(12): p. 6124-6136.
419. Van Poznak, C., et al., *Oral gossypol in the treatment of patients with refractory metastatic breast cancer: a phase I/II clinical trial.* Breast cancer research and treatment, 2001. **66**(3): p. 239-248.
420. Jin *et al*., *Serum lactic dehydrogenase strongly predicts survival in metastatic nasopharyngeal carcinoma treated with palliative chemotherapy.* Eur J Cancer, 2013. **49**(7): p. 1619-26.
421. Zhuang *et al*., *Lactate dehydrogenase 5 expression in melanoma increases with disease progression and is associated with expression of Bcl-XL and Mcl-1, but not Bcl-2 proteins.* Mod Pathol, 2010. **23**(1): p. 45-53.
422. Soncini *et al*., *Ras -GAP SH3 domain binding protein (G3BP) is a modulator of USP10, a novel human ubiquitin speci®c protease.* Oncogene, 2001.
423. Cohen, M., et al., *Ubp3 requires a cofactor, Bre5, to specifically de-ubiquitinate the COPII protein, Sec23.* Nat Cell Biol, 2003. **5**(7): p. 661-7.

424. Cohen, M., F. Stutz, and C. Dargemont, *Deubiquitination, a new player in Golgi to endoplasmic reticulum retrograde transport.* J Biol Chem, 2003. **278**(52): p. 51989-92.
425. Willers, I.M., et al., *Selective inhibition of β-F1-ATPase mRNA translation in human tumours.* Biochemical Journal, 2010. **426**(3): p. 319-326.
426. Jin, L., et al., *Phosphorylation-mediated activation of LDHA promotes cancer cell invasion and tumour metastasis.* Oncogene, 2017. **36**(27): p. 3797-3806.
427. Guan, M., et al., *Lapatinib Inhibits Breast Cancer Cell Proliferation by Influencing PKM2 Expression.* Technol Cancer Res Treat, 2018. **17**: p. 1533034617749418.
428. Wong, N., J. De Melo, and D. Tang, *PKM2, a Central Point of Regulation in Cancer Metabolism.* Int J Cell Biol, 2013. **2013**: p. 242513.
429. Lüftner, D., et al., *Tumor type M2 pyruvate kinase expression in advanced breast cancer.* Anticancer Res, 2000. **20**(6d): p. 5077-82.
430. Eigenbrodt, E., et al., *Quantification of tumor type M2 pyruvate kinase (Tu M2-PK) in human carcinomas.* Anticancer research, 1997. **17**(4B): p. 3153.
431. Mazurek, S., et al., *Pyruvate kinase type M2 and its role in tumor growth and spreading.* Seminars in Cancer Biology, 2005. **15**(4): p. 300-308.
432. Luo, W., et al., *Pyruvate kinase M2 is a PHD3-stimulated coactivator for hypoxia-inducible factor 1.* Cell, 2011. **145**(5): p. 732-744.
433. Pfaffl, M.W., *A new mathematical model for relative quantification in real-time RT-PCR.* Nucleic Acids Res, 2001. **29**(9): p. e45.
434. Rizwan, A., et al., *Relationships between LDH-A, lactate, and metastases in 4T1 breast tumors.* Clinical Cancer Research, 2013. **19**(18): p. 5158-5169.
435. Vander Heiden, M.G., L.C. Cantley, and C.B. Thompson, *Understanding the Warburg effect: the metabolic requirements of cell proliferation.* Science, 2009. **324**(5930): p. 1029-33.
436. Warburg, O., F. Wind, and E. Negelein, *THE METABOLISM OF TUMORS IN THE BODY.* J Gen Physiol, 1927. **8**(6): p. 519-30.
437. Taniuchi, K., I. Nishimori, and M.A. Hollingsworth, *The N-terminal domain of G3BP enhances cell motility and invasion by posttranscriptional regulation of BART.* Mol Cancer Res, 2011. **9**(7): p. 856-66.
438. Winslow *et al.*, *Regulation of PMP22 mRNA by G3BP1 affects cell proliferation in breast cancer cells.* Molecular Cancer, 2013.

439. Atlas *et al*., *The insulin-like growth factor mRNA binding-protein IMP-1 and the Ras-regulatory protein G3BP associate with tau mRNA and HuD protein in differentiated P19 neuronal cells.* J Neurochem, 2004. **89**(3): p. 613-26.
440. Abdellatif, M., et al., *A Ras-dependent pathway regulates RNA polymerase II phosphorylation in cardiac myocytes: implications for cardiac hypertrophy.* Molecular and cellular biology, 1998. **18**(11): p. 6729-6736.
441. Lypowy, J., I.-Y. Chen, and M. Abdellatif, *An alliance between Ras GTPase-activating protein, filamin C, and Ras GTPase-activating protein SH3 domain-binding protein regulates myocyte growth.* Journal of Biological Chemistry, 2005. **280**(27): p. 25717-25728.
442. Yang, J.-Y., et al., *Impaired Akt activity down-modulation, caspase-3 activation, and apoptosis in cells expressing a caspase-resistant mutant of RasGAP at position 157.* Molecular biology of the cell, 2005. **16**(8): p. 3511-3520.
443. Costa *et al*., *Human DNA helicase VIII: a DNA and RNA helicase*

corresponding to the G3BP protein, an element of the Ras transduction pathway. Nucleic Acids Research, 1999.
444. Srivastava, M. and H.B. Pollard, *Molecular dissection of nucleolin's role in growth and cell proliferation: new insights.* Faseb j, 1999. **13**(14): p. 1911-22.
445. Niesen *et al*., *The use of differential scanning fluorimetry to detect ligand interactions that promote protein stability.* Nat Protoc, 2007. **2**(9): p. 2212-21.
446. Nachiappan *et al*., *Structural and functional analysis of Glutaminyl-tRNA synthetase (TtGlnRS) from Thermus thermophilus HB8 and its complexes.* Int J Biol Macromol, 2018. **120**(Pt B): p. 1379-1386.
447. Vera *et al*., *The conformational quality of insoluble recombinant proteins is enhanced at low growth temperatures.* Biotechnol Bioeng, 2007. **96**(6): p. 1101-6.
448. Longley, D.B., D.P. Harkin, and P.G. Johnston, *5-fluorouracil: mechanisms of action and clinical strategies.* Nature reviews cancer, 2003. **3**(5): p. 330.
449. Zhang, Q., et al., *APR-246 reactivates mutant p53 by targeting cysteines 124 and 277.* Cell death & disease, 2018. **9**(5): p. 439.
450. Wassman *et al*., *Computational identification of a transiently open L1/S3 pocket for reactivation of mutant p53.* Nat Commun, 2013. **4**: p. 1407.

451. Vedadi, M., et al., *Chemical screening methods to identify ligands that promote protein stability, protein crystallization, and structure determination.* Proceedings of the National Academy of Sciences, 2006. **103**(43): p. 15835-15840.
452. Senisterra, G., I. Chau, and M. Vedadi, *Thermal denaturation assays in chemical biology.* Assay and drug development technologies, 2012. **10**(2): p. 128-136.
453. Korcsmáros, T., et al., *How to design multi-target drugs.* Expert Opin Drug Discov, 2007. **2**(6): p. 799-808.
454. Cimmperman, P., et al., *A quantitative model of thermal stabilization and destabilization of proteins by ligands.* Biophysical journal, 2008. **95**(7): p. 3222-3231.
455. Wang, Z., et al., *Pattern of distant metastases in inflammatory breast cancer - A large-cohort retrospective study.* Journal of Cancer, 2020. **11**(2): p. 292-300.
456. Hance, K.W., et al., *Trends in inflammatory breast carcinoma incidence and survival: the surveillance, epidemiology, and end results program at the National Cancer Institute.* J Natl Cancer Inst, 2005. **97**(13): p. 966-75.
457. Sahai, E., *Illuminating the metastatic process.* Nat Rev Cancer, 2007. **7**(10): p. 737-49.
458. Meng, X.G. and S.W. Yue, *Dexamethasone disrupts cytoskeleton organization and migration of T47D Human breast cancer cells by modulating the AKT/mTOR/RhoA pathway.* Asian Pac J Cancer Prev, 2014. **15**(23): p. 10245-50.
459. Yamaguchi, H. and J. Condeelis, *Regulation of the actin cytoskeleton in cancer cell migration and invasion.* Biochim Biophys Acta, 2007. **1773**(5): p. 642-52.
460. Condeelis, J., R.H. Singer, and J.E. Segall, *The great escape: when cancer cells hijack the genes for chemotaxis and motility.* Annu Rev Cell Dev Biol, 2005. **21**: p. 695-718.
461. Arpaia, E., et al., *The interaction between caveolin-1 and Rho-GTPases promotes metastasis by controlling the expression of alpha5-integrin and the activation of Src, Ras and Erk.* Oncogene, 2012. **31**(7): p. 884-96.
462. Koestler, S.A., et al., *F- and G-actin concentrations in lamellipodia of moving cells.* PLoS One, 2009. **4**(3): p. e4810.
463. Pollard, T.D. and J.A. Cooper, *Actin, a central player in cell shape and movement.* Science, 2009. **326**(5957): p. 1208-12.
464. Suzuki, R., K. Hotta, and K. Oka, *Spatiotemporal quantification of subcellular ATP levels in a single HeLa cell during changes in morphology.* Sci Rep, 2015. **5**: p. 16874.

465. Campello, S., et al., *Orchestration of lymphocyte chemotaxis by mitochondrial dynamics.* J Exp Med, 2006. **203**(13): p. 2879-86.
466. Kalluri, R. and R.A. Weinberg, *The basics of epithelial-mesenchymal transition.* J Clin Invest, 2009. **119**(6): p. 1420-8.
467. Eger, A., et al., *Epithelial mesenchymal transition by c-Fos estrogen receptor activation involves nuclear translocation of beta-catenin and upregulation of beta-catenin/lymphoid enhancer binding factor-1 transcriptional activity.* J Cell Biol, 2000. **148**(1): p. 173-88.
468. Tepass, U., et al., *Cadherins in embryonic and neural morphogenesis.* Nat Rev Mol Cell Biol, 2000. **1**(2): p. 91-100.
469. Edelman, G.M., et al., *Early epochal maps of two different cell adhesion molecules.* Proceedings of the National Academy of Sciences of the United States of America, 1983. **80**(14): p. 4384-4388.
470. Rodilla, V., et al., *Possible relationship between micronucleated and binucleated cells induced by cisplatin in cultured CHO cells.* Mutat Res, 1993. **291**(1): p. 35-41.
471. Guerreiro, P.S., et al., *Differential effects of methoxyamine on doxorubicin cytotoxicity and genotoxicity in MDA-MB-231 human breast cancer cells.* Mutat Res, 2013. **757**(2): p. 140-7.
472. Ramos, D.L., et al., *Genotoxic effects of doxorubicin in cultured human lymphocytes with different glutathione S-transferase genotypes.* Mutat Res, 2011. **724**(1-2): p. 28-34.
473. Liang, L., et al., *Dkk1 exacerbates doxorubicin-induced cardiotoxicity by inhibiting the Wnt/beta-catenin signaling pathway.* J Cell Sci, 2019. **132**(10).
474. Pandey, S., et al., *Upregulation of IGF-IIRalpha intensifies doxorubicin-induced cardiac damage.* J Cell Biochem, 2019.
475. Mancilla, T.R., B. Iskra, and G.J. Aune, *Doxorubicin-Induced Cardiomyopathy in Children.* Compr Physiol, 2019. **9**(3): p. 905-931.
476. Rebucci, M. and C. Michiels, *Molecular aspects of cancer cell resistance to chemotherapy.* Biochem Pharmacol, 2013. **85**(9): p. 1219-26.
477. Wurz, G.T. and M.W. DeGregorio, *Activating adaptive cellular mechanisms of resistance following sublethal cytotoxic chemotherapy: implications for diagnostic microdosing.* Int J Cancer, 2015. **136**(7): p. 1485-93.

478. Graham, C.H., et al., *Rapid acquisition of multicellular drug resistance after a single exposure of mammary tumor cells to antitumor alkylating agents.* J Natl Cancer Inst, 1994. **86**(13): p. 975-82.
479. Yoshida, T., et al., *Repeated treatment with subtoxic doses of TRAIL induces resistance to apoptosis through its death receptors in MDA-MB-231 breast cancer cells.* Mol Cancer Res, 2009. **7**(11): p. 1835-44.
480. Amalina, N.D., I.P. Nurhayati, and E. Meiyanto, *Doxorubicin Induces Lamellipodia Formation and Cell Migration.* Indonesian Journal of Cancer Chemoprevention, 2017. **8**(2): p. 61-67.
481. Sylvia S. Gayle, S.L.M.A., Ruth M. O'Regan, and Rita Nahta, *Pharmacologic Inhibition of mTOR Improves Lapatinib Sensitivity in HER2-Overexpressing Breast Cancer Cells with Primary Trastuzumab Resistance.* Anticancer Agents Med Chem, 2012.
482. Kaczynska *et al*., *Combination of lapatinib with isothiocyanates overcomes drug resistance and inhibits migration of HER2 positive breast cancer cells.* Breast Cancer, 2017. **24**(2): p. 271-280.
483. Dai, C.L., et al., *Lapatinib (Tykerb, GW572016) reverses multidrug resistance in cancer cells by inhibiting the activity of ATP-binding cassette subfamily B member 1 and G member 2.* Cancer Res, 2008. **68**(19): p. 7905-14.
484. Janser, F.A., et al., *Her2-Targeted Therapy Induces Autophagy in Esophageal Adenocarcinoma Cells.* Int J Mol Sci, 2018. **19**(10).
485. Boccardo, F., et al., *Evaluation of lapatinib (Lap) plus capecitabine (Cap) in patients with brain metastases (BM) from HER2+ breast cancer (BC) enrolled in the Lapatinib Expanded Access Program (LEAP) and French Authorisation Temporaire d'Utilisation (ATU).* Journal of Clinical Oncology, 2008. **26**(15_suppl): p. 1094-1094.
486. Cameron, D., et al., *Lapatinib plus capecitabine in women with HER-2-positive advanced breast cancer: final survival analysis of a phase III randomized trial.* The oncologist, 2010. **15**(9): p. 924-934.
487. Crown, J.P., et al., *Safety and tolerability of lapatinib in combination with taxanes (T) in patients with breast cancer (BC).* Journal of Clinical Oncology, 2007. **25**(18_suppl): p. 1027-1027.
488. PIRCHER, M., et al., *Lapatinib-plus-Pegylated Liposomal Doxorubicin in Advanced HER2-positive Breast Cancer Following Trastuzumab: A Phase II Trial.* Anticancer Research, 2015. **35**(1): p. 517-521.

489. Kimball, K.J., et al., *A phase I study of lapatinib in combination with carboplatin in women with platinum sensitive recurrent ovarian carcinoma.* Gynecol Oncol, 2008. **111**(1): p. 95-101.
490. Bartsch, R., et al., *Impact of anti-HER2 therapy on overall survival in HER2-overexpressing breast cancer patients with brain metastases.* Br J Cancer, 2012. **106**(1): p. 25-31.
491. Bachelot, T., et al., *[Systemic treatment of brain metastases from breast cancer: cytotoxic chemotherapy and targeted therapies].* Bull Cancer, 2013. **100**(1): p. 7-14.
492. Morten, B.C., R.J. Scott, and K.A. Avery-Kiejda, *Comparison of three different methods for determining cell proliferation in breast cancer cell lines.* JoVE (Journal of Visualized Experiments), 2016(115): p. e54350.
493. Yano, S., et al., *Preparation of photocrosslinked fish elastin polypeptide/microfibrillated cellulose composite gels with elastic properties for biomaterial applications.* Marine drugs, 2015. **13**(1): p. 338-353.
494. Schönborn, I., et al., *PCNA as a potential prognostic marker in breast cancer.* The Breast, 1994. **3**(2): p. 97-102.
495. Juríková, M., et al., *Ki67, PCNA, and MCM proteins: Markers of proliferation in the diagnosis of breast cancer.* Acta Histochem, 2016. **118**(5): p. 544-52.
496. Sidani, M., et al., *Cofilin determines the migration behavior and turning frequency of metastatic cancer cells.* J Cell Biol, 2007. **179**(4): p. 777-91.
497. Zebda, N., et al., *Phosphorylation of ADF/cofilin abolishes EGF-induced actin nucleation at the leading edge and subsequent lamellipod extension.* J Cell Biol, 2000. **151**(5): p. 1119-28.
498. Nahta, R., et al., *Lapatinib induces apoptosis in trastuzumab-resistant breast cancer cells: effects on insulin-like growth factor I signaling.* Molecular Cancer Therapeutics, 2007. **6**(2): p. 667.
499. Shah, A.N. and W.J. Gradishar, *Adjuvant Anthracyclines in Breast Cancer: What Is Their Role?* The oncologist, 2018. **23**(10): p. 1153-1161.
500. Bandyopadhyay, A., et al., *Doxorubicin in combination with a small TGFbeta inhibitor: a potential novel therapy for metastatic breast cancer in mouse models.* PLoS One, 2010. **5**(4): p. e10365.
501. Alam, S.R., et al., *Investigation of mitochondrial metabolic response to doxorubicin in prostate cancer cells: an NADH, FAD and tryptophan FLIM assay.* Scientific reports, 2017. **7**(1): p. 10451.

502. van Wijngaarden, J., et al., *Celecoxib enhances doxorubicin-induced cytotoxicity in MDA-MB231 cells by NF-kappaB-mediated increase of intracellular doxorubicin accumulation.* Eur J Cancer, 2007. **43**(2): p. 433-42.
503. Li, X., et al., *Intrinsic resistance of tumorigenic breast cancer cells to chemotherapy.* J Natl Cancer Inst, 2008. **100**(9): p. 672-9.
504. Avtanski, D., et al., *Resistin induces breast cancer cells epithelial to mesenchymal transition (EMT) and stemness through both adenylyl cyclase-associated protein 1 (CAP1)-dependent and CAP1-independent mechanisms.* Cytokine, 2019. **120**: p. 155-164.
505. Ridley, A.J., *Life at the leading edge.* Cell, 2011. **145**(7): p. 1012-22.
506. Insall, R.H. and L.M. Machesky, *Actin dynamics at the leading edge: from simple machinery to complex networks.* Dev Cell, 2009. **17**(3): p. 310-22.
507. Zhao, J., et al., *Mitochondrial dynamics regulates migration and invasion of breast cancer cells.* Oncogene, 2013. **32**(40): p. 4814-24.
508. Cunniff, B., et al., *AMPK activity regulates trafficking of mitochondria to the leading edge during cell migration and matrix invasion.* Mol Biol Cell, 2016. **27**(17): p. 2662-74.
509. Rivadeneira, D.B., et al., *Survivin promotes oxidative phosphorylation, subcellular mitochondrial repositioning, and tumor cell invasion.* Sci Signal, 2015. **8**(389): p. ra80.
510. Licon-Munoz, Y., et al., *F-actin reorganization by V-ATPase inhibition in prostate cancer.* Biol Open, 2017. **6**(11): p. 1734-1744.
511. Lee, E., E.A. Shelden, and D.A. Knecht, *Formation of F-actin aggregates in cells treated with actin stabilizing drugs.* Cell motility and the cytoskeleton, 1998. **39**(2): p. 122-133.
512. Martin, T.A., et al., *Cancer invasion and metastasis: molecular and cellular perspective*, in *Madame Curie Bioscience Database [Internet]*. 2013, Landes Bioscience.
513. Singh, R. and J. Valcárcel, *Building specificity with nonspecific RNA-binding proteins.* Nature structural & molecular biology, 2005. **12**(8): p. 645.
514. Solomon, S., et al., *Distinct structural features of caprin-1 mediate its interaction with G3BP-1 and its induction of phosphorylation of eukaryotic translation initiation factor 2alpha, entry to cytoplasmic stress granules, and selective interaction with a subset of mRNAs.* Mol Cell Biol, 2007. **27**(6): p. 2324-42.

515. Sorrell, F.J., et al., *Development of a differential scanning fluorimetry based high throughput screening assay for the discovery of affinity binders against an anthrax protein.* Journal of pharmaceutical and biomedical analysis, 2010. **52**(5): p. 802-808.
516. Morita, E., et al., *Attenuated protein expression vectors for use in siRNA rescue experiments.* Biotechniques, 2012: p. 1.
517. Eastlack, S.C., et al., *Suppression of PDHX by microRNA-27b deregulates cell metabolism and promotes growth in breast cancer.* Mol Cancer, 2018. **17**(1): p. 100.
518. Xu, M., et al., *FGFR4 Links Glucose Metabolism and Chemotherapy Resistance in Breast Cancer.* Cellular Physiology and Biochemistry, 2018. **47**(1): p. 151-160.